The role of the amyloid precursor protein following traumatic brain injury

Frances Corrigan BHlthSc (Hons)

Discipline of Anatomy and Pathology
School of Medical Sciences
The University of Adelaide

November 2011

A thesis submitted in partial fulfilment of the requirements for the degree of Doctor of Philosophy

Table of Contents

Abstract

The amyloid precursor protein (APP) is known to increase following traumatic brain injury (TBI). It has been hypothesised that this increase in APP may be deleterious to outcome due to the production of neurotoxic Aβ. Conversely, this upregulation may be beneficial as cleavage of APP via the alternative non-amyloidogenic pathway produces the soluble alpha form of APP (sAPPα), which is known to have many neuroprotective and neurotrophic functions. Indeed a previous study showed that treatment with sAPPα following a diffuse injury in rats reduced apoptotic cell death and axonal injury which corresponded with an improvement in motor outcome. However, it is not yet known whether endogenous APP plays a similar beneficial role following TBI, or which specific region within sAPPα conferred this protective activity.

In order to investigate this the effect of post-traumatic administration of various regions within sAPPα was examined following severe-impact acceleration TBI in Sprague Dawley rats. Furthermore the outcome of male C57BL6j x 129sv APP-/- mice was compared to that of APP+/+ mice following two types of traumatic brain injury; a diffuse lesion caused by a weight drop model and a focal lesion induced by a controlled cortical impact (CCI) injury.

Knockout of APP was found to worsen outcome following both a mild diffuse and moderate focal injury, with an exacerbation of motor and cognitive deficits associated with an increase in neuronal injury and an impaired reparative response. These deficits could be rescued with treatment with sAPPα, suggesting that it was lack of this APP metabolite which caused the increase in vulnerability of APP-/- mice. Furthermore initial investigations in Sprague Dawley rats found that only the domains of sAPPα that contained heparin binding sites were able to improve functional outcome and decrease axonal injury following diffuse TBI. This suggested that the neuroprotective activity of sAPPα related to its ability to bind to heparin sulphate proteoglycans. Indeed a preliminary investigation found that the peptide APP96-110, which encompassess one of the heparin binding sites within sAPPα, was sufficient to reduce functional deficits and neuronal injury in APP-/- mice.

These results demonstrate that the upregulation of APP seen following TBI is a protective response, with the benefits of sAPPα outweighing any negative effects of other APP metabolites like Aβ. The neuroprotective properties of sAPPα, may relate to its heparin binding sites, with one of these regions, APP96-110, warranting further investigation as a putative neuroprotective agent following TBI.

Declaration

This work contains no material which has been accepted for the award of any degree or diploma in any university or other tertiary institution to Frances Corrigan and, to the best of my knowledge and belief, contains no material previously published or written by another person, except where due reference has been made in the text.

I give consent to this copy of my thesis when deposited in the University Library, being made available for loan and photocopying subject to the provisions of the Copyright Act 1968. The author acknowledges that copyright of published works contained within this thesis, as listed below, resides with the copyright holders of those works.

I also give permission for the digital version of my thesis to be made available on the web, via the University's digital research repository, the Library catalogue, the Australasian Digital Theses Program (ADTP) and also through web search engines, unless permission has been granted by the University to restrict access for a period of time

Frances Corrigan

Date:

Publications and Presentations

Publications

Corrigan F, Pham C, Vink R, Blumbergs P, Masters C, Van den Heuvel C and Cappai R. *The neuroprotective domains of the amyloid precursor protein, in traumatic brain injury, are located in the two growth factor domains.* Brain Research (2011) 1378:137-43.

Corrigan F, Ziebell J and Vink R. *Motor cortical trauma / fluid percussion models* in Animal Models of Movement Disorders, Neuromethods (2011) 62:193-209

Corrigan F, Pham C, Vink R, Blumbergs P, Masters C, Cappai R and Van den Heuvel C. Characterising the effects of the knockout of the amyloid precursor protein following mild diffuse traumatic brain injury. Experimental Neurology (Submitted)

Ziebell J, **Corrigan F** and Vink R. *Models of traumatic brain injury: What have we learnt over the past 30 years* in Traumatic Brain and Spinal Cord Injury (In Press)

Cook N, **Corrigan F,** Van den Heuvel C. *The Role of Magnesium in Traumatic CNS Injury* in Magnesium in the Central Nervous System, University of Adelaide Press (2011)

Abstracts/Presentations

Corrigan F, Vink R, Blumbergs P, Masters C, Cappai R and Van Den Heuvel C (2011). *Characterising the effects of amyloid precursor protein knockout on outcome following traumatic brain injury* 28(5): A28, 10th International Neurotrauma Symposium, Shanghai, China

Corrigan F, Vink R, Blumbergs P, Masters C, Cappai R and Van Den Heuvel C (2011). *sAPPα prevents the exacerbation of deficits seen in amyloid precursor knockout mice*. Journal of Neurotrauma 28(5): A67, 10th International Neurotrauma Symposium, Shanghai, China

Corrigan F, Vink R, Blumbergs P, Masters C, Cappai R and Van Den Heuvel C (2011), *Exacerbation of deficits seen in amyloid precursor protein knockout mice following traumatic brain injury is rescued with sAPPα.* Abstracts of 31st Annual Meeting of the Australian Neuroscience Society, P128, Auckland, New Zealand

Cappai R, **Corrigan F**, Pham CL, Vink R, Masters CL, Blumbergs PC, van den Heuvel C (2011), *Defining the neuroprotective activity of endogenously expressed amyloid precursor protein in traumatic brain injury.* Abstracts of the 23rd Meeting of the International Society for Neurochemistry, PS08.X, Athens, Greece

Corrigan F, Vink R, Blumbergs P, Masters C, Cappai R and Van den Heuvel C (2010). *Characterisation of the effects of knockout of the amyloid precursor protein on outcome following traumatic brain injury*. Abstracts of the Australasian Trauma Society Annual Scientific Meeting, P13, Melbourne, Australia

Corrigan F, Vink R, Blumbergs P, Masters C, Cappai R and Van den Heuvel C (2010). *Exacerbation of deficits in amyloid precursor protein knockout mice following mild traumatic brain injury.* Abstracts of the South Australian Meeting of the Australian Medical Science Research Society, P74, Adelaide

Corrigan F, Vink R, Blumbergs P, Masters C, Cappai R and Van den Heuvel C (2010). *The amyloid precursor protein is neuroprotective following mild traumatic brain injury.* Abstracts of the Australian Neuroscience Society, O16, Sydney Australia

Corrigan F, Vink R, Cappai R and Van den Heuvel C (2009). *Determining the neuroprotective properties of the amyloid precursor protein in vivo.* Journal of Neurotrauma 26(9):A9, 2nd Joint Symposium of the National And International Trauma Societies, Santa Barbara, USA

Acknowledgements

The work within this thesis would not have been possible without the support and assistance of many other people.

My primary supervisor Dr Corinna Van den Heuvel, thank you for providing me with the opportunity to undertake my PhD and for your continual support, guidance and knowledge. Throughout my PhD your door has always been open for chats about the progress of this work.

My second superivisor, Professor Robert Vink was always generous in sharing his extensive research knowledge and experience.

Associate Professor Roberto Cappai provided much of the theoretical underpinnings to the peptide studies conducted within this thesis. In particular, his extensive knowledge of the amyloid precursor protein, including its three dimensional structure and its specific active sites were crucial.

Dr Chi Pham was also critical in producing many of the proteins that were used throughout this thesis.

Dr Mark Habgood provided invaluable assistance in setting up the controlled cortical impact model, going above and beyond what was required to ensure that I had a working model. This not only included assisting in its construction, but also being willing to provide detailed and helpful answers to my many questions.

Jim Manavis, whose encyclopedic knowledge of immunohistochemistry, meant that he could assist with technical details about almost any antibody I could think to ask for. I also extend thanks to the rest of the IMVS staff, including Kathy, Serg, Sophie, Sven and Yvonne for their help throughout my studies.

The post-docs within the laboratory, Dr Stephen Helps, Dr Emma Thornton, Dr Jenna Ziebell and Dr Renee Turner provided assistance with many aspects of these studies, particularly in setting up the mouse diffuse injury model .

John Hallett for constructing many of the different functional testing apparatus used throughout this thesis including the Y Maze, Barnes Maze and ledged beams.

To my fellow PhD students, past and present who have shared part of this journey, Adam, Anna, Chris, Kate, Levon, Liz and Tim, who have made this an enjoyable experience through their help and support.

Finally, the IMVS Animal Facility, particularly Briony and Kelly for taking excellent care of my animals.

Abbreviations

Aβ	Amyloid beta
AD	Alzheimer's disease
AICD	Amyloid precursor protein intracellular domain
AIF	Apoptosis inducing factor
ANOVA	Analysis of variance
APLP	Amyloid precursor like protein
APOE	Apolipoprotein E
APP	Amyloid precursor protein
ATP	Adenosine triphosphate
BACE	Beta amyloid precursor protein cleaving enzyme
BDNF	Brain derived neurotrophic factor
CCI	Controlled cortical impact
CDK5	Cyclin dependent kinase 5
CNS	Central nervous system
CuBD	Copper binding domain
DAI	Diffuse axonal injury
DAB	3,3' Diaminobenzidine
DNA	Deoxyribonucleic acid
ER	Endoplasmic reticulum
FJC	Fluoro Jade C
FP	Fluid percussion
GFLD	Growth factor like domain
GSK-3β	glycogen synthase kinase-3β
H&E	Haematoxylin and eosin
HSPG	Heparin sulphate proteoglycans
ICV	Intracerebroventricular
IAP	Inhibitor of apoptosis
IGF-2	Insulin growth factor
IL	Interleukin
IP	Intraperitoneal
JNK3	c-Jun N-terminal kinase 3
KPI	Kunitz type protease inhibitor
LTP	Long term potentiation
NF-κB	Nuclear factor kappa B

NGF	Nerve growth factor
NT	Neurotrophin
MAP-2	Microtubule associated protein-2
MAPK	Mitogen activated protein kinase
PAT1a	Protein interacting with amyloid precursor protein tail 1a
PCD	Programmed cell death
PBS	Phosphate buffered saline
PI_3K	Phosphotidylinositol-3-kinase
PKC	Protein kinase C
PS	Presenilin
PTB	Phosphotyrosine binding
ROS	Reactive oxygen species
RGB	Red green blue
sAPPα	Serum amyloid precursor protein alpha
sAPPβ	Serum amyloid precursor protein beta
SEM	Standard error of the mean
SP	Substance P
TBI	Traumatic brain injury
TBS	Tris buffered saline
TNF-α	Tumour necrosis factor alpha

Table of Figures

Chapter 1: Introduction to traumatic brain injury and the role of the amyloid precursor protein

Traumatic brain injury (TBI) is a major health problem, causing more deaths in Australians under 45 years of age than any other cause (Finfer and Cohen, 2001). Furthermore many survivors are left with permanent neurologic deficits at a substantial social and economic cost to the community. Following TBI, cell death is not only caused by the initial insult, but is ongoing due to the initiation of a number of secondary factors such as excitotoxicity, oxidative stress and inflammation (Maas et al., 2008). Despite this knowledge, to date there are no currently accepted therapies to limit this injury (Faden and Stoica, 2007; Vink and Van Den Heuvel, 2004).

TBI also leads to the upregulation of a number of neuroprotective pathways, which attempt to limit the amount of neuronal damage and to activate the repair response within the brain (Keyvani and Schallert, 2002). It has been suggested that novel therapeutic strategies for TBI should attempt to stimulate these endogenous repair-regeneration mechanisms while antagonising deleterious processes (Faden and Stoica, 2007). Recent evidence suggests that the amyloid precursor protein (APP) may play such a role following TBI. It is acutely upregulated following injury (Van Den Heuvel et al., 2000), with its metabolite sAPPα shown to attenuate neuronal death induced by a number of secondary injury factors such as excitotoxicity (Goodman and Mattson, 1994; Mattson, 1994) and to also facilitate reparative activities like synaptogenesis (Bell et al., 2006). As such this thesis aims to establish whether APP is a neuroprotective molecule following TBI, and to determine the region of APP which contains this activity in order to facilitate drug development. In order to explain the basis of this project, the mechanisms of injury following TBI and the potential role of APP will be outlined.

1.1 Epidemiology

According to the World Health Organisation, motor accidents and their sequelae, particularly TBI will surpass many diseases as the major cause of death and disability by the year 2020 (Hyder et al., 2007). An estimated 10 million people are affected annually by a TBI serious enough to result in death or hospitalisation, with a mortality rate of 15-30 per 100,000 reported in industrialised countries (Finfer and Cohen, 2001; Tagliaferri et al., 2006). TBI is a major public health and medical problem with an estimated 1% of the US population living with long-term or lifelong disability associated with a TBI that required hospitalisation (Corrigan et al., 2010). Indeed, the cost globally for rehabilitation of individuals following head injury is estimated to be around US $500 billion a year (Jacobs et al., 2000).

.

Similar to the global situation, in Australia TBI is a significant health problem, with the rate of hospitalisation for TBI recorded as 107 per 100,000 people in the population in 2004 (Fortune and Wen, 2007). This evidently underestimates the actual incidence of TBI, as the majority are mild cases which do not require hospitalisation. There were two sharp peaks of incidence, in males between the ages of 15 and 25 and in males and females over the age of 70. This second rise in prevalence reflected an increase in injuries caused by falls, although the most common overall cause was vehicular accidents.

It is evident that TBI causes a substantial economic burden, not only due to medical costs, but because it predominantly affects individuals of working age. Many survivors do not return to their pre-injury functioning levels, with recovery from moderate-severe TBI often a long arduous process. Most recovery gains occur within the first 6 months and are influenced by a number of factors including pre-injury functioning capacities, age, level of unconsciousness and magnitude of neurologic damage (Connor, 2002). However many survivors are left with severe permanent neurological deficits, which adversely affect their quality of life. Even mild TBI is associated with a number of symptoms including headaches, blurred vision, poor concentration, sleep disturbance, depressed mood and irritability, which are broadly classed as post-concussion syndrome (Bryant et al., 2010; Petchprapai and Winkelman, 2007; Vanderploeg et al., 2005). Memory deficits in particular can impair a patient's ability to resume normal daily activities. With more severe injuries more significant motor and cognitive deficits, as well as behavioural problems can occur such as a decreased ability to plan, control or execute activities, disordered thought processes, personality changes, violent mood swings and depression, which can prevent patients from returning to work or resuming family responsibilities (Halcomb et al., 2005; Kneafsey and Gawthorpe, 2004). In addition a small group of patients will be left in a vegetative state, unable to meaningfully respond to external stimuli and thus requiring constant care (Blumbergs, 1997).

1.2 Neuropathology and physiology of head injury

TBI results from the head impacting with an object or from acceleration/deceleration forces that produce vigorous movement of the brain within the skull or varying combinations of these mechanical forces (Finnie and Blumbergs, 2002). The resultant injury is caused by two mechanisms, either primary or secondary, although there is some degree of overlap (Gaetz, 2004; Maas et al., 2008). Indeed it has been suggested that the mechanisms of TBI could be extended out to 4 phases:

the primary injury, the delayed consequences of the primary injury, the secondary injury and finally recovery (Graham et al., 2002). Whereas the primary injury is not reversible, its delayed consequences and the secondary injury cascade it sets in motion over minutes to days are potentially reversible (Graham et al., 2000a). Therefore, as many of the neurological deficits seen following TBI are the result of the secondary injury cascade, this provides an opportunity to improve outcome with appropriate therapeutic intervention (Bramlett and Dietrich, 2004).

1.2.1 Primary Injury

Mechanical forces (rotation, acceleration/deceleration and direct force applied to the head) acting at the moment of injury damage the blood vessels, axons, nerve cells and glia of the brain in a focal, multifocal or diffuse pattern of involvement. The type and severity of the resulting injury depend on the nature of the initiating force, as well as its site, direction and magnitude (Smith et al., 2003). Contact forces generated when the head strikes or is struck by an object generally produce focal injuries such as skull fractures, extradural haemorrhages, and contusions. In contrast acceleration/deceleration forces that result from violent unrestrained head movement are associated with diffuse axonal injury (DAI) (Blumbergs, 1997). When the head suffers a sudden mechanically induced load two types of motion can be induced in translation or rotation. Translation occurs when the head's centre of gravity moves along a straight line, whilst rotational injuries allow the head to move around its centre of gravity. The latter induces the most devastating forces that affect the brain after injury, as it places stress on the connections between the brain and skull distorting axons, and potentially disrupting the bridging veins within the subdural space (Ommaya et al., 2002).

Structural damage

Structural damage following injury is traditionally classified as focal, which encompasses lacerations, skull fractures, intracerebral haemorrhages and cortical contusions, or diffuse, comprising DAI and diffuse microvascular damage. However both focal and diffuse injuries can co-exist, with, for example, direct impacts to the head seen in falls, motor vehicle accidents and assaults capable of producing significant acceleration/deceleration forces leading to DAI, as well as the move obvious contact forces causing focal injuries (Gaetz, 2004).

Cerebral Haemorrhage

Traumatic brain haemorrhages generally result from tearing of blood vessels at the moment of head impact and are classed as intracerebral, extradural, subdural or subarachnoid (Povlishock and Katz, 2005). The most common vascular injury is subarachnoid haemorrhage, the result of disrupted small subarachnoidal vessels, with this potentially leading to a number of secondary complications including vasospasm and hydrocephalus (Blumbergs, 1997). Epidural haematomas are usually the result of a skull fracture disrupting the middle meningeal artery, whilst subdural haematomas are commonly due to the stretching or tearing of cortical veins which occurs during an acceleration/deceleration injury (Besenski, 2002). Intracerebral haemorrhages follow stretching and rupture of small-calibre arterioles within either the basal ganglia or the ventricles and are thus commonly distributed throughout the central white matter and basal ganglia (Cifu et al., 1999). All intracranial haemorrhages have the potential to increase intracranial pressure, leading to secondary cell death due to reductions in cerebral perfusion pressure and brain herniation.

Cortical Contusions

Contusions are a common feature of TBI and result from localised mechanical forces damaging the small blood vessels (capillaries, veins and/or arteries) and other tissue components (nerve and glial cells) of the neural parenchyma (Gaetz, 2004). Contusions and lacerations form a continuum of tissue injury, with lacerations defined as a disruption of the pia membrane, as well as tearing of the underlying tissue (Blumbergs, 1997). Bleeding is usually the most obvious feature of contusions on macroscopic and microscopic examination and it ranges from microhaemorrhages to confluent haemorrhage disrupting the tissue. Surface contusions occur at the crest of gyri, where the brain encounters the rough and irregular surfaces of the skull during the contact or deceleration phase of a force. These can be classified as coup (occurring directly beneath the site of impact) contrecoup (occurring opposite to the site of impact), fracture (beneath the site of a fracture) or herniation contusions (when the parahippocampal gyri and cerebellar tonsils are forced against the tentorium and foramen magnum) (Davis, 2000; Farkas and Povlishock, 2007; Graham et al., 2000a). Along with surface contusions that occur from contact forces, gliding contusions can be produced with rotational motion and are thus associated with DAI. They are principally found in the parasagittal regions of the brain, where the brain is more adherent to the dura (Davis, 2000). Contusions can increase in size over hours to days due to evolving events related to the interplay of haemorrhage,

early ischaemic necrosis and breakdown of the blood-brain barrier (BBB) with vasogenic oedema formation (Blumbergs, 1997).

Diffuse Axonal Injury

One of the most harmful consequences of TBI is the widespread or diffuse disruption and disconnection of axons through a process known as diffuse axonal injury (DAI) or traumatic axonal injury (TAI). DAI is a term applied to TBI-induced scattered destruction of white matter tracts, with the corticomedullary junctions, particularly those located in the frontal and temporal areas, as well as the corpus callosum, the upper brainstem and the deep grey matter the most susceptible regions (Adams et al., 1989). Diffuse vascular injury is thought to represent the severe end of the spectrum of DAI. It is only seen in patients who die very soon after head injury and consists of multiple small haemorrhages throughout the brain (Blumbergs, 1997)

Although axonal injury was initially considered to constitute a primary injury mechanism following TBI (primary axotomy), it has since been discovered that only a small subpopulation of axons that sustain the most severe injury rupture at the moment of impact. Indeed, axonal injury is currently considered to principally be a progressive event which evolves from an initial focal perturbation of the axon to ultimate axonal disconnection (secondary axotomy) (Buki and Povlishock, 2006; Gentleman et al., 1993b; Povlishock et al., 1992). The initiating event is thought to be an alteration in axolemmal permeability involving mechanoporation of the axolemma evoked by the shearing forces of the injury (Maxwell et al., 1997; Pettus et al., 1994; Povlishock and Pettus, 1996). This allows local intra-axonal calcium accumulation with subsequent activation of various calcium-dependent cysteine protease (calpain) pathways capable of degrading the cytoskeletal network within the axon. Calpain-mediated degradation of the cytoskeleton has been shown to occur at sites of axonal damage and disconnection in numerous Immunohistochemical studies employing antibodies directed towards its specific proteolytic breakdown products (Buki et al., 1999; Saatman et al., 2003; Serbest et al., 2007). Another member of the cysteine protease family, the caspases, is also thought to be activated within damaged axons (Buki et al., 2000). Although caspases are principally mediators of apoptotic cell death, in severely injured axons they are thought to participate in the terminal degradation of the cytoskeleton leading to irreversible collapse of the subaxolemmal membrane skeleton, rather than causing direct apoptotic changes in the soma (Buki and Povlishock, 2006). This cytoskeletal breakdown disrupts axonal transport causing organelle and

vesicular accumulation with resultant axonal swelling and eventual detachment (Smith et al., 2003). Once detached from its distal, downstream segment, the axonal segment in continuity with its sustaining soma continues to swell with the persistent delivery of organelles via anterograde transport (Buki and Povlishock, 2006). This results in the formation of a retraction bulb, the classically described hallmark of axonal injury. In contrast the disconnected downstream axonal profiles undergo Wallerian degeneration over weeks to months post-injury, with this widespread deafferentiation of downstream targets thought to cause many of the functional deficits observed post-TBI (Povlishock, 2000).

As DAI cannot be detected using routine imaging studies, it can only be definitively diagnosed post-mortem, using immunohistochemical methods, with an antibody targeting APP most commonly used as it is known to be delivered by axonal transport (Blumbergs et al., 1995). Following axonal injury, the anterograde transport of APP is impeded, allowing it to accumulate to detectable levels. APP immunohistochemistry is thought to offer significant advantages over other methods because it can be seen within 2 hrs following injury and only stains injured axons, unlike a neurofilament stain which also stains normal axons (Abou-Hamden et al., 1997). However later research suggested that local cytoskeletal collapse associated with DAI may not always cause impaired transport with axonal swelling and bulb formation (Stone et al., 2001). It is proposed that with more severe forms of axonal injury, massive influxes of calcium may trigger the conversion of anterograde to retrograde transport thereby attenuating the development of axonal swelling (Buki and Povlishock, 2006; Marmarou et al., 2005). Thus a staining technique, like APP, which only detects impairment in anterograde transport, may underestimate the amount of axonal injury present, with suggestions that multiple markers may be necessary to assess the full extent of an injury.

1.2.2 Secondary Injury

Secondary injury is a gradual process that occurs over minutes to days as the result of cellular, neurochemical and metabolic alterations initiated by the primary insult (Hall et al., 2005). Injury factors that contribute to this phenomenon include metabolic changes, oedema formation, calcium influx, increased oxidative stress, excitotoxicity, inflammation and ultimately cell death via necrosis or apoptosis (Saatman et al., 1996). Eventually the insult leads to the activation of neuroprotective pathways that promote the reparative activity of the brain, although the mechanisms behind this are not yet fully understood.

Metabolic dysfunction

Cerebral metabolism (oxygen and glucose consumption) and cerebral energy state (tissue concentrations of phosphocreatine and ATP or lactate/pyruvate ratio) are reduced after TBI, with the degree dependent on the severity of the primary insult (Clark et al., 1997a; Glenn et al., 2003). This is caused by a number of factors including reductions in cerebral blood flow and mitochondrial dysfunction. Stretch induced mechanical injury alters mitochondrial membrane potential and decreases ATP levels in neurons, with this further exacerbated by intramitochondrial calcium overload which interferes with electron transport (Tavazzi et al., 2005; Verweij et al., 2000).

Ionic changes

Ionic homeostasis is also compromised following trauma with massive ion fluxes across the neuronal membrane causing an influx of calcium and sodium with a corresponding efflux of potassium into the extracellular space (Blumbergs, 1997). This has a number of deleterious effects including the widespread loss of membrane potential and rapid release of neurotransmitters, the formation of cytotoxic oedema and the activation of calcium dependent proteases which can cause extensive cellular damage (Maas et al., 2008). Trauma also disrupts magnesium levels, causing a decline in brain intracellular free magnesium, exacerbating a number of secondary injury processes such as energy depletion, cytotoxic oedema formation and excitotoxicity (van den Heuvel and Vink, 2004; Vink et al., 2003a).

Excitotoxicity

Following TBI under both experimental and clinical settings, levels of extracellular glutamate increase acutely (Bullock et al., 1998; Faden et al., 1989; Globus et al., 1995; Palmer et al., 1993). This is the result of its uncontrolled release due to the aforementioned loss of membrane potential (Vink and Van Den Heuvel, 2004), as well as a decrease in its reuptake caused by impaired glutamate transporter activity (Yi and Hazell, 2006) and a reduction in the numbers of astrocytic transporters (van Landeghem et al., 2006). These high levels of glutamate cause excessive activation of excitatory amino acid receptors leading to excitotoxicity, an important process in secondary damage and cell death following TBI (McIntosh, 1996). The NMDA receptor plays a particularly important role, as its overstimulation promotes substantial calcium influx. Calcium overload activates a number of

calcium-dependent enzymes including proteases, lipases, translocases and endonucleases which degrade cellular structures and eventually cause neuronal degeneration. Further damage can also be initiated through the generation of reactive oxygen species (ROS) via the activation of phospholipases and cyclooxygenases (Maas et al., 2008). High levels of calcium within mitochondria not only allow additional ROS production due to structural alterations of the inner mitochondrial membrane with disorganisation of the electron transport chain, but also decrease available ATP levels, exacerbating energy depletion following TBI (Kowaltowski et al., 1995).

Oxidative stress

TBI dramatically increases the production of ROS through a variety of mechanisms including excitotoxicity, the arachidonic acid cascade, increased leakage of superoxide from mitochondrial electron transport, auto-oxidation of catecholamines, activation of neutrophils and breakdown of haemoglobin (Awasthi et al., 1997; Lewen et al., 2000). Oxidative stress ensues when their production overwhelms the antioxidant mechanisms within the brain. ROS, which contain an unpaired electron in the outermost orbit, are highly reactive inducing tissue damage via peroxidation of cellular and vascular structures, protein oxidation, cleavage of DNA and inhibition of the mitochondrial electron transport chain (Lewen et al., 2000 387). Membrane lipids are particularly vulnerable, with lipid peroxidation altering the structure, fluidity and transport function of the membrane, ultimately causing membrane lysis (Werner and Engelhard, 2007). Furthermore, oxidative stress not only causes irreversible loss of mitochondrial functions such as mitochondrial respiration and oxidative phosphorylation, but may also modulate translocation of cytochrome c from the mitochondria into the cytosol, a key step in the initiation of apoptotic cell death (Mbye et al., 2008).

Inflammation

A robust inflammatory response is also invoked following TBI, involving the activation of glia and neurons as well as cerebral accumulation of monocytes and lymphocytes. This is signified by elevated levels of a number of inflammatory mediators such as IL-1β, IL-1α, IL-6 and TNFα within hours in the CSF and brain parenchyma after trauma in humans and rodents (Hutchinson et al., 2007; Morganti-Kossman et al., 1997; Semple et al., 2010a; Taupin et al., 1993; Zhu et al., 2004). IL-1 is thought to be a key inflammatory mediator as it provokes the release of other neurotoxic mediators

such as prostaglandins, ROS, COX-2 and cytotoxic proteases (Molina-Holgado et al., 2000; Rothwell, 2003). TNFα also plays a major role, promoting the release of proteolytic enzymes which are associated with breakdown of the BBB and subsequent oedema formation (Shohami et al., 1999). Furthermore it is able to induce intracellular signalling pathways that promote both necrotic and apoptotic cell death (Reid et al., 1989). Although inflammation may facilitate tissue damage early following injury, it is also thought to be involved in the later reparative response, with cytokines such as IL-1, IL-6 and TNF-α known to induce the release of the neurotrophic nerve growth factor (NGF) from astrocytes (Lenzlinger et al., 2001; Morganti-Kossmann et al., 2007).

In addition to the typical inflammatory response, neurogenic inflammation is thought to play a significant role in the secondary injury process. It is a neurally elicited response, mediated by the release of neuropeptides such as substance P (SP), with the typical features of an inflammatory response in vasodilation and increased microvascular permeability. Indeed experimental studies have shown that SP immunoreactivity within the brain is increased following TBI, with its release temporally correlated with breakdown of the BBB and subsequent vasogenic oedema formation (Vink et al., 2003b).

Oedema

There are primarily two forms of oedema initiated after TBI, vasogenic oedema and cytotoxic oedema (Marmarou, 2003; O'Connor et al., 2006). Whilst vasogenic oedema is associated with breakdown of the BBB and accumulation of water in the extracellular space as osmotic substances escape the vasculature, cytotoxic oedema involves flow of fluid from the extracellular to intracellular space due to the creation of an osmotic gradient. Vasogenic oedema develops early after diffuse TBI (O'Connor et al., 2006; Vink et al., 2003b), with this thought to be permissive for the later gradual development of cytotoxic oedema (Beaumont et al., 2000). The increase in volume associated with the development of vasogenic oedema, can cause raised intracranial pressure. This has many deleterious consequences including reductions in cerebral blood flow and perfusion pressure, which decrease tissue oxygenation and can also result in brain herniation, causing further cell death.

1.2.3 Cell Death Following TBI

After TBI, cell death involves a phenotypic spectrum ranging from programmed cell death (PCD) to unregulated cell death (necrosis); necrotic cell death predominates early, whilst the more delayed second peak of cell death is mainly due to PCD (Clark et al., 1997b; Portera-Cailliau et al., 1997; Rink et al., 1995). There are a number of recognised forms of programmed cell death including apoptosis, autophagy, paraptosis, calcium dependent death and oncosis (Bredesen, 2008; Stoica and Faden, 2010). These can be divided into caspase depedent cell death, in apoptosis, and caspase independent cell death (all other forms of PCD). The proportion of necrotic cell death and the role of different PCD pathways is dependent upon the extent of injury, brain region and other secondary factors. Indeed, a continuum between forms of PCD and necrosis exists, as the pathways that lead to each form of cell death are not mutually exclusive. For example, if a cell in which the apoptotic program has been initiated runs out of sufficient energy, the cell will eventually die via other mechanisms including necrosis or autophagy (Bredesen, 2008; Nicotera et al., 1999). Of the forms of PCD, apoptosis is the best characterised, with research ongoing into the contribution of other forms of PCD to neuronal degeneration following TBI.

Necrosis

Necrosis is a form of cell death that is uncontrolled and caused by supraphysiological conditions which disrupt cellular integrity by interfering with the permeability barrier function of the plasma membrane causing a loss of cellular homeostasis (Lenzlinger et al., 2001; Zong and Thompson, 2006). This loss of cellular integrity can be the result of a number of mechanisms including energy depletion, loss of structural integrity of the lipid bilayer, disruption to ion channel proteins and breakdown of the cytoskeleton. The characteristic features of necrosis are cell and organelle swelling, ATP depletion, increased plasma membrane permeability, release of macromolecules and the eventual stimulation of the inflammatory response (Sastry and Rao, 2000). Immediately following TBI cells predominantly die by necrosis because of mechanically induced membrane disruption and cell lysis related to osmolar shifts and intracellular swelling (Lenzlinger et al., 2001). In addition the massive calcium influxes caused by excitotoxicity can also lead to necrosis through the activation of a number of destructive calcium dependent proteases which degrade the cellular membrane and cytoskeleton (Kampfl et al., 1997; Rubin, 1998).

Apoptosis

In contrast apoptosis is a form of PCD which involves the activation of an intrinsic cellular suicide program when cells are no longer needed or become seriously damaged (Sastry and Rao, 2000). The endpoint of apoptosis is the systematic fragmentation of cellular DNA and collapse of nuclear structure followed by formation of membrane wrapped apoptotic bodies (Zhang et al., 2005). These are cleared by macrophages or microglia, without the induction of an inflammatory response. Although apoptosis is required in the developing nervous system to establish appropriate cell numbers (Pettmann and Henderson, 1998) inappropriate induction of apoptotic cell death contributes to the neuropathology associated with TBI (Yakovlev et al., 1997; Yang et al., 2002).

Apoptosis is primarily induced through the activation of a family of cell suicide cysteine-dependent aspartate-proteases referred to as caspases. This occurs via two major pathways, involving either activation of death receptors (e.g TNFR 1 or Fas) in response to ligand binding (death receptor pathway) or the release of cytochrome c from the mitochondria following the formation of a mitochondrial permeability transition pore (MPTP)(mitochondrial pathway) (Ashkenazi and Dixit, 1998; Hengartner and Bryant, 2000; Zhang et al., 2005). A MPTP is formed following a non-selective increase in the permeability of the mitochondrial inner membrane, which results in a loss of matrix components and swelling of the organelle with eventual outer membrane rupture (Sullivan et al., 2002). Both pathways converge to activate executioner caspases such as caspase-3, which execute cell death in a controlled manner by cleaving a number of substrates including structural proteins, nucleic acid associated proteins, regulatory proteins and apoptotic regulators (Raghupathi et al., 2000). In addition formation of the MPTP is also associated with caspase-independent cell death pathways, with release of other proteins such as apoptosis inducing factor (AIF) associated with chromatin condensation and large scale DNA fragmentation that cannot be prevented by a caspase inhibitor (Susin et al., 1999).

The induction of apoptosis is controlled by a number of regulatory proteins. This includes the Bcl family which regulates the permeability of the mitochondrial outer membrane and formation of the MPTP (Graham et al., 2000c). Pro-apoptotic members of this family such as bax, bad and bak translocate to the mitochondria in response to various cell death signals and facilitate the release of cytochrome c, whilst anti-apoptotic family members such as Bcl-2, Bcl-xl and bak are integral mitochondrial proteins that stabilise the mitochondria and prevent the efflux of cytochrome c

(Graham et al., 2000c). Other regulatory proteins include the IAPs (inhibitors of apoptosis) which are able to directly inhibit active caspases and also interfere with pro-caspase activation and p53 which promotes apoptosis through a number of mechanisms including an increase in transcription of bax (Raghupathi et al., 2000).

Cell death at later time-points following TBI (24-72 hrs) is thought to be primarily due to forms of PCD, primarily apoptosis, as a result of a number of secondary mechanisms of injury including disruption of axonal transport, oxidative stress, inflammation and excitotoxicity. Inflammation leads to an increase in the levels of TNFα (Taupin et al., 1993), with evidence that levels of its receptor, TNFR1 are also higher in neurons following trauma (Beer et al., 2000b). Another mediator of the extrinsic pathway, Fas is also upregulated within the injured cortex and remains elevated for up to 3 days (Beer et al., 2000a; Minambres et al., 2008; Qiu et al., 2002). The intrinsic pathway is also activated as mitochondria suffer extensive damage following TBI, with increased ROS production and excessive intracellular calcium major contributors to the opening of the MPTP with release of cytochrome c and AIF (Robertson, 2004). Indeed, cytochrome c has been shown to be released from mitochondria after a number of experimental models of trauma (Buki et al., 2000; Lewen et al., 2001; Sullivan et al., 2002), with one study also showing translocation of AIF to the nucleus with associated DNA fragmentation following a controlled cortical impact (CCI) injury (Zhang et al., 2002). Furthermore, other downstream events like caspase-3 activation have been well documented and correlated with the appearance of the morphological features of apoptosis such as DNA strand breaks and nuclear fragmentation (Cernak et al., 2002; Keane et al., 2001; Knoblach et al., 2002; Yakovlev et al., 1997).

This apoptotic cell death following TBI may be further facilitated by an imbalance between the pro- and anti-apoptotic members of the bcl-2 family. Levels of the pro-apoptotic bax have been found to be elevated for up to three days following experimental injury in rats, whilst the expression of Bcl-2 and bcl-xl is unchanged early after severe injury (Cernak et al., 2002; Raghupathi, 2004; Strauss et al., 2004; Yao et al., 2005), with a significant upregulation only occurring from day 3 in one study (Cernak et al., 2002). Interestingly human studies have suggested that higher Bcl-2 levels within the CSF or in debrided contusional tissue may correlate with improved outcome (Clark et al., 2000; Harter et al., 2001; Minambres et al., 2008). Indeed the absence of Bcl-2 expression within the peri-contusional zone has been associated with increased mortality (Beaumont et al., 2000) and poorer Glasgow Outcome Score (GOS) 18 months after TBI (Nathoo et al., 2004).

1.2.4 Endogenous Neuroprotective & Neurotrophic Pathways

As well as promotion of anti-apoptotic factors, there are a number of other neuroprotective and neurotrophic pathways that are activated following TBI which facilitate the brain's reparative response. This is thought to involve multiple pathways which alter cortical representation areas, modify synaptic activity and increase neurogenesis, synaptogenesis and neurite outgrowth (Keyvani and Schallert, 2002; Nudo et al., 2001). For example, synaptogenesis has been observed in the CA1 region of the hippocampus from day 10 following a moderate CCI injury and continued for at least 60 days. This was associated with a gradual recovery of cognitive performance in the Morris Water Maze, although the injured animals did not return to sham level (Scheff et al., 2005).

In addition to restoring synapse numbers, the adult brain retains a limited capacity for neurogenesis following TBI, with neural stem cells residing in the subgranular zone of the hippocampus and the subventricular zone capable of differentiating into neurons, oligodendrocytes or astrocytes (Gage et al., 1998; Garcia-Verdugo et al., 1998; McKay, 1997). Although most proliferating neural stem cells following trauma appear to differentiate into astrocytes post-injury (Chen et al., 2003), several studies have identified replicating cells in the dentate gyrus (Braun et al., 2002; Dash et al., 2001; Wang et al., 2011; Yu et al., 2008), subventricular zone (Chen et al., 2003) and neocortical zones (Braun et al., 2002) which stained for a variety of neuronal markers. However, research is ongoing into whether, following TBI, these neurons are capable of becoming functionally integrated and thus contribute to recovery. TBI has also been shown to increase dendritic arborisation and spine density in both the peri-injury and intact cortical areas, with all of the aforementioned processes potentially contributing to functional recovery after TBI (Keyvani and Schallert, 2002). However, it appears that with more severe injuries the body may be less able to initiate a reparative response. Indeed, Thompson *et al* showed that whilst a moderate CCI injury caused an increase in GAP-43, a protein associated with synaptic remodelling and neuronal sprouting, a more severe injury elicited no changes in the levels of this protein (Thompson et al., 2006).

Several factors are thought to mediate the repair response, with the neurotrophin family comprising NGF, BDNF (brain-derived neurotrophic factor), NT-3 (neurotrophin-3) and NT-4/5, amongst others, thought to be particularly important as they are involved in the development, maintenance and ultimate survival of neurons (Kalish and Phillips, 2010; Pardon, 2010). Studies have shown increased NGF in the injured cortex and hippocampus following experimental TBI (DeKosky et al., 2004; Goss et

al., 1998; Truettner et al., 1999) and in the cerebrospinal fluid (CSF) of brain-injured patients (Kossmann et al., 1997), with high levels of NGF in the CSF correlated with improved outcome in children (Chiaretti et al., 2008). BDNF has also been reported to increase after TBI in the hippocampus and cortical areas (Griesbach et al., 2002; Oyesiku et al., 1999). Furthermore NT-4/5 is transiently elevated in the injured rat cortex and hippocampus following a CCI injury, with NT-4/5 knockout mice exhibiting greater levels of neuronal death in the hippocampus than wild-type mice (Royo et al., 2006). It is thought that these neurotrophins may attenuate neuronal cell death induced by a variety of secondary injury factors, whilst also being involved in repair processes such as axonal regeneration and neuronal plasticity (reviewed in Conte et al., 2004).

Similarly to neurotrophins, it is hypothesised that APP may play a role in the repair response following injury, as it is acutely upregulated, with its metabolite sAPPα known to promote cell survival, neurogenesis, neurite outgrowth and synaptogenesis (Reinhard et al., 2005).

1.3 Amyloid precursor protein

APP is a ubiquitous transmembrane protein, which is found in all neurons and some glial cells in the central and peripheral nervous system, as well as being expressed in platelets, endothelial cells and fibroblasts (Kawarabayashi et al., 1991; Mattson, 1997). It serves a synaptic function and is located predominantly in neuronal cell bodies, concentrated at axosomatic and other synaptic sites (Beyreuther et al., 1993), with smaller quantities found in vesicular structures in axons and dendrites.

1.3.1 APP Isoforms

The APP gene is located on chromosome 21 and consists of 19 exons, of which exons 7 (encoding a Kunitz-type protease inhibitor (KPI) domain), 8 (encoding an OX-2 domain) and 15 can be alternatively spliced to produce the three major isoforms of APP, in APP695, APP751 and APP770. APP695 lacks the amino acid sequences coded by exon 7 and 8 and is the dominant isoform found in neurons (Sandbrink et al., 1996). Both APP751 and APP770 contain the KPI domain, whilst only APP770 has the OX-2 domain, with these isoforms predominating in glial and other non-neuronal cells (Garcia-Ladona et al., 1997; Sisodia et al., 1993).

1.3.2 Protein structure of APP

The APP protein consists of an ectodomain, a transmembrane (TM) region and an APP intracellular domain (AICD) (Mattson, 1997). The ectodomain can consist of up to 6 different domains, a growth factor like domain (D1), a copper binding region (D2), an acidic region (D3), the KPI (D4) and OX-2 (D5) domains depending on the isoform, and a carbohydrate domain (D6). This carbohydrate domain can be further divided into an E2 domain (D6a) and a juxtamembrane region (D6b) (Reinhard et al., 2005; Storey and Cappai, 1999; Wang and Ha, 2004). In addition the combination of the D1 and D2 domains is sometimes referred to as the E1 domain (Fig 1.1) (Soba et al., 2005). Apart from the CuBD, the ectodomain contains several other binding sites for zinc (Bush et al., 1993), heparin (Rossjohn et al., 1999; Wang and Ha, 2004) and collagen (Beher et al., 1996). Only the acidic domain and the juxtamembrane region do not participate in secondary structure formation, as they provide flexible linkers that connect the individual folding units, regulating their relative distance to each other and providing mobility in three dimensions (Reinhard et al., 2005).

Unlike the domains of the extracellular region, the AICD does not adopt a stable conformation in solution. This allows it to form `specific' interactions with different intracellular proteins, with its structure thought to vary depending on the binding partner (Reinhard et al., 2005). In particular, proteins containing a phosphotyrosine binding (PTB) domain such as those in the Fe65, JIP (c-Jun N-terminal kinase-interacting protein), Numb and X11/Mint families (reviewed in (De Strooper and Annaert, 2000; King and Scott Turner, 2004) are able to bind to a YENPTY motif (a.a residues 682-687) contained within this region. This binding may be influenced by phosphorylation of APP, with phosphorylation at the threonine residue by kinases such as CDK5 (cyclin-dependent kinase 5), JNK3 (c-Jun N-terminal kinase 3) and GSK-3β (glycogen synthase kinase-3β), known to be crucial for Fe65 binding, but to have little or no impact on the interaction with X11α (Ando et al., 2001).

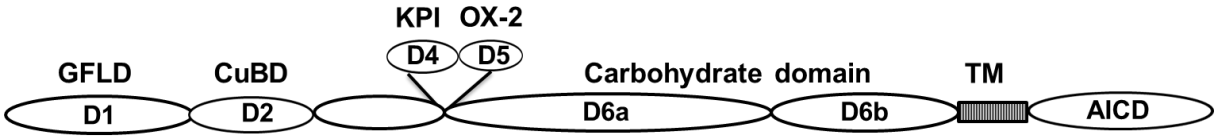

Fig 1.1: Representative image of APP, demonstrating the domains within the extracellular sequence.

1.3.3 Proteolytic Processing

Different segments of the APP protein can be released depending on its proteolytic processing. Following synthesis within the endoplasmic reticulum (ER), APP becomes O-glycosylated and tyrosyl sulphated while moving through the *trans*-Golgi network (Tomita et al., 1998). After delivery to the cell surface via this secretory pathway, APP can be re-internalised and transported to the endosomal/lysosomal system (Koo et al., 1996). APP only has a short half-life of 30-90 mins (Herreman et al., 2003), as once mature it can undergo proteolytic processing by proteases known as α-, β- and γ-secretases. The three proteases process APP in two mutually exclusive pathways, the non-amyloidogenic pathway and the amyloidogenic pathway (Fig 1.2). The former leads to the production of neuroprotective sAPPα (Mattson, 1997), whilst the latter results in the formation of amyloid-beta (Aβ), the main protein component of senile plaques in the cerebral cortex of patients afflicted with Alzheimer's disease (Selkoe, 2000). This is a progressive neurologic disorder, typically affecting the elderly, which is characterised clinically by loss of memory, cognitive impairment and

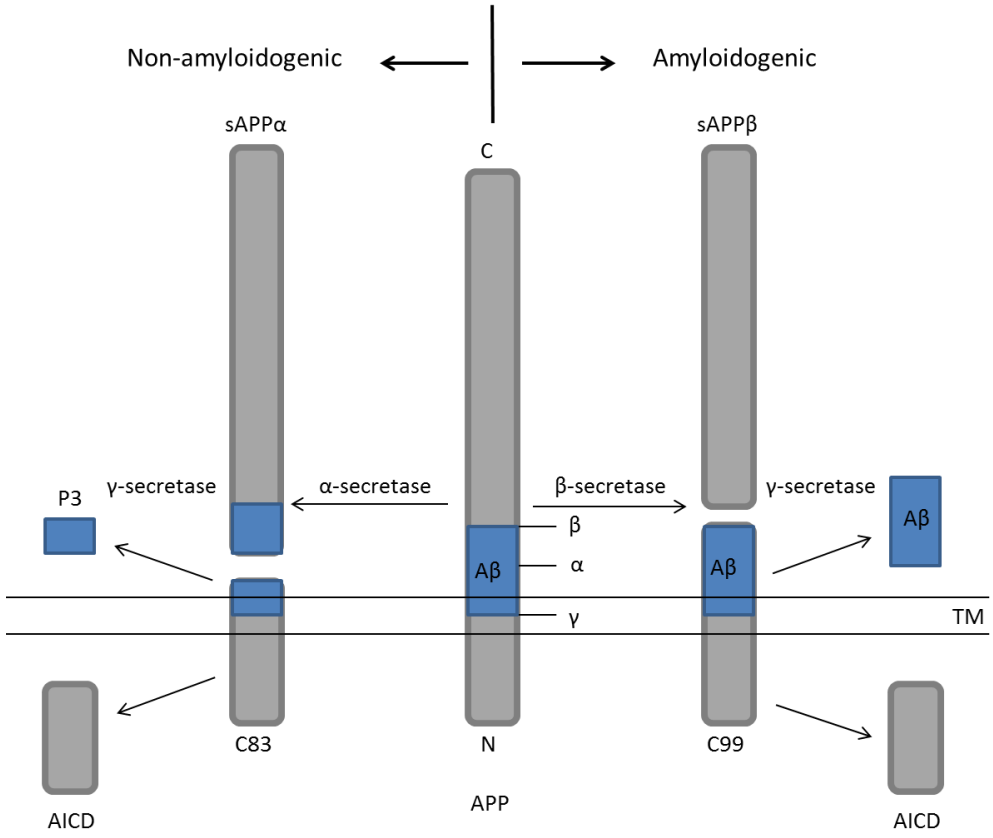

Fig 1.2: Representative image of the proteolytic processing of APP along the non-amyloidogenic and amyloidogenic pathways.

eventual dementia. Thus it is evident that processing of APP can produce either a beneficial or a detrimental product depending on the way in which it is post-translationally processed.

Non amyloidogenic processing

APP is principally cleaved by α-secretase, (Koo et al., 1996; Suh and Checler, 2002), with this mainly occurring within the secretory pathway in the *trans* Golgi network (De Strooper et al., 1993; Tomita et al., 1998) and at the cell surface (Haass et al., 1992; Ikezu et al., 1998), with α-secretase cleaving between the Lys16-Leu17 bond of APP, 12 amino acids on the extracellular side of the plasma membrane, within the Aβ sequence (Simons et al., 1996; Zhong et al., 1994). This produces a neuroprotective soluble protein, sAPPα, which is secreted from the cell, leaving behind a membrane bound 83 amino-acid C-terminal APP fragment (C83). C83 is then cleaved within the transmembrane helix by γ secretase, resulting in the formation of a 3kDA peptide called p3, as well as an AICD of 57-59 amino acids.

Specific membrane-bound disintegrin metalloproteinases (ADAMs) have been shown to be capable of cleaving APP at the α-cleavage site in several different cell systems, with ADAM-10 (Kojro et al., 2001; Lammich et al., 1999) and ADAM-17 (Buxbaum et al., 1998; Slack et al., 2001) the most likely candidates. These enzymes are synthesised in an inactive form and require activation through cleavage of their pro-domain, either by pro-hormone convertases (furin proteases) or by autocatalysis. Numerous cells including neurons and astrocytes possess a basal level of α-secretase activity (Allinson et al., 2003; Lammich et al., 1999), with its activity also upregulated by the activation of a number of intracellular pathways (Mills and Reiner, 1999). ADAM-10 is thought to be responsible for basal and regulated APP metabolism, whilst ADAM-17 activity appears to be restricted to regulated APP cleavage (Bandyopadhyay et al., 2006; Buxbaum et al., 1998).

Amyloidogenic processing

Alternatively, APP may be sequentially cleaved by β- and γ-secretases to generate the potentially neurotoxic compound, Aβ. Preferential cleavage by β–secretase occurs in the endosomal/lysosomal system and the ER (Kinoshita et al., 2002), with this initial cleavage generating a soluble protein sAPPβ, as well as a 99 amino acid C-terminal fragment (C99). The γ-secretase complex then processes C99 to form an AICD of 57 or 59 amino acids and Aβ, which varies in length depending on the γ-

cleavage site. Cleavage at Val40 produces Aβ (1-40) the most common Aβ species, whereas cleavage at Ala42 produces Aβ (1-42), a less abundant but more aggregating and hence more toxic species (Cappai and White, 1999). Proteolysis by γ-secretase also occurs at other positions including the ε-(Aβ 49) and δ -sites (Aβ 46), which are located downstream of the γ-site, proximal to the membrane-intracellular boundary (Ren et al., 2007; Zhao et al., 2005). It has been proposed that γ secretase may cut at the ε site first, with subsequent cuts at every helical turn of the substrate (every 3-4 residues), ultimately producing the 39-43 residue Aβ peptides that are secreted from the cell (Kakuda et al., 2006; Wolfe, 2007). Thus, the major product of ε-cleavage would be a shorter AICD (AICD 50), which currently appears to have similar attributes to the longer forms (AICD 57 and AICD 59) (Checler et al., 2007; Leissring et al., 2002).

The membrane –anchored aspartyl protease β-APP cleaving enzyme (BACE-1) has been identified as β-secretase (Bennett et al., 2000; Hussain et al., 1999; Vassar et al., 1999) and consists of a signal peptide, a pro-domain and a single trans-membrane domain. During maturation the pro-domain is removed and BACE-1 is then phosphorylated, N-glycosylated and palmitolyated, following a similar trafficking route to APP (Capell et al., 2000). Subcellular localisation of BACE-1 revealed that the protein exists primarily at two intracellular sites, the *trans*-Golgi network and the endosomal system (Capell et al., 2000; Haniu et al., 2000), although significant quantities of the glycoprotein are also present in the ER and on the cell surface (Capell et al., 2000; Huse et al., 2000). Neurons, but not astrocytes, are known as the major source of Aβ because astrocytes normally express low levels of BACE-1, although it can be upregulated following chronic stress (Hartlage-Rubsamen et al., 2003).

The γ-secretase complex is a membrane-embedded tetrametric complex with presenilin (PS) as the catalytic component (Haass, 2004). There are two isoforms, PS1 and PS2, which are similar in size and both found predominantly in the ER and Golgi membranes (Annaert and De Strooper, 1999; Kaether et al., 2002), although the proteins have also been detected to varying degrees in the endosomal system (Lah and Levey, 2000), the nucleus (Li et al., 1997), and the plasma membrane (Dewji and Singer, 1997; Nowotny et al., 2000). Apart from PS1 or PS2, which provide the active core, the γ-secretase complex includes other proteins in nicastrin, Aph 1 (anterior pharynx-defective phenotype) and Pen2 (presenilin enhancer) (Laudon et al., 2007; Suh and Checler, 2002). As this complex cannot efficiently cleave full length type I proteins, either α or β cleavage is required first to remove most of the ectodomain to enable intramembrane cleavage of the remaining stub (Selkoe and Wolfe, 2007).

Caspases

In addition to these two pathways, APP may also be a substrate of caspases, which predominantly cleave after aspartate at position 664 (APP695 numbering), liberating a 31 amino acid C-terminal peptide (C31) shown to have pro-apoptotic properties (Pellegrini et al., 1999). This pattern of cleavage has been show to occur both *in vitro* (Lu et al., 2003) and *in vivo* (Gervais et al., 1999), with the truncated APP molecule still able to be processed along the normal proteolytic pathways.

1.3.4 Functions of APP

APP is thought to play a fundamental role in cellular physiology as it is ubiquitously expressed during development and highly conserved across phyla. Indeed APP-/- mice show a range of deficits including reductions in body weight, grip strength, locomotor activity and brain weight, as well as age-related deficits in spatial learning. Furthermore, histological analysis of the brain also reveals areas of gliosis, decreased neocortical and hippocampal levels of synaptophysin and reduced dendritic lengths of hippocampal neurons with age (Dawson et al., 1999; Zheng et al., 1995). This supports a role for APP in a variety of cellular functions such as cellular adhesion, neurite outgrowth and synaptogenesis, although its physiological functions have yet to be fully elucidated. It is thought that more severe effects from knockout of APP may be prevented by compensation from the amyloid precursor-like proteins (APLP1 and APLP2), which share a close homology with APP. Indeed a combined APP and APLP2 knockout in mice is perinatally lethal, suggesting that APP and APLPs are together involved in normal metabolism (Heber et al., 2000; von Koch et al., 1997). Interestingly the deficits seen in APP-/- mice were rescued by a knock-in allele of sAPPα, indicating that the ectodomain of APP may be sufficient for the physiological function of APP in the adult brain (Ring et al., 2007). In fact, over-expression of other APP metabolites like Aβ and C31 can be neurotoxic, inducing apoptotic cell death and increasing susceptibility to other insults (Kim et al., 2004; Mattson, 1997). The following section will discuss research into the putative functions of APP, beneficial and detrimental, associated with the APP ectodomain, the intracellular domain and the Aβ peptide.

The APP ectodomain

Cell Adhesion

Intercellular adhesion may be promoted by homo-and hetero-dimerisation between the ectodomain of APP family members in adjacent cells, with such a mechanism analogous to that of known cell adhesion molecules such as cadherins and nectins (Wolfe and Guenette, 2007). A cell culture study found that the E1 domain (D1 & D2) was critical for this process, as APP constructs lacking this domain showed poor or no detectable interaction (Soba et al., 2005). Interestingly, in this study the D6 domain was not found to be important for this process, despite X-ray analysis earlier demonstrating that it can form anti-parallel dimers which could potentially function in trans-cellular adhesion (Wang and Ha, 2004). Instead, the E2 domain may be important in mediating the adhesive properties of sAPPα, as Sabo *et al* (2005) only studied the interactions of full length APP. Furthermore, both regions may participate in APP mediated cell-substratum adhesion as they interact with extracellular matrix (ECM) proteins and heparin sulphate proteoglycans (HSPGs) (Cappai and White, 1999), with this important for mediating the effects of APP on other processes such neurite outgrowth and synaptic plasticity.

Neurogenesis, neurite outgrowth and synaptogenesis

Indeed, a neurotrophic and synaptotrophic role for APP has been consistently documented, with a reduction in APP expression associated with impaired neurite outgrowth and synaptic activity *in vivo* (Allinquant et al., 1995; Herard et al., 2006; Perez et al., 1997). sAPPα appears to be particularly important, with its *in vitro* application causing neurite outgrowth in cultured fibroblasts (Bhasin et al., 1991; Saitoh et al., 1989), cortical hippocampal neuronal cells (Araki et al., 1991; Ohsawa et al., 1997; Qiu et al., 1995) and human neuroblastoma cell lines (Jin et al., 1994; Wang and Ha, 2004), whilst raising levels of sAPPα *in vivo* increases cortical synaptogenesis (Bell et al., 2006). Interestingly, sAPPα also acts synergistically with EGF (epidermal growth factor), as a growth factor for neuronal progenitor cells in the subventricular zone of adult mice (Caille et al., 2004). This suggests a role for sAPPα in adult neurogenesis, as these cells retain the capacity to produce new neurons throughout adulthood.

Memory and Cognition

The involvement of APP in synaptogenesis, cell adhesion and neurite extension may also assist in the structural changes at the synapse involved in long term memory consolidation. Indeed, APP-/- mice have age-related cognitive deficits including impairment in conditioned avoidance and Morris Water Maze tasks supporting a role for APP in processes underlying learning and memory (Dawson et al., 1999; Tremml et al., 1998; Tremml et al., 2002). This association was further illustrated by Huber *et al*, as exposure of animals to an enriched environment, which improves performance in cognitive tasks, is associated with a 4-fold increase in APP protein levels and an overall increase in the percentage of APP containing synapses in the hippocampus (Huber et al., 1997).

Several studies have highlighted the important role of sAPPα, with its *in vivo* administration increasing memory retention in the Morris Water Maze (Roch et al., 1994) and a variety of other tasks involving short and long term memory, with higher doses able to overcome the amnestic effects of scolopamine, an acetylcholine antagonist (Meziane et al., 1998). Indeed memory deficits with aging are associated with a reduction in the CSF levels of the APP metabolite, sAPPα in rats (Anderson et al., 1999). This is supported by an *in vitro* study which indicated that sAPPα administration can facilitate long-term potentiation (LTP), a key cellular correlate of learning and memory, in hippocampal cells. Indeed, APP-/- mice show a partial reduction in LTP that can be rescued by restoring sAPPα expression (Ring et al., 2007), whilst APP over-expression causes a notable, but not significant increase in LTP (Ma et al., 2007).

Neuroprotection

In addition, APP has been shown to have neuroprotective properties, with its overexpression in cultured neuroblastoma cells protecting against glutamate toxicity (Schubert and Behl, 1993). Its metabolite, sAPPα plays a central role in this process as its application to cultured neuronal cells increases their resistance to excitotoxic, metabolic and oxidative insults (Furukawa et al., 1996; Goodman and Mattson, 1994; Mattson et al., 1993). Similar results have been shown *in vivo,* with intracerebroventricular infusion of sAPPα able to decrease levels of neuronal death following TBI (Thornton et al., 2006) and transient global cerebral ischaemia (Smith-Swintosky et al., 1994). Furthermore transgenic mice with elevated levels of APP and overexpression of ADAM-10 to increase

sAPPα levels, show reduced seizure duration following kainate injections than ADAM-10 null mice, indicating a reduction in excitotoxicity (Clement et al., 2008).

Several mechanisms have been proposed whereby sAPPα may provide neuroprotection. It activates high conductance potassium channels, hyperpolarising the cell and suppressing calcium entry through voltage-dependent channels and NMDA receptors (Furukawa and Mattson, 1998; Furukawa et al., 1996; Mattson, 1999). As discussed earlier, excessive calcium influx seen with excitotoxicity activates a number of destructive enzymes which initiate cytoskeletal collapse, as well as causing opening of the mitochondrial permeability transition pore, thereby promoting necrotic and apoptotic cell death (Bramlett and Dietrich, 2004). Thus, any reduction in intracellular calcium concentration caused by sAPPα can reduce levels of cell death by maintaining mitochondrial integrity and reducing protease activity. Furthermore sAPPα may reduce levels of apoptosis through an upregulation in the expression of IGF-2 (insulin growth factor) (Stein et al., 2004) and activation of the phosphotidylinositol-3-kinase (PI_3K)-Akt kinase signalling pathway (Cheng et al., 2002). These lead to the phosphorylation and inactivation of the pro-apoptotic protein bad and an increase in the expression of anti-apoptotic members of the Bcl-2 family of proteins. Furthermore, sAPPα activates nuclear factor kappa B (NFκB) (Cheng et al., 2002), a transcription factor which promotes neuronal survival by repressing pro-apoptotic genes such as bax, whilst upregulating the expression of anti-apoptotic genes such as c-FLIP (caspase-8/FADD-like-IL-1b-converting enzyme inhibitory protein) and IAPs (Yang et al., 2007).

Despite the positive effects seen with exogenous application of sAPPα, studies on the physiological neuroprotective function of APP have been less consistent. Han *et al* showed that cultured cortical and hippocampal neurons from APP-/- mice were more susceptible to glutamate exposure, exhibiting less than 20% survival compared to 50% in wild-type neurons (Han et al., 2005). This deficit was primarily restored with the addition of sAPPα, further supporting the notion that APP chiefly exerts its neuroprotective actions through sAPPα. In contrast, other *in vitro* studies detected no difference in survival rates between APP null and wildtype cortical neurons exposed to oxidative stress (Harper et al., 1998; White et al., 1998) or excitotoxicity (White et al., 1998). It is unclear what caused the inconsistency between these studies, but it may be due to differences in the use of media, density of the cells or the concentration of toxins used. Furthermore, as these studies were conducted *in vitro*, it is uncertain how these findings may relate to the role of APP in response to insults *in vivo*, which will be discussed in Section 1.3.6.

Intracellular Domain

sAPPα is not the only APP metabolite thought to play a physiological role, with the AICD also believed to function in multiple signalling pathways ranging from calcium signalling (Leissring et al., 2002) and apoptosis (Kim et al., 2004; Kinoshita et al., 2002; Ozaki et al., 2006) to gene transcription regulation (Cao and Sudhof, 2001; Kinoshita et al., 2002; Pardossi-Piquard et al., 2005; von Rotz et al., 2004). Many of these processes seem to be mediated through interactions between the YENPTY motif and intracellular proteins. Particular interest has been generated by the discovery that a complex comprising the AICD, Fe65 and a histone acetyltransferase, Tip60, was able to cause transcriptional activation in a reporter gene system (Cao and Sudhof, 2001). However, this finding has been disputed, with evidence showing that Fe65 may regulate transcription independently of its interaction with APP (Yang et al., 2006), and that γ-secretase cleavage of APP, presumably necessary for the production of AICD, is not required for transcriptional activation (Hass and Yankner, 2005). Despite these conflicting results, a trans-activating role of the AICD/Fe65/Tip60 complex has been documented, particularly in overexpression systems (Slomnicki and Lesniak, 2008). Genes purported to be affected include APP itself, Tip60, neprilysin, KAI1, and others, including several potentially pro-apoptotic genes (Baek et al., 2002; Belyaev et al., 2010; Checler et al., 2007; Pardossi-Piquard et al., 2005; von Rotz et al., 2004).

Activation of neprilysin has drawn particular attention, as it suggests the presence of a negative feedback control on Aβ production. Generation of Aβ is coupled with the production of AICD, which may then induce expression of neprilysin, a neutral endopeptidase with Aβ degrading activity. However, this finding remains controversial, with other authors reporting difficulty in consistently reproducing this observation (Chen and Selkoe, 2007). Furthermore such feedback would be inefficient if AICD produced from both α and β secretase activity was involved in regulating neprilysin activity. To address this inconsistency it has recently been suggested that the β-secretase amyloidogenic pathway of APP metabolism primarily mediates AICD-dependent nuclear signalling (Hoey et al., 2009). Indeed Goodger *et al* demonstrated that by blocking endocytosis or inhibiting β-secretase, translocation of AICD to the nucleus was reduced, whilst inhibition of α-secretase had no effect (Goodger et al., 2009). It has been postulated that this is because α-secretase activity primarily occurs at the plasma membrane, with the cytosolic AICD formed then rapidly metabolised by insulin-degrading enzyme making it non-functional (Edbauer et al., 2002). In contrast the preferential cleavage by β-secretase that occurs within endosomes may circumvent this degradation and allow

the retrograde transport of AICD to the nucleus following formation of a protein complex with Fe65 (Belyaev et al., 2010). However, it should be noted that Sala Frigerio *et al* have disputed this claim finding that β-secretase cleavage was not required for the generation of AICD (Sala Frigerio et al., 2010), with research ongoing into this issue.

AICD has also been shown to regulate phosphoinositide mediated Ca^{2+} signalling, which involves the release of ER calcium stores. Cells lacking APP show deficits in calcium signalling that can be rescued by constructs containing the AICD region, but not by constructs lacking this domain (Leissring et al., 2002). This has been suggested to be one mechanism through which AICD may contribute to memory formation (Wolfe, 2007), as it has been suggested that AICD was the APP proteolytic product responsible for enhanced spatial memory in mice overproducing wild-type human APP (Ma et al., 2007).

Apart from these beneficial functions, over-expression of C31 and AICD (C50, C57 and C59) has also been shown to be neurotoxic and pro-apoptotic *in vitro* (Bertrand et al., 2001; Kim et al., 2004; Kim et al., 2003; Lu et al., 2000; Ohkawara et al., 2011). It is thought that one of the mechanisms behind the cytotoxicity of AICD and C31 may be due to their association with Fe65 and induction of pro-apoptotic genes, as mentioned previously. Indeed Kim *et al* showed that cells transfected with a mutated form of C31 or AICD (59) that lacked the YPENTY domain, essential for interaction with Fe65, had a significant reduction in apoptotic cell death, compared to those transfected with the full construct (Kim et al., 2003). To date two genes in p53 and GSK-3β have been identified as potential targets (Checler et al., 2007; Kim et al., 2003; Ozaki et al., 2006; Ryan and Pimplikar, 2005). Over-expression of AICD (C50 and C59) increases the transcription and activity of p53 (Checler et al., 2007), a tumour suppressor protein involved in the direct transcriptional activation of a series of pro-apoptotic effectors such as caspase-1 and bax. Furthermore both C31 and AICD (C57 and C59) can increase the mRNA and protein levels of GSK-3β, by forming a complex with Fe65 and the GSK-3β promoter, CP2/LSF/LBP1 (Kim et al., 2003; Ryan and Pimplikar, 2005). GSK-3β is a proline-directed serine/threonine kinase that phosphorylates cytosolic proteins, including tau, β-catenin and mitochondrial pryuvate dehydrogenase (Graef et al., 1999). Excessive phosphorylation of tau and β-catenin is thought to induce apoptosis through a variety of mechanisms including the disruption of cytoskeletal and axonal transport (Kim et al., 2003). However another study failed to replicate this finding, with no AICD-dependent activation of GSK3β in transgenic mice expressing AICD 50, 57 or 59 (Giliberto et al., 2010).

It is important to note that nearly all of the aforementioned studies on AICD involve overexpression systems. Thus given the relaxed conformation of AICD, it has been suggested that its exogenous overexpression might perturb many different protein-protein interactions in non-specific ways, making interpretation of these experiments difficult (Reinhard et al., 2005). It is evident that further investigation is necessary to determine if these findings reflect the *in vivo* role of the AICD.

Amyloid beta

A similar neurotoxic role is attributed to Aβ peptides, with the secreted peptides varying in size from 39 to 43 amino acids. Aβ exists as monomers, dimers and higher oligomers (Walsh et al., 2000), with further aggregation of oligomers, which is dependent on time and concentration, yielding protofibrils and then fully fledged insoluble fibrils. Whilst in its monomeric form, it has been suggested that Aβ has a physiological function in depressing synaptic activity, thus providing feedback to prevent synaptic activity from becoming excessive (Kamenetz et al., 2003). Indeed these Aβ monomers have been postulated to enhance survival of developing neurons under conditions of trophic deprivation and protect mature neurons against excitotoxic death (Giuffrida et al., 2009). However, levels of soluble Aβ (Lue et al., 1999; McLean et al., 1999; van Helmond et al., 2010a), oligomeric Aβ (Kuo et al., 1996; van Helmond et al., 2010b; Xia et al., 2009) and insoluble fibrillar Aβ (Svedberg et al., 2009; van Helmond et al., 2010a; Wang et al., 1999; Xia et al., 2009) are all increased in post-mortem brain tissue from patients with late onset AD compared to age matched controls. Neurons that degenerate in AD exhibit increased oxidative damage, impaired energy metabolism and perturbed calcium homeostasis, with the soluble oligomeric forms of Aβ in particular thought to be important instigators of these abnormalities (Dahlgren et al., 2002; Mattson, 2004; Shankar et al., 2009; Townsend et al., 2006). Indeed oligomeric forms of Aβ have been shown to cause neurite damage (Ivins et al., 1998; Pike et al., 1992), interfere with synaptic plasticity (Lambert et al., 1998; Walsh et al., 2002; Wang et al., 2002), increase susceptibility to other insults (Mattson et al., 1998) and ultimately cause neuronal death (Hartley et al., 1999; Lorenzo and Yankner, 1994; Pike et al., 1991; Simmons et al., 1994).

These toxic effects are thought to be the result of oxidative stress, increased intracellular calcium levels and an upregulation of pro-apoptotic proteins. Indeed, exposure of Aβ to neurons and synaptosomes *in vitro* leads to free radical production and oxidative stress (Mattson, 1999). The resultant oxidative modification and inhibition of membrane transporters, receptors, ion channels

and GRP-coupled transmembrane signalling proteins can cause loss of cell potential, accumulation of excitotoxic glutamate, decreased glucose availability and decreased intracellular communication with a resultant increase in cell death (Lauderback et al., 2001). Furthermore aggregation of Aβ at the cell membrane leads to membrane associated oxidative stress and lipid peroxidation of neuronal and glial membranes (Mattson, 2004). This disrupts membrane integrity, further disturbing ionic gradients and if severe enough leads to membrane lysis (Enriquez and Bullock, 2004).

The induction of oxidative stress also disrupts calcium regulation by impairing membrane calcium pumps and enhancing calcium influx through voltage dependent channels and ionotropic glutamate receptors (Mattson and Chan, 2003). Aβ may also promote calcium influx directly by forming calcium permissive channels in the cell membrane (Kawahara and Kuroda, 2000; Lin et al., 2001) or by activating cell surface receptors coupled to calcium influx (Le et al., 2001; Mattson and Chan, 2003). This increase in intracellular calcium can cause a decrease in ATP, disrupt the cellular membrane and increase the cellular response to glutamate, leading to irreversible cell injury and cell death (Suh and Checler, 2002). Raised intracellular calcium levels are also proposed to be one of the mechanisms behind Aβ-induced apoptosis through the induction of the mitochondrial permeability transition pore (Ferreiro et al., 2004; Mattson, 2004). *In vitro* experiments have demonstrated that exposure to Aβ induces an apoptotic cascade that involves the down-regulation of anti-apoptotic members of the Bcl-2 family (Forloni, 1996; Paradis et al., 1996; Tamagno et al., 2003), upregulation of pro-apoptotic proteins like Bax and p53 (Paradis et al., 1996; Yin et al., 2002), cytosolic release of cytochrome c (Canevari et al., 2004; Kim et al., 2002) and ultimately the activation of executioner caspases such as caspase-3 (Chan et al., 1999; Ferreiro et al., 2004; Xiao et al., 2002).

1.3.5 Factors which affect APP processing

Some proteins interact with APP to alter its trafficking or maturation in such a way that they alter the rate of its proteolytic processing to cause an increase or decrease in the levels of sAPPα and Aβ concurrently, with neither pathway favoured over the other. Conversely, a variety of other extracellular and intracellular signals modulate the processing of APP to promote either the non-amyloidogenic or amyloidogenic pathway. This has important implications due to the divergent functional roles of the metabolites of each pathway. Indeed, an imbalance between the production of Aβ and sAPPα is thought to underlie the pathogenesis of AD (Bandyopadhyay et al., 2007; Turner et al., 2003).

Positive and negative regulators of APP processing

A number of proteins that interact with the YENPTY motif of APP located within the intracellular domain, such as members of the Fe65 and X11 family, are known to affect its processing. X11α and X11β appear to prolong the half-life of APP, as when their levels are raised *in vitro*, cellular APP levels increase, whilst secretion of its catabolites, sAPPα and Aβ diminish. In contrast, several *in vitro* studies have indicated that overexpression of Fe65 stimulates the maturation of APP with a resultant increase in the secretion of Aβ and sAPPα (Guenette et al., 1999; Sabo et al., 1999; Tanahashi and Tabira, 2002). However, it has also been shown that elevated levels of Fe65 may stabilise immature APP, inhibiting its proteolytic breakdown (Ando et al., 2001). This latter study was supported *in vivo,* as levels of sAPPα and Aβ were reduced in transgenic APP mice when they were crossed with mice overexpressing human Fe65 (Santiard-Baron et al., 2005). It was hypothesised that the disparate effects of Fe65 in various cell types and in transgenics could be explained by different levels of a trimeric complex comprising APP, Fe65 and low-density lipoprotein receptor-related protein (LRP). Fe65 acts as a functional linker between the cytoplasmic domains of APP and LRP, and thus when a significant proportion of Fe65 is bound to LRP it may facilitate the proteolysis of APP, whereas unbound Fe65 may impair its breakdown (Pietrzik et al., 2004).

In addition, transport proteins such as SORLA and PAT1a (protein interacting with APP tail 1), can alter APP trafficking and thus its processing. The SORLA receptor shuttles proteins between the Golgi, plasma membrane and endosomes, determining the residence time of APP in the various intracellular compartments (Nielsen et al., 2007). It appears to promote the retention of APP in Golgi compartments (Andersen et al., 2006), which are less favourable for its processing, reducing the extent of its proteolytic breakdown into both amyloidogenic and non-amyloidogenic products. Indeed, it has been shown that increasing SORLA expression in cells reduces the conversion of APP to Aβ and sAPPα (Andersen et al., 2006), while low levels of the receptor activity accelerate generation of these processing products (Nielsen et al., 2007; Spoelgen et al., 2006). In contrast PAT1 is thought to increase transport of APP to the cell surface, thereby promoting its proteolytic processing, with knockdown of the gene in human neuroblastoma cells decreasing levels of sAPPα and Aβ (Kuan et al., 2006).

Promoters of the non amyloidogenic pathway

Activation of many cell surface receptors, such as muscarinic M_1 and M_3 (Buxbaum et al., 1992; Davis et al., 2010; Nitsch et al., 1992), metabotropic glutamate (Lee et al., 1995; Ulus and Wurtman, 1997), serotonin 5-HT_{2a} and 5-HT_{2c} (Nitsch et al., 1996), growth factor (Clarris et al., 1994; Ringheim et al., 1997), nicotinic (Kim et al., 1997; Nie et al., 2010), vasopressin (V1a) and bradykinin (B2) types (Nitsch et al., 1995) can enhance the production of sAPPα by activating pathways involving phospholipase C, phosphatdylinositol 3-kinase, protein kinase C (PKC), and the MAPKs (mitogen-activated protein kinases) (reviewed in Checler, 1995; Mills and Reiner, 1999). In particular PKC is thought to be the key mediator of the regulated secretion of sAPPα, as it represents the final common pathway of the majority of these factors (Mills and Reiner, 1999). Several *in vitro* studies have shown that direct activation of PKC by phorbol esters increases sAPPα secretion, whilst decreasing Aβ formation (Buxbaum et al., 1993; Caporaso et al., 1992; Gabuzda et al., 1993; Jacobsen et al., 1994). PKC belongs to a family of at least 12 isoenzymes of serine/threonine protein kinases which are central to many signal transduction pathways (Carey et al., 2005), with the α and ε isoforms thought to be important in mediating the effects on APP proteolysis (Racchi et al., 2003; Zhu et al., 2001).

Although this action of PKC has been extensively documented, the mechanism behind it remains unclear. It has been hypothesised that inhibition of endocytosis may increase sAPPα release by prolonging the interaction of APP with α-secretases on the cell surface (Mills et al., 1997), but it has been demonstrated that activation of PKC does not significantly alter APP internalisation (Carey et al., 2005). Instead, PKC activation increases the formation of APP-containing secretory vesicles from the *trans*-Golgi network suggesting that accelerated trafficking of APP to the cell surface might underlie the increase in sAPPα release induced by PKC.

In addition, other factors may promote non-amyloidogenic processing directly by increasing the transcription of α-secretases. Of note, *In vitro* studies indicate that the cytokines, IL-1α and IL-1β, raise levels of sAPPα through this mechanism. Application of IL-1α to astrocytoma cells upregulated ADAM-17 mRNA and protein levels with a corresponding increase in the production of sAPPα and decrease in the amounts of cell surface APP and extracellular Aβ (Bandyopadhyay et al., 2006). Similarly, administration of IL-1β led to a significant increase in levels of sAPPα in human neuroglioma cells (Ma et al., 2005) and mouse primary neurons (Tachida et al., 2008), with an associated 2-fold increase in the mature form of ADAM-17 and a reduction in levels of sAPPβ. These

findings correlate with the theory that the inflammatory response, while promoting damage early following TBI, may also facilitate the brain's reparative response through induction of neurotrophic factors such as sAPPα and NGF (Lenzlinger et al., 2001). Interestingly NGF itsself has been shown to increase the expression of ADAM-17, whilst decreasing levels of BACE-1, shifting the processing of APP towards the non-amyloidogenic pathway (Fragkouli et al., 2011).

Promoters of the amyloidogenic pathway

In contrast to these beneficial pathways, other factors are associated with increasing the levels of the potentially detrimental Aβ. Mutations of the APP gene around the secretase cleavage sites and also in the presenilins are associated with an increase in Aβ deposition and the development of early onset familial Alzheimer's disease in an autosomal dominant fashion (reviewed in (Tanzi and Bertram, 2005). Not only do these mutations increase Aβ generation, but the majority also increase the production of the more toxic Aβ42 species as opposed to Aβ40 by an unknown mechanism (Price et al., 1998; Scheuner et al., 1996). Another genetic risk factor for AD is the ε4 allele of apolipoprotein E. APOE plays a key role in lipoprotein metabolism and redistribution of lipoproteins and cholesterol by facilitating the cellular uptake of remnants of triglyceride rich chylomicrons and LDLs (Mahley, 1988). There are three different isoforms, ε2, ε3 and ε4, with the presence of an ε4 allele known to be a major susceptibility factor associated with approximately 40-50% of sporadic and familial AD compared with 30% of the normal population (Roses, 1996). In addition, Aβ deposition occurs more prominently following head injury in those who possess an APOE ε4 allele (Van Den Heuvel et al., 2007). It is unknown how APOE ε4 facilitates Aβ deposition, it does not appear to directly relate to changes in APP processing, but may instead be through a decrease in Aβ clearance (Hirsch-Reinshagen and Wellington, 2007).

In addition to these genetic causes, a number of factors associated with TBI have been shown to promote amyloidogenic processing of APP. The induction of apoptosis *in vitro* increases Aβ secretion at the expense of sAPPα production in cerebellar granule cells (Galli et al., 1998), human primary neurons (LeBlanc, 1995) and NT2 cells (Gervais et al., 1999). Caspase cleavage of APP appears to mediate this effect, with caspases,-3, -6 and -8 shown to process APP C-terminally during apoptosis with increased Aβ production as a result (Gervais et al., 1999; LeBlanc et al., 1999; Pellegrini et al., 1999). Indeed application of a caspase inhibitor was able to return Aβ levels to that seen in uninjured cells (Gervais et al., 1999). It has been suggested that during apoptosis the selective activation of

ERK1 causes an increase in the phosphorylation of the APP cytoplasmic tail at T668, thereby facilitating the internalisation of APP with sorting to early endocytic compartments where β-secretase processing preferentially occurs (Sodhi et al., 2008).

Cultured cells exposed to oxidants or the lipid peroxidation product 4-hydroxynonenal (HNE) also demonstrate an increase in the levels of intracellular and extracellular Aβ 1-40 and 1-42, with a resultant reduction in sAPPα production (Kao et al., 2004; Tamagno et al., 2005; Tamagno et al., 2003; Tong et al., 2005). This appears to be independent of the ability of oxidative stress to induce apoptosis, as similar results were obtained using levels of HNE that preserved neuronal viability (Paola et al., 2000). Indeed, oxidative stress is associated with an increase in the expression and activity of BACE 1 (Quiroz-Baez et al., 2009; Tamagno et al., 2005), an increase in the transcription of the components of the γ-secretase complex, PS1 and PEN 2 (Quiroz-Baez et al., 2009; Tamagno et al., 2008), as well as a decrease in the levels of the α-secretases, ADAM-10 and -17 (Quiroz-Baez et al., 2009).

Exposure of cortical neurons to a sublethal concentration (7.5um) of NMDA also increased the production and secretion of Aβ, with a corresponding decrease in the levels of sAPPα (Lesne et al., 2005). This shift towards amyloidogenic processing of APP was accompanied by an increase in the mRNA levels of APP770 and APP751, whilst levels of the normally predominant APP695 transcripts declined. As antibodies to the KPI domain were found to reverse the amyloidogenic effect of NMDA exposure, it was hypothesised that the KPI domain may interact with ADAM-17, inhibiting its activity, In contrast to this study, Hoey *et al* reported that calcium influx through NMDA receptors increased non-amyloidogenic processing of APP in primary cortical neurons, with a 2 to 2.5 fold increase in α-secretase generated C83 levels, with an accompanying decrease in Aβ40 production (Hoey et al., 2009). It is evident that further investigation is needed to determine the effect of activation of NMDA receptors on APP processing.

As apoptotic cell death, excitotoxicity and oxidative stress contribute to the secondary injury process following TBI, they may explain why BACE-1 protein levels were found to be transiently increased from 24-72 hrs, with an accompanying increase in activity at 48 hrs, following a CCI injury in rats (Blasko et al., 2004). As it has not been assessed whether there is a similar increase in α-secretase activity, it is unclear how this would affect the balance between the production of sAPPα and Aβ following injury, with the role of APP following TBI yet to be determined.

1.3.6 APP and TBI

APP protein levels are increased within neuronal cell bodies and reactive astrocytes following experimental TBI in the rat (Bramlett et al., 1997; Pierce et al., 1996), sheep (Van den Heuvel et al., 1999) and pig (Chen et al., 2004), with similar findings in humans (Gentleman et al., 1993a). This is correlated with an increase in APP mRNA levels suggesting that this is due to an increase in production of APP rather than its accumulation due to disruption of normal axoplasmic flow (Van den Heuvel et al., 1999). It is hypothesised that this is a normal acute phase response to neuronal stress (Gentleman et al., 1993a), as APP mRNA expression is regulated by many genes and proteins that are acutely increased following TBI including heat shock proteins and immediate early genes such as *c-fos* and *c-jun* (Dewji and Do, 1996). Indeed, a similar upregulation of APP is seen in cells exposed to a variety of other stressors such as ischaemia (Nihashi et al., 2001; Popa-Wagner et al., 1998), and excitotoxicity (Gordon-Krajcer and Gajkowska, 2001), but the functional significance of this nerve injury response remains poorly understood.

It has been proposed that this upregulation of APP following TBI in rats was associated with increased hippocampal cell death (Murakami et al., 1998). This was attributed to an increase in the production of the Aβ, which may have been facilitated by the aforementioned transient elevation in BACE-1 levels and activity. Indeed, co-accumulation of Aβ with APP in swollen axons and neuronal cell bodies has been observed within days in a pig model of diffuse traumatic injury (Smith et al., 1999). Damaged axons are thought to provide a key source of Aβ following TBI (Uryu et al., 2004), as impaired axonal transport allows long term pathological co-localisation of BACE-1 and PS1 with APP within injured axons (Kamal et al., 2001; Uryu et al., 2007), assisting in a shift towards amyloidogenic processing. Therefore Aβ could play a role in delayed post-injury mechanisms associated with TBI, by promoting secondary injury factors such as membrane disruption, loss of calcium homeostasis and activation of apoptotic pathways (Stone et al., 2002). Furthermore, other APP fragments such as AICD and C31 could enhance apoptotic cell death (Kim et al., 2003; Lu et al., 2000). Indeed it has been hypothesised that following TBI caspase-3 activation may initiate a vicious cycle, as it increases the production of Aβ, AICD and C31 (Gervais et al., 1999), which can in turn promote apoptotic cell death with further caspase activation (Abrahamson et al., 2006). This correlates with a study which demonstrated that APP accumulation and increased Aβ production occur in parallel with caspase-3 activation after a diffuse injury in rats (Stone et al., 2002). In addition, treatment with caspase inhibitors prevented the increase in Aβ following TBI in mice with the human Aβ coding sequence

knocked in (Abrahamson et al., 2006). This was associated with a reduction in cell death, but this evidently cannot be completely attributed to changes in the levels of Aβ. Indeed, a direct link between increased APP levels and increased Aβ deposition and toxicity in TBI has never demonstrated (Iwata, 2003).

It is also thought that the increase in Aβ following TBI increases the risk for the later development of AD (Fleminger et al., 2003; Mortimer et al., 1991; Salib and Hillier, 1997), especially in susceptible individuals with the APOE ε4 allele (Guo et al., 2000; Mayeux et al., 1995). However, this supposition has not been conclusively proven, with studies producing contradictory results. Epidemiologically whilst reports have suggested there is a positive association between TBI and AD (Guo et al., 2000; Rasmusson et al., 1995; Salib and Hillier, 1997), other studies have found that TBI may not be a risk factor for the later development of AD (Fratiglioni et al., 1993; Launer et al., 1999). Similarly while some histopathological studies of individuals who died after suffering a single severe TBI demonstrate widespread Aβ deposition irrespective of age (Gentleman et al., 1997; Ikonomovic et al., 2004; Roberts et al., 1991), others have concluded that Aβ deposition in victims below the age of 60 is a rare occurrence (Adle-Biassette et al., 1996; Braak and Braak, 1997). Furthermore, Chen *et al* found that Aβ plaques present after TBI decrease over time, with this attributed to an increase in the levels of the Aβ degrading enzyme, neprilysin (Chen et al., 2009). This correlates with experimental studies employing transgenic mice with mutations which enable the development of AD-like pathology, which have not found that TBI accelerates Aβ deposition (Murai et al., 1998; Nakagawa et al., 2000; Smith et al., 1998), unless a repetitive model of injury was used (Uryu et al., 2002). It is thought that repeated blows to the head may facilitate Aβ deposition due to an increase in the levels of oxidative stress, with a similar situation seen in boxers who are known to be predisposed to a form of dementia associated with diffuse Aβ plaque deposition (Clinton et al., 1991).

Alternatively, it is thought that the upregulation of APP following TBI may represent a protective cellular response, as the APP metabolite, sAPPα, can attenuate neuronal cell death induced by excitotoxicity, ischaemia and oxidative stress, which are all important components of the pathophysiology of TBI. Furthermore it may promote repair processes such as axonal regeneration and neuronal plasticity, which are critical for recovery after TBI, through its previously discussed effects on neurite outgrowth, synaptogenesis and neurogenesis. Although not studied as extensively as Aβ production, one study showed that following head injury in humans levels of sAPPα within the CSF rise by 2033% from day 1 to day 11 post injury, when measurements ceased (Olsson et al., 2004).

Interestingly, knockout of the APP orthologue, APPL, in *Drosophilia* led to an increase in mortality compared to wild-type files at 1 and 2 weeks following brain trauma induced by a needle injury (Leyssen et al., 2005). The increased survival in wild-type flies was attributed to the effects of APPL on axonal outgrowth and arborisation, which was hypothesised to be essential to compensate for the neuronal death associated with the injury. In order to determine whether APP may play a similar role in humans following TBI, these results need to be replicated in higher order animals using a more consistent form of injury.

1.3.7 Therapeutic Potential of APP

Although it is yet to be demonstrated whether the endogenous upregulation of APP following TBI is neuroprotective, exogenous intracerebroventricular administration of sAPPα has been shown to reduce apoptotic cell death and axonal injury after a diffuse injury in rats, with a resultant improvement in motor outcome (Thornton et al., 2006). The neuroprotective properties of sAPPα are supported by another study which showed that treatment with the PKC activator bryostatin, which promotes non-amyloidogenic processing of APP, was found to improve cognitive outcome by preserving synaptic structure post-injury following mild TBI in mice (Zohar et al., 2010)

Currently there are no accepted pharmacologic interventions available for the treatment of TBI, with phase II/III clinical neuroprotection trials, involving compounds such as NMDA antagonists, free radical scavengers and calcium channel blockers, failing to show any consistent improvement in outcome for TBI patients (Faden and Stoica, 2007). It is thought that compounds that show promise in experimental work may fail to translate to humans because they only modulate a single proposed injury factor such as excitotoxicity or oxidative stress (Tolias and Bullock, 2004; Vink and Van Den Heuvel, 2004). A more effective therapeutic strategy may be to target several injury factors given the complexity and heterogeneity of clinical TBI. This suggests that designing a drug based on sAPPα may be a viable option for TBI treatment, as it reduces neuronal death induced by a number of secondary factors and also enhances the reparative response within the brain. In order for this to eventuate the neuroprotective active site within sAPPα has to be determined, with several likely sites identified from previous research.

For example the pentapeptide motif `RERMS' (a.a residues 328-332) contained within the D6a domain, has been shown to promote survival of cultured rat cortical cells (Ohsawa et al., 1997; Yamamoto et al., 1994). It also has neurotrophic properties, with infusion of a 17 mer peptide

containing the sequence enhancing synaptic density in the frontoparietal cortex of rats, with an associated increase in memory retention, as demonstrated by performance in the Morris Water Maze (Roch et al., 1994). Furthermore, neurite extension was promoted following transfection of B103 cells with APP plasmid constructs containing the RERMS sequence, with the surrounding amino acid found to contribute to its biological activity as constructs containing RERMS alone had less effect than longer sequences (Jin et al., 1994).

Conversely, Ohsawa *et al* found that an extended version of the N-terminal domain (D1-D3) promoted neurite outgrowth in cultured rat neurons, whilst a 17 amino acid sequence containing RERMS did not (Ohsawa et al., 1997). It is unclear what caused the contradictory results, but it may relate to the differences in cell lines used. However, other studies have also suggested that the D1 domain has neurotrophic properties. This was attributed to a disulphide bridge within the growth factor like domain which stabilises a β-hairpin loop (Small et al., 1994), as similar structures have been identified in other known growth factors (Chirgadze et al., 1998; Kadomatsu and Muramatsu, 2004). It is evident that further studies are needed to determine the functional properties of the various regions of sAPPα and whether their administration may be beneficial following TBI.

1.4 Experimental TBI models

In order to investigate the mechanisms behind brain injury and possible treatment options, appropriate experimental models are required. Animal models are designed to produce the functional and pathological changes resulting from head injury in a closely monitored setting in sufficient numbers to enable statistical interpretation (Povlishock et al., 1994). Experimental models need to be able to produce damage as part of a continuum, increasing in severity as the mechanical forces applied are increased (Graham et al., 2000a; Laurer and McIntosh, 1999).

Rodents and mice have become the most commonly used animals for neurotrauma research. The advantages of using rodents include extensive normative data, relatively small size and modest cost, which allow a large number of structural and functional studies not possible in higher order animals due to technical and functional limitations. Indeed, rodents are often used as an initial step in testing the efficacy of a particular drug treatment. In contrast mice are generally employed as they can be genetically modified, with the specific neurologic, histopathologic and behavioural sequelae of TBI in the absence or overexpression of certain gene products providing valuable insight into the secondary

injury process following injury (Fujimoto et al., 2004). However there are disadvantages to using these animals as they can differ to humans in their systemic, physiological and behavioural responses to TBI. For example, the lissencephalic nature of the cortex in rodents and mice does not allow complete modelling of the changes that occur in the gyri and sulci of traumatically injured patients (Povlishock et al., 1994). To compensate for the disadvantages within an individual model, a number of different models have been developed to reproduce specific aspects of injury in human TBI including focal and/or diffuse damage (Finnie and Blumbergs, 2002). The most extensively used models include fluid percussion injury (FP), controlled cortical impact (CCI), and the impact-acceleration (closed skull-weight drop) model.

1.4.1 Fluid Percussion Injury

FP involves the injection of an extradural fluid pulse through a central, lateral or parasagittal skull craniotomy onto the dura thus causing transient deformation of the brain (Cernak, 2005). The model predominantly causes a focal injury, although limited DAI has also been observed within the subcortical white matter, thalamus and brain stem (Graham et al., 2000b; Iwamoto et al., 1997). It is commonly used for the study of TBI pathology, physiology and pharmacology in a number of animal species including rodents and mice, with both central and lateral versions of the FP injury, at moderate severity, causing transient hypertension, elevated intracranial pressure, alteration in cerebral blood flow, increased permeability of the blood-brain barrier, altered ionic homeostasis and neuronal cell death (Graham et al., 2000b; McIntosh et al., 1987; McIntosh and Raghupathi, 1995; McIntosh et al., 1989; Raghupathi et al., 1995; Schmidt and Grady, 1993). Furthermore cognitive impairment is seen following FP injury, with deficits noted on the Morris Water Maze up to to 30 days post-injury (Baranova et al., 2006). In addition motor deficits in rodents have been reported on a variety of tasks including the beam balance and beam walk test (Dixon et al., 1987; Lyeth et al., 1990) and the rotarod (Hamm et al., 1994). The response to injury is graded with post-injury haemorrage, BBB disruption and neurological outcome correlated with severity of injury (McIntosh et al., 1987).

1.4.2 Controlled Cortical Impact Injury

The CCI injury is the most commonly used model to produce a non-penetrating focal injury, characterised by the presence of a contusion with intraparenchymal petechial haemorrhages,

extensive tissue loss and cell death. The model was first characterised in the ferret (Lighthall, 1988), before being adapted for use in the rat (Dixon et al., 1991), mouse (Smith et al., 1995) and pig (Manley et al., 2006). In the original model a midline location was used (Lighthall, 1988), but like fluid percussion, a lateral location is now preferred (Dixon et al., 1991), allowing the area of damage to be concentrated in one hemisphere. Indeed, this injury model causes significant cell loss within the cortex, hippocampus, dentate gyrus and thalamus of the damaged hemisphere, with smaller degrees of contralateral damage observed with higher degrees of injury (Goodman and Mattson, 1994). Although it is thought of as a predominantly focal model, studies over the last 5 years have demonstrated extensive axonal degeneration following CCI involving ipsilateral cortex, including the frontal, somatosensory, parietal and occipital cortices, the hippocampus, dorsalteral thalamus, parts of the caudate nucleus, hypothalamus and the optic tectum. As well, areas of the contralateral cortex and hippocampus are affected to a lesser extent, due to anterograde degeneration of fibres arising from the ipsilateral cortical and hippocampal neurons which project via the corpus callosum or hippocampal commisure (Hall et al., 2008). Apart from axonal injury and cell death, the CCI model is also associated with significant oedema formation, with increases in brain water content seen as early as 2 hrs post-injury and peaking at 24 hrs (Baskaya et al., 1997). This oedema formation as well as the intraparenchymal haemorrhage causes a rise in ICP and reduction in cerebral perfusion pressure (Cherian et al., 2000). Motor and cognitive deficits have been detected using a variety of different tasks including the rotarod (Brody et al., 2007; Lindner et al., 1998; Shear et al., 2004), grid walk (Onyszchuk et al., 2007), Morris Water Maze (Saatman et al., 2006; Smith et al., 1995; Yu et al., 2009) and Barnes Maze (Fox et al., 1998), with these deficits still present a year after the injury (Scheff et al., 1997; Shear et al., 2004).

1.4.3 Impact-acceleration injury model

Unlike the predominantly focal models of injury described above, the impact-acceleration model of TBI, developed by Marmarou and colleagues, aimed to reproduce the DAI often associated with severe clinical TBI (Marmarou et al., 1994). The trauma device consists of a brass weight which falls freely by gravity from a designated height through a Plexiglas tube onto a stainless steel disc that is rigidly fixed to the animal's skull to prevent skull fracture (Marmarou et al., 1994). This model has also been adapted so that a similar injury can be invoked using a hydraulic-driven piston impactor to contact the steel disc, rather than a free falling weight (Cernak et al., 2004). In both situations the animal is placed on a foam platform or gel filled base in order to decelerate the head after impact,

mimicking the acceleration-deceleration injuries observed in humans. This results in graded widespread injury of neurons and microvasculature as well as axonal damage, and is thus suitable for studying the neuronal, axonal and vascular changes associated with diffuse brain injury (Cernak, 2005). Indeed this model is associated with widespread DAI, particularly in the corpus callosum, internal capsule, optic tracts, cerebral and cerebellar peduncles and the long tracts of the brainstem (Foda and Marmarou, 1994). In addition it induces motor and cognitive deficits (O'Connor et al., 2007; Thornton et al., 2006; Vink et al., 2003a), which increase with injury severity (Marmarou et al., 2009), similar to those observed after FP or CCI. It is the most commonly used model for the production of diffuse injury in rats.

1.5 Conclusion and Aims

Following TBI, cell death is ongoing due to the initiation of a number of secondary injury factors as a result of cellular, neurochemical and metabolic changes caused by the primary insult. In response the body upregulates a number of neuroprotective and neurotrophic pathways to limit the amount of damage occurring, whilst also instigating a reparative response. It is thought that APP may play a crucial role in this process, as it is acutely upregulated following TBI, with its metabolite sAPPα shown to be protective against a number of insults both *in vitro* and *in vivo*. Furthermore, if the neuroprotective region within the APP molecule can be determined, it could be possible to develop a drug based on this to improve outcome following TBI. As such the broad aims of this thesis are:

1. To determine the active region of the sAPPα by assessing the benefit of different regions within sAPPα, including the D1, D2 and D6a domains, on improving outcome following their admistration post-TBI.
2. That assess the effects of knockout of the APP on functional deficits and extent of neuronal injury following TBI in mice.

Chapter 2: Materials and Methods

2.1 Ethics

Experimental protocols were approved by the ethics committees of the Institute of Medical and Veterinary Science and the University of Adelaide in accordance to guidelines established for the use of rats and mice in experimental research as outlined by the Australian National Health and Medical Research Council.

2.2 Animals

Male Sprague Dawley rats weighing between 390-460gm were used for the experiments outlined in Chapter 3. They were obtained at least a week prior to experiments and housed at a minimum of two to a cage. For the experiments outlined in Chapters 4-7, male C57BL6j x 129sv mice were used, with the generation of APP-/- mice explained in detail elsewhere (Zheng, 1995). Animals were bred within the animal facility of the Institute of Medical and Veterinary Science and were at least 8 weeks of age before inclusion within experiments. All animals were subject to a 12 hour light-dark cycle and fed and watered *ad libitum*. Animal numbers used in each experiment are detailed in the relevant chapters.

2.3 Experimental Procedures

2.3.1 Anaesthesia

Isoflurane

For induction of anaesthesia animals were placed in a transparent plastic induction chamber with isoflurane (Independent Veterinary Supplies) delivered at 3% in 1.5L/min O_2 for rats and at 2% in 800ml/min O_2 for mice. Maintenance was achieved via a nose cone covering the nose and mouth with 1.5% isoflurane at 1.5L/min O_2 for rats and 1% at 800ml/min O_2 for mice.

Avertin

Avertin was made by dissolving 1.25g of 2.2.2-Tribomethanol (Sigma T48402) in 2.5ml 2-methyl-2-butanol (Sigma 240486) and then diluting this solution with 100ml of dH_20. Avertin was used instead

of isoflurane to induce anaesthesia for the experiments utilising the CCI model of injury, as the necessity of a nose cone was found to be impractical whilst the mice were within the stereotaxic frame. Mice were given an intraperitoneal (IP) injection of 0.4-0.7mL with a 25G needle, with the dose titrated until the pedal foot and blink reflexes were absent.

Pentobarbital

Pentobarbital (300mg/ml; Rhone Merieux) was obtained from Independent Veterinary Supplies and stored at room temperature. Animals requiring perfuse fixation were administered 0.2-0.5 ml for rats and 0.5-1ml ml for mice of pentobarbital IP via a 25 gauge needle with dose titration until all responses to pain were abolished.

2.3.2 Rat Impact-Acceleration Model of Traumatic Brain Injury

Animals were injured using the impact-acceleration model of diffuse TBI as described previously (Fig 2.1) (Marmarou et al., 1994). Briefly, animals were anaesthetized with isoflurane as described and the skull exposed by a midline incision so that a stainless steel disc (10mm in diameter and 3mm thick) could be fixed rigidly with polyacrylamide adhesive to the animal's skull centrally between lambda and bregma. The rats were subsequently placed on a 12cm foam bed, held securely with masking tape and subjected to brain injury by dropping a 450g brass weight a distance of 2m onto the stainless steel disc. Care was taken to remove the animals before a rebound injury could occur. Animals typically suffered a period of apnea following the injury and were resuscitated manually until they were able to maintain their blood oxygenation at greater than 80%, as monitored using a pulse oximeter (Harvard Apparatus). This injury led to a mortality rate of 15.5%, with rats typically dying in the hour following injury due to the

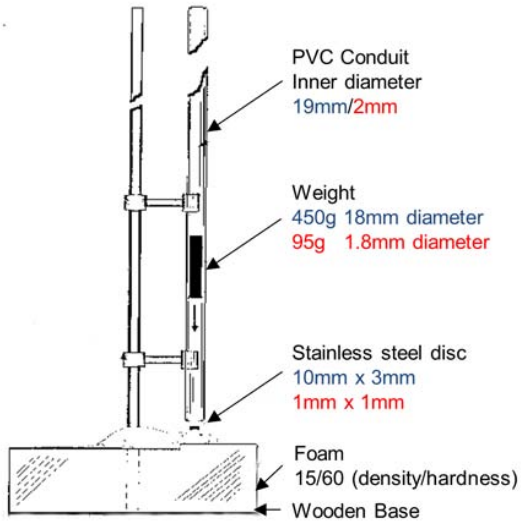

Fig 2.1: Injury apparatus used for induction of the impact acceleration model in rats and mice, demonstrating how the weight is positioned over the stainless steel disc helmet. Specifications for the rat model are seen in blue, for mice in red.

presence of large subarachnoid bleeds. Previous studies have shown that this level of injury results in moderate to severe functional deficits (Heath and Vink, 1999). Sham operated animals were surgically prepared but were not injured.

2.3.2 Mouse Impact-Acceleration Model of Traumatic Brain Injury

The impact-acceleration model of injury used above was modified for use in mice, as detailed in Fig 2.1, in order to produce a mild diffuse axonal injury. Under isoflurane anaesthesia a midline incision was made to allow fixation of a stainless steel disc (1mm in diameter and 1mm thick) centrally between the lambda and bregma using a polyacrylamide adhesive. Mice were then placed on a 10cm foam bed (15/60 density/hardness) and secured with a velcro strap before being subjected to a brain injury by dropping a 95g steel weight (1.8mm in diameter) along a PVC tube onto the steel helmet from either 1.2m for APP-/- mice or 1.3m for APP+/+ mice, with no mortalities recorded with these parameters. The differences in impact height were to compensate for the slightly smaller brain size reported in APP-/- mice (Ring et al., 2007), with this outlined in detail in Section 4.2.2. Preliminary studies identified that 1.3m was the ideal height from which to injure the APP+/+ mice, as release from greater than 1.4m led to a substantial increase in mortality (3/5) due to the presence of extensive subarachnoid bleeding. Furthermore in 1 of the 2 survivors a substantial bleed was noted within the cerebellum which was associated with balance deficits. At lower heights minimal injury was noted in APP+/+ mice, however at 1.3m axonal injury was evident within the corpus callosum and brain stem as would be expected in a mild diffuse injury (Fig 2.2).

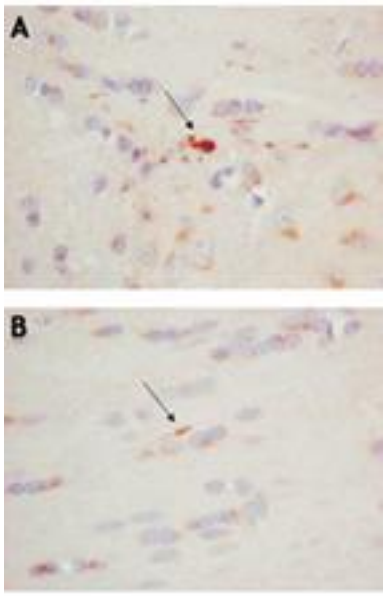

Fig 2.2: Evidence of axonal injury, with both retraction bulbs (A) and APP immunopositive lengths (B) evident at 3 days following injury induced by releasing a 95g weight from 1.3m.

2.3.3 Mouse Controlled Cortical Impact Model of Traumatic Brain Injury

In order to induce a focal injury the CCI model of TBI was used which involves the placement of an impactor tip against the intact dura, with the consequent impact causing the formation of a focal

cortical contusion (Dixon et al., 1991). An impactor device like that described by Ek *et al* (2010) was utilised which consists of a LinMot linear motor and slider which are mounted onto a manipulator of a stereotaxic frame, a Linmot servo controller unit and a PC computer running Linmot control software (LinTalk Version 2.6) (Fig 2.3) (Ek et al., 2010). Plastic tip pieces 2mm in diameter were fabricated (Alternative Engineering) and fitted to the end of the slider to provide a flat impacting surface. Electromagnetic forces are used by the linear motor to propel the slider along the central hollow tube of the motor casing. The Linmot control software through the servo unit allows the precise specification of the movements made by the slider, thus permitting modification of the depth and velocity of impact, as well as the dwell time.

In order to perform the CCI injury, an intraperitoneal injection of Avertin (250mg/kg) was used to anaesthetise the mice, with surgery commencing once pedal foot reflexes were absent. Following a midline scalp incision, a craniotomy (3mm diameter) was performed in the centre of the right parietal bone, being careful to ensure that the integrity of the dura was not disrupted. Mice were then placed in a stereotaxic frame with the head positioned in the horizontal plane and nose bar set at zero. The impactor tip was then manoeuvred into position so that it was just touching the surface of the tissue to be impacted, with this confirmed with an operational microscope. Once in position the computer software was used to operate the device, with the slider moving in accordance with user set parameters which control the acceleration and depth of the impact, as well as the dwell

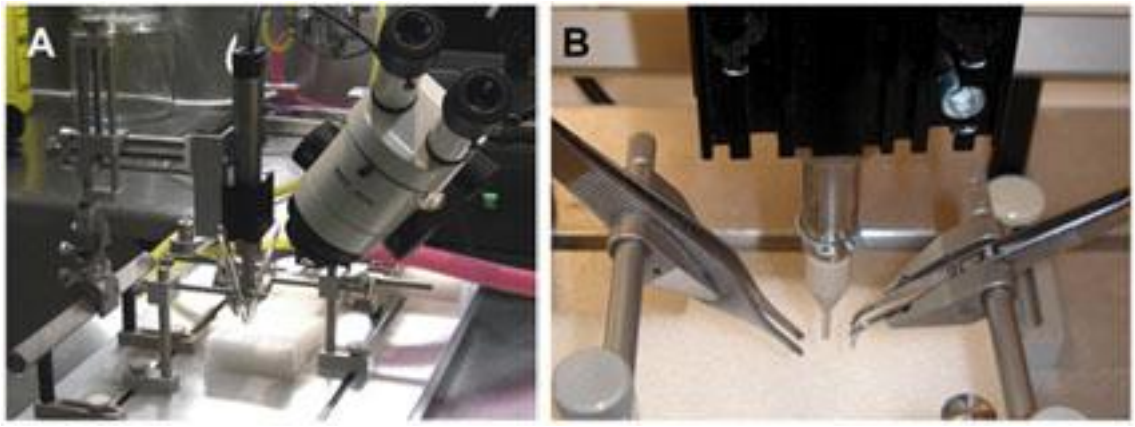

Fig 2.3: Representative images of the CCI device used, taken from Ek *et al* (2010). The linear motor is mounted onto the stereotaxic frame, with the tip lowered manually using the manipulator arm controls until it is just touching the surface of the dura mater which has been exposed via a craniotomy. An impact is then delivered by sending a command from the Linmot Control Software on a PC to the servo-controller unit, which precisely controls the acceleration of the tip, depth of tip penetration and well time, with this preset by the user.

time, resulting in a cortical impact injury. The position of the slider is monitored in real-time and displayed graphically allowing the impact velocity and the depth of impact to be recorded.

Preliminary experiments in APP+/+ mice are outlined in Chapter 5, characterising the effects of impact at depths of 1, 1.5 and 2mm at 5m/sec with a dwell time of 100ms on functional and histological outcome. Having determined that 1.5mm was the optimal depth at which to achieve a moderate level of injury, the impact depth in APP-/- mice had to be adjusted slightly in order to compensate for the 10% reduction in brain weight noted in these mice (Ring et al., 2007) . Righting reflex could not be used to assess injury severity following injury as the effects of Avertin take much longer to wear off than the inhalation anaesthetic isoflurane. Instead histological outcome was compared at 5 hrs post-injury to ensure that the level of primary injury received was the same. With an impact depth of 1.3cm for APP-/- mice and 1.5mm for APP+/+ mice, it was found that there was no difference between APP-/- and APP+/+ mice in terms of lesion volume or in the number of degenerating neurons within the dentate gyrus and CA region of the hippocampus as detected with Fluoro Jade C (FJC) staining (Fig 2.4).

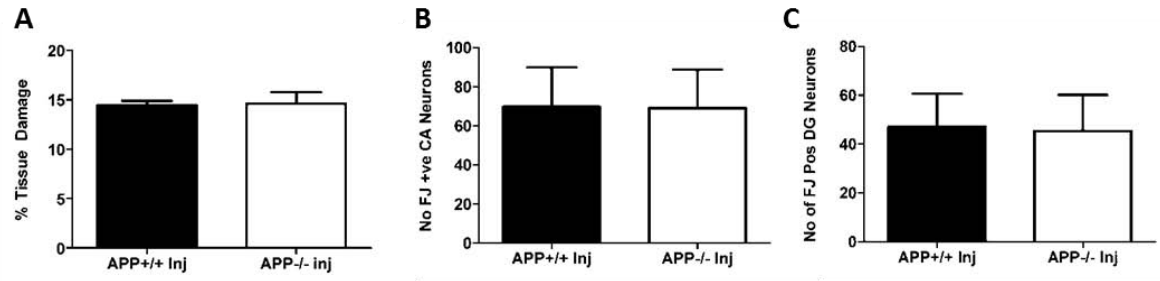

Fig 2.4: Lesion volume (A) and degenerating neurons as detected by FJC staining within the CA region of the hippocampus (B) and dentate gyrus (C) at 5 hrs post-injury demonstrating that the primary injury level is the same between APP+/+ and APP-/- mice. (n=3 per group)

2.3.4 Drug Treatment

The studies within this thesis employed the following treatments: full length sAPPα (APP18-611) its D1 (APP28-123), D2 (APP124-189) or D6a (APP316-498) domains, the regions encompassing its heparin binding sites, APP96-110 and APP416-47, or artificial CSF vehicle (Fig 2.5), with the specific details found in the relevant chapters. Briefly, sAPPα, the D1, D2 and D6a peptides were expressed as

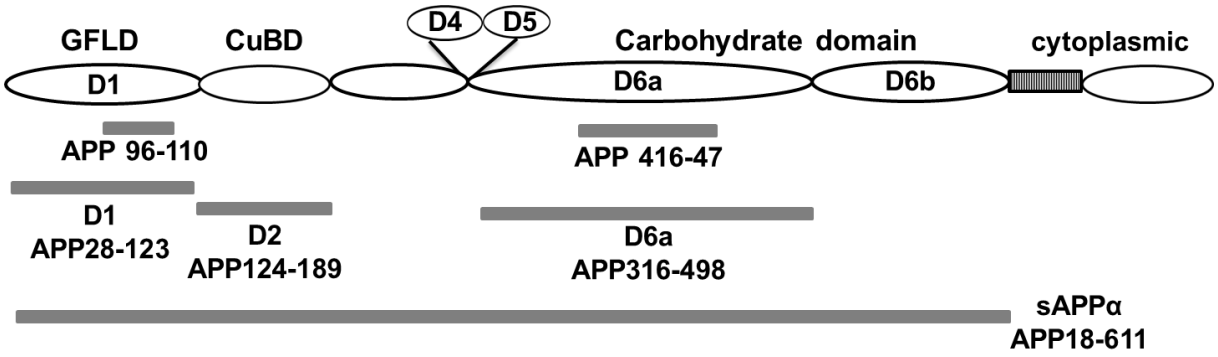

Fig 2.5: Schematic of the different peptides administered in relation to full length APP

a secreted protein in the methylotrophic yeast, *Pichia pastoris* as previously described (Henry et al., 1997). They were then purified from the media by anion exchange chromatography using a Hiload Q sepharose column (26 x 12 mm, GE Healthcare, Sweden), followed by affinity chromatography using a Hitrap heparin HP column (5mL, GE Healthcare, Sweden). APP96-110 and APP416-447 were produced through custom peptide synthesis (Auspep) using the following sequences, NWCKRGRKQCKTHPH and FNMLKKYVRAEQKDRQHTLKHFEHVRMVDPKK, and were N-terminally acetylated and C-terminally amidated, with the disulphide bridge preserved between Cys-98 and Cys-105 within APP96-110. 150µl of the appropriate treatment (25µM) was then mixed with 75µL of artificial CSF vehicle (Roch et al., 1994; Thornton et al., 2006) prior to administration. This concentration was based a preliminary dose response study in Sprague Dawley rats which investigated the effects of 0.25, 2.5 or 25µM of sAPPα on motor outcome following TBI. This found that although each dose reduced motor deficits when compared to vehicle controls, there was a slight improvement in those in the 25µM group in days 1-4 post-injury in comparison to the other treatment groups (Fig 2.6).

To facilitate treatment following injury in rats a 0.7mm craniotomy was performed at the stereotaxic coordinates relative to the bregma: posterior 0.6mm, lateral 1.5mm (Paxinos, 1998; Thornton et al., 2006). A 30-gauge needle attached to a 5µl syringe was then stereotaxically lowered 4.0 mm then retracted 0.5 mm to facilitate administration into the left ventricle. 5µL of the appropriate

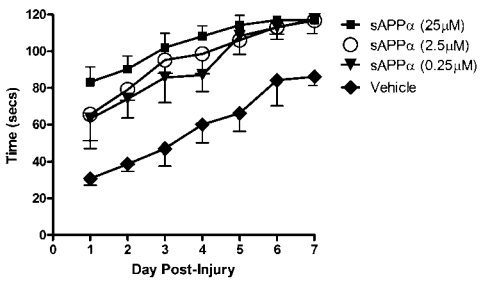

Fig 2.6: Dose-response study demonstrating a small improvement in rats treated with 25µM rather than 2.5µM or 0.25µM sAPPα in terms of performance on the rotarod, although all treatment groups performed better than the vehicle controls. (n=5 per group)

treatment was administered at a rate of 0.5µL/min, with the needle left in place for 2 mins prior to retraction. In mice a similar protocol was followed with a 0.3mm craniotomy performed on the left side, at the stereotaxic coordinates relative to bregma: posterior 0.5mm, lateral 1mm (Paxinos and Franklin, 2007), with the needle lowered 2.5mm and retracted 0.3mm to allow injection of 2µL of the appropriate treatment which was administered at a rate of 0.5 µL/min. This method of administration was selected on the basis of our previous work which showed that administering sAPPα via an intracerebroventricular (ICV) injection improved outcome following TBI (Thornton et al., 2006), in line with previous research which used autoradiography to show that ICV administration results in a homogenous distribution of sAPPα throughout the rat brain and a higher concentration compared to shams (Roch et al., 1994).

2.3.5 Post-surgery recovery

Following surgery all animals were placed in a recovery box on a 37°C heatpad until they had regained their righting reflex and were showing interest in their environment. They were then returned to their home cage with unlimited access to food and water and checked regularly to ensure there were no adverse effects from surgery.

2.4 Neurological Assessment

2.4.1 Cognitive Testing

Before choosing a cognitive test for assessment of post-injury deficits, a group of uninjured animals were subjected to a battery of cognitive tests each spaced a week apart, in order to determine the task at which the animals were most adept at performing. The tasks chosen for the Sprague Dawley rats were the Y Maze, Object Recognition Task and Shuttlebox, while those for the mice were the Object Recognition Task, Y Maze and Barnes Maze. All assessments were conducted within a quiet darkened room between 7:00-9:00a.m to improve the likelihood of gaining meaningful results.

Shuttlebox

The shuttlebox has previously been used to assess two-way active avoidance learning in rodents (Escorihuela et al., 1999; Gershtein et al., 2000; Sansone et al., 1999). The test is conducted in a two-chambered box, with the chambers separated by a swinging door which allows animals to move freely between the compartments. Animals are placed into one of the compartments and presented with a light for 10 secs, which acts as a conditioned stimulus. The animals are required to move to the other compartment in order to avoid an electrical foot shock (the unconditioned stimulus) which is applied to the stainless steel bars of the grid floor. If the animal fails to make an escape response the electric shock is turned off after 5 secs. Compartment changes during the presentation of the conditioned stimulus are counted as conditioned (correct) avoidance reactions, while changes during the unconditioned stimulus are counted as unconditioned avoidance reactions. If animals do not move from the compartment in which the shock is being delivered this is counted as a failure, with the test terminated if rats had greater than 3 failures in a row. Each animal was subject to 15 trials a day for 5 days to observe their ability to learn to perform this task.

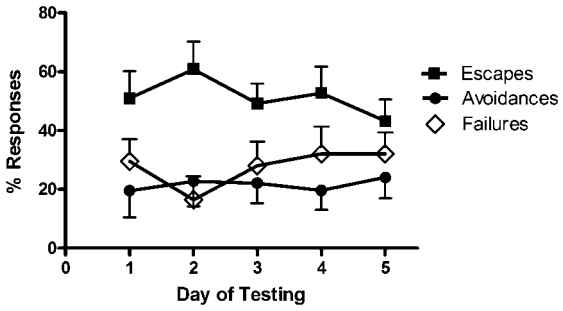

Fig 2.7: Responses elicited during shuttlebox training in naïve Sprague Dawley rats, showing an inability to learn the task as there was no increase in the number of avoidances over the testing period (n=6-8 per day).

As seen in Fig 2.7, these Sprague Dawley rats did not learn to perform this task, with no improvement in the number of correct avoidance responses seen in 5 days of testing. Indeed, these rats had a quite high failure rate, where they were unable to escape the shock, which steadily increased over the testing period. As this was associated with freezing behavior, it suggests that the task may have induced such high anxiety levels within these rats that they were unable to learn the correct response (Shors and Dryver, 1994).

Object Recognition

The Object Recognition task is based on the observation that rats spend more time exploring a new object than a familiar one (Ennaceur and Delacour, 1988). In order to conduct the test naïve animals

were first subjected to habituation, with the animals being placed in the empty box for 10 mins each morning for three consecutive days (1m x 1m for Sprague Dawley rats; 70cm x 70cm for the C57BL6jx129sv mice). This is to familiarise the animals with the environment in which the test is to be conducted to increase the likelihood that they will be interested in the objects.

On the day of testing, animals were first placed in the box for the sample phase of the experiment whereby they were exposed to two identical objects (cylinders) over a 5 min period. At either 15 or 60 mins after the sample phase animals were reintroduced into the box for the choice phase of the experiment. In the choice phase, two objects were presented in the same location, one a cylinder identical to those used in the sample phase and the other a lego block, so the animals were exposed to a familiar and a novel object (Fig 2.8). The time spent exploring each object was then recorded with a stop watch over a 5 min period. Exploration was defined as directing the nose at and actively sniffing the object when less than 2cm away, and/or touching the nose to the object. After each animal the box and objects were cleaned thoroughly with 70% alcohol to remove scent trails.

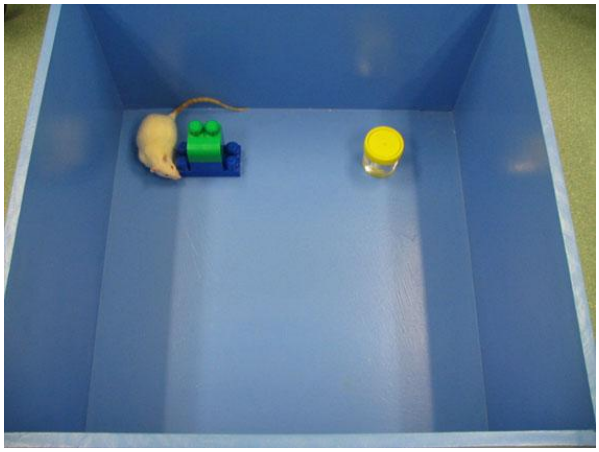

Fig 2.8: Representative photograph of the object recognition task during the choice phase. The rat is able to explore both a novel (lego block) and familiar object (cylinder) with time spent exploring each object recorded.

As can be seen in Fig 2.9 the rats demonstrated a small non-significant increase in the amount of time spent with the novel rather than the familiar object. This was similar with either a 15 min (53.6%) or 60 min (58.1%) interval between the two phases of the experiment, indicating that this was not due to an inability to remember the familiar object with increasing time after the sample phase. These findings support our

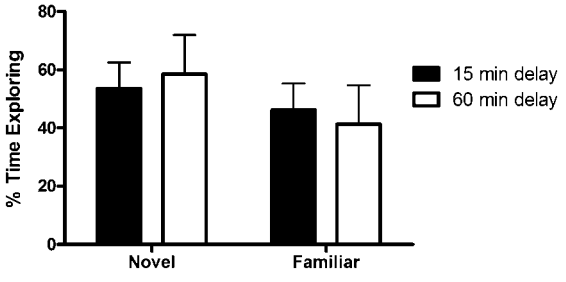

Fig 2.9: Performance by Sprague Dawley rats on the object recognition task, showing a small increase in the percentage of time exploring the novel rather than the familiar object with either a 15 or 60 min delay before exposure to the novel object (n=6 per group).

observations that this particularly colony of rats have poor vision and thus were not overly interested in the visual stimuli presented. Indeed they often spent less than 30 secs over the 5 min testing period exploring the objects provided. As such this was not thought to be an appropriate test to determine cognitive deficits following TBI with this colony of rats.

In the C57BL6j x 129sv mice we were unable to tabulate the results as they were even less interested in the objects, often spending fewer than 10 secs over the 5 min period attending to the objects. As this occurred repeatedly during the sample phase of the experiments, many mice (5/8) were not thought to have been sufficiently familarised with the objects to allow for their inclusion within the novel phase of the experiment. This may relate to the particular strain of mice in use, or that these mice may have needed a more lengthy period of habituation, which was not practical for these particular experiments.

Y Maze

The Y maze tests spatial and recognition memory and has been shown to be a sensitive test for detecting hippocampal damage in rodents (Conrad et al., 1996). The maze consists of three arms (30 x 10 x 15cm for rat, 20 x 5 x 10cm for mice, length x width x height) with 3 cylinders at the end of each arm. Each cylinder was covered with either sandpaper, bubble wrap or plastic to provide different tactile stimulus and aid the animals in distinguishing between the arms (Fig 2.10). These also provided a support for the animals to climb on and rear so as to better see the environment

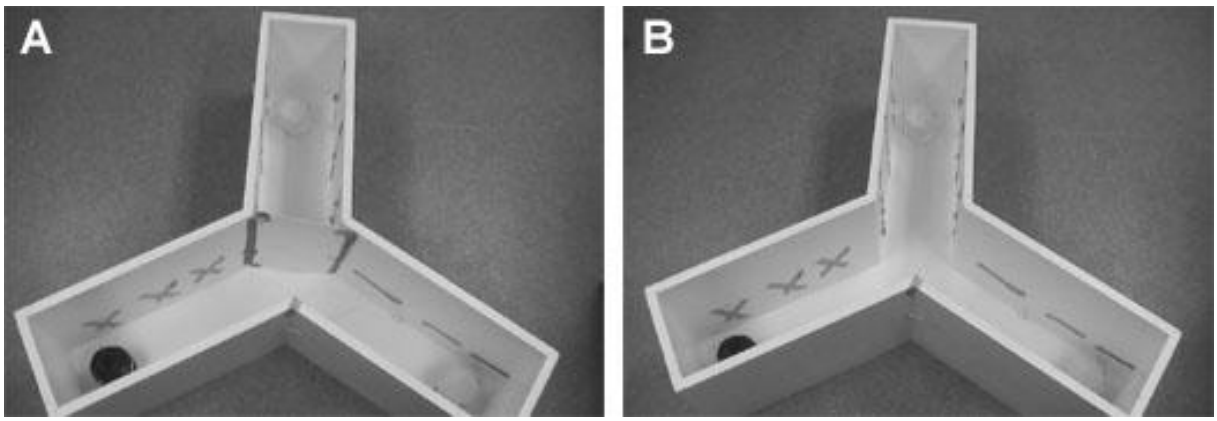

Fig 2.10: The Y Maze apparatus as set up for the first phase (A) of the experiment with one of the arms blocked, and for the second phase (B) where all arms are open for the animal to explore. Note the presence of cylinders which are covered with sandpaper, plastic and bubblewrap as viewed clockwise from the left. These provide spatial information and also provide an impetus for the animals to keep exploring.

outside the maze, whilst also provided a stimulus for the rats to continue to explore. Distinct spatial clues were located around the maze and kept constant throughout the study in order to allow the animals to orientate themselves and thus differentiate between the arms without examining the objects. The arms are arbitrarily designated as the start, other and novel arms, with this randomly alternated among the rats. In the first phase of the experiment, rats are introduced into the maze in which one of the arms (novel) has been closed and allowed to explore for 3 mins. This means that the animals were able to explore the start and other arms, but not the novel arm. An hour later the animals are placed back into the maze in their start arm, with all the arms (start, other and novel) open, and allowed to explore for another 3 mins. This test works on the basis that an uninjured animal will spend more time exploring the novel arm to which they have not been previously exposed, rather than the other two arms. In order to remove scent trails the maze was wiped thoroughly with 70% alcohol after each trial. The experimenter was not in the room during the trials, with all trials captured on video, and the number of times each arm was visited and the time spent in each arm analysed. Animals that did not enter the other arm during the first part of the experiment were not included.

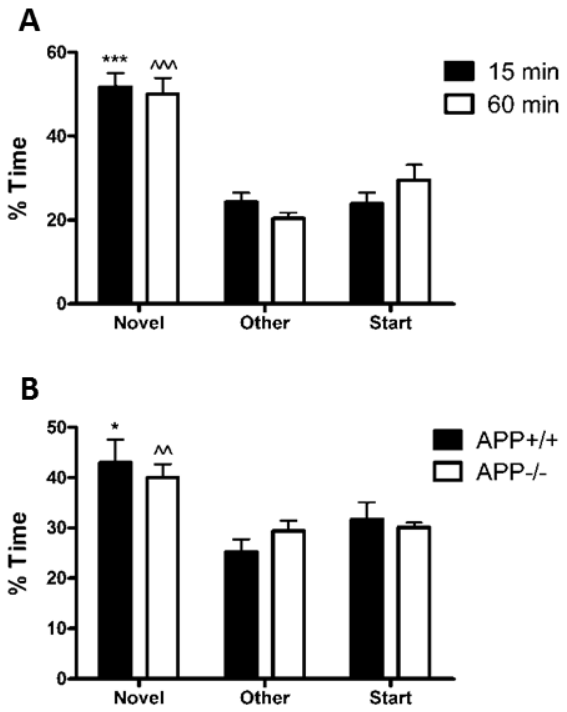

Fig 2.11: Performance by Sprague Dawley rats on the Y Maze (A) shows they spend a significantly greater amount of time in the novel arm rather than the start or other arms following either a 15 or 60 min delay (n=6 per group). Similarly APP+/+ or APP-/- C57BL6j x 129sv mice spend a significantly greater percentage of time within the novel arm than the other 2 arms, with a 60 min delay (B). (APP+/+ mice n=6, APP-/- mice n=5) (*p<0.001, *p<0.05 compared to start and other arms; ^^^p<0.001, ^^p<0.01 compared to start and other arms)**

Sprague Dawley rats were found to spend a significantly greater amount of time within the novel arm than the other two arms with either a 15 or 60 min delay between the two phases of the experiment (Fig 2.11A). The rats spent more time exploring than in the Object Recognition task, suggesting that they may have been more comfortable within the confines of the Y maze where they were always close to a wall, rather than in an open box. The addition of tactile objects also seemed

to help the animals orientate themselves within the maze, with this task chosen as the appropriate test to assess post-injury cognitive deficits in these animals.

Preliminary investigations in both APP+/+ and APP-/- mice also showed that they were capable of distinguishing the novel arm from the other two arms within the Y Maze following a 60 min delay (Fig 2.11B). However, we decided to test whether the Barnes Maze would be suitable in these animals before choosing between the two tasks. Although the Y Maze had proved successful in demonstrating a treatment effect following injury in rats, it was thought that it may not be sensitive enough to discern between subtle graduations in injury, with animals either performing the task correctly or incorrectly. Thus, as the hypothesis in these studies was that the lack of APP would worsen outcome following TBI, it would be impossible to discern between two groups who performed the task incorrectly.

Barnes Maze

The Barnes maze paradigm exploits the natural inclination of small rodents to seek escape to a darkly lit, sheltered environment when placed in an open arena under bright, aversive illumination (Barnes, 1979). The maze consists of a white circular platform (diameter 120cm) elevated 70cm above the floor, from which the mouse could escape into 1 of 40 holes (5cm in diameter) evenly spaced around the perimeter (Fig 2.12). The escape hole was connected to an escape box (10 x 15cm), with distinct spatial clues located all around the maze which were kept constant throughout the study to aid the animals in finding the correct hole. As such animals have to use a hippocampal dependent spatial strategy in order to find the escape hole (Koopmans et al., 2003), with previous studies showing a correlation between hippocampal damage and decrease in performance on this test (Fox et al., 1998; Raber et al., 2004).

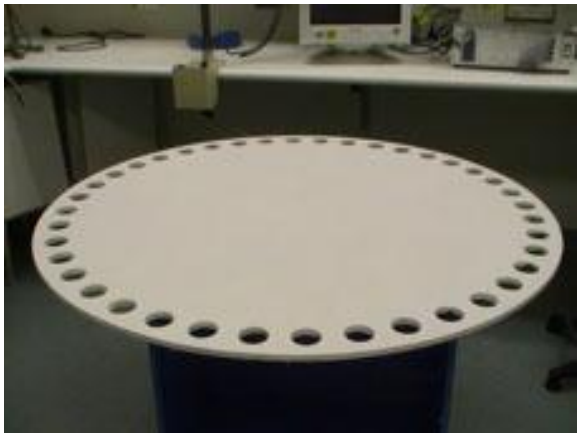

Fig 2.12: Representative photograph of the Barnes Maze showing the white circular platform with 40 holes around the perimeter, one of which is attached to an escape box.

During pre-training, animals were initially habituated by placing them into the escape box and leaving them there for 3 mins. One min later, the first trial started, with the animal placed in a start chamber, comprising a plastic box in the centre of the platform. After 10 secs the start chamber was removed, a buzzer and a bright light turned on and the mouse was set free to explore the maze. The trial finished when the mouse had either entered the escape box or 3 mins had passed. If the mouse did not find the escape box within 3 mins, the experimenter gently guided the animal there. Once the mouse had entered the escape tunnel, the buzzer and light were turned off and the mouse was allowed to remain for 1 min. If a mouse failed to find the escape box they were given a second trial that day, with a period of approximately 1 hr between trials. As can be seen in Fig 2.13, both the APP+/+ and APP-/- mice were able to learn this task over a 5 day habituation period, with improvement over the testing period, occurring most sharply between days 3 and 4 (Fig 2.13). With the mice able to perform this task adequately it was chosen as that to be used for post-injury cognitive assessment. Their ability to find the escape hole following the 5 day period of pre-training was assessed on days 2, 4 and 6 post-injury, as outlined in Chapters 4- 7.

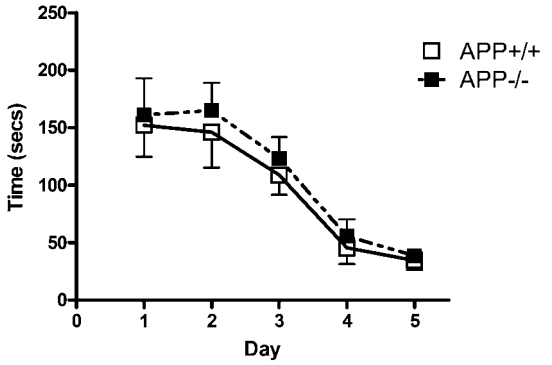

Fig 2.13: The ability of APP+/+ and APP-/- C57BL6j x 129sv mice to find an escape hole on the Barnes Maze over a 5 day training period.

2.4.2 Motor Testing

Rotarod

Motor deficits produced by diffuse TBI were assessed using the rotarod (Fig 2.14), which has been described as the most sensitive test for the detection of motor deficits in rodents (Hamm et al., 1994). The rotarod device which was used to test the rats consists of a motorised rotating assembly of eighteen 1mm metal rods. In order to walk as the rods rotated beneath them the animals were required to grip the rods, thus introducing a grip test component to the assessment (Lighthall, 1988). After being placed on the stationary device for 10 secs, rotational speed was then increased from 6 to 36 revolutions per minute (rpm), at a rate of 3rpm/10 secs. The duration in seconds, up to a

maximum of 120 secs, was recorded at the point when animals had either completed the task, clung to the rods for 2 consecutive rotations without actively walking or had fallen off. All animals were pre-trained daily on the device for 5 days prior to injury and assessed daily for 7 days after injury. A smaller scale model was used to test motor deficits in mice, comprising a motorised assembly of 12 rods that are 0.2mm in diameter, with speed increasing from 0 to 30rpm at a rate of 3rpm/10 secs. Similarly, the mice were required to walk on the rods, with the latency to fall from the rotating bars or to grip the rods and spin two consecutive rotations recorded. APP+/+ mice were expected to complete 180 secs on the rotarod, whilst APP-/- mice were only expected to complete 120 secs due to the forearm weakness that is part of their phenotype (Zheng et al., 1995). All mice were pre-trained daily for 5 days, with their best time taken as their pre-injury baseline level and then assessed for 7 days after injury.

Fig 2.14: Photograph of the rotarod device used to test motor deficits following impact-acceleration TBI in rats. A similar but smaller scale model was used for assessment of deficits in mice.

Ledged Beam

For assessment of motor deficits following a focal injury, the ledged beam was used as it has previously been shown to be a sensitive test of unilateral deficits (Bye et al., 2007; Semple et al., 2010b). This involves use of beam that is 1m in length tapering from 3.5cm to 0.5cm with underhanging ledges 1.0cm in width on either side (Fig 2.15). The beam was placed at a 30° angle of incline, with the narrowest end at the highest point. Mice were placed at the widest end of the beam and required to walk to the narrowest end, where an enclosed box was situated. Within this box, bedding material and tissues were placed in order to provide an incentive for the mice to cross the beam. Animals were pre-trained for 3 days prior to injury in order to habituate them to the task, and then tested each day for 7 days following injury, with each mouse given 2 trials which were videotaped for later analysis. The number of times the underhanging ledge was used (foot faults) by

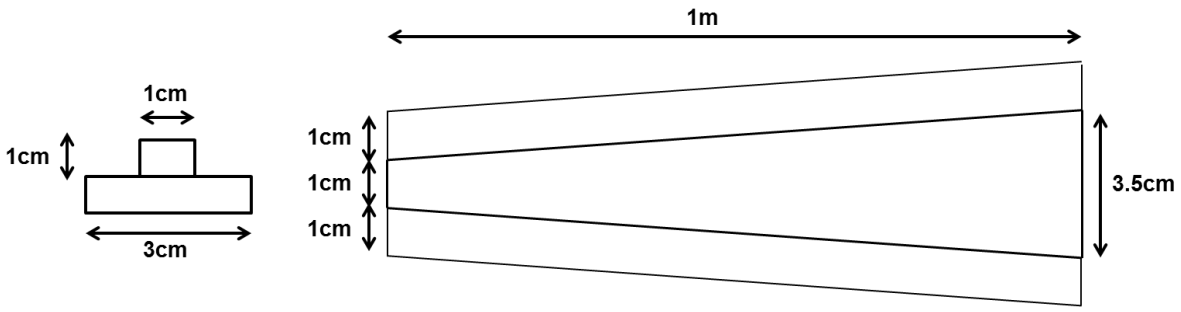

Fig 2.15 : A diagram depicting the ledged beam as viewed from the side (left) and from above (right) showing the 1m long beam tapering from 1 to 3.5cm with underhanging ledges 1cm in length present on either side.

limbs on the left side, which was contralateral to the CCI injury, were counted and averaged across the two trials.

2.5 Histological Analysis

2.5.1 Perfuse Fixation

Before perfuse fixation animals were first administered an IP injection of pentobarbital, with the dose titrated until all pain reflexes were absent. The upper peritoneal cavity was then exposed, the diaphragm incised and the thorax opened bilaterally. The left ventricular apex was then pulled down slightly with a towel clip in rats and a suture in mice, to allow the insertion of a blunt 20 (rat) or 23 (mice) gauge needle through the left ventricle into the aorta. The right atrium was then excised and 10% neutral buffered formalin driven under either 120mmHg (rats) or 80mmHg (mice) of pressure until the fluid from the right atrium was clear. Animals were decapitated 1 hr later to minimise artefactual damage to blood vessels, with brains extracted and placed in formalin for processing a minimum of 24 hrs later.

2.5.2 Tissue Processing

For histological assessment of animals who underwent diffuse injury the brains were cut into 14 (rats) or 7 (mice) 2mm coronal slices and placed in cassettes in neutral buffered formalin. They were then processed overnight according to the following protocol, 20 mins in ethanol baths of increasing concentration (50%, 70%, 80%, 95%, 100%, 100%), followed by 2 xylene baths (90 mins) and then

paraffin baths of increasing duration (30, 60, 60, 90 mins). These brain slices were then embedded in paraffin wax, sectioned with a microtome (Leica RM2245) and floated onto glass slides (Menzel-Glaser, Superfrost plus). Sections were taken from the region -4.5 from bregma for rats and -2.3mm from bregma in mice. Slides were then air dried before being stored in a humidified oven at 37°C.

For mice subjected to the focal injury, the entire brain was placed into a cassette before undergoing a two day processing protocol. The brains were embedded in paraffin wax and then trimmed on the microtome until the region +0.5mm from bregma was reached. Serial sections were than taken at 200µm intervals until the region -4 from bregma to allow assessment of the entire cortical contusion, with slides stored as above.

2.5.3 Haematoxylin and Eosin Staining

For H&E staining slides were first placed on a blower for 2 mins to remove the majority of the wax before being placed in 2 x 2 mins of xylene and 2 x 2 mins of alcohol. Following a brief wash in dH_20 slides were placed in haematoxylin for 5 mins. After washing in dH_20 for 30secs, slides were briefly dipped in acid alcohol and then in saturated lithium carbonate, rinsed with dH_20 and placed in eosin for 1 min. Slides were then dehydrated with 2 x 2 mins of 100% alcohol, followed by 2 x 2 mins of histolene before being coverslipped using DePeX. These slides were then scanned (Nanozoomer, Hamamatsu City, Japan) and viewed using the associated software (NDP View Version 1.2.2.5).

Lesion Volume

To determine the extent of cortical damage after the focal CCI injury (Chapters 5-7), 5 sections per brain (400µm apart) were stained with H&E, representing the region Bregma -0.5 to -4 due to the shrinkage associated with tissue processing. The unaffected area of the cortex of each hemisphere was outlined within the NDP View software, with damaged tissue defined by a decrease in H&E staining intensity (Fig 2.16). The volume of undamaged tissue in each hemisphere was then calculated using the following equation:

$$(Area_1 \; x \; D) + \frac{(Area_2 - Area_1 \; x \; D)}{2}$$

$Area_1$ is the area of undamaged tissue (μm^2) in section 1 (the smaller area of the 2 sections) and $Area_2$ is the area of undamaged in section 2. *D* is the distance (in µm) between section 1 and section 2 (i.e. 5 µm × the number of sections between). The volumes of healthy tissue between successive pairs of sections across the lesion were then added to determine the total volume. The percentage of cortical tissue damage was then calculated as (uninjured cortical volume – injured cortical volume) / uninjured cortical volume × 100 (Semple et al., 2010b).

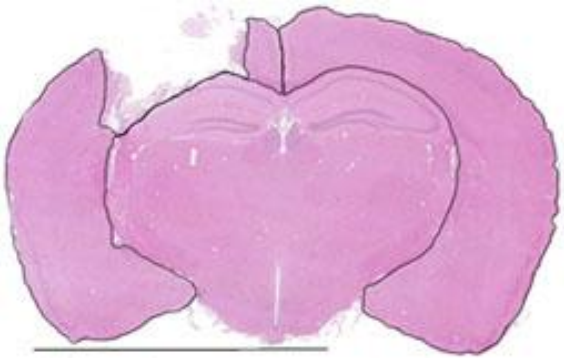

Fig 2.16: Representative micrograph demonstrating how the area of the cortex was outlined in order to determine the extent of cortical damage. The area of the damaged right cortex is 7.46mm^2 and the left 11.9 mm^2. Scale bar = 5mm

Neuronal Counts

Following the diffuse injury in mice neuronal numbers were assessed within the selectively vulnerable CA3 region and the cortex directly underneath the impact site. The CA3 region was sequentially imaged at 40x magnification and digitally reconstructed into a montage, to allow manual counting of the neurons using the cell count software associated with Image J. Similarly, 4 macroscopic fields (40x) directly underneath the impact site were examined. For each animal 2 slides were counted from the region -2.1 from bregma and the average then taken. Only histologically normal appearing neurons with a clearly defined cell body and nucleus were counted, those that were only partially seen due to the level of sectioning were not included nor were those that appeared pyknotic (dark, shrunken with no visible nucleus) (Fig 2.17).

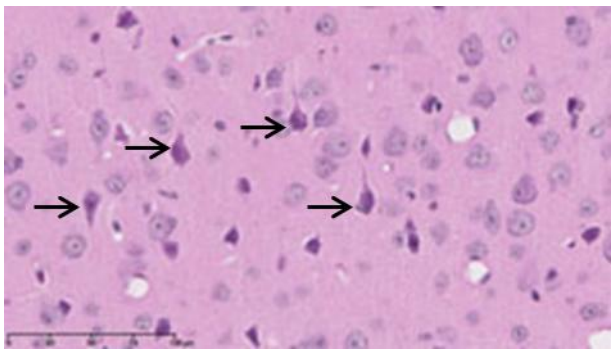

Fig 2.17: Representative micrograph of the cortex of an APP-/- mouse following the mild diffuse impact-acceleration injury. Arrows denote pyknotic cells which were not included within neuronal counts.

Following the focal injury the neuronal damage is not evenly distributed like that seen with a diffuse injury. Thus three sections located 200µm apart representing the region Bregma -1.2 to -2.1 were analysed, with the number of neurons within the CA region counted. To determine the effects of injury on the dentate gyrus, the area of the granular layer of the dentate gyrus was determined in 5 sections located 200µm apart (Bregma -1.5 to -3), with the volume calculated using the equation described above:

$$(Area_1 \; x \; D) + \frac{(Area_2 - Area_1 \; x \; D)}{2}$$

2.5.4 Fluoro Jade C Staining

FJC is an anionic fluorescein derivative that specifically labels neurons undergoing neurodegeneration. To stain slides with FJC they were first dewaxed through immersion in xylene for 2 x 3 mins, then placed in 100% ethanol for 3 mins, 70% ethanol for 3 mins and then for 2 mins in dH_20. Sections were then incubated in 0.06% potassium permanganate for 10 min to reduce non-specific staining and washed with dH_20. All remaining steps were conducted in the dark, with slides incubated with FJC for 20mins. FJC was prepared by adding 1ml of 0.01% FJC stock to 99ml of 0.01% glacial acetic acid solution. Slides were then rinsed in dH_20, before being placed in a 45°C oven until fully dry and coverslipped with DePeX mounting media from histolene.

Counts of degenerating neurons

Following the focal CCI injury 3 sections located 200µm apart representing the region Bregma -1.2 to -2.1 were analysed for FJC staining, as it labels degenerating neurons (Schmued et al., 1997). Sections were viewed with the Olympus BX61 microscope using a FITC fluorescence filter cube, with the CA region and granular dentate gyrus layer sequentially photographed at 40x magnification. These images were then imported into ImageJ, with the number of FJC+ve neurons within these regions counted using the associated cell count software.

2.5.5 Immunohistochemistry

Sections were immunostained with 3,3' diaminobenzidene (DAB) method for APP (Novocastra 122703), which allows identification of injured axons, GAP-43 (Novacastra 1222203), a marker of the

reparative response, synaptophysin (DakoA0010), which labels pre-synaptic boutons, microtubule associated protein-2 (MAP-2) (Abcam 24645), a dendritic marker and doublecortin (Millipore, 2253), which labels immature neurons.

Following dewaxing and dehydration, endogenous peroxidase activity was blocked by incubation with 0.5% hydrogen peroxide in methanol for 30 mins. Slides were then washed in 2 x 3 mins in phosphate buffered saline (PBS) before antigen retrieval retrieved by heating at close to boiling point for 10 mins (TRIS for doublecortin, citrate for others). Once the slides had cooled below 40°C they were washed with PBS before being blocked with 3% normal horse serum in PBS for 30 mins. The appropriate primary antibody was applied to the slides which were left to incubate overnight (APP, GAP-43, MAP-2, synaptophysin 1:1000, doublecortin 1:8000). The next day slides were washed in 2 x 3 mins of PBS before the appropriate species of IgG biotintylated antibody was added for 30 min (Dako). After a further PBS wash, slides were incubated with streptavidin peroxidase conjugate for 60 mins followed by another rinse with PBS. The immunocomplex was then visualised with precipitation of DAB (Sigma D-5637) in the presence of hydrogen peroxide. Slides were washed to remove excess DAB and lightly counterstained with haematoxylin, dehydrated and mounted with DePeX from histolene.

Axonal Injury

To assess axonal injury following the diffuse impact-acceleration injury in rats the number of APP immunopositive lengths within the corpus callosum at the level -4.5mm from bregma were counted for each animal.

Neurogenesis

For semi-quantification of neurogenesis, the number of doublecortin-positive cells embedded within the granule cell layer of the dentate gyrus were counted in 3 sections spanning the dorsal hippocampus, as increased rate of neurogenesis correlates with an increased number of cells expressing doublecortin (Couillard-Despres et al., 2005). The length of the dentate gyrus was measured, and the number of cells/mm calculated, as described elsewhere (Dash et al., 2010).

Colour Deconvolution

To objectively assess the level of GAP-43, synaptophysin and MAP-2 following injury the colour deconvolution method was employed to determine the amount of DAB and hence antigen that was present within each image. This technique is based on the Ruifork and Johnston method for separation and quantification of immunohistochemical staining by deconvolution of colour information in RGB, which separates the amount of blue from brown within an image (Ruifrok and Johnston, 2001). This allows the relative brownness of each pixel to be obtained from a histogram which is weighted from 0-255, with the total number of pixels multiplied by 255 giving the maximal theoretical brownness of an image. If the actual brownness values for all pixels are added together and divided by the maximal theoretical number, a result is given which is a measure of actual versus maximum possible brownness which is expressed as a fraction of 1 (%DAB weight). Pixels with a value of 0 or 1 are discarded as these represent white areas such as empty blood vessels and ventricles. This algorithm was coded as an NIH Image J macro, with background subtraction and colour correction applied to the images before processing with the `rolling ball' method of Castle and Keller (2007) using the staining vectors included within the macro. The deconvolved DAB channel was semi-quantitated by performing a histogram analysis as described above. The end result is given as the %DAB weight within an image thus allowing comparison of this value to that of other images. Previous experiments have shown the reliability of this method with a linear correlation demonstrated (extinction coefficient 0.96) between increasing antibody concentration and DAB weight (Kleinig, 2010).

2.6 Caspase-3 ELISA

At either day 3 or 7 post-injury animals were re-anaesthetised with isoflurane and once a surgical level of anaesthesia was reached they were rapidly decapitated and the brain removed, with the peak of apoptotic cell death following diffuse injury occurring at 3 days. The hippocampus and the region of cortex directly under the impact site were removed and rapidly frozen in liquid nitrogen. Tissue was later thawed and placed in a tissue homogeniser with 10 x brain region weight of homogenisation buffer (Roche) and vortexed on ice every 5 mins for 20 mins. The sample was then centrifuged at 8500 rpm for 15 mins with the pellet discarded and the supernatant frozen.

A 30µl aliquot was then used to estimate protein concentration against a standard curve derived from serial solutions of bovine serum albumin (BSA Sigma A21543). 5µl of supernatant or BSA was added to the recommended amounts of Biorad protein assay reagents (500-0113, -0114 and 0115). Three wells were performed for each specimen and averaged and the absorbance read at 620nm. Each sample was then diluted with tris-buffered saline (TBS) to achieve a final concentration of 400ng protein per 100µl of TBS.

To perform the ELISA, 100µl of each sample was loaded in triplicate to a 96 well plate (Nunc F96 Maxisorp) and allowed to coat the wells overnight. A minimum of 6 blank wells were included as controls. The wells were then blocked with 0.2% gelatine for 30 mins and rinsed with TBS before being incubated with anti-active caspase 3 (1:1000 BioVision) in a 37°C oven for 30 mins. After rinsing with TBS, secondary anti-rabbit horseradish peroxidise conjugate (1:2000 Rockford) was added, with the plates placed in a 37°C oven for 30 mins. TBS was applied to thoroughly rinse the plates, before the liquid substrate system 3,3'5,5'-tetramethylbenzidine (Sigma) was used to reveal protein expression. The reaction was stopped after 100 secs with 0.5M sulphuric acid and levels of expression determined by reading absorbance at 450nm on an Ascent Multiscan plate reader. To demonstrate repeatability the ELISA was performed 3 times.

2.7 Statistical Analysis

All parametric data were assessed using two-tailed unpaired student's t tests or analysis of variance (ANOVA -one or -two way and/or repeated measures as necessary), followed by Bonferonni tests for multiple comparisons. A p value of less than 0.05 was considered significant. All graphical data is presented as mean ± standard error of the mean (SEM).

Chapter 3: The neuroprotective domains of the amyloid precursor protein, in traumatic brain injury, are located in the two growth factor domains

3.1 Introduction

TBI is a leading cause of morbidity and mortality with an estimated 10 million people affected annually by an injury serious enough to result in death or hospitalisation (Hyder et al., 2007). Following TBI, cell death is caused by the initial insult and the ongoing contribution of secondary factors such as excitotoxicity, oxidative stress and inflammation (Bramlett and Dietrich, 2004; Enriquez and Bullock, 2004). Although this delayed tissue damage provides a therapeutic window with opportunity for to limit neuronal damage (Vink and Van Den Heuvel, 2004), there are currently no accepted pharmacological interventions available for the treatment of TBI (Maas et al., 2010). As such it seems imperative that the identification of factors within the endogenous neuroprotective and neurotrophic pathways may facilitate the development of novel therapeutic strategies. This is especially important as the upregulation of these pathways appears to be inhibited with more severe injuries (Thompson et al., 2006).

Recent evidence suggests that APP may play a role in these neuroprotective and neurotrophic pathways following TBI, with the metabolite sAPPα shown to improve motor outcome with an associated reduction in axonal injury and apoptotic cell death when administered to rats following TBI (Thornton et al., 2006). Indeed, multiple studies have highlighted the role of sAPPα in providing neuroprotection (Goodman and Mattson, 1994; Masliah et al., 1997), enhancing neurite outgrowth (Ohsawa et al., 1997; Qiu et al., 1995), promoting synaptogenesis (Bell et al., 2006) and increasing neurogenesis (Caille et al., 2004).

sAPPα can consist of up to 6 different domains, although the predominant isoform of APP which is present in the CNS, APP695, does not contain the 4^{th} (KPI) or 5^{th} (OX-2) domains (Sandbrink et al., 1996). Thus sAPPα from APP695 can be divided into a growth factor like domain (D1), a copper binding region (D2), an acidic region (D3), and a carbohydrate domain (D6), with the carbohydrate domain further divided into an E2 domain (D6a) and a juxtamembrane region (D6b) (Reinhard et al., 2005; Storey and Cappai, 1999). It should also be noted that the combination of the D1 and D2 domains is sometimes referred to as the E1 domain (Soba et al., 2005). Only the D1, D2 and D6a domains participate in secondary structure formation with the D3 and D6b domains providing flexible linkers to connect the individual folding units (Reinhard et al., 2005) The beneficial actions of sAPPα have previously been linked to the D1 and D6a domains (Jin et al., 1994; Ohsawa et al., 1997; Qiu et al., 1995). However, their efficacy *in vivo,* and their ability to improve outcome following TBI, is yet to be determined. As such the

present study examined the effects of *in vivo* post-traumatic administration of the D1, D2 and D6a domains of sAPPα on functional outcome following severe impact acceleration TBI compared to that of animals treated with the full length sAPPα.

3.2 Experimental Design

3.2.1 Induction of Traumatic Brain Injury

A total of 90 adult male Sprague-Dawley rats weighing between 390- 460 g were randomly assigned into two broad groups, outcome studies (n=60) or histological studies (n=30). These animals were then further randomly assigned into sham, vehicle control, sAPPα, D1, D2 or D6a treatment groups (n=15). Animals were injured using the impact-acceleration model of diffuse traumatic brain injury as described in Section 2.3.2. Briefly, animals were anaesthetised with isoflurane and the skull exposed by a midline incision so that a stainless steel disc (10mm in diameter and 3mm in depth) could be fixed rigidly with polyacrylamide adhesive to the animal's skull centrally between lambda and bregma. The rats were subsequently placed on a 12cm foam bed and subjected to brain injury by dropping a 450g brass weight a distance of 2m onto the stainless steel disc. Sham operated animals were surgically prepared but were not injured.

Animals were treated with 25µM of either the D1 (APP28-123), D2 (APP124-189), D6a (APP316-498) domains of sAPPα, the full length peptide (APP18-611) or artificial CSF vehicle (Fig 3.1), via an intracerebroventricular (IVC) injection as described in Chapter 2. Following the injection, the rat was removed from the stereotaxic device, and the midline incision closed using 9-mm surgical clips. Rats

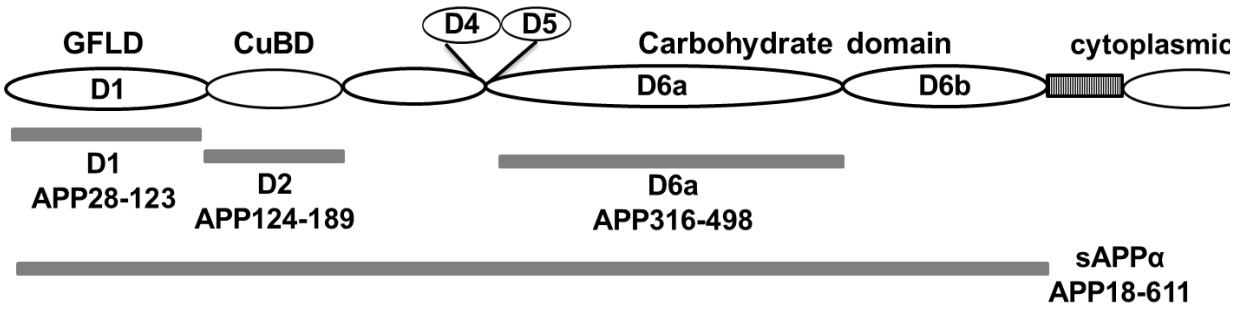

Fig 3.1: Schematic of the different peptides administered within this study

were maintained at a rectal temperature of 37°C throughout surgery, recovery, and drug administration using a thermostatically controlled heating pad.

3.2.2 Motor Outcome

Motor deficits produced by TBI were assessed using the rotarod, which consists of a motorised rotating assembly of eighteen 1mm metal rods. Rotational speed of the device was increased from 6 to 36 rpm in intervals of 3 rpm every 10 secs. The duration in seconds, up to a maximum of 120 secs, was recorded at the point when animals had either completed the task, clung to the rods for 2 consecutive rotations without actively walking or had fallen off. All animals were pre-trained daily on the device for 1 week prior to injury and assessed daily for 7 days after injury.

3.2.3 Cognitive Outcome

Cognitive deficits produced by TBI were assessed using the Y maze, which tests spatial and recognition memory. The maze consists of three arms with cylinders covered with a different tactile substance (bubblewrap, sandpaper or plastic) placed at the end of each arm. The arms are arbitrarily designated as the start, other and novel arms, with this randomly alternated among the rats.

In the first phase of the experiment, rats are introduced into the maze in which one of the arms (novel) has been closed and allowed to explore for 3 mins. This means that the animals were able to explore the start and other arms, but not the novel arm. An hour later the animals are placed back into the maze in their start arm with all the arms (start, other and novel) open and allowed to explore for another 3 mins. This test works on the basis that an uninjured animal will spend more time exploring the novel arm to which they have not been previously exposed, rather than the other two arms. In contrast an injured animal will spend an equal amount of time in each of the arms as they will not remember the maze. In order to remove scent trails the maze was wiped thoroughly with 70% alcohol after each trial. The experimenter was not in the room during the trials, with all trials captured on video, and the number of times each arm was visited and the time spent in each arm analysed. Animals that did not enter the novel arm during the first part of the experiment were not included.

3.2.4 Histological Analysis

Rats were sacrificed by perfusion at day 3 post-injury, as described earlier, with brains then blocked and embedded. For each animal a section was cut from the region -4.5 mm from the bregma, as this was located directly underneath the impact site. These sections were incubated overnight with a 1:1000 dilution of a biotintylated monoclonal antibody specific to APP (Novocastra 122703), followed by biotintylated secondary antibody (1:250 Sigma-Aldrich) and then streptavidin peroxidase conjugate. Bound antibody was detected with 3,3-diaminobenzidine tetrahydrochloride and sections were counterstained with haematoxylin. All slides were scanned (Nanozoomer, Hamamatsu, Japan) and viewed with the associated software to allow the number of APP immunopositive lengths along the corpus callosum to be counted.

3.2.5 Statistical Analysis

All parametric data were assessed using two-tailed unpaired student's t tests or analysis of variance (ANOVA -one or -two way and/or repeated measures as necessary), followed by Bonferonni tests for multiple comparisons. A p value of less than 0.05 was considered significant**.**

3.3. Results

3.3.1 The D1 and D6a domains of sAPPα are as effective as the full length peptide at improving motor outcome post-injury

Following TBI, motor outcome was determined using the rotarod (Fig 3.2), with sham rats performing at close to the maximum time of 120 secs, ranging from 111.5 secs to 118.7 secs over the testing period. The vehicle animals were significantly impaired on all days following injury ($p<0.01$), and although they did improve from 45 secs on day 1 to 85.5 secs on day 7 post-injury, they never returned to sham level. Similarly, the D2 treated rats (Fig 3.2C) were significantly worse than sham rats on days 1 to 5 following injury ($p<0.001$), with scores from 46.2 secs on day 1 to 94 secs on day 7. In contrast the D1 (Fig 3.2A) and D6a (Fig 3.2B) groups were almost identical to the sAPPα treatment group, being significantly different from shams only on day 1 post-injury. At this time point they were, however, still performing

significantly better than the vehicle ($p<0.001$) and D2 ($p<0.01$) treated animals with scores of 80 secs (sAPPα), 86 secs (D1) and 75 secs (D6a). By day 3 the times for the sAPPα, D1 and D6a groups were similar to those for sham animals at 113.7 secs, 108.6 secs and 108.2 secs respectively, and remained at this level for the week of assessment. Indeed, they were significantly different to vehicle treated animals on all days (1 to 7) post-injury ($p<0.01$). In contrast treatment with the D2 domain was ineffective, with these animals showing no significant difference as compared to the vehicle treated rats on all days tested.

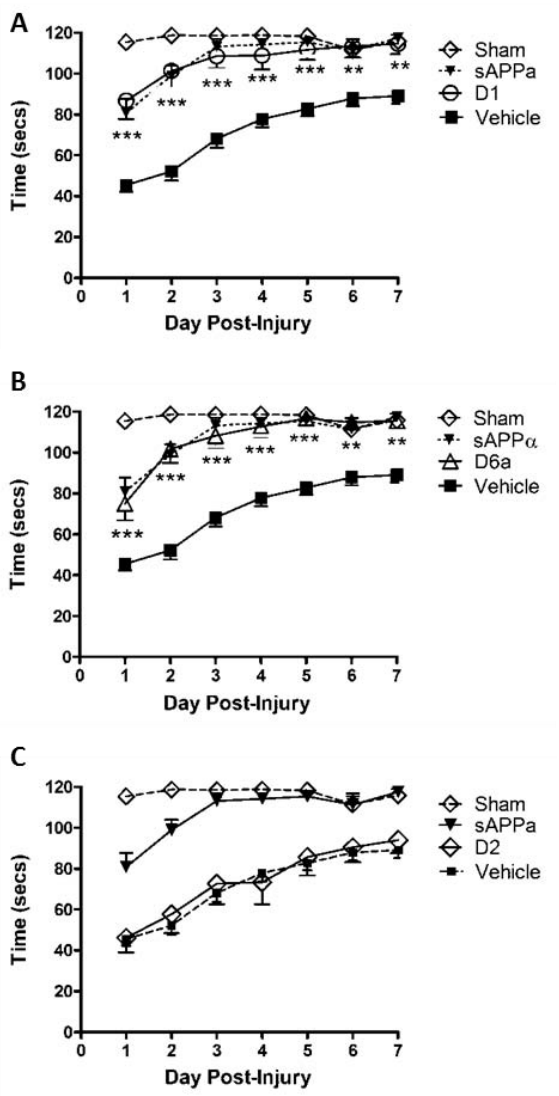

Fig. 3.2 Motor (rotarod) scores for rats following TBI, showing that whilst treatment with the D1 (A) or D6a (B) domains was as effective as the full length peptide at improving motor outcome following TBI, treatment with the D2 domain (C) had no effect. (n=10 per group)(*p<0.001, **p<0.01 compared to vehicle controls)**

3.3.2 The D1 and D6a domains of sAPPα are as effective as the full length peptide at improving cognitive outcome post-injury

Cognitive outcome was tested using the Y Maze on day 5 (Fig 3.3A) and 10 (Fig 3.3B) post-injury. At both day 5 and day 10 post-injury, the sAPPα, D1 and D6a treated rats were similar to sham animals in that they spent significantly more time ($p<0.01$) in the novel arm than either the start or other arm. Indeed the amount of time spent in the novel arm was similar in these groups with sham animals spending 80.33 secs on day 5 and 84.4 secs on day 10 in the novel arm compared to 83.22 and 81.67 secs for the sAPPα treated group, 89.1 and 75.91 secs in the D6a treated group and 85.4 and 83.4 secs for the D1 treated group. In contrast the vehicle and D2 treated animals did not spend significantly more time in any of the arms. On day 10 the vehicle treated animals spent 58.3 secs in the novel arm, 64.17 secs in the start arm and 57.5 secs in the other arm. Similarly at day 10 the D2 treated animals spent 64.3 secs in the novel arm,

54.1 secs in the start arm and 61.5 secs in the other arm. There was no significant difference between the groups in number of arm entries on either day 5 or 10 post-injury.

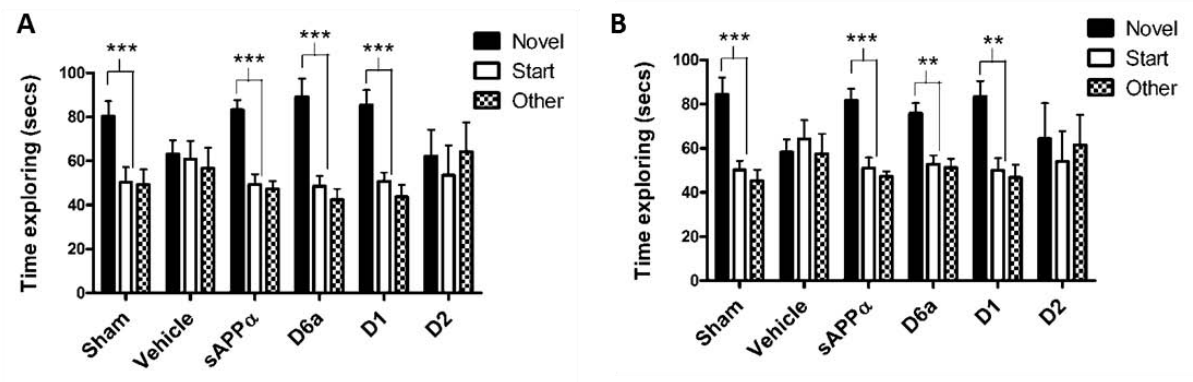

Fig. 3.3: Cognitive outcome (Y Maze) on day 5 (A) and 10 (B) following injury, showing that treatment with the D1 and D6a domains was as effective as the full length peptide at improving cognitive performance, with these rats spending significantly more time within the novel arm of the maze. In contrast D2 treated rats were indistinguishable from vehicle treated rats spending an equal amount of time within each of the arms. (vehicle, sAPPα and D6a groups n=10, Sham, D1 and D2 groups n=9) (*p<0.001 compared to start and other arms)**

3.3.3 The D1 and D6a domains of sAPPα are as effective as the full length peptide at reducing axonal injury post-injury

To determine if the improvement in motor function and cognition correlated to the neuroprotective activity of APP, axonal injury was determined by counting the numbers of APP immunopositive lengths within the corpus callosum (Fig 3.4 & 3.5). The vehicle and D2 treated animals had a significant increase ($p<0.05$) in the number of injured axons when compared to sham animals. In contrast, the sAPPα, D1 and D6a treated animals were not significantly different to sham controls and had significantly less injured axons than the vehicle or D2 treated animals ($p<0.05$).

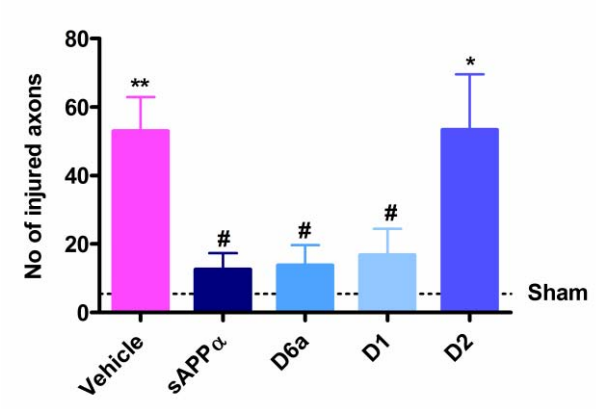

Fig 3.4: Axonal injury within the corpus callosum following TBI, showing a clear reduction within rats treated with either the D1 or D6a domain of sAPPα, but not the D2 domain. (n=5 per group) (*p<0.05, **p<0.01 compared to sham animals, #p<0.05 compared to vehicle controls)

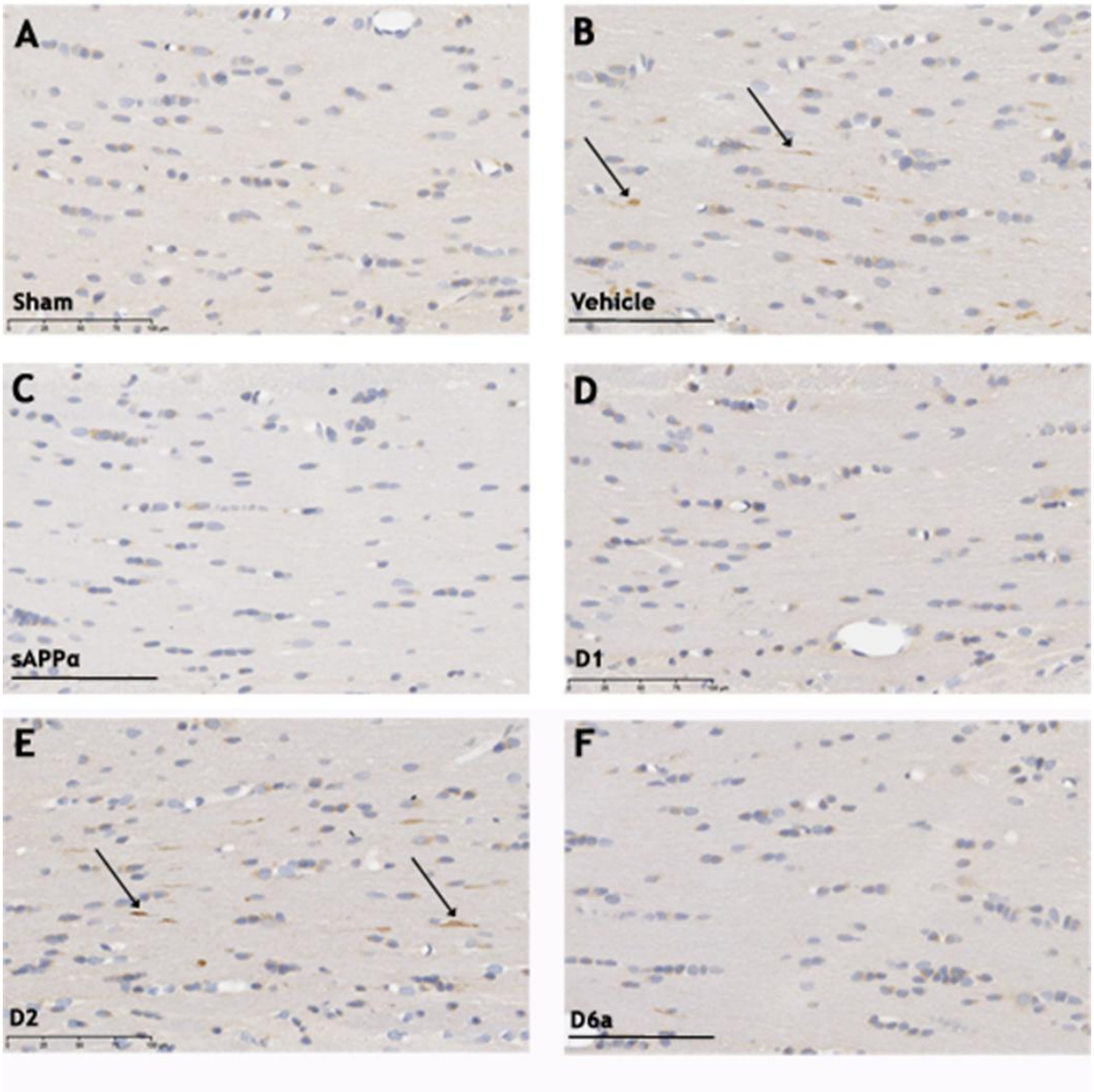

Fig 3.5: Representative micrographs showing the presence of a number of APP immunopositive lengths representing axonal injury within the corpus callosum of a vehicle treated rat. Treatment with the D1 or D6a domains of sAPPα, like the full length peptide, led to a decrease in the amount of axonal injury, whilst D2 domain treatment had no effect. (Arrows denote examples of APP immunopositive lengths) (Images are representative of n=5 per group)

3.4 Discussion

This study found that the D1 and D6a, but not the D2 domain of sAPPα were as effective as the full length peptide at improving outcome following TBI. Animals treated with the D1 and D6a domains showed a significant improvement in motor and cognitive outcome, with a corresponding decrease in axonal injury that was identical to that seen in those treated with sAPPα. Indeed these animals returned to a sham level of performance on the rotarod by day 3 post-injury and were indistinguishable from shams in their performance in the Y maze. In contrast treatment with the D2 domain had no effect, with these animals performing in an identical fashion to vehicle controls.

The neuroprotective properties of the D1 domain most likely relate to its heparin binding site, which spans residues 96-110 and contains a disulphide bridge (Rossjohn et al., 1999). Although this region has not previously been linked specifically to neuroprotective actions, it is known that the binding of this region to HSPGs promotes neurite outgrowth from central and peripheral neurons (Small et al., 1994). Furthermore, an antibody that binds to this region inhibits functional synapse formation (Morimoto et al., 1998) and completely abolishes depolarisation induced neurite outgrowth (Gakhar-Koppole et al., 2008).

Similar to D1, the neuroprotective properties of the D6a domain may relate to its heparin binding site which encompasses six basic residues from helices αC and αD of one monomer (Arg-375, His-382, Arg-424, Lys-428, His-432, His-439) and a conserved Arg-336 from helix αB′ of the second monomer (Wang and Ha, 2004). This region may regulate intracellular calcium since sAPPα reduces neuronal excitability, stabilises calcium homeostasis and protects neurons against excitotoxicity, most likely through activation of high conductance potassium channels which hyperpolarise the cell. These actions were blocked by an antibody that partially covers the heparin binding site (Mattson et al., 1993). Excessive calcium influx seen with excitotoxicity following TBI activates a number of destructive enzymes which can worsen secondary axotomy (Buki et al., 2006). Thus any reduction in calcium concentration due to the actions of this region would help maintain cytoskeletal integrity and reduce axonal injury. Furthermore, this region also has neurotrophic properties, whereby deletion of amino acids 305-591 abolished the promotion of neurite extension in cells exposed to APP (Qiu et al., 1995).

Alternatively, the D6a active site may involve the pentapeptide motif `RERMS' (a.a residues 328-332) which was originally found to be responsible for the growth regulating activity of APP in fibroblasts (Ninomiya et al., 1993). The same sequence can promote survival of rat cortical cells (Ohsawa et al., 1997; Yamamoto et al., 1994). An extended 17 mer peptide enhances synaptic density in the frontoparietal cortex of rats with an associated increase in memory retention (Roch et al., 1994). The surrounding amino acids may contribute to the biological activity of the RERMS sequence, as neurite extension activity in B103 cells was enhanced with longer sequences, than RERMS alone (Jin et al., 1994). However, other studies have found that small peptides encompassing the RERMS sequence did not protect cells against glutamate or Aβ toxicity (Furukawa et al., 1996) or promote neurite outgrowth in cultured rat neurons (Ohsawa et al., 1997).

The D2 domain, which does not contain a heparin binding site, had no effect on functional outcome or the amount of injured axons following TBI. This supports the model that the protective properties of sAPPα may relate to its heparin binding sites contained within the D1 and D6a domains. Heparin and heparin sulphate are components of the glycosaminoglycan sidechains of proteoglycans which are present in cell membranes, extracellular matrices and basement membranes. The majority of binding sites for APP in the extracellular matrix are these HSPGs (Ninomiya et al., 1994), with the interaction of APP with HSPGs promoting cell adhesion, neuron-cell or cell-matrix interactions (Reinhard et al., 2005), which are important for a number of functions including cell signaling and growth. The role of heparin binding sites in facilitating the neuroprotective activities of sAPPα were highlighted by the ability of heparinases to prevent the ability of sAPPα to protect cultured cells from a number of insults including glutamate toxicity and glucose deprivation (Furukawa et al., 1996). In addition, binding of the heparin like molecules glypican and perlecan was capable of inhibiting APP-induced neurite outgrowth, presumably by competing with endogenous proteoglycans which mediate this activity (Williamson et al., 1996).

Binding to heparin also appears to induce dimerisation, with this phenomenon occurring with an extended version of the D1 domain (D1 and D2 domains) (Dahms et al., 2010 ; Soba et al., 2005) and the D6 domain (Wang and Ha, 2004). This could potentially initiate intracellular signaling cascades important for physiological cellular events, although these have yet to be fully elucidated (Reinhard et al., 2005). Indeed, the effects of sAPPα may be mediated in part through an interaction with full length membrane bound APP (Gralle et al., 2009; Young-Pearse et al., 2008), with heparin induced dimerisation a possible mechanism of action.

This study shows that the D1 and D6a domains are as effective as full length sAPPα at improving functional outcome and reducing axonal injury following TBI. As the D1 and D6a domains contain heparin binding sites, but the inactive D2 does not, this suggests the neuroprotective ability of sAPPα may relate to its ability to bind HSPGs. Further research on the exact mechanisms on how the binding of sAPPα to HSPGs provides neuroprotection may allow the development of exogenous agents to improve functional outcome following TBI.

Characterisation of the effect of knockout of the amyloid precursor protein on outcome following mild traumatic brain injury

4.1 Introduction

The previous chapter delineated the regions within sAPPα that can confer neuroprotection when applied exogenously. However, the role of endogenous APP following TBI has yet to be fully elucidated. After TBI, a number of neuroprotective and neurotrophic pathways are activated in response to this injury in order to facilitate a reparative response. It is thought that APP, through its metabolite sAPPα, may be involved in these processes as it is acutely upregulated within injured neurons and reactive astrocytes following TBI (Chen et al., 2004; Van den Heuvel et al., 1999). Indeed this significant post-traumatic upregulation appears to be a normal acute phase response to neuronal stress (Gentleman et al., 1993a), with a similar increase seen in cells exposed to ischaemia (Nihashi et al., 2001; Popa-Wagner et al., 1998) and excitotoxicity (Gordon-Krajcer and Gajkowska, 2001). The functional significance, however, remains poorly understood.

As outlined in chapter 1, the majority of APP is processed within the non-amyloidogenic pathway via the action of α secretase, to form the protective α form of APP (sAPPα) (Suh and Checler, 2002), whilst a small proportion is cleaved by β and γ secretases within the amyloidogenic pathway to produce toxic Aβ (Koo et al., 1996), the main component of plaques associated with Alzheimer's disease. The disparate actions of these APP metabolites highlights why the role of APP following TBI remains controversial.

It has been proposed that the upregulation of APP seen following TBI is associated with increased hippocampal cell death (Murakami et al., 1998). This was attributed to an increase in the production of Aβ, which may be facilitated by a transient elevation in β-secretase activity post-injury (Blasko et al., 2004). Indeed co-accumulation of Aβ with APP in swollen axons and neuronal cell bodies has been observed within days in both rodent (Stone et al., 2002) and swine models (Chen et al., 2004; Smith et al., 1999) of diffuse TBI. In swine sparse diffuse Aβ plaques were also observed up to 6 months following injury, the first animal model to replicate findings that Aβ plaques are found in up to 30% of people who die acutely of TBI (Roberts et al., 1991). Reports on levels of soluble Aβ following human TBI have been contradictory with Brody *et al* finding a persistent decrease in intraparenchymal levels, whilst Markland *et al* found no change (Brody et al., 2008; Marklund et al., 2009). Similarly, within the ventricular cerebrospinal fluid, both an increase (Olsson et al., 2004; Raby et al., 1998) and a decrease (Kay et al., 2003) in levels of Aβ have been reported. Regardless, a direct

link between increased levels of APP, enhancement of Aβ production and toxicity has never been demonstrated (Iwata et al., 2002).

Alternatively, it is thought that the upregulation of APP following TBI may represent a protective cellular response, with sAPPα shown to attenuate neuronal cell death induced by excitotoxicity, ischaemia and oxidative stress (Furukawa et al., 1996; Goodman and Mattson, 1994; Mattson et al., 1993). In addition sAPPα can promote repair processes, through its well characterised effects on neurite outgrowth (Ohsawa et al., 1997; Qiu et al., 1995; Wang and Ha, 2004), synaptogenesis (Bell et al., 2006) and neurogenesis (Caille et al., 2004). The importance of APP post-injury was highlighted by the finding that knocking out the APP orthologue in *Drosophilia*, APPL, leads to an increase in mortality compared to wild-type flies at 1 and 2 weeks following brain trauma induced by a needle injury (Leyssen et al., 2005). Therefore the aim of the current study was to assess the importance of endogenous APP by determining whether knockout of APP would worsen functional outcome, increase neuronal damage and inhibit the reparative response following mild diffuse TBI (mTBI) in mice.

4.2 Materials and Methods

Generation of APP-/- mice has been described previously (Zheng et al., 1995), with both the APP+/+ and APP-/- mice being on the same background strain, C57BLbj x 129sv. All studies were performed within the guidelines established by the NHMRC of Australia and were approved by the Animal Ethics Committees of the Institute of Medical and Veterinary Sciences and the University of Adelaide.

4.2.1 Induction of Traumatic Brain Injury

A total of 30 APP+/+ and 30 APP-/- male mice were used in this experiment comprising 20 injured and 10 uninjured mice. Injury was induced using a modified version of the Marmarou model of diffuse axonal injury (Marmarou et al., 1994). Ten to sixteen week old mice were anaesthetised with isoflurane and the skull exposed by midline incision so that a stainless steel disc (1mm in diameter, 1mm thick) could be fixed rigidly to the mouse's skull centrally between the lambda and bregma. After being placed on a foam bed, injury was induced by dropping a 95g steel weight from 1.2 or 1.3m, with the APP-/- mice injured from the lower height.

In other models of TBI, such as the closed head injury model, it has been found that knockout strains can display different susceptibility to the impact (Flierl et al., 2009). This was of particular concern due to reported differences in brain weight of around 10% in APP-/- mice (Ring et al., 2007), which correspond with overall decreases in body weight. Indeed in this study the APP-/- mice were approximately 10% lighter than APP+/+ mice (APP+/+ 29.2±1.42g, APP-/- 26.2±2.36g). Thus the injury parameters were adjusted so that the level of primary injury in the wildtype and knockout animals was the same, by ensuring that time for the righting reflex to return was the same. The righting reflex has been shown to be a reliable indicator of injury severity (Fujimoto et al., 2004; Hallam et al., 2004) and is measured as the time taken for an animal to return to a spontaneous upright position following injury. With the injury parameters stated, as to deliver 10% less force to APP-/- mice, there was no significant difference between righting times between APP-/- (329±33 secs) and APP+/+ mice (348±52 secs), although both were significantly greater than their shams (APP+/+ 135±31 secs; APP-/- 127±26 secs).

4.2.2 Motor Outcome

Post-traumatic motor deficits were assessed using a rotarod device. Briefly, this device consists of a motorised assembly of 12 rods that are 0.2mm in diameter, which increases in speed from 0 to 30 rpm at a rate of 3rpm/10 secs. The mice were required to walk on the rods, with the latency to fall from the rotating bars or to grip the rods and spin two consecutive rotations recorded. APP+/+ mice were expected to complete 180 secs on the rotarod, whilst APP-/- mice were only expected to complete 120 secs due to the forearm weakness that is part of their phenotype (Zheng et al, 1995). All mice were pre-trained daily for 5 days, with their best time taken as their pre-injury baseline level and then assessed for 7 days after injury.

4.2.3 Cognitive Outcome

The Barnes maze paradigm exploits the natural inclination of small rodents to seek escape to a darkly lit, sheltered environment (Barnes, 1979) and consists of a white circular platform elevated above the floor, from which the mouse could escape into 1 of 40 holes evenly spaced around the perimeter. The escape hole was connected to an escape box with distinct spatial clues located all around the maze to aid the mice in finding the correct hole. As such mice have to use a hippocampal dependent spatial strategy in order to find the escape hole (Koopmans et al., 2003).

The Barnes Maze protocol has been described within Chapter 2. Animals were pre-trained for 5 days prior to injury, with their best time taken as their pre-injury baseline level. Assessment was conducted on days 2, 4 and 6 post-injury, with escape latency (time in seconds) for the mice to find and enter the escape box with front paws and trunk recorded, as well as the number of errors, which were counted each time the mouse placed its head within a hole which did not contain the escape box.

On day 7 post-injury the escape box was switched to a different, randomly chosen hole to test the ability of mice to learn a new spatial contingency. Mice were allowed three trials, spaced 1 hr apart, to learn the location of the new hole with their escape latency recorded as above.

4.2.4 Histological Analysis

Mice were transcardially perfused with 10% formalin on day 3 or 7 post-injury. Serial sections of 5µm thickness were taken from paraffin embedded tissue in the region -2.1mm from the bregma, with this region directly underneath the impact site, and stained with standard H&E, GAP-43 (1:1000) or synaptophysin (1:1000). Following overnight incubation with either of the specific monoclonal antibodies, secondary antibody was applied (1:250), followed by streptavidin peroxidase conjugate, with bound antibody then detected with 3,3-diaminobenzidine tetrahydrochloride and sections counterstained with haematoxylin.

These slides were digitally scanned (Nanozoomer, Hamamatsu) and images exported as a jpeg file using the software associated with the slide scanner. For GAP-43 analysis the entire CA1 region was photographed sequentially with each image then cropped to contain only the pyramidal layer of the hippocampus, with the average value across the CA1 region determined. For synaptophysin analysis, the CA1 region was also sequentially photographed, with the stratum pyramidale and radiatum layers subjected to analysis. DAB and haematoxylin were separated using Ruifork and Johnston's colour deconvolution method (Ruifrok and Johnston, 2001), with 2 slides per stain analysed for each animal and an average taken to determine the final %DAB weight.

Sections were also stained with H&E to assess neuronal numbers within the selectively vulnerable CA3 region of the hippocampus and the cortex directly underneath the impact site on the right side

analysed (Fig 4.1). The CA3 region was sequentially imaged at 40x magnification and digitally reconstructed into a montage, to allow manual counting of the neurons using the cell count software associated with Image J. Similarly, 4 macroscopic fields (40x) directly underneath the impact site were examined. For each animal 2 slides were counted and the average then taken. Only histologically normal appearing neurons with a clearly defined cell body and nucleus were counted, those that were only partially seen due to the level of sectioning were not included nor were those that appeared pyknotic (dark, shrunken with no visible nucleus).

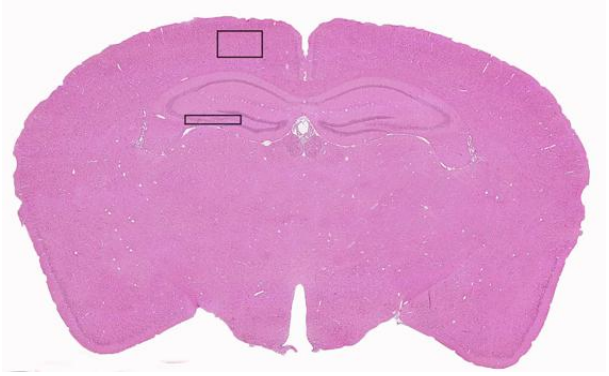

Fig 4.1: Micrograph showing the regions that were used to determine the number of healthy neurons within APP+/+ and APP-/- mice following TBI

4.2.5 Caspase- 3 ELISA

At either day 3 or 7 post-injury (n=5 per group) mice were re-anaesthetised with isoflurane, decapitated and the brain removed. The hippocampus and the region of cortex directly under the impact site were dissected and rapidly frozen in liquid nitrogen. Following homogenisation, the amount of protein was determined using the Biorad protein assay, with each sample diluted with TBS to 400ng protein per 100µl of TBS. 100µl of each sample was loaded in triplicate, and the wells blocked with 0.2% gelatine before being incubated with anti-active caspase 3 (1:1000 BioVision). Secondary anti-rabbit horseradish peroxidise conjugate (1:2000 Rockford) was added before the liquid substrate system 3,3'5,5'-tetramethylbenzidine (Sigma) was used to reveal protein expression. The reaction was stopped after 100 secs with 0.5M sulphuric acid and levels of expression determined by reading absorbance at 450nm on an Ascent Multiscan plate reader. To demonstrate reproducibility the ELISA was conducted 3 times.

4.2.6 Statistical Analysis

All data was analysed using a two-way ANOVA (repeated measures for functional outcome data) followed by Bonferonni t tests using Graphpad Prism software. A p value of less than 0.05 was considered significant in all experiments.

4.3 Results

4.3.1 APP-/- Mice Have Impaired Motor Outcome following mTBI

Motor outcome was determined using the rotarod. Results are expressed as a percentage of each mouse's own pre-injury baseline level, to compensate for phenotypic affects as APP-/- mice demonstrate forearm weakness (Zheng et al., 1995). Although there is a significant difference between APP-/- and APP+/+ sham animals when the data is expressed as raw scores (Fig 4.2A), there is no significant difference when expressed as a percentage of each mouse's own baseline level (Fig 4.2B), allowing a direct comparison between APP-/- and APP+/+ injured mice. This injury model did not produce detectable motor deficits in APP+/+ mice, with these mice performing at between 101.02% and 103.14% of their pre-injury time (Fig 4.2B). In contrast, injured APP-/- mice remained significantly impaired on all days of testing post-injury when compared to their shams ($p<0.05$) and to the injured APP+/+ mice ($p<0.05$). Although the APP-/- mice improved over the testing period from 75.15% of pre-injury level on day 1 to 86.51% on day 7, they did not return to an uninjured baseline level.

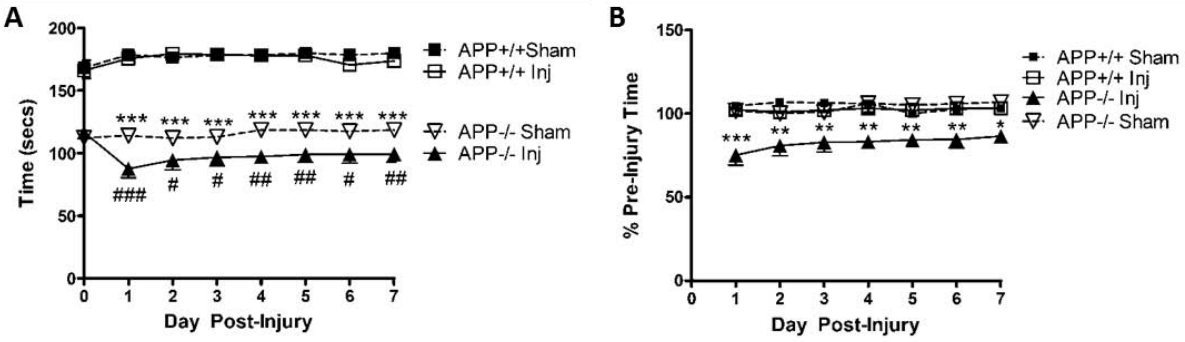

Fig 4.2: Motor outcome, as assessed on the rotarod, expressed as raw scores (A) and % pre-injury time (B). APP-/- mice have a small, but significant, impairment in motor performance following TBI, which was not present in APP+/+ mice. Results are expressed as means ± SEM. (n=8 per group) (*p<0.001 compared to APP+/+ shams, ###p<0.001, ##p<0.01, #p<0.05 compared to APP-/- shams (A); ***p<0.001, **p<0.01, *p<0.05 compared to APP+/+ injured mice (B)).**

4.3.2 APP-/- Mice Have Impaired Cognitive Outcome Following mTBI

The cognitive performance of the mice post-injury was measured using the Barnes Maze, which assesses the ability to find a previously learned escape hole. There were no significant differences between APP-/- and APP+/+ shams, with both groups showing improvement in escape latency compared to their pre-injury time, APP-/- shams from 38.6.1 to 22.3 secs and APP+/+ shams from 34.5 to 16.1 secs (Fig 4.3A). Although injured APP+/+ mice were not significantly different to their shams on any day tested post-injury there was an increase in the escape latency on day 2 following injury, in 44 secs compared to 23.6 secs in APP+/+ shams at this time point. Injured APP+/+ mice then returned to sham level taking 24.0 and 15.5 secs to locate the escape hole on days 4 and 6 post-injury compared to 16.25 and 22 secs in their shams. In contrast the APP-/- mice were significantly impaired when compared to injured APP+/+ mice on days 2, 4 and 6 post-injury ($p<0.05$). However, they did improve over the testing period; with an escape latency of 71.37 secs on day 2 compared to 51.02 and 41.75 secs on days 4 and 6.

The ability of mice to learn a new location for the escape hole over 3 trials is shown in Fig 4.3B. The APP+/+ injured mice were no different to their shams with performance improving steadily over the 3 trials from 73.75 secs on trial 1 to 31.625 secs by trial 3, compared to 83.62 secs to 25.37 secs in APP+/+ shams. On the other hand APP-/- mice were significantly impaired in their ability to learn the new location, seen as a significant increase in the amount of time taken on trial 2 when compared to APP-/- shams ($p<0.05$) and APP+/+ injured mice ($p<0.05$). However, by the third trial there were no differences between the 4 groups.

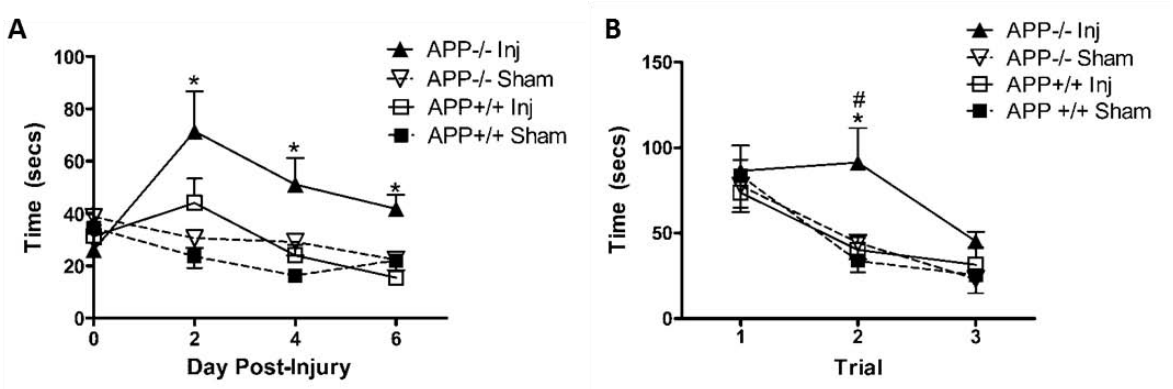

Fig 4.3: Cognitive outcome as determined by escape latency (A) and ability to learn a new spatial contingency (B) on the Barnes Maze. Results are expressed as means ± SEM (APP+/+ sham, APP-/- sham, APP-/-inj n=8 per group; APP+/+ inj n=7). (*p<0.05, **p<0.01 compared to injured APP+/+ mice, #p<0.05

compared to APP-/- shams)

4.3.3 APP-/- Mice Have Increased Neuronal Loss Following mTBI

Vulnerability of cells post-injury was assessed by evaluating the number of healthy neurons within the CA3 region of the hippocampus (Fig 4.4) and the cortex directly under the impact site (Fig 4.5). Following injury the CA3 region of the APP+/+ mice looked similar to their sham controls, whereas in the APP-/- mice there were increasing numbers of pyknotic neurons from 3 to 7 days with evidence of neuronal loss by day 7 post-injury (Fig 4.5). Similarly within the cortex although APP+/+ mice had some pyknotic neurons and appeared to have have some neuronal loss, this was exacerabated in APP-/- mice. Indeed at day 3 post-injury there appeared to be greater numbers of pyknotic neurons and by day 7 there appeared to be less neurons within this area of the cortex directly underneath the impact site. These observations were confirmed by a count of the number of healthy neurons within the CA3 region (Fig 4.6G) and cortex underneath the impact site (Fig 4.6F), with APP-/- mice exhibiting significantly lower numbers at 3 and 7 days post-injury at both these sites ($p<0.05$).

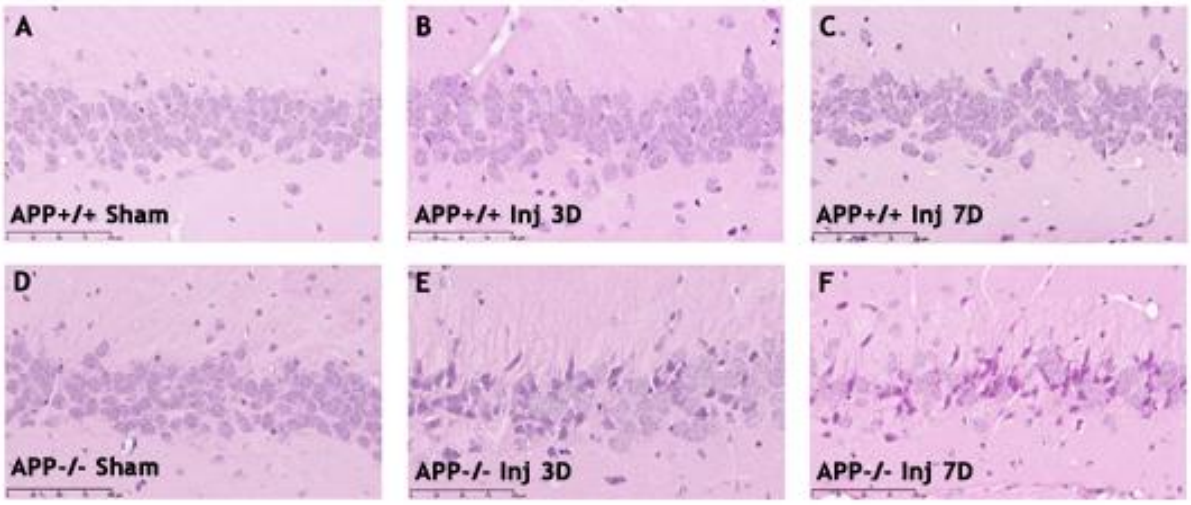

Fig 4.4: H&E labeled sections within the CA3 region of the hippocampus. Compared to APP+/+ (A) and APP-/- (D) shams, greater cell damage is evident in APP-/- mice at 3 (E) and 7 (F) days post-injury, than in APP+/+ mice at these time points (B&C) (Images are representative of n=5 per group) (scale bar = 100µm).

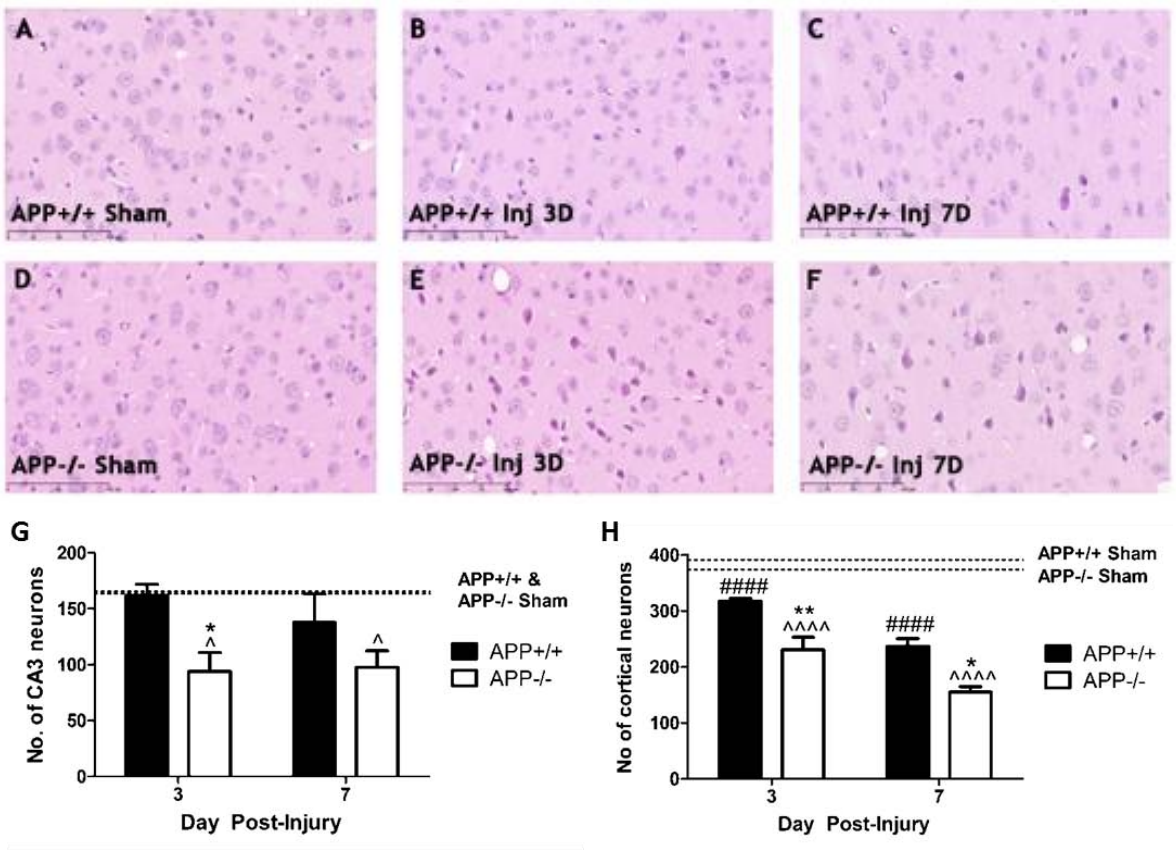

Fig 4.5: H&E labeled sections within cortex directly underneath the impact site (A-F). Compared to the APP+/+ (A) and APP-/- (D) shams, neuronal damage is evident in APP+/+ mice increasing from 3 (B) to 7 (C) days post-injury. However, neuronal damage is exacerbated in APP-/- mice with greater amounts of damage at both 3 (E) and 7 (F) days. (scale bar = 100µm). These observations were confirmed with neuronal counts within the CA3 region of the hippocampus (G) and cortex underneath the impact (H), showing that APP-/- have significantly greater neuronal damage than APP+/+ mice in both these regions. (n=5 per group). (*p<0.05, **p<0.01 compared to injured APP+/+ mice; ^^^^p<0.0001, ^ p<0.05 compared to APP-/- shams; ####p<0.0001 compared to APP+/+ shams)

4.3.4 APP-/- Mice Have Decreased GAP-43 Expression Following mTBI

Levels of GAP-43 within the hippocampus and cortex were used to determine the strength of the reparative response seen post-injury (Fig 4.6). GAP-43, is a neural specific membrane associated phosphoprotein which is one component of injury-induced plasticity as it is associated with promotion of neuronal sprouting and neurite extension which facilitate synaptic remodelling (Bendotti et al., 1997). The APP+/+ animals had an upregulation of GAP-43 within the CA1 region of the hippocampus at days 3 and 7 following injury and in the cortex at day 7 post-injury, with levels clearly higher than that seen in the APP+/+ or APP-/- shams. In contrast GAP-43 remained at sham level at both time points in APP-/- animals following mTBI. This observation was supported with

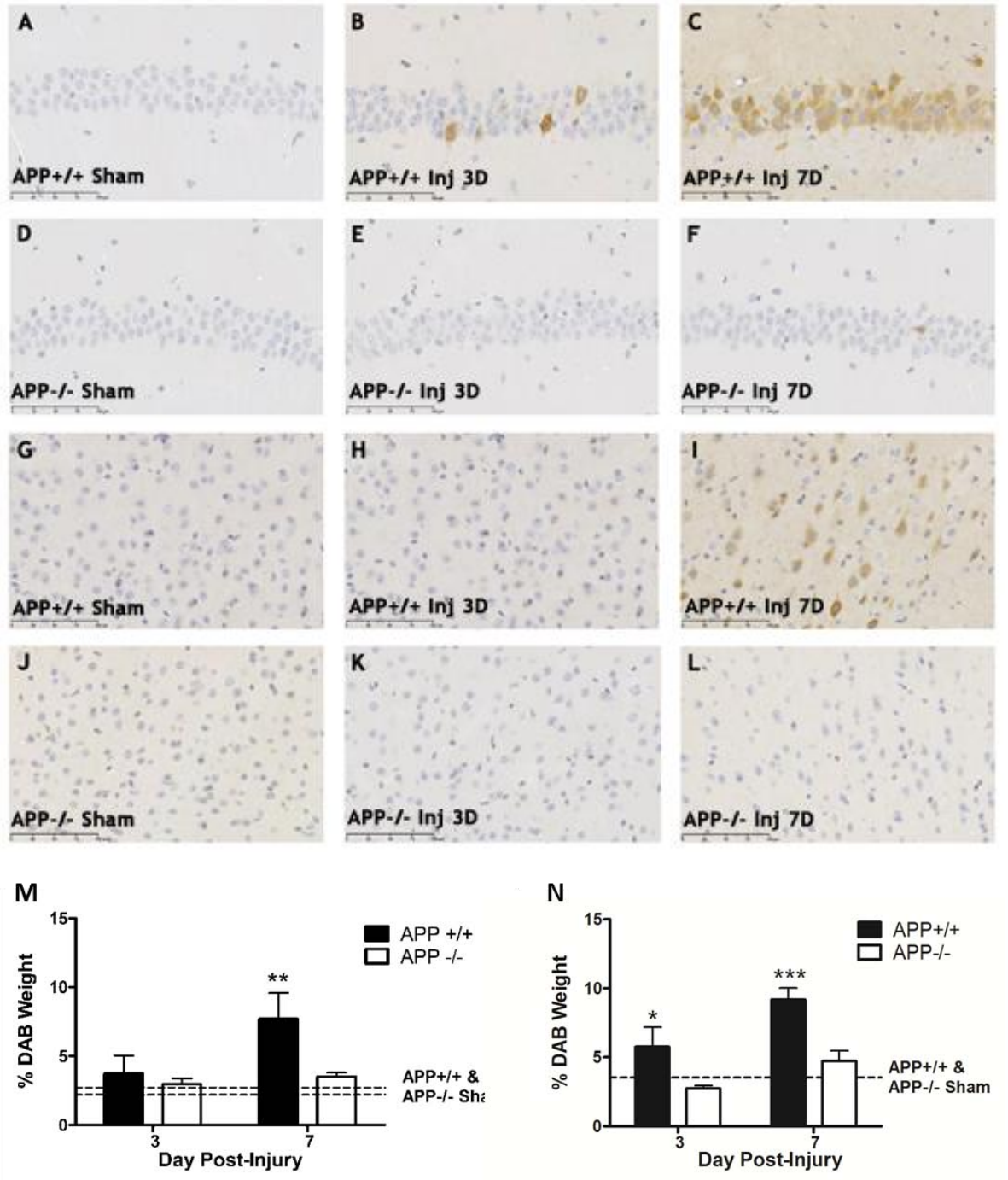

Fig 4.6: GAP-43 immunolabeled sections within the CA1 region of the hippocampus (A-F) and cortex (G-L). Within the hippocampus levels of GAP-43 are increased in APP+/+ mice at 3 (B) and 7 (C) days post-injury when compared to their shams (A), whilst in APP-/- mice levels at 3 (E) and 7 (F) days post-injury resemble those in APP-/- shams (D). Similarly, there is no increase in levels of GAP-43 evident in APP-/- mice at either 3 (K) or 7 (L) days post-injury in the cortex underneath the impact site when compared to their shams (J), whilst in APP+/+ mice a clear increase is evident by day 7 post-injury (I) when compared to APP+/+ shams (G). Scale bar = 100µm. These observations were confirmed with colour deconvolution within the CA1 region of the hippocampus (M) and cortex (N), showing that levels of GAP-43 are increased in APP+/+, but not APP-/- mice following injury. (n=5 per group). (*p<0.05, ***p<0.001 compared to APP+/+ injured mice)

colour deconvolution showing a significant increase in %DAB weight at day 3 and 7 following TBI in the CA1 region in the APP+/+ animals ($p<0.05$) (Fig 4.7M). Indeed levels in the APP+/+ animals, at 9.17%, were almost double that of the APP-/- animals, at 4.74%, at day 7 post-injury. Similarly in the cortex a significant upregulation occurred at day 7 following TBI ($p<0.01$) with APP+/+ animals having a DAB weight of 7.7% compared to 3.5% in APP-/- animals (Fig 4.7N).

4.3.5 APP-/- Mice Have Decreased Synaptophysin Levels Following mTBI

Synaptophysin levels were examined within the CA1 region of the hippocampus (Fig 4.7 & 4.8) in order to evaluate the effects of injury induced neuronal remodelling and rearrangement on synapse numbers (Masliah, 1990), with synaptophysin levels shown to increase following injury (Thompson, 2006). There was no obvious differences between APP+/+ and APP-/- shams. At day 3 post-injury both APP+/+ and APP-/- animals had a similar staining pattern to sham animals. However by day 7 APP+/+ animals

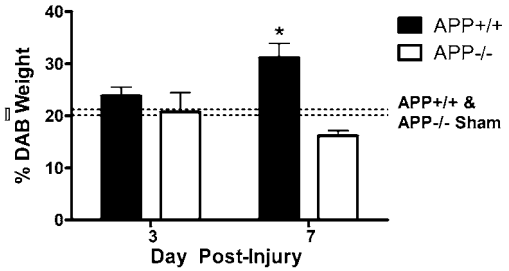

Fig 4.7: Colour deconvolution of synaptophysin immunohistochemistry shows a significant increase in APP+/+, but not APP-/- mice at 7 days post-injury. (n=5 per group) (*p<0.05 compared to APP-/- injured mice).

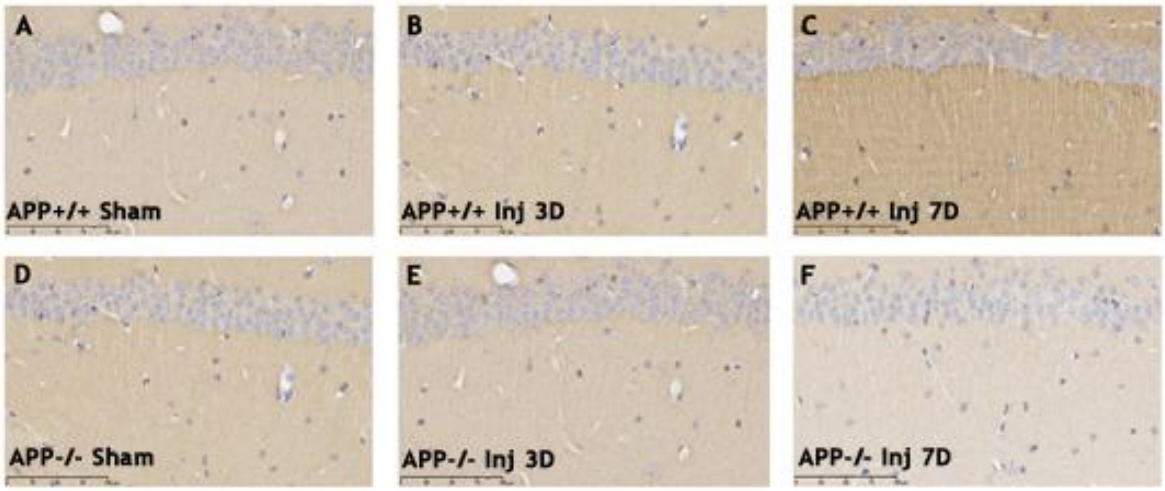

Fig 4.8: Synaptophysin immunolabeled sections within the CA1 region of the hippocampus (40x). No changes in synaptophysin levels are evident at 3 days post-injury in APP+/+ (B) or APP-/- (E) mice when compared to their respective shams (A&D). However by day 7 post-injury an increase in synaptophysin can be seen in APP+/+ mice (C), whilst levels appear slightly decreased in APP-/- mice (F).(Images are representative of n=5 per group) Scale bar = 100µm

had an obvious increase in immunostaining, whilst APP-/- animals appeared to have a slight decrease in synaptophysin levels (Fig 7A-F). This was corroborated with colour deconvolution (Fig 4.8), which showed a significant increase in the APP+/+ animals at day 7 following injury ($p<0.05$), with a %DAB weight of 31.33% compared to 18.16% in the APP-/- animals.

4.3.6 APP-/- Mice Have Increased Levels of Activated Caspase-3 Following TBI

Levels of activated caspase-3 were determined within the hippocampus (Fig 4.9A) and cortex (Fig 4.9B) in order to reflect apoptotic cell death following injury using an ELISA. The APP-/- mice had significantly higher levels at day 3 post-injury in the hippocampus ($p<0.001$) and cortex ($p<0.01$) when compared to APP+/+ mice. At this time point activated caspase-3 levels were 3 times higher in the cortex, and 2 times higher in the hippocampus in the APP-/- mice. By day 7, levels remained elevated in the APP-/- mice, with an absorbance level of 0.314 in the hippocampus compared to 0.218 in the APP+/+ mice, with a similar pattern in the cortex, with APP-/- mice at 0.224 compared to 0.163 in the APP+/+ mice, but this was not significant. There was no significant difference in activated caspase-3 levels between APP+/+ and APP-/- shams.

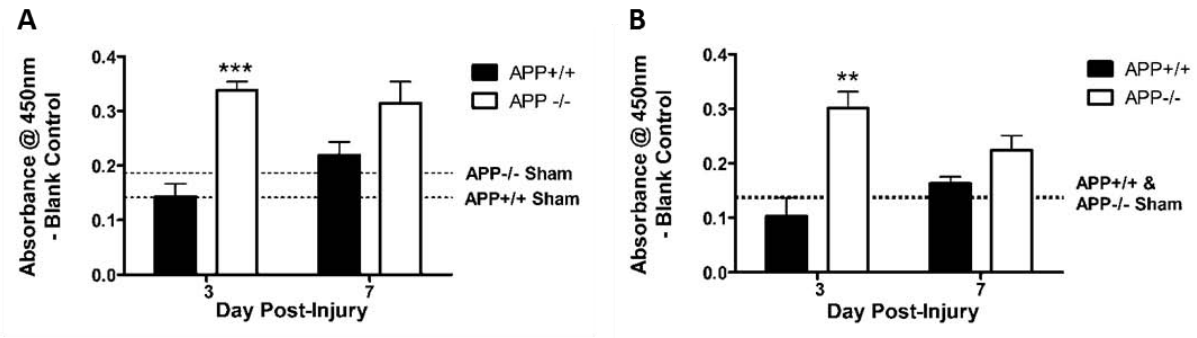

Fig 4.9: Levels of activated caspase-3 within the hippocampus (A) and cortex (B), showing a significant increase in APP-/- but not APP+/+ mice at day 3 post-injury. (n=5 per group)(p<0.01, ***p<0.001 compared to APP+/+ injured mice)**

4.1 Discussion

This study demonstrates that lack of APP appears to make mice more vulnerable following mTBI, with APP-/- mice demonstrating greater functional deficits, increased vulnerability of neurons and an impaired reparative response. This model of mTBI allows the study of the role of endogenous

neuroprotective pathways without the complications of large amounts of tissue loss, representing a situation similar to a mild concussive injury in humans.

Following injury, APP+/+ mice had significant cortical cell loss under the impact site and a non-significant increase in escape latency on day 2 following injury when compared to their shams. In contrast APP-/- mice had a significant increase in escape latency on the Barnes Maze on days 2-6 post-injury, which was associated with an increase in the number of errors, which reached significance on day 4. They also displayed significant impairment in learning a new spatial contingency when the escape hole was moved. In addition APP-/- mice had a small but significant impairment in rotarod performance in the first week post-injury. These cognitive and motor deficits were correlated with increased neuronal cell loss, an increase in levels of active caspase-3 and a decrease in levels of GAP-43 and synaptophysin when compared to APP+/+ mice.

The changes seen in APP-/- mice cannot be accounted for by a more severe injury, as the APP-/- mice were injured from a lower height than the APP+/+ mice in part to compensate for reported differences in brain weight. This was calibrated to ensure that both APP+/+ and APP -/- mice had a similar time for the righting reflex to return, as this has been found to be a reliable indicator of injury severity (Fujimoto et al., 2004; Hallam et al., 2004). Thus as the level of primary injury was the same, exacerbation of deficits in the APP-/- mice can be assumed to be caused by changes in the level of secondary injury sustained**.** Indeed, despite the lower height from which the weight was released, APP-/- mice demonstrated more severe histological and functional deficits. Furthermore the APP-/- phenotype, which includes forearm weakness (Zheng et al., 1995) and age related cognitive deficits (Dawson et al., 1999) is not the cause of the impairments observed in these mice following injury. Although there is a difference between APP+/+ and APP-/- sham animals in terms of raw rotarod scores, only the APP-/- injured animals demonstrated a motor deficit following injury. Furthermore, at this age (10-16 weeks), the APP-/- animals did not demonstrate cognitive deficits on the Barnes Maze, with no significant differences between escape latency in APP+/+ and APP-/- sham animals.

The exacerbation in functional deficits was associated with increased neuronal damage and elevated levels of active-caspase 3 in APP-/- mice following injury. The increased vulnerability of cells post-injury is most likely due to the lack of neuroprotective sAPPα. Adding sAPPα to cultured neuronal cells increases their resistance to excitotoxic, metabolic and oxidative insults (Furukawa et al., 1996; Goodman and Mattson, 1994; Mattson et al., 1993), whilst ICV infusion of sAPPα decreases levels of

neuronal death following TBI (Thornton et al., 2006), and transient global cerebral ischaemia (Smith-Swintosky et al., 1994).

In addition to increasing the vulnerability of cells, the lack of APP impedes the ability to initiate a reparative response, in the current study this was reflected by a decrease in levels of GAP-43 and synaptophysin in the APP-/- mice post-injury when compared to APP+/+ mice. GAP-43 is elevated following TBI (Christman et al., 1997; Emery et al., 2000; Hulsebosch et al., 1998; Thompson et al., 2006), and is associated with the period of synaptic organisation and axonal organisation (Bendotti et al., 1997). This occurs through its ability to promote neuronal sprouting and neurite extension and to enhance synaptic remodelling through formation of novel neuronal connections (Bendotti et al., 1997), although this response may be inhibited with increasing injury severity (Thompson et al., 2006). Previous studies have shown that cells that are GAP-43 positive are responsible for formation of new axon collaterals following transection of mature axons in CA3 pyramidal cells (McKinney et al., 1999) and lesions of the perforant pathway (Lin et al., 1992). The lack of GAP-43 in APP-/- mice following injury can be seen as an inhibition of axonal plasticity that would normally occur in response to post-traumatic axonal damage.

The suppression of synaptophysin upregulation may also reflect impaired hippocampal synaptic remodelling. Synaptophysin is a calcium binding glycoprotein found in membranes of pre-synaptic vesicles in neurons (Navone et al., 1986) and can be used as a marker protein to quantify synapse numbers (Loncarevic-Vasiljkovic et al., 2009; Shojo and Kibayashi, 2006). Levels of synaptophysin increase following permanent focal ischaemia (Stroemer et al., 1995) and moderate CCI (Thompson et al., 2006). This correlates with the increase in synaptogenesis seen in the CA1 region from day 10 to 60 following moderate CCI as determined by counting total synapse numbers through stereology and transmission electron microscopy (Scheff et al., 2005). Following injury the hippocampus undergoes extensive and long-lasting synaptogenesis and synaptic reorganisation, which is impaired in APP-/- mice. This may relate directly to the failure to upregulate GAP-43, as this facilitates synaptogenesis by promoting hippocampal axonal sprouting (Thompson et al., 2006). This is seen in the APP+/+ mice where GAP-43 levels are increased at day 3 before an increase in synaptophysin is seen at day 7 following injury.

The deficits seen in these APP-/- mice can be attributed to lack of sAPPα since its *in vitro* application causes neurite outgrowth (Araki et al., 1991; Bhasin et al., 1991; Ohsawa et al., 1997; Qiu et al., 1995;

Saitoh et al., 1989), whilst raising the levels of sAPPα *in vivo* increases cortical synaptogenesis (Bell et al., 2006). APP can act synergistically with NGF to enhance its neurotrophic effects (Wallace et al., 1997), with this important for promoting the plasticity associated with recovery following brain injury.

This study identifies a potential role for endogenous APP in maintaining cognitive and motor abilities following a mild diffuse TBI in mice by reducing cell death and promoting a reparative response, with this most likely due to the actions of sAPPα. Long term recovery after brain injury is known to involve processes such as neurite outgrowth, synaptic plasticity and neuron regeneration. As such it could be beneficial to either modulate the proteolytic processing of endogenous APP to enhance levels of sAPPα post-injury, or to develop an exogenous agent that replicates this activity in order to improve functional outcome following TBI.

Chapter 5: Characterisation of the controlled cortical impact model of traumatic brain injury

5.1 Introduction

In order to fully elucidate the role of APP following TBI, it is necessary to use a model of injury in which a more severe injury can be inflicted. As outlined in Chapter 2, attempts to increase the severity of the diffuse injury model in mice led to a drastic increase in the mortality rate, due to the presence of large subarachnoid haemorrhages. This is similar to observations from another laboratory (K Saatman private communication), suggesting that the biomechanics of this type of injury in mice mean that it is difficult to increase injury severity without the complications of large amounts of bleeding.

In contrast, focal injury models have been shown to produce graded injury in mice with the severity of histological and behavioural changes increasing with the amount of mechanical force applied, without undue increases in mortality (Brody et al., 2007; Fox et al., 1998; Saatman et al., 2006). The CCI model is the most commonly used and involves the use of a piston with a tip of a specific diameter to strike the exposed dura at a precise velocity and depth, causing rapid cortical deformation (Smith et al., 1995). This leads to the formation of a focal cortical contusion with intraparenchymal petechial haemorrhages, extensive tissue loss and cell death. The advantage of this model is that the user is easily able to manipulate injury severity, with the shape of the impactor and depth of impact found to be the key parameters in determining injury severity (Mao et al., 2010).

The impactor device used to induce the injury in these experiments is described in Ek *et al* and comprises a LinMot linear motor and slider, which acts as the piston, which are mounted onto a manipulator of a stereotaxic frame (Ek et al., 2010). These are connected to a PC computer via a Linmot servo controller unit. Plastic tip pieces 2mm in diameter were fitted to the end of the slider to provide a flat impacting surface. Electromagnetic forces are used by the linear motor to propel the slider with the plastic tip attached along the central hollow tube of the motor casing. The precise specification of the movements made by the slider are controlled via Linmot control software on the PC computer to which it is connected. This program allows precise specification of injury parameters including depth and velocity of impact and dwell time.

As this device has primarily been used to create spinal contusions, it is necessary to determine the ideal parameters for CCI injury, by determining the histological and behavioural response to varying

impact depth. This is important as the depth of impact needed to produce histologically similar injuries varies with the use of different CCI devices, with a 2mm depth of impact in one study utilising electromagnetic force to drive the tip (Brody et al., 2007) most closely resembling the histological damage seen with a 1mm depth utilising an older pneumatic device in another (Saatman et al., 2006). This was attributed to a greater amount of overshoot in the older pneumatic devices. However, slight differences in techniques across laboratories can also alter the characteristic of the injury such that that injuries produced in different laboratories with different parameters can produce histologically similar injuries (Hanell et al., 2010), whilst the same parameters in different laboratories can produce dissimilar injuries. For example an injury produced using a pneumatic device set to deliver a 1mm deformation at 6.0m/s caused greater cortical ablation and hippocampal cell loss in one study (Smith et al., 1995) than another (Fox et al., 1998). Thus the aim of this study is to characterise the use of a Linmot impactor device to produce CCI injury in mice, and determine the effects of exogenous sAPPα treatment on outcome following a moderate level of injury.

5.2 Methods

In the first part of the study, effects of varying depth of impact was characterised, with mice injured with either 1mm (n=5), 1.5mm (n=5) or 2mm (n=5) of deformation and their functional and histological outcome examined. In the second part of the study, having determined that the 1.5mm depth was the most amenable to treatment given that the hippocampus was not directly deformed by the impact, a further 12 mice were injured with these parameters and then treated with either sAPPα (n=7) or vehicle aCSF treatment (n=5).

5.2.1 Mouse Controlled Cortical Impact Model

In order to perform the CCI injury, an IP injection of Avertin (250mg/kg) was administered to anaesthetise the mice, with surgery commencing once pedal foot reflexes were absent. Following a midline scalp incision, a craniotomy (3mm diameter) was performed in the centre of the right parietal bone, being careful to ensure that the integrity of the dura was not disrupted. Mice were then placed in a stereotaxic frame with the head positioned in the horizontal plane and nose bar set at zero. They were then subjected to a cortical impact injury with the 2mm flat impactor tip used to cause either 1 (mild), 1.5 (moderate) or 2mm (severe) of deformation at a velocity of 5m/sec with a

dwell time of 100ms. Following the impact a cranioplasty was performed to cover the injured tissue. Sham animals underwent all surgical procedures, but were not injured (n=5).

Following injury a subgroup of those receiving an impact depth of 1.5mm were randomised to receive an ICV injection of 25 μM sAPPα (APP18-611) (n=8) or artificial CSF vehicle (n=5) at 30 mins post-injury. To facilitate treatment a 0.3mm craniotomy was performed on the left side, at the stereotaxic coordinates relative to bregma: posterior 0.5mm, lateral 1mm (Paxinos and Franklin, 2007). A 30-gauge needle attached to a 5μl syringe was then stereotaxically lowered 2.5mm and retracted 0.3mm to facilitate administration into the left ventricle. At 15 mins post-injury 2μL of either sAPPα or aCSF was administered at a rate of 0.5 μL/min. Bone wax was used to close the craniotomy and the surgical wound sutured.

5.2.2 Motor Outcome

Motor deficits were assessed using the ledged beam test, as previously described (Bye et al., 2007). Briefly, a beam was used which was 1m in length tapering from 3.5cm to 0.5cm with underhanging ledges 1.0cm in width on either side. The beam was placed at a 30° angle of incline, with the narrowest end at the highest point. Mice were placed at the widest end of the beam and required to walk to the narrowest end, where an enclosed box was situated. Animals were pre-trained for 3 days prior to injury in order to habituate them to the task, and tested each day for 7 days following injury, with each mouse given 2 trials which were videotaped for later analysis. The number of times the underhanging ledge was used (foot faults) by both the hind and front limb on the side contralateral to the CCI injury were counted and averaged across the two trials.

5.2.3 Cognitive Outcome

Cognitive deficits were assessed using the Barnes Maze which consists of a white circular platform (120cm in diameter) elevated 70 cm off the floor with 40 holes (5 cm in diameter) evenly spaced around the perimeter. One of these holes was connected to an escape box, which the mouse was required to locate. Distinct spatial clues were located around the maze and kept constant throughout the study to aid the animals in finding the correct hole. As such animals have to use a hippocampal dependent spatial strategy in order to find the escape hole (Koopmans et al., 2003), with previous

studies showing a correlation between hippocampal damage and a decrease in performance in this test (Fox et al., 1998; Raber et al., 2004).

As previously described for the Barnes Maze, mice were pre-trained for 5 days prior to injury, with their best time taken as their pre-injury baseline level. Assessment was conducted on days 2, 4 and 6 post-injury, with escape latency (time in seconds) for the mice to find and enter the escape box with front paws and trunk recorded. On day 7 post-injury the escape box was switched to a different, randomly chosen hole to test the ability of mice to learn a new spatial contingency. Mice were allowed three trials, spaced 1 hr apart, to learn the location of the new hole with their escape latency recorded as above.

5.2.3 Histological Analysis

At day 7 post-injury mice were terminally anaesthetised with Pentobarbital and perfused transcardially with 10% formalin. Brains were then embedded in paraffin prior to sectioning. To ensure inclusion of the entire lesioned cortex, 5 µm sections were collected from Bregma -0.5 to -4mm. To determine the extent of damaged tissue after CCI, 5 sections per brain (400µm) apart were stained with haematoxylin and eosin (H&E), representing the region Bregma -0.5 to -4 due to the shrinkage associated with processing. The unaffected area of the cortex of each hemisphere was outlined, with damaged tissue defined by a decrease in H&E staining intensity. The volume of undamaged tissue in each hemisphere was then calculated using the following equation, as described within the Methods section:

$$(Area_1 \; x \; D) + \frac{(Area_2 - Area_1 \; x \; D)}{2}$$

The volumes of healthy tissue between successive pairs of sections across the lesion were then added to determine the total volume, with the percentage of cortical tissue damage was then calculated as (uninjured cortical volume − injured cortical volume) / uninjured cortical volume × 100 (Semple et al., 2010b).

To assess hippocampal damage, 3 H&E stained sections located 200µm apart, representing the region Bregma -1.2 to -2.1, from each animal were assessed for the number of remaining neurons within the CA region of the hippocampus. The CA region was sequentially imaged at 40x

magnification and digitally reconstructed into a montage, to allow manual counting of the neurons using the cell count software associated with Image J. To determine the effects of injury on the dentate gyrus, the area of the granular layer of the dentate gyrus was determined in 5 sections located 200µm apart (Bregma -1.5 to -3) with the volume calculated using the equation described above:

$$(Area_1 \; x \; D) + \frac{(Area_2 - Area_1 \; x \; D)}{2}$$

5.2.4 Immunohistochemistry

To characterise the effects of increasing depth of impact on hippocampal integrity and the reparative response, levels of MAP-2, a dendritic marker and GAP-43, a reparative protein were determined via immunohistochemistry which was performed on 3 sections per mouse. For GAP-43 slides were used which were 400µm apart representing Bregma -1.2 to -3.5, whilst for MAP-2 slides were used which were 200µm apart representing Bregma -1.2 to -2.1 to allow specific analysis of the dorsal hippocampus. Briefly, dewaxed sections were immersed in 1% hydrogen peroxide solution to quench endogenous peroxidases before undergoing antigen retrieval by microwave treatment in sodium citrate buffer (pH 6.0). The sections were then incubated with biotintylated anti-mouse GAP-43 (Novocastra 1:1000) or MAP-2 (Abcam 1:1000) overnight, followed by the appropriate secondary antibody (1:250) for 30 mins and then streptavidin peroxides conjugate for 1 hr (1:1000). Bound antibody was then detected with 3,3-diaminobenzidene tetrahydrochloride (Sigma) and sections counterstained with haematoxylin.

Immunohistochemical Analysis

For analysis, the slides were digitally scanned (Nanozoomer, Hamamatsu) and images exported as a jpeg file using the software associated with the slide scanner. To assess the reparative response, post-injury levels of GAP-43 were assessed with sequential stepwise 40x images of the cortex taken at approximately 400, 800 and 1200µm from the edge of the lesion and exported as jpeg files (Fig 5.1). MAP-2 immunostaining was used to assess dendritic integrity post-injury, with sequential 40x images of the CA2 stratum radiatum layer, the CA3 region and the dentate hilus taken. For both GAP-43 and MAP-2 analysis, images then underwent colour deconvolution using Ruifork and Johnston's method with DAB and haematoxylin separated to allow objective analysis of staining intensity

(Ruifrok and Johnston, 2001). This protocol is described in detail within Chapter 2 and calculates the %DAB weight within an image allowing the comparison of this value to that of other images.

5.2.5 Statistical Analysis

All parametric data were assessed using two-tailed unpaired student's t tests or analysis of variance (ANOVA -one or -two way and/or repeated measures as necessary), followed by Bonferonni tests for multiple comparisons. A p value of less than 0.05 was considered significant**.**

Fig 5.1: Representative image depicting the regions (black boxes) that were used to analyse GAP-43 immunohistochemistry. Scale bar = 5mm

5.3 Results

5.3.1 Effects of varying impact depth on motor deficits following CCI injury

The number of foot faults made by the impaired left side on the ledged beam were counted post-injury to determine levels of motor deficits following CCI injury (Fig 5.2). There was a small increase in foot faults between mice injured at the mild 1mm depth compared to the moderate 1.5mm depth which reached significance on day 1 post-injury ($p<0.05$). However there was rapid improvement in the moderately injured mice so that by day 4 post-injury there was minimal difference between the two groups. There was a greater difference between the severely (2mm depth) and moderately injured mice, with a significant increase in the number of foot faults to day 4 post-injury. Nonetheless by day 7 after injury the severely injured mice were only slightly more impaired than the mildly and moderately injured mice on the ledged beam.

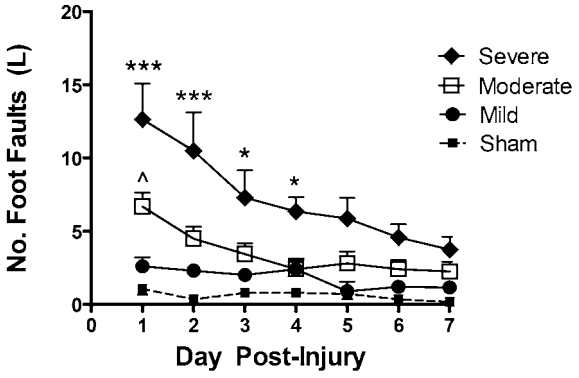

Fig 5.2: Motor deficits, as detected on the ledged beam following graded CCI injury. (Mild, severe and sham n=5; moderate n=10) (^p<0.05 compared to mildly injured mice, ***p<0.001, *p<0.05 compared to moderately injured mice)

5.3.2 Effects of varying impact depth on cognitive deficits following CCI injury

Following injury, both the moderately (1.5mm depth) and severely (2mm depth) injured mice demonstrated cognitive deficits on the Barnes Maze (Fig 5.3), whilst the mildly injured (1mm depth) mice were no different to uninjured shams. Following a severe injury mice had a significant increase in escape latency on all days tested post-injury when compared to shams (98.8, 62 and 48 secs vs 25.1, 20.9 and 22 secs). In the moderately injured mice the increase in escape latency was less than that seen in the severely injured mice (51.5, 41 and 26.4 secs), with this group only significantly different to shams on days 2 and 4 post-injury.

On day 7 post-injury the ability of the mice to learn a new location for the escape hole was tested (Fig 5.3B). The severely injured mice were significantly impaired in their ability to learn the new location, taking longer than shams on each of the trials, in 78, 67.5 and 41 secs compared to 59.9, 30 and 27 secs, with this reaching significance on trial 2 ($p<0.005$). The moderately injured mice also had an increase in time taken to find the escape hole on trial 2 (52 secs) when compared to shams, but this did not reach significance. Furthermore, the time taken was less than the severely injured mice, and by trial 3 they were no different to the shams. In contrast the mildly injured animals were no different to shams.

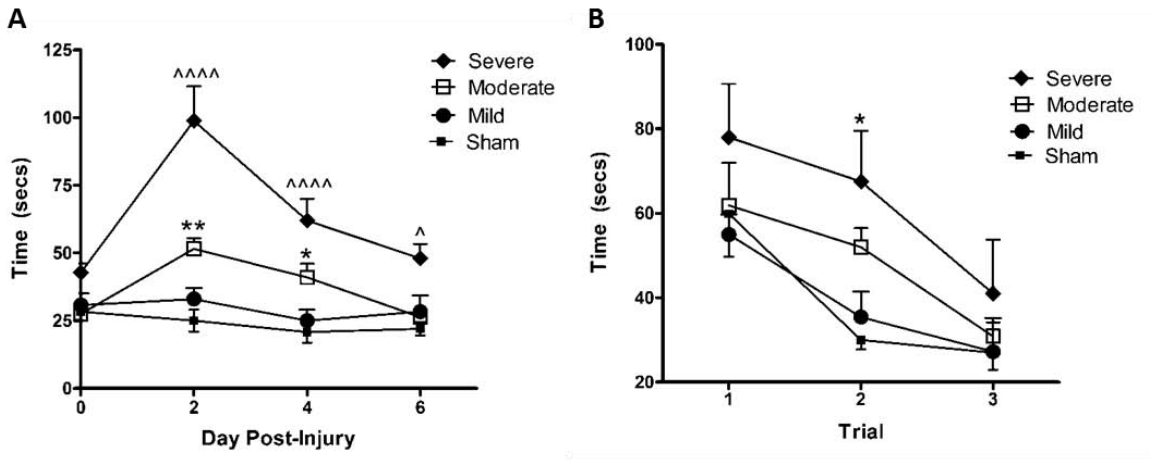

Fig 5.3: Cognitive outcome, as determined by the time taken to find the location of a previously learnt escape hole (A), and the ability to learn a new location for the escape hole (B). This shows a clear increase in cognitive deficits with increasing injury severity, with mice injured at the mild 1mm depth similar to uninjured shams, whilst severely injured mice had a significant deficit when performing both these tasks. (Mild, severe and sham n=5; moderate n=10) (p<0.01, *p<0.05, ^^^p<0.001, ^p<0.05 compared to shams)**

5.3.3 Histological characterisation of varying impact depth in the CCI model of TBI

Representative images seen in Fig 5.4A-C, demonstrate that as depth of impact increases there was a progressive loss of cortical and hippocampal tissue, with obvious distortion in the morphology of the remaining hippocampus at the 2mm depth which is not evident at the lower impact depths. Closer examination of the hippocampus reveals increasing loss of vulnerable CA3 neurons as impact death increases from 1 to 2mm. At the 2mm impact depth there is an almost complete loss of CA2 neurons, whilst at the moderate or mild level of injury there is only minor damage to this region (5.4D-F). Determination of cortical damage by comparing the remaining volume of the injured left hemisphere to that of the uninjured right hemisphere, demonstrates a step wise increase in lesion volume, with significant increases in damage from the 1 to 1.5mm impact depth ($p<0.001$), and from the 1.5 to

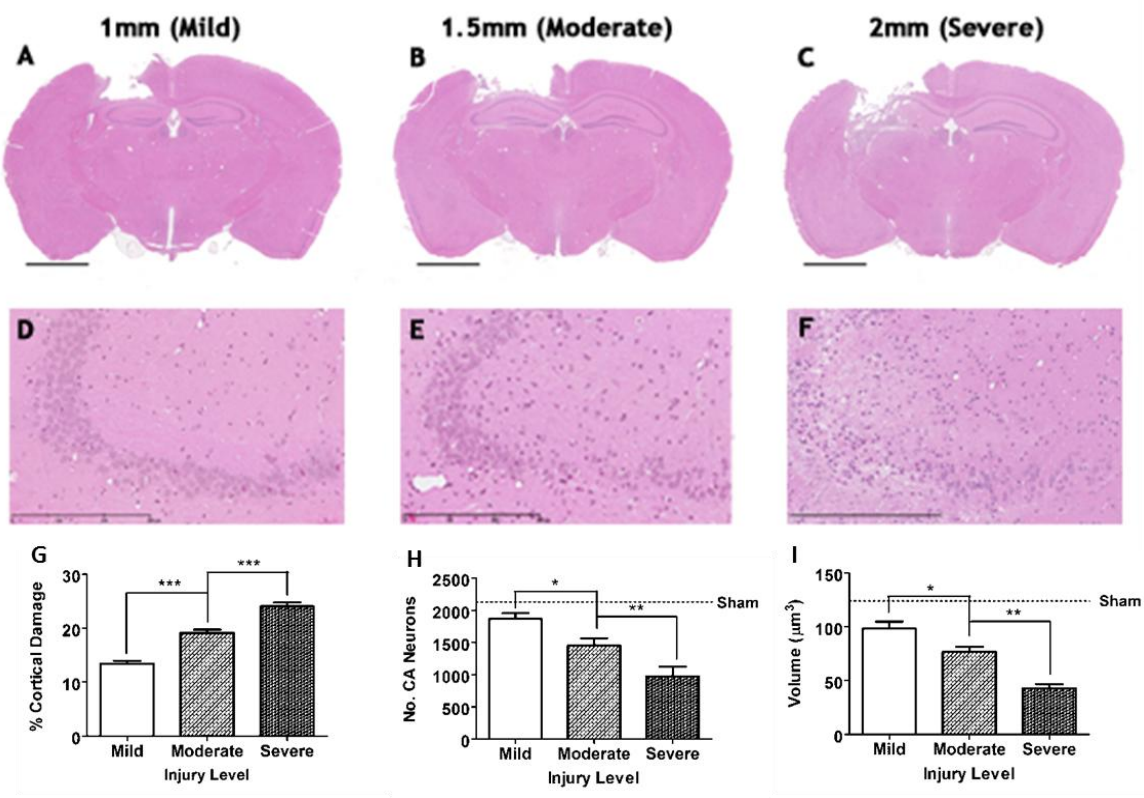

Fig 5.4: Representative images taken from the region -2.1 from Bregma, demonstrating the increasing cortical and hippocampal damage that accompany increasing impact depth. These observations were confirmed with step wise increases in the amount of cortical damage (G), decreases in the number of remaining CA neurons (H) and decreases in the volume of the dentate gyrus (I) as impact depth increased. (Scale bar = 5mm (A-C) or 300µm (D-F)) (n= 5 per group)

2mm impact depth ($p<0.001$) (Fig 38G). A similar step wise pattern is seen in analysis of hippocampal damage, with number of CA neurons and volume of the dentate gyrus decreasing with increasing injury severity caused by increasing impact depth (Fig 5.4H&I).

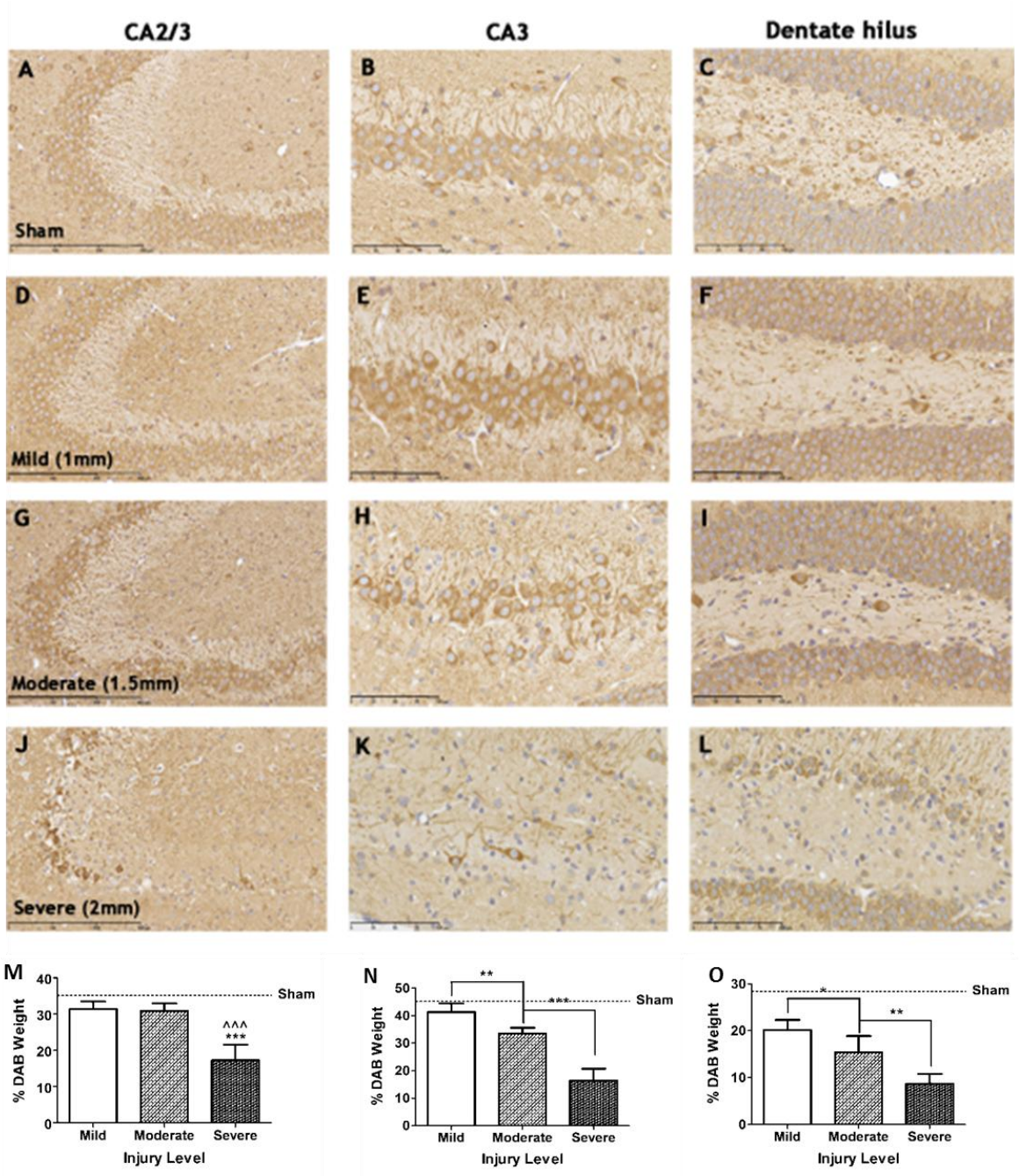

Fig 5.5: Representative images (A-L) taken from the region -2.1 from the Bregma, showing increasing damage to the hippocampus as depth of impact increased. These observations were confirmed with colour deconvolution of the CA2 (M), CA3 (N) and dentate hilus (O) regions of the hippocampus. A step wise pattern of increasing damage is seen in the CA3 and dentate hilus regions, whilst significant damage to the CA2 region only occurs with 2mm depth of impact. (A, D, G, J scale bar = 300µm, otherwise scale bar = 100µm)

Hippocampal damage was confirmed with MAP-2 immunohistochemistry, which allows assessment of dendritic integrity (Fig 5.5). The dentate hilus region was most susceptible to injury (Fig 5.5O), with significant reductions in staining intensity at all levels of injury ($p<0.05$), although the disruption was greater as severity of injury increased. Similarly damage to the CA3 region worsens with increasing depth of impact, with an injury caused by a 1mm depth of impact causing minimal loss of MAP-2 staining, whilst at the 2mm depth there is almost a complete loss of staining associated with extensive cell death. Staining at the moderate level of injury is between these two extremes (Fig 5.5N). As seen within the H&E images, in the CA2 region, noticeable loss of levels of MAP-2 staining only occurs at the most severe 2mm depth of impact, but not at the 1.5 or 1mm impact depths (Fig 5.5M).

5.3.4 The effect of varying impact depth on levels of GAP-43 following CCI injury

Levels of GAP-43 within the cortex at increasing distance from the impact site were immunohistochemically assessed to determine the strength of the reparative response following graded CCI injury. Levels of GAP-43 were increased in the region closest to the lesion in all injury severity groups (Fig 5.7). At greater distance, although levels increase from a mild to a moderate level of injury, there was no further increase seen following a severe injury. Instead, levels actually decrease in the mice injured at the 2mm depth when compared to those injured at the 1.5mm depth. These observations were confirmed with colour deconvolution (Fig 5.6), showing a significant increase in levels 0.8mm from the lesion in the moderate injury group when compared to the mild and severe injury groups ($p<0.05$).

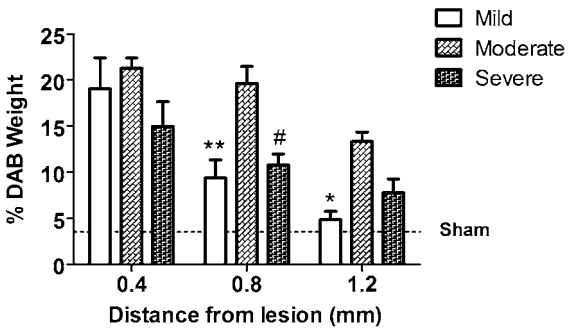

Fig 5.6: Levels of GAP-43 within the cortex expressed as %DAB weight, confirming that as distance from the lesion increases, levels in the moderately but not severely injured mice are higher than those in the mild injury group. (n=5 per group) (*p<0.05, **p<0.01, #p<0.05 compared to moderate injury group)

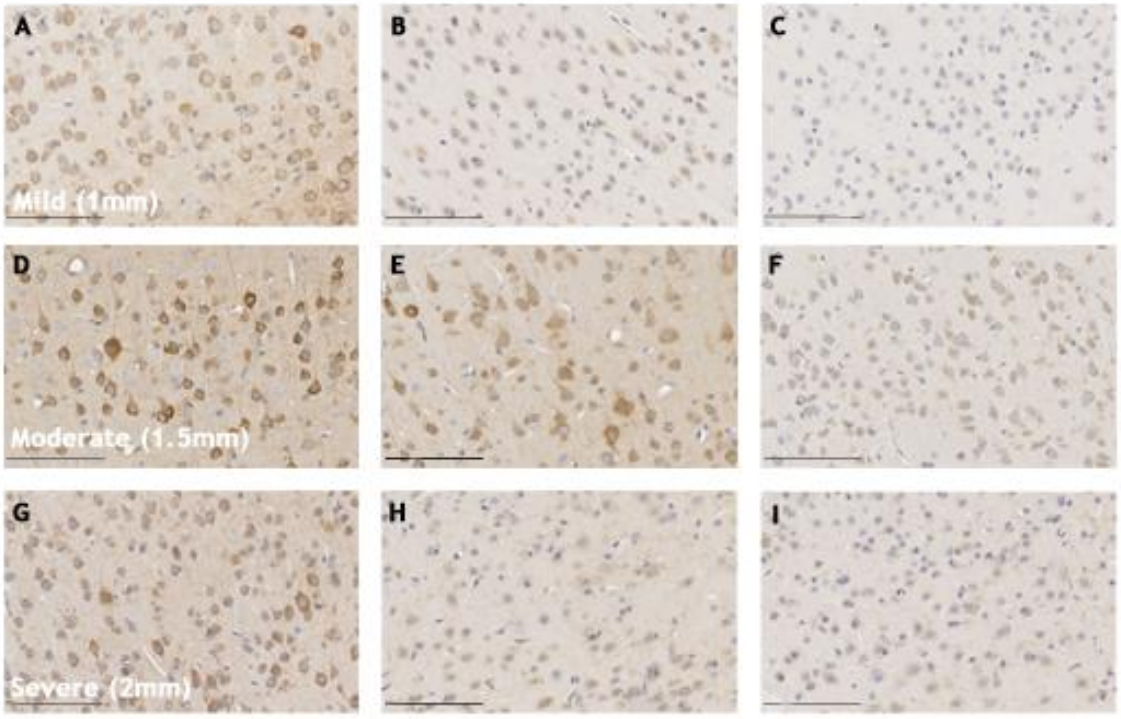

Fig 5.7: Representative images of GAP-43 immunohistochemistry at increasing distance from the lesion site (left-right) following graded CCI injury. Whilst levels of reparative GAP-43 increase from a mild to a moderate injury, following a severe injury there is no further increase, and in fact levels appear to be less.

5.3.5 Effects of sAPPα treatment on functional outcome following moderate CCI injury

Given the preliminary studies above, it was determined that the moderate level of injury induced by cortical deformation of 1.5mm would be most amenable to treatment due to the presence of functional deficits without extensive distortion of the underlying hippocampus. Following treatment with sAPPα, motor deficits, as determined by the number of foot faults on the ledged beam were

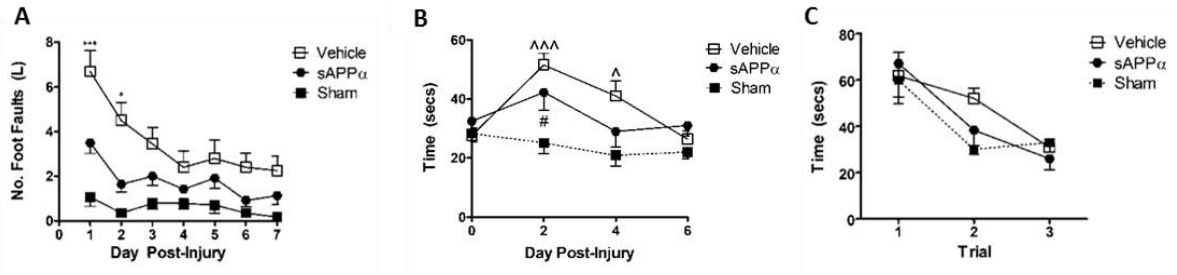

Fig 5.8: Effect of treatment with sAPPα on motor (A) and cognitive outcome (B&C) following moderate CCI injury. Treatment ensures a more rapid rate of recovery in all tasks. (Vehicle n=10, sAPPα n=7, sham n=5) (*p<0.001, *p<0.05 compared to sAPPα treated mice (A), ^^^p<0.001, ^p<0.05, #p<0.05 compared to shams (B))**

significantly reduced on days 1-2 following injury, indicating a more rapid rate of recovery in these mice (Fig 5.8A). Similarly, sAPPα treated mice improved more rapidly on the Barnes Maze, returning to a sham level of performance on day 4 compared to day 6 in vehicle treated mice (Fig 5.8B). There was no significant difference between the ability of vehicle and sAPPα mice to learn a new location for the escape hole over 3 trials, with both groups showing a slight increase in time taken on trial 2 when compared to shams (Fig 5.8C).

5.3.6 Effects of sAPPα treatment on histological outcome following moderate CCI injury

Following injury there was a small but significant reduction in cortical damage in sAPPα treated mice, when the volume of the injured right side was compared to that of the uninjured left side (Fig 5.9D). More evident, was the reduction in damage to the CA region of the hippocampus in sAPPα treated mice compared to their vehicle treated counterparts, with in particular, a greater preservation of the CA3 region (Fig 5.9A-C). This was confirmed with a count of the number of remaining CA neurons within 3 sections showing a significant increase in sAPPα compared to vehicle treated mice, although there was still significant damage when compared to shams ($p<0.05$) (Fig 5.9E). There was also a greater preservation of the dentate gyrus, represented by an increase in its calculated volume, although this did not reach signficance (Fig 5.9F).

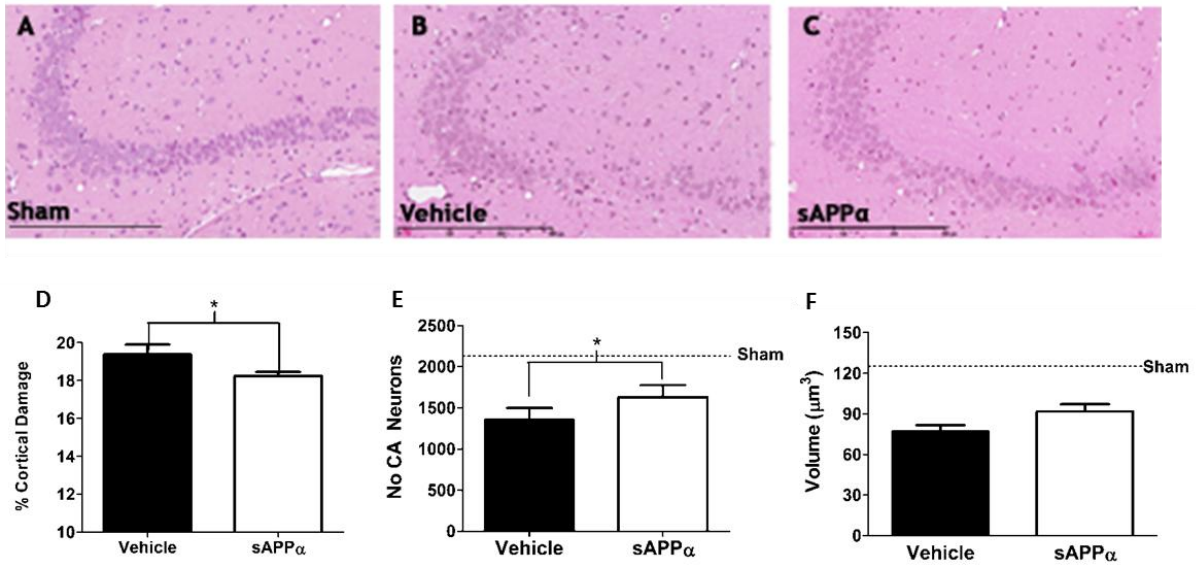

Fig 5.9: Representative images from the CA2/3 region of sham (A), vehicle (B) and sAPPα treated mice. Treatment with sAPPα led to a significant reduction in cortical damage (D) and hippocampal damage, seen as an increase in the number of remaining CA neurons (E). There was also an increased preservation of the volume of the dentate gyrus, but this did not reach significance (F). Scale bar = 300μm (n=5 per group)

5.4 Discussion

This study has characterised the use of a Linmot Linear Motor system for induction of CCI injury, demonstrating that varying the depth of impact causes graded motor and cognitive deficits in the week following injury. These behavioural deficits were accompanied by progressive cortical and hippocampal damage, the extent of which was dependent on injury severity. A moderate level of injury, produced by 1.5mm of cortical deformation, was found to be amenable to treatment, with a significant improvement in motor and cognitive deficits accompanied by a reduction in histological damage seen in response to sAPPα treatment. However, the beneficial effects were not as dramatic as those seen following a diffuse injury in rats.

Increasing depth of CCI impact has previously been shown to cause graded functional deficits at 2 days (Saatman et al., 2006) and at 2-4 weeks post-injury (Brody et al., 2007), using tasks including the grid walk, rotarod and Morris Water Maze. This study adds to this body of evidence, demonstrating worsening performance on the ledged beam and the Barnes Maze with increasing impact depth in the week following injury. Although the number of foot faults on the ledged beam, even for the most severely injured group, were quite low, the task was sensitive enough to discern between the different groups particularly on days 1-4 post-injury. Similar responses to the task following TBI are reported elsewhere (Bye et al., 2007), suggesting this is a normal level of performance for this task. This relates to the phenomenon whereby injury effects in mice are known to disappear faster than if the same task was performed in rats (Fujimoto et al., 2004). It is unclear whether this can be attributed to injury models being less severe in mice or that mice have a faster rate of spontaneous recovery. In addition daily testing immediately after injury accelerates the rate of the recovery (O'Connor et al., 2003), contributing to the rapid return towards a sham level of performance in these mice.

Similarly in terms of cognitive performance, all mice showed improvement in escape latency on the Barnes Maze in the week following injury, with the rate of improvement correlating with injury severity and hence the degree of hippocampal damage. Mice subject to 1mm cortical deformation were no different to shams, those at 1.5mm had returned to a sham level of performance by day 6 and the severely injured mice were still impaired at this time point. The performance on the Barnes Maze is like that reported by other studies (Fox et al., 1998; Wang et al., 2011), indicating that it is a suitable alternative to the more commonly used Morris Water Maze (Mannix et al., 2010; Sheibani et al., 2004; Varma et al., 2002; You et al., 2008), to assess cognitive deficits following TBI.

Histologically, as well as prominent damage to the cortex, CCI brain injury typically results in neuronal loss in the hippocampal dentate gyrus and CA3 pyramidal layers (Baldwin et al., 1997; Hall et al., 2008; Saatman et al., 2006). This is seen within this study with progressive increases in the amount of cortical damage, as well as to the vulnerable hippocampal CA3 and dentate gyrus regions as depth of impact increased. The histological damage seen in this study at the depths of 1, 1.5 and 2mm appears to correlate most closely with the injury caused by cortical deformation of 1.5, 2 and 2.5mm within the Brody study (Brody et al., 2007). This is most likely due to the use of ear bars in this study, rather than the cup holders used by Brody *et al* (2007) which were observed to cause approximately 0.4mm of protusion of the surface of the brain through the craniotomy. In comparison to studies utilising the older pneumatic CCI device, our moderate level of injury at a 1.5mm depth, most closely resembles the histological damage caused by 1mm of cortical deformation (Hall et al., 2008; Hanell et al., 2010; Saatman et al., 2006). This is presumably due to a reduction in the amount of overshoot in the electromagnetic device used in this study, although this was not specifically measured. However the injury caused by 1.5mm of cortical deformation also appeared comparable to one produced with 0.6mm cortical deformation at a velocity of 6m/sec (Mannix et al., 2011; Whalen et al., 2008). It is unclear what caused the difference in these results, but may relate to factors such as the strain of mouse used, the anaesthesia employed or other slight differences in technique. This highlights the necessity of characterising the functional and histological response to particular injury parameters to ensure that the desired level of injury is produced.

Interestingly the reparative response, as determined by levels of GAP-43, appeared to be impaired within the cortex following a severe injury. GAP-43 is a well characterised marker of regenerative sprouting (Christman et al., 1997; Emery et al., 2000; Thompson et al., 2006), with levels known to increase following TBI (Hall and Lifshitz, 2010; Hulsebosch et al., 1998). Whilst levels of GAP-43 increased within the cortex directly around the contusion from a mild to a moderate level of injury, there was no further increase with a severe injury and instead a significant decline in levels was observed. This did not appear to be due to a greater loss of cortical neurons as measurements were taken from the lesion edge, to account for the greater cortical damage with increasing injury severity. Furthermore, no differences were seen in levels of cortical MAP-2 between the groups (data not shown). These results support an earlier study that showed that levels of GAP-43 increased following a moderate, but not a severe CCI injury (Thompson et al., 2006). This suggests that the greater amount of neuronal damage resulting from the primary injury and the resultant secondary injury

cascade with a more severe injury make the environment less conducive for repair, with further research needed to investigate this issue.

Having characterised the functional and histological outcome to injury caused by 1, 1.5 and 2mm of cortical deformation, it was determined that the 1.5mm depth of injury represented a moderate level of injury seen in other studies. This level of injury was thought to be ideal for investigation of the therapeutic effects of sAPPα following a focal injury. Following the mild 1mm injury functional deficits were not present, whilst with the severe 2mm injury, there was a considerable amount of primary damage to the hippocampus. Indeed, other treatments like hypothermia, have been shown to be effective against moderate but not a mild or severe CCI injury due to the reasons outlined above (Markgraf et al., 2001).

Following treatment with sAPPα mice showed a significant improvement in motor and cognitive function, relating to a more rapid rate of recovery. However by day 4 on the ledged beam and day 6 on the Barnes Maze, the peformance of the treated mice was no different to the vehicle controls. Nonetheless, these improvements in functional outcome were accompanied by a small but significant improvement in the amount of cortical and hippocampal damage seen at 7 days post-injury. The effect of treatment with sAPPα was not as dramatic as that seen following diffuse injury in rats. In terms of motor deficits treated rats returned to a sham level of performance on the rotarod by day 4 following injury, whereas vehicle treated rats were still impaired by day 7. Similarly levels of axonal injury in sAPPα treated rats were dramatically reduced so that they were indistinguishable from shams (Chapter 3.3). The differences between these studies can be accounted for by the more rapid rate of recovery in mice on functional tests compared to rats as discussed above, as well as the more rapid rate of neurodegeneration in a focal injury (Hall et al., 2008), making it more difficult to observe a large treatment effect. To enhance the neuroprotective effect of sAPPα following a focal injury, repeated applications of the treatment may be necessary. In other studies which have observed treatment effects following CCI injury in mice, the animals are commonly treated more than once (Clausen et al., 2009; Han et al., 2011; Mbye et al., 2008) or very early (<15 mins) after impact (Longhi et al., 2009; You et al., 2008). As the ability to treat at later time points is more clinically relevent, exploration of the benefits of repeated treatments of sAPPα following focal injury could be examined in the future.

This study has demonstrated that increasing the depth of impact of a CCI injury utilising a Linear Linmot system, causes a proportionate increase in motor and cognitive deficits, the amount of damage to the cortex and hippocampal neuronal loss. However there was not a commensurate increase in the reparative response, with levels of GAP-43 decreasing from a moderate to severe level of injury. Further evidence was also provided of the neuroprotective activity of sAPPα, with treatment following a moderate CCI injury, significantly improving functional and histological outcome.

Chapter 6: Treatment with sAPPα is sufficient to rescue deficits in amyloid precursor protein knockout mice following focal traumatic brain injury

6.1 Introduction

Although the presence of endogenous APP conferred protection against a mild diffuse TBI as detailed in Chapter 4, it is unknown whether it would remain protective against a more severe focal injury. The difference between these two types of injuries was highlighted by the greater effectiveness of exogenous sAPPα treatment in improving functional outcome following a diffuse TBI in rats, as outlined in Chapter 3, rather than the focal CCI injury in mice, as detailed in Chapter 5. A similar situation has been described regarding the actions of endogenous neuroprotective agents with the presence of estrogen and progesterone in females shown experimentally to be more effective against diffuse (Kupina et al., 2003), rather than focal injuries (Brody et al., 2007; Hall et al., 2005). The disparity is thought to be due to the slower nature of degeneration seen in diffuse injuries.

In addition, the greater levels of oxidative stress, excitotoxicity and apoptotic cell death evident following a more severe injury could shift the processing of APP towards the amyloidogenic pathway, as these factors are known to increase the activity of the β-secretase, BACE (Lesne et al., 2005; Sodhi et al., 2008; Tamagno et al., 2008; Tong et al., 2005), thus potentially reducing levels of neuroprotective sAPPα.

Furthermore, it is unclear whether endogenous APP is required for sAPPα to exert its neuroprotective effects *in vivo*, as *in vitro* studies have suggested that both the neuroprotective (Gralle et al., 2009) and neurotrophic (Young-Pearse et al., 2008) actions of sAPPα require the presence of full length APP. However, knock in of sAPPα was sufficient to rescue deficits seen in APP-/- mice such as a reduction in grip strength and age related decreases in long term potentiation (Ring et al., 2007). Thus, this study aimed to assess whether the presence of APP would remain protective following a focal TBI and to determine what affect treatment with sAPPα would have on APP-/- mice.

6.2 Methods

Generation of APP-/- mice has been described previously (Zheng et al., 1995), with both the APP+/+ and APP-/- mice on the same background strain, C57BLbj x 129sv, with this study utilising a total of 40 animals comprising 5 APP+/+ and 40 APP-/- mice, with incorporation of the APP+/+ sham and vehicle mice from the previous chapter, as these studies were conducted concurrently.

6.2.1 Mouse Controlled Cortical Impact Model

TBI was induced using the CCI model of injury, utilising an impactor device described in the previous chapter. In order to perform the CCI injury, an IP injection of Avertin (250mg/kg) was administered to anaesthetise the mice, with surgery commencing once pedal foot reflexes were absent. A 3mm craniotomy was performed in the centre of the right parietal bone, with mice then subjected to a CCI injury with a 2mm flat impactor tip used to cause either 1.5 mm of deformation in APP+/+ mice or 1.3mm of deformation in APP-/- mice at a velocity of 5m/sec with a dwell time of 100ms.

The difference in deformation depths is to account for the smaller brain size of the APP-/- mice, with previous studies showing a reduction of brain weight of about 10% in APP-/- mice (Ring et al., 2007). Impact depth was varied as computer modelling has suggested that the most important factors in determining injury severity are impact depth and impactor shape, with the diameter of the impactor having less effect (Mao et al., 2010). As stated within Chapter 2, with these parameters it was found that at 5 hrs post injury there was no difference between APP-/- and APP+/+ mice in terms of lesion volume or in the number of degenerating neurons within the dentate gyrus and CA region of the hippocampus as detected with FJC staining.

Following injury a randomised subset of the APP-/- mice received treatment via an ICV injection of 2µL of sAPPα (APP18-611) as previously described, with all other mice receiving an equal volume artificial CSF vehicle.

6.2.2 Motor Outcome

Motor deficits were assessed using the ledged beam test, as previously described. Mice were pre-trained for 3 days prior to injury and tested each day for 7 days following injury, with each mouse given 2 trials which were videotaped for later analysis. The number of times the underhanging ledge was used (foot faults) by limbs on the side contralateral to the CCI injury were counted and averaged across the two trials.

6.2.3 Cognitive Outcome

Cognitive deficits were assessed using the Barnes Maze, as previously described. Animals were pre-trained for 5 days prior to injury, with their best time taken as their pre-injury baseline level. Assessment was conducted on days 2, 4 and 6 post-injury, with escape latency (time in seconds) for the mice to find and enter the escape box with front paws and trunk recorded. On day 7 post-injury the escape box was switched to a different, randomly chosen hole to test the ability of mice to learn a new spatial contingency. Mice were allowed three trials, spaced 1hr apart, to learn the location of the new hole with their escape latency recorded as above.

6.2.4 Tissue processing

For histological analysis animals were perfuse fixed at 24 hrs or 7 days after CCI (n=5 per group), with 7 day animals randomly chosen from those undergoing functional assessment. Mice were terminally anaesthetised with pentobarbital and perfused transcardially with 10% formalin. Brains were then embedded in paraffin prior to sectioning. To ensure inclusion of the entire lesioned cortex, 5 µm sections were collected from Bregma +0.5 to -4m.

6.2.5 Assessment of cortical tissue damage

To determine the extent of damaged tissue after CCI, 5 sections per brain (400µm) apart were stained with haematoxylin and eosin (H&E), representing the region Bregma -0.5 to -4 due to the shrinkage associated with processing. The volume of undamaged tissue in each hemisphere was then calculated, as described in Chapter 5, with volumes of healthy tissue between successive pairs of sections across the lesion were then added to determine the total volume. This was then used to calculate a percentage of cortical tissue damage.

6.2.6 Assessment of hippocampal damage

Three sections located 200µm apart representing the region Bregma -1.2 to -2.1 from each animal at 24 hrs post-injury were stained with FJC to determine the extent of hippocampal cell damage. Slides were immersed in xylene for 2 x 3 mins, 100% ethanol for 3 mins, 70% ethanol for 3 mins and then for 2 mins in dH_20. Sections were then incubated in 0.06% potassium permanganate for 10 min to reduce non-specific staining, followed by incubation in 0.004% solution of FJC solution in 0.1% acetic acid for 20 mins. The slides were rinsed in dH_20 before being placed in a slide warmer until fully dry and then coverslipped with DePeX mounting media from histolene. Sections were viewed with the Olympus BX61 microscope using a FITC fluorescence filter cube, with the CA region and granular dentate gyrus layer sequentially photographed at 40x magnification. These images were then imported into ImageJ, with the number of FJC+ve neurons within these regions counted using the associated cell count software.

Sections from 7 day post-injury mice were stained with H&E to assess the number of remaining neurons within the CA region of the hippocampus. Slides were scanned and viewed with the associated software. The CA region was sequentially imaged at 40x magnification and digitally reconstructed into a montage, to allow manual counting of the neurons using the cell count software associated with Image J. To determine the effects of injury on the dentate gyrus, the area of the granular layer of the dentate gyrus was determined in 5 sections located 200µm apart (Bregma -1.5 to -3), with the volume calculated using the equation described previously.

6.2.7 Immunohistochemistry

Immunohistochemistry was performed on 3 sections per mouse to analyse levels of GAP-43, MAP-2 and doublecortin. Briefly, for GAP-43 immunohistochemistry slides were used which were 400µm apart representing Bregma -1.2 to -3.5 for GAP-43, whilst for MAP-2 and doublecortin staining, slides were used which were 200µm apart representing Bregma -1.2 to -2.1 to allow specific analysis of the dorsal hippocampus. Sections were incubated with either biotintylated anti-mouse GAP-43 (Novocastra 1:1000), MAP-2 (Abcam 1:1000) or anti-guinea pig doublecortin (Millipore 1:8000), followed by the appropriate secondary antibody, then streptavidin peroxidase conjugate, with bound antibody finally detected with 3,3-diaminobenzidene tetrahydrochloride (Sigma) and sections counterstained with haematoxylin.

Immunohistochemical Analysis

For analysis the slides were digitally scanned (Nanozoomer, Hamamatsu) and images exported as a jpeg file using the software associated with the slide scanner. GAP-43 and MAP-2 immunohistochemistry were analysed as detailed in Chapter 5. For quantification of neurogenesis, the number of doublecortin-positive cells embedded within the granule cell layer of the dentate gyrus were counted in 3 sections spanning the dorsal hippocampus, as increased rate of neurogenesis correlates with an increased number of cells expressing doublecortin (Couillard-Despres et al., 2005). The length of the dentate gyrus was measured, and the number of cells/mm calculated.

6.2.8 Statistical Analysis

All data was analysed using either a one or two-way ANOVA as appropriate, (repeated measures for functional outcome analysis), followed by Bonferonni t tests using Graphpad Prism software. A p value of less than 0.05 was considered significant in all experiments.

6.3 Results

6.3.1 sAPPα rescues motor deficits in APP-/- mice following CCI injury

Motor deficits following CCI injury were assessed using the ledged beam, with the number of foot faults on the contralateral side (left) counted (Fig 6.1). Both APP+/+ and APP-/- mice had an increase in the number of foot faults following injury when compared to their respective shams, which was significant from days 1-4 for the APP+/+ mice ($p<0.05$) and from days 1-7 in APP-/- mice ($p<0.01$). However, motor deficits were exacerbated in APP-/- mice. Although there was only a slight increase

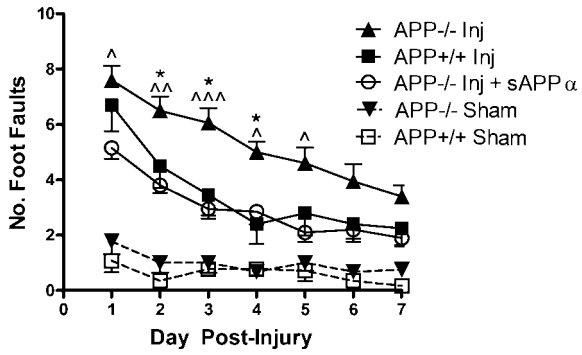

Fig 6.1: Motor outcome, as assessed on the ledged beam, showing that exacerbation of motor deficits in APP-/- mice was rescued with sAPPα treatment. (n=10 per group) (^p<0.05; ^^p<0.01, ^^^p<0.001 compared to sAPPα treated APP-/- mice; *p<0.05 compared to APP+/+ injured mice)

in the number of foot faults on day 1 when compared to APP+/+ mice, these mice demonstrated a slower rate of improvement, such that they had a significant increase in the number of foot faults on days 2-4 post-injury ($p<0.05$), with numbers remaining elevated for the rest of the testing period. With sAPPα treatment the motor performance of APP-/- mice was no longer significantly different to the APP+/+, such that they had a significant reduction in the number of foot faults when compared to untreated APP-/- mice on days 1-5 post-injury ($p<0.05$).

6.3.2 Exacerbation of cognitive deficits in APP-/- mice is prevented with sAPPα treatment

After CCI injury the presence of cognitive deficits was determined using the Barnes Maze, with the time taken to find a previously learned escape hole recorded. APP+/+ mice demonstrated a significant increase in escape latency on days 2 ($p<0.001$) and 4 ($p<0.05$) following injury before returning to a sham level of performance (Fig 6.2A). In contrast APP-/- mice were significantly impaired on all days following injury when compared to their shams ($p<0.001$). Indeed APP-/- mice had an increase in escape latency when compared to APP+/+ mice on all days tested post injury (68.3, 65.3 and 45.1 secs vs 51.5, 41.0 and 26.4 secs) which reached significance on day 4 ($p<0.01$). When APP-/- mice were treated with sAPPα, they were no longer significantly different to APP+/+ mice, with a significant improvement in escape latency on days 2 and 4 post-injury when compared to untreated APP-/- mice ($p<0.01$). The ability of mice to learn a new location for the escape hole was also tested on day 7 post-injury (Fig 6.2B). There were no differences in escape latency during trial 1 whilst mice were being familiarised to the new paradigm. On trial 2 APP+/+ and sAPPα APP-/- mice had a small but not significant increase in escape latency compared to their respective shams (52 vs 30.4 secs and 58.2 vs 27.5 secs respectively). However this deficit was exacerbated in APP-/- mice (96.3 secs) such that they were significantly impaired when compared to their shams ($p<0.001$) and APP+/+ injured mice ($p<0.05$). By trial 3 there were no significant differences between the groups.

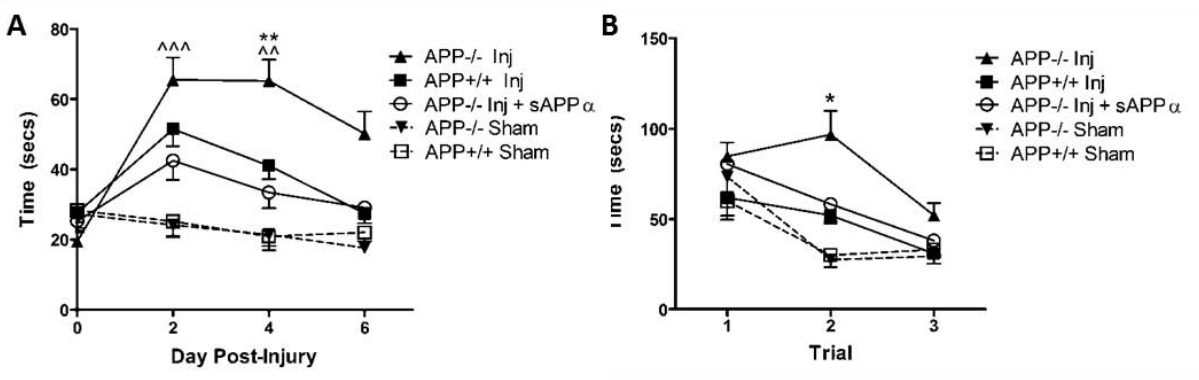

Fig 6.2: Cognitive outcome as determined by escape latency on the Barnes Maze. Following CCI animals were assessed on their ability to find a previously learned escape hole (A), with the increase in escape latency observed in APP-/- compared to APP+/+ mice following injury prevented with sAPPα treatment. Mice were also tested on their ability to learn a new spatial contingency (B). (n=10 per group) (p<0.01, *p<0.05 compared to APP+/+ mice; ^^^p<0.001, ^^p<0.01 compared to APP-/- sAPPα treated mice)**

6.3.3 Exacerbation of cortical damage in APP-/- mice is rescued with sAPPα after CCI injury

To determine the role of APP in secondary cortical degeneration following focal TBI, the extent of tissue damage resulting from CCI injury was assessed by H&E staining (Fig 6.3). By 24 hrs post-injury there was a small, but not significant increase in lesion volume in the APP-/- mice compared to the APP+/+ mice. From 24 hrs to 7 days post-injury the progression of cortical damage in APP-/- mice was greater than in APP+/+ mice, such that there was now a significant increase in tissue damage between the groups (p<0.01). Furthermore, although sAPPα treatment had a negligible effect on the extent of tissue damage at 24hrs post-injury, there was minimal expansion of lesion volume by 7 days, so that these mice now had a significantly smaller lesion volume than untreated APP-/- mice (p<0.01). There was no significant difference between lesion volume size between the APP+/+ and APP-/- sAPPα treated animals at either time point.

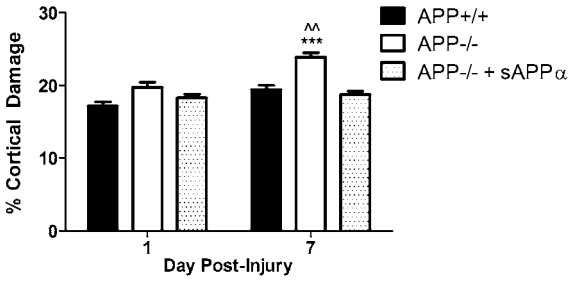

Fig 6.3: Cortical damage, as expressed as a percentage of the uninjured left cortex. (n=5 per group) (*p<0.001 compared to APP+/+ mice; ^^p<0.01 compared to APP-/- sAPPα treated mice)**

6.3.4 Increased hippocampal damage in APP-/- mice following CCI Injury is prevented with sAPPα treatment

The level of hippocampal cell damage was determined by assessing both the number of FJC+ve neurons at 24 hrs (Fig 6.4) and the number of remaining neurons within H&E stained sections at 7 days following the CCI injury (Fig 6.5). Although considerable neuronal degeneration within the hippocampus was evident in all injured animals following CCI, it appeared to be far greater in the vehicle treated APP-/- mice (Fig 6.4A-E). This was confirmed by a count of the number of FJC+ve neurons within 3 sections spanning Bregma -1.2 to 2.1, which demonstrated a significant increase following injury in APP-/- mice within both the CA region (Fig 6.4F) and the dentate gyrus (Fig 6.4G) when compared to APP+/+ mice ($p<0.05$) and sAPPα treated APP-/- mice ($p<0.05$). As suggested by the FJC staining, by 7 days post-injury there was an obvious reduction in the number of remaining neurons within the CA region of the hippocampus in APP-/- mice compared to APP+/+ mice and sAPPα treated APP-/- mice, with the CA2/3 region particularly vulnerable (Fig 6.5A-E). A count of the remaining neurons within this region confirmed this observation, with a significant increase in APP+/+ mice ($p<0.001$) and sAPPα treated mice ($p<0.001$) compared to APP-/- mice, although both these groups showed significant neuronal loss when compared to their shams ($p<0.01$) (Fig 6.5F). Similarly, both APP+/+ and APP-/- mice had a significant reduction in the volume of the granular layer of the dentate gyrus when compared to their respective shams ($p<0.01$) (Fig 6.5G). However, the reduction was significantly greater in APP-/- mice, with this rescued following treatment with sAPPα.

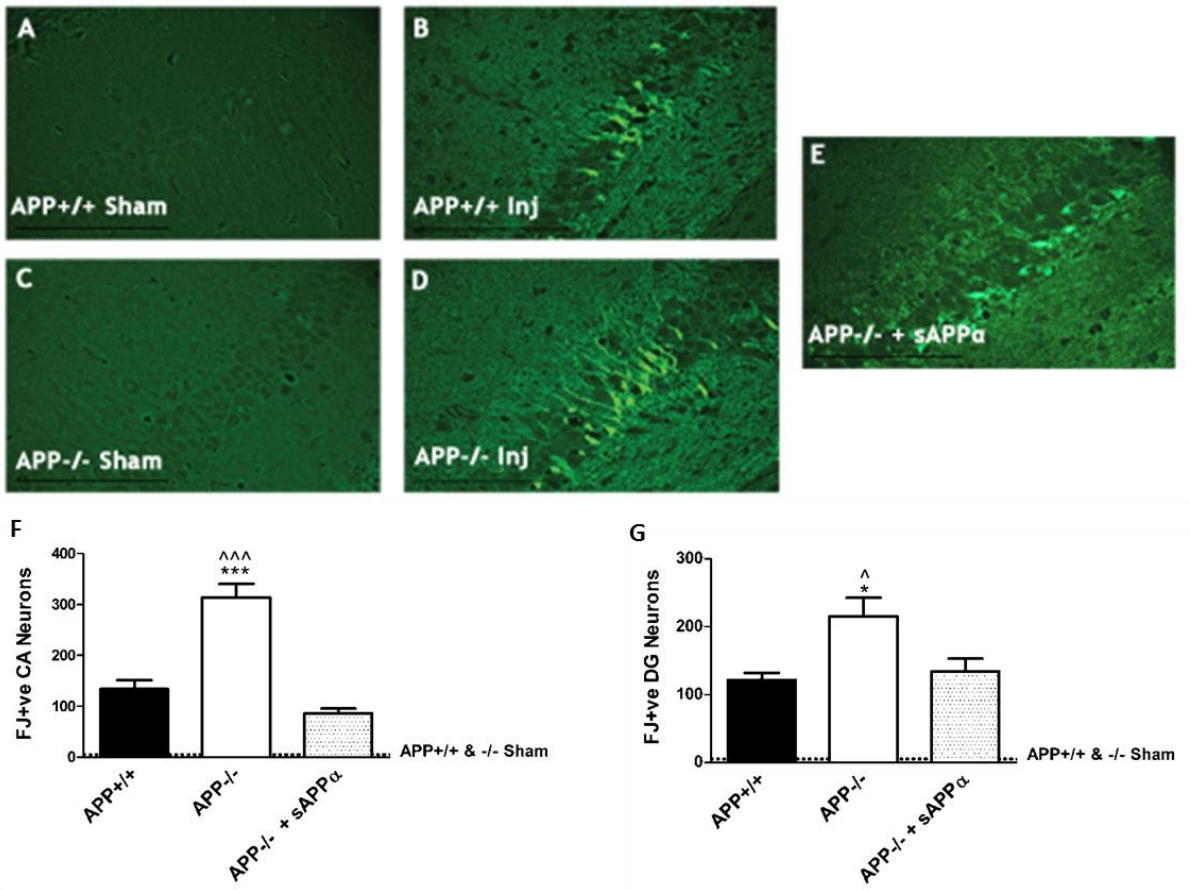

Fig 6.4: Hippocampal neuronal degeneration as assessed by FJC staining at 24 hrs following injury. APP+/+ sham (A), APP+/+ injured (B), APP-/- sham (C), APP-/- injured (D) and sAPPα treated APP-/- mice (E). Evidence of increased FJC staining in APP-/- mice was confirmed by a count of the number of positive neurons within the CA region (F) and dentate gyrus (G). (n=5 per group) (Scale bar = 100µm) (*p<0.001, *p<0.01 compared to APP+/+ injured mice, ^^^p<0.001, ^p<0.05 compared to sAPPα treated APP-/- mice)**

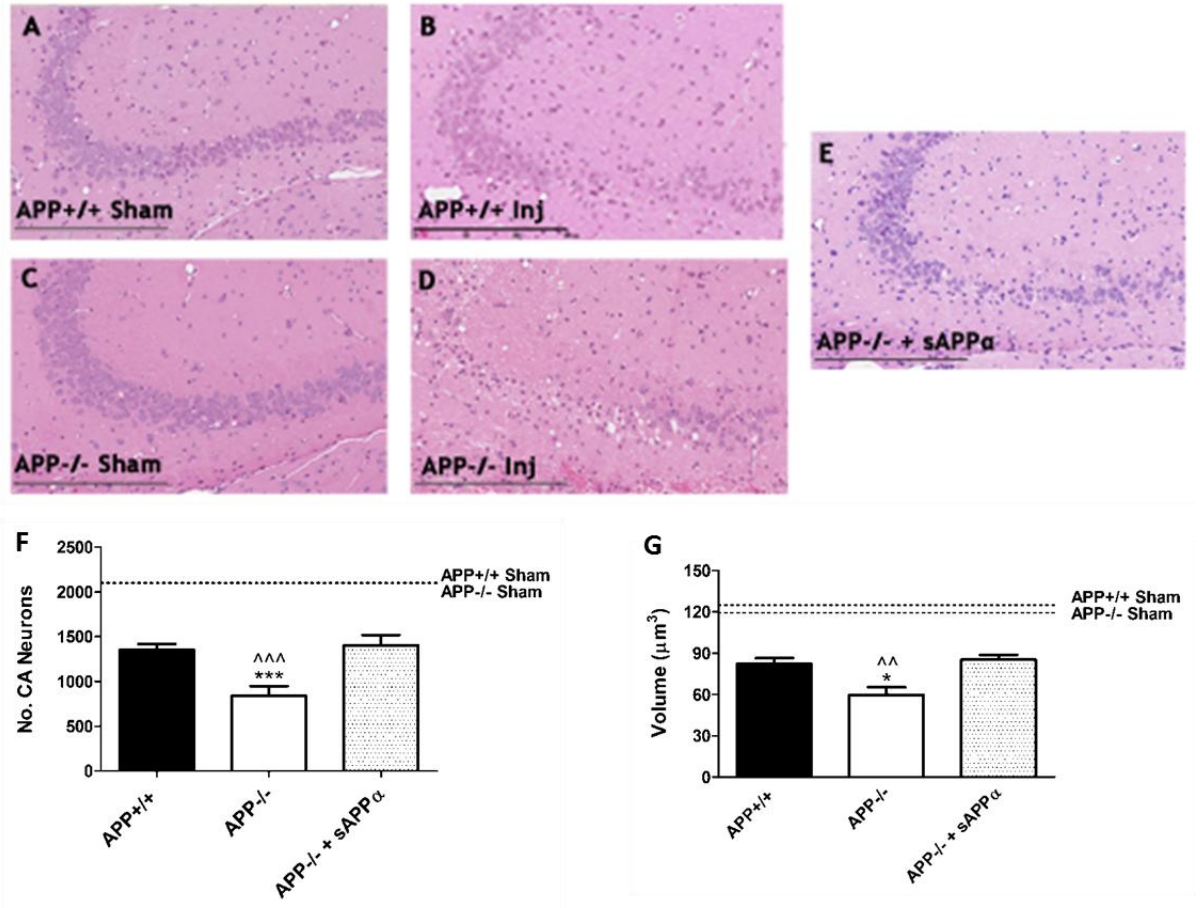

Fig 6.5: Hippocampal neurodegeneration as assessed with H&E staining at 7 days post-injury. There is a clear reduction in the number of remaining hippocampal neurons in APP-/- mice (D) when compared to APP+/+ (B) and APP-/- sAPPα treated animals (E) following injury. These observations were confirmed with a count of the number of remaining neurons within the CA region (F), with a significant reduction in the volume of the granular layer of the dentate gyrus also noted in APP-/- mice (G). (n=5 per group) (Scale bar = 100μm) (*p<0.05, ***p<0.001 compared to APP+/+ mice; ^^p<0.01, ^^^p<0.001 compared to sAPPα treated APP-/- mice)

.

6.3.5 sAPPα treatment prevents the decrease in hippocampal levels of MAP-2 following CCI Injury seen in APP-/- mice

To assess hippocampal dendritic integrity following CCI injury, immunohistochemistry was performed using the dendritic marker MAP-2, with results from colour deconvolution of images in Fig 6.6 and representative images at 7 days post injury seen in Fig 6.7. Decreases in MAP-2 staining were evident in all animals following injury within the dentate hilus, although this appeared greater in APP-/- mice, with an almost complete loss of dendrites and MAP-2 positive cells within this region by 7 days post-

injury. Supporting the hippocampal cell damage reported above, the APP-/- mice had an obvious greater loss in the number of MAP-2 positive cells within the CA2 and CA3 regions of the hippocampus in comparison to APP+/+ and sAPPα treated APP-/- mice. Similarly there was a decrease in the amount of dendritic staining, although those that remained appeared thickened. These observations were confirmed with colour deconvolution which calculated the density of staining within each image, with levels of MAP-2 assessed at 24 hrs and 7 days post-injury. Following CCI injury APP+/+ mice had a significant decrease in the intensity of MAP-2 staining within the CA3 region ($p<0.05$) and the dentate hilus ($p<0.001$) at both time points, with an almost 50% reduction within the dentate hilus. Within the stratum radiatum layer of the CA2 region a significant reduction was observed at 24 hrs ($p<0.05$), but not 7 days post-injury, with levels at this time point similar to that seen in shams. Similarly in sAPPα treated APP-/- mice significant reductions in levels of MAP-2 were observed at both time points in the CA2 ($p<0.05$) and CA3 ($p<0.05$) regions of the hippocampus as well as the dentate hilus ($p<0.05$) in comparison to their shams, with the most dramatic reduction within the vulnerable dentate hilus. In APP-/- mice the loss of MAP-2 staining was exacerbated with significant decreases compared to APP+/+ and sAPPα treated APP-/- mice within each of these regions ($p<0.05$), with an almost 70% reduction in staining in comparison to their shams with the dentate hilus.

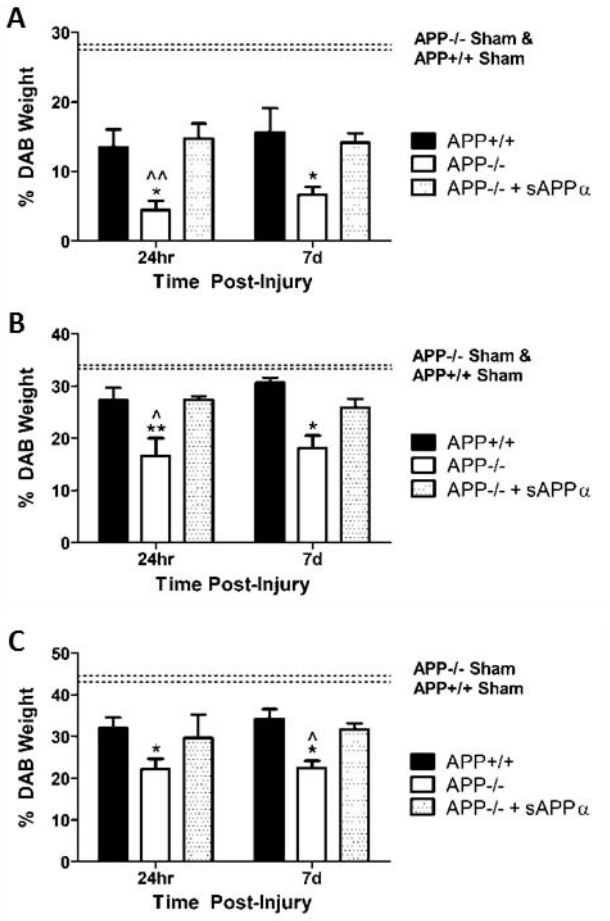

Fig 6.6: Levels of MAP-2, as determined by colour deconvolution within the stratum radiatum layer of the CA2 region (A), the CA3 region (B) and the dentate hilus (C). (n=5 per group) (*p<0.05, p<0.01 compared to APP+/+ mice, ^p<0.05, ^^p<0.01 compared to sAPPα treated APP-/- mice)

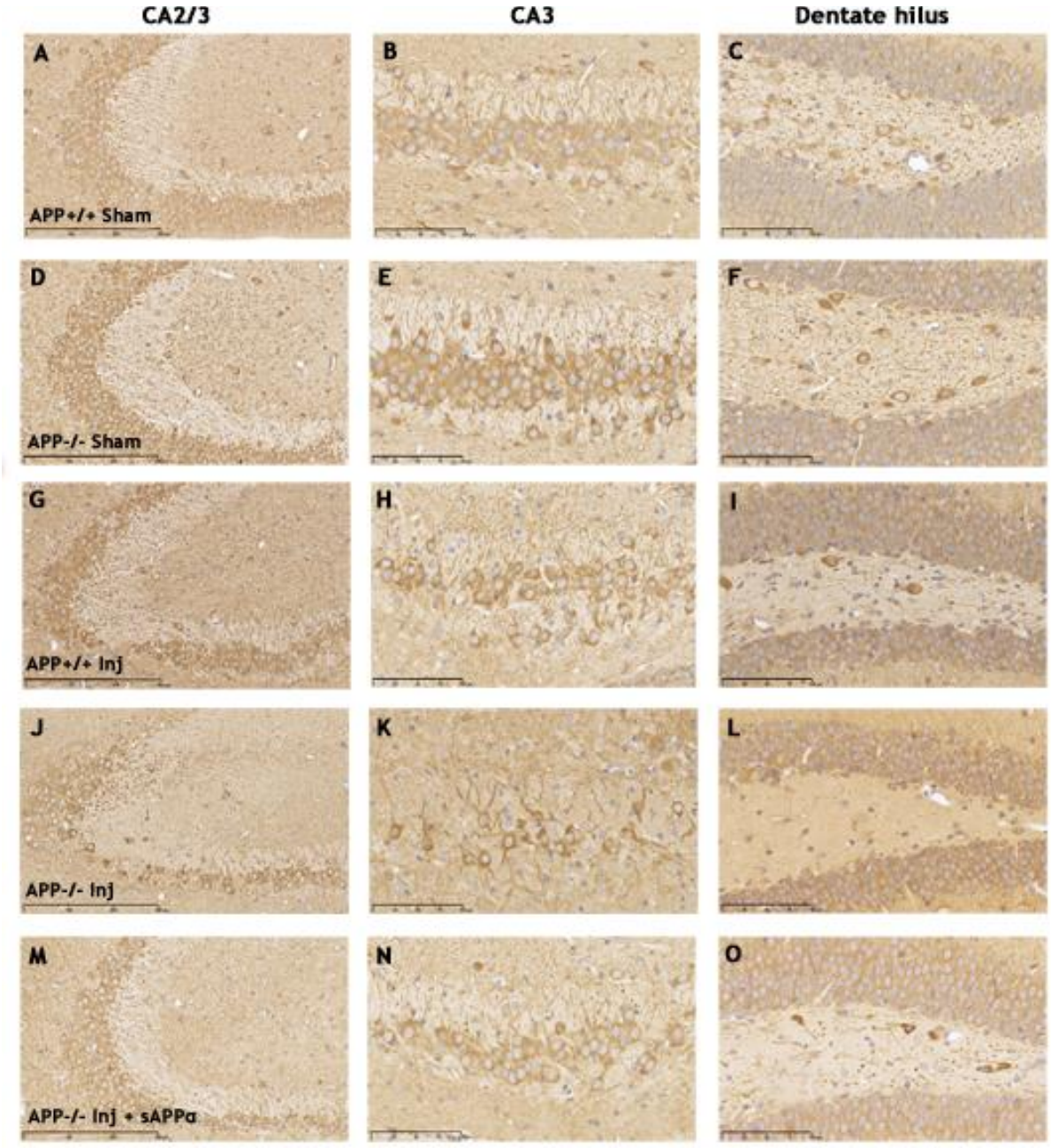

Fig 6.7: Representative images of MAP-2 immunohistochemistry showing the clear reduction in MAP-2 staining within the CA2, CA3 and dentate hilus regions of the hippocampus in APP-/- (J-L) mice following injury when compared to APP+/+ (G-I) and sAPPα treated APP-/- mice (M-O). Images are representative of n=5 per group. (A, D, J, M scale bar = 300µm, otherwise scale bar = 100µm)

6.3.6 APP-/- Mice have decreased numbers of doublecortin positive cells following CCI injury

To determine the effects of knockout of APP on neurogenesis following CCI injury the number of doublecortin positive cells within the subgranular layer of the dentate gyrus was assessed (Fig 6.8), with this quantified by calculating the number of cells/mm of dentate gyrus (Fig 6.9). By 24 hrs following injury there was a clear reduction in the number of doublecortin positive cells in all injured animals when compared to shams, reflecting their vulnerability following CCI injury. By 7 days post-injury, the number of doublecortin positive cells had significantly increased in both the APP+/+ mice

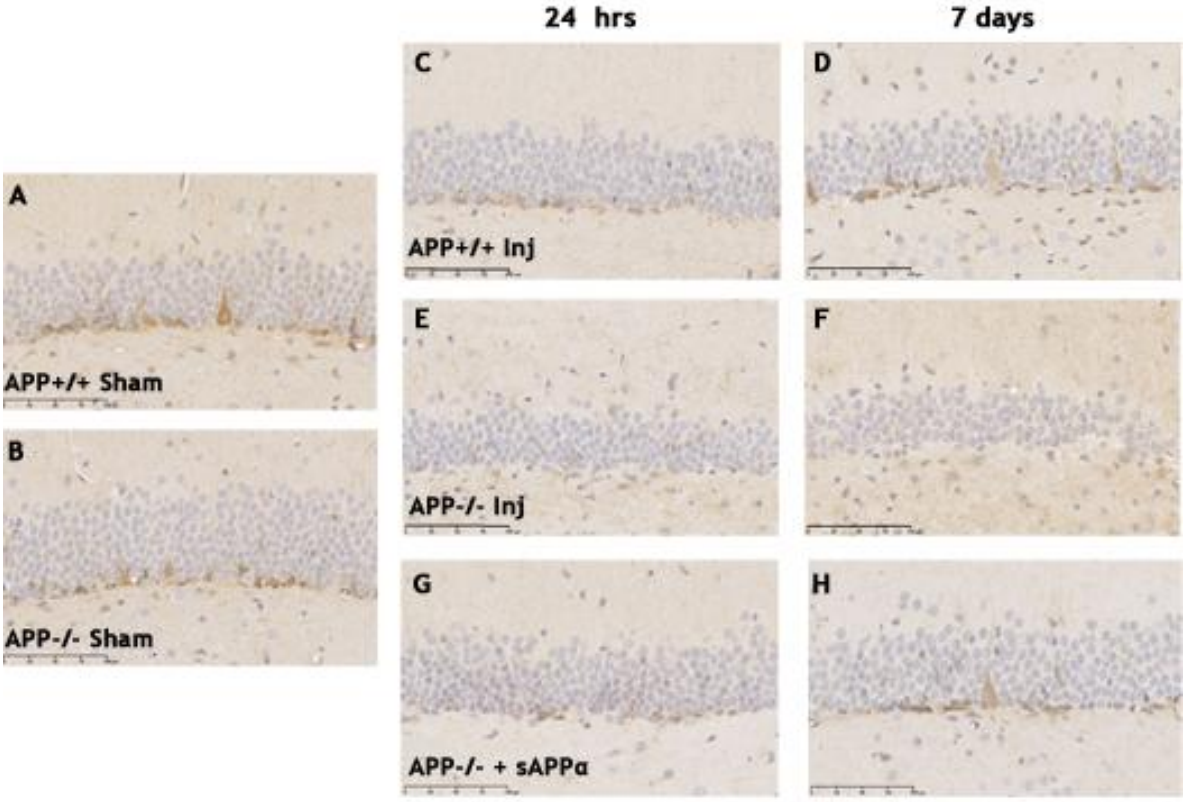

Fig 6.8 : Representative images of doublecortin immunohistochemistry in an APP+/+ sham (A), APP-/- sham (B) and injured mice at 24 hrs (C,E,G) and 7 days (D,F,H) post-injury. At 24 hrs post-injury all injured mice show a reduction in numbers of doublecortin positive cells in comparison to sham mice. However by 7 days post-injury there was an increase relative to 24 hr injured mice in the numbers of doublecortin positive cells in APP+/+ and sAPPα treated APP-/- mice, but not vehicle treated APP-/- mice. (Images are representative of n=5 per group) (Scale bar = 100μm)

and the sAPPα treated APP-/- mice ($p<0.05$), with some of these cells seen to be migrating into the granular layer of the dentate gyrus and extending their dendrites towards the molecular layer. However in APP-/- mice numbers of doublecortin positive cells remained low, such that they were now significantly decreased when compared to the APP+/+ ($p<0.01$) and sAPPα treated APP-/- mice ($p<0.05$), with little evidence of the incorporation of any immature neurons into the dentate gyrus.

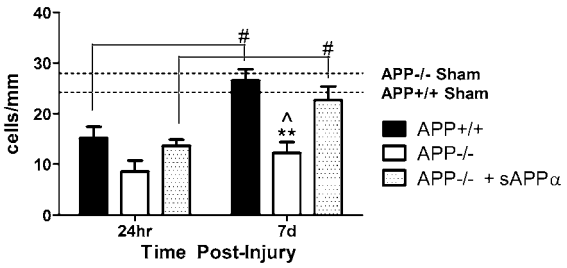

Fig 6.9: Quantitative counts of the number of doublecortin positive cells within the dentate gyrus expressed as cells/mm. There is a significant increase from 24hrs to 7 days in the APP+/+ and sAPPα treated APP-/- mice that is not present in vehicle treated APP-/- mice. (n=5 per group) (p<0.01 compared to APP+/+ mice; ^p<0.05 compared to APP-/- sAPPα treated mice; #p<0.05 compared to 24 hr time point)**

6.3.7 Knockout of APP Decreases Levels of GAP-43 Following CCI Injury

To assess the reparative response following CCI injury levels of GAP-43 were determined immunohistochemically at 7 days post-injury, as GAP-43 is known to be involved in activities such as neurite sprouting and neurite extension which facilitate synaptic plasticity. Following injury, APP-/- mice only had a significant increase in levels of GAP-43 when compared to their shams in the region closest to the lesion, with levels similar to that seen in shams as distance from the lesion increased (Fig 6.10 & 6.11). In contrast both APP+/+ and sAPPα treated APP-/- mice had a significant increase in levels of GAP-43 up to 1.2mm from the lesion site when compared to their respective shams, with these observations confirmed with colour deconvolution ($p<0.0001$ for APP+/+; $p<0.01$ for sAPPα treated APP-/- mice) (Fig 6.10). This showed that APP+/+ mice had significantly higher levels of GAP-43 than APP-/- mice up to 1.2mm from the injury site, including the region closest to the contusion ($p<0.01$). Treatment

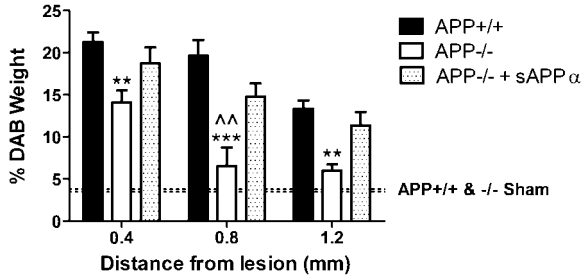

Fig 6.10: Levels of GAP-43 within the cortex expressed as %DAB weight, confirming the decrease in levels observed in APP-/- mice compared to APP+/+ mice and sAPPα treated APP-/- mice post-injury. (n=5 per group) (p<0.01, ***p<0.001 compared to APP+/+ mice, ^^p<0.01 compared to sAPPα treated APP-/- mice)**

with sAPPα meant that APP-/- mice were no longer significantly different to APP+/+ mice with increases in levels of GAP-43 at each of the sites measured when compared to APP-/- mice, with this reaching significance at a distance of 0.8m from the lesion.

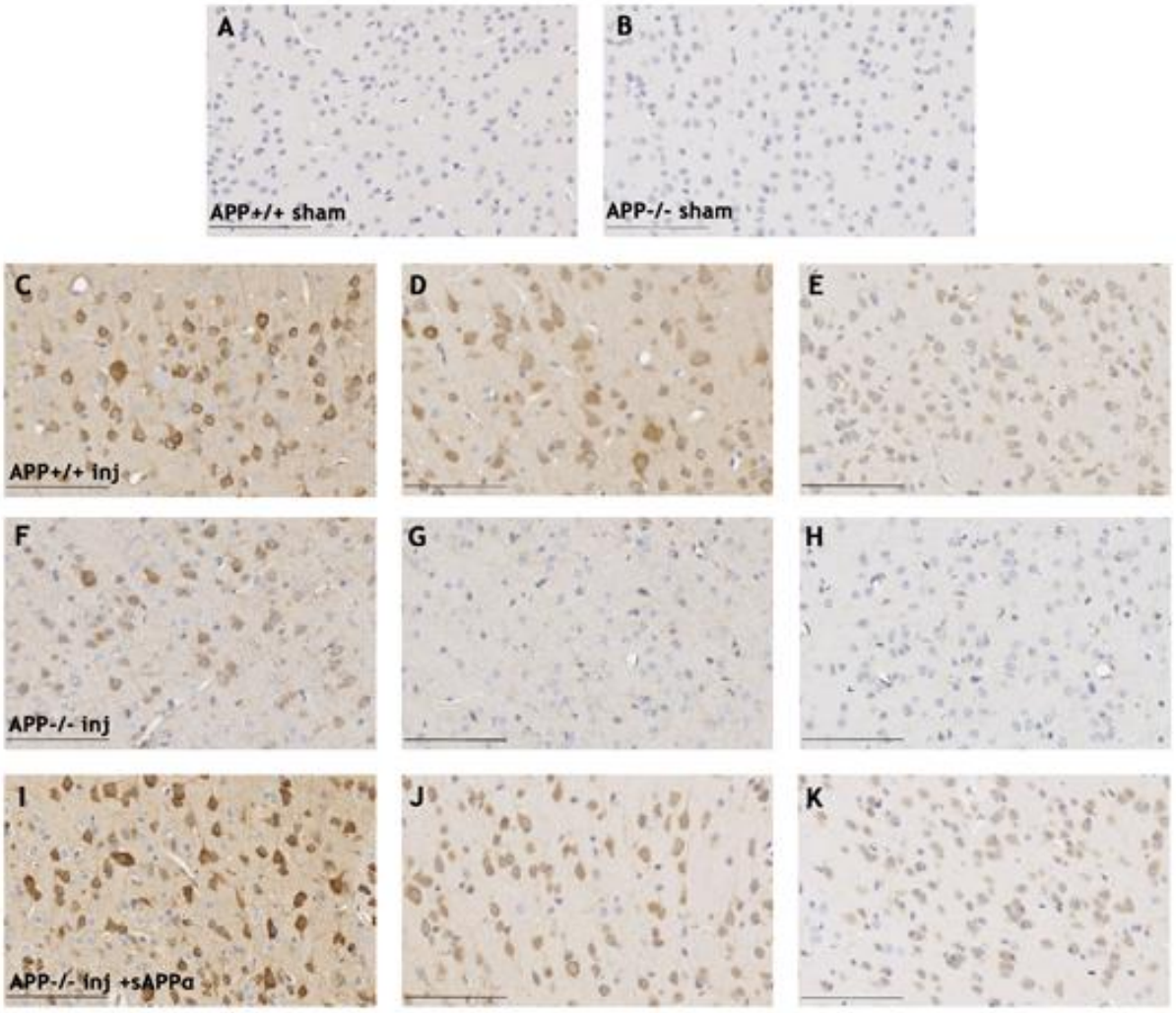

Fig 6.10: Representative images of GAP-43 immunohistochemistry in an APP+/+ (A) and APP-/- (B) sham, with images C-K representing sections taken at increasing distance from the lesion from APP+/+ injured (C-E), APP-/- injured (F=H) and sAPPα treated APP-/- mice (I-K), with the images on the left the closest and those on the right furthest away from the lesion.

6.4 Discussion

This study demonstrates that following a moderate focal injury knockout of APP makes mice more vulnerable, with these mice exhibiting greater functional deficits. These deficits correlated with increased levels of cortical and hippocampal cell damage, as well as an impaired reparative response. This is most likely due to lack of the APP metabolite, sAPPα, as post-injury treatment with this protein was able to prevent the exacerbation of deficits seen in APP-/- mice.

Following injury APP-/- mice exhibited greater motor and cognitive deficits, as detected by increased numbers of foot faults on the ledged beam and increased escape latency on the Barnes Maze in both learning and memory tasks. These were associated with an increase in lesion volume and greater hippocampal cell damage within both the CA region and the dentate gyrus, with an increase in neuronal degeneration, as determined with FJC staining at 24 hrs post-injury, leading to a decrease in hippocampal cell numbers within H&E stained sections by 7 days post-injury. This hippocampal cell loss was also reflected by MAP-2 immunoreactivity, which allows assessment of dendritic integrity (Folkerts et al., 1998), with a significantly greater loss of staining in APP-/- mice within the CA2, CA3 and dentate hilus regions of the hippocampus. Furthermore APP-/- mice had much lower levels of GAP-43, a protein which is unregulated during the repair response to injury (Thompson et al., 2006), with increased GAP-43 levels evident only in the area closest to the lesion, whereas in APP+/+ mice evidence of upregulation extended up to 3 times further.

These changes are not due to a greater amount of primary injury in APP-/- mice as the level of injury was adjusted, with depth of impact decreased from 1.5 to 1.3mm to compensate for the reported decrease in brain size in APP-/- mice (Ring et al., 2007). It should be noted that this has not been associated with major neuronal loss within the cortex or hippocampus of adult APP-/- mice (Herms et al., 2004; Phinney et al., 1999). This is supported by our findings that there was no significant difference in cell numbers within the CA region of the hippocampus nor in the volume of the dentate gyrus between APP+/+ and APP-/- mice. The decision to alter depth rather than impactor tip size was due to a report which indicated that depth is one of the most important factors in determining injury severity, with the other being impactor shape which would have been impossible to alter between groups in a meaningful manner (Mao et al., 2010).This adjustment meant that cortical damage, as assessed by lesion volume and expressed as a percentage of the uninjured hemisphere, and hippocampal damage, as determined by FJC positive neurons, were not significantly different

between the APP+/+ and APP-/- mice at 5 hrs post-injury, with this outlined in the Section 2.3.3. As such the exacerbation of deficits in APP-/- mice is due to an increase in the level of secondary injury received, rather than due to the primary insult. It should also be reiterated that the APP-/- phenotype which includes reduced grip strength (Zheng et al., 1995) and age related cognitive deficits (Phinney et al., 1999; Dawson et al., 1999; Senechal et al., 2008), is not the cause of the impairments observed in these mice following injury, as there was no difference in performance on either the ledged beam or the Barnes Maze between APP+/+ and APP-/- shams.

This study provides evidence that even with increasing injury severity knockout of APP remains detrimental. Thus in APP+/+ mice the production of sAPPα appears to be more important in determining outcome than the presence of other toxic APP metabolites in the week following injury. Indeed, following treatment with sAPPα, APP-/- mice were no longer significantly different to APP+/+ mice, suggesting that lack of sAPPα is the cause of the enhanced deficits in APP-/- mice. This treatment led to a significant improvement in functional outcome, a reduction in cortical and hippocampal cell damage and a restoration of the reparative response when compared to untreated APP-/- mice, further supporting the role of sAPPα as a neuroprotective agent (Copanaki et al., 2010; Goodman and Mattson, 1994; Smith-Swintosky et al., 1994; Thornton et al., 2006). This can partially be attributed to its ability to activate high conductance potassium channels which hyperpolarise the cell and prevent further calcium entry thus reducing levels of excitotoxic cell death (Furukawa and Mattson, 1998), as well as activation of a number of anti-apoptotic pathways (Cheng et al., 2002; Stein et al., 2004), although the full mechanisms of action are yet to be determined.

As well as providing neuroprotection, the neurotrophic role of sAPPα has also been extensively characterised (Araki et al., 1991; Bhasin et al., 1991; Ohsawa et al., 1997; Qiu et al., 1995; Saitoh et al., 1989), with the assessment of MAP-2 staining originally intended to assess the ability of the hippocampus to regenerate dendrites following TBI (Huh et al., 2003). However the results seen within this study appear to predominantly reflect the greater amounts of cell loss evident in APP-/- mice. Thus the increase in MAP-2 levels seen in APP+/+ and sAPPα treated APP-/- injured mice can be accounted for by a greater preservation of hippocampal neuronal cells and hence dendritic integrity, rather than due to an increase in neurite outgrowth.

Nonetheless, evidence for the loss of the neurotrophic role of sAPPα in APP-/- mice is seen through the reduction in GAP-43 levels within the cortex following injury, which is restored following sAPPα

treatment. GAP-43 is a neural specific membrane associated phosphoprotein which is known to be increased following injury (Christman et al., 1997; Emery et al., 2000; Hulsebosch et al., 1998; Thompson et al., 2006) and is an important regulator of synaptic plasticity as it promotes neuronal sprouting and neurite outgrowth (Bendotti et al., 1997). During regeneration GAP-43 is transported along neuronal fibres and distributed in growth cones (Thompson et al., 2006), with its upregulation following injury reflecting an attempt by the injured CNS to promote axonal regeneration and compensate for neuronal loss by creating new synaptic connections (Emery et al., 2003). Indeed increased GAP-43 expression has been hypothesised to correlate with behavioural recovery in tasks such as the beam balance following TBI (Hulsebosch et al., 1998). As such the reduced levels of GAP-43 observed in APP-/- mice reflect an inhibition of intrinsic recovery mechanisms that can facilitate improvement in motor performance following TBI. Interestingly the upregulation of GAP-43 is known to be impaired with increasing injury severity, which may relate to an overwhelming of the post traumatic neural repair response with resultant failure to elicit a plasticity response, as well as increased degradation of plasticity related proteins (Thompson et al., 2006). Thus it is unclear whether knockout of APP in this instance creates an environment which is less conducive for repair, as injury severity was greater in APP-/- than APP+/+ mice, or whether APP itself, through sAPPα, is required to facilitate GAP-43 production and trafficking following TBI.

sAPPα has also previously been shown to affect neurogenesis as it acts synergistically with EGF, as a growth factor for neuronal progenitor cells (Caille et al., 2004). Therefore to examine the effects of APP knockout on neurogenesis, doublecortin immunohistochemistry was used, as it is a reliable marker of immature neurons (Couillard-Despres et al., 2005; von Bohlen Und Halbach, 2007). Within the subgranular zone of the dentate gyrus new neurons are born throughout life (Eriksson et al., 1998). These neurons are capable of migrating into the granular cell layer where they can connect to the CA3 region, their target area (Markakis and Gage, 1999). Predictably at 24 hrs post-injury all mice exhibited a decrease in the number of doublecortin cells within the dentate gyrus, as these cells have been found to be particularly vulnerable following TBI (Rola et al., 2006). However, by 7 days post-injury the APP+/+ and sAPPα treated APP-/- mice had shown a significant increase in the number of doublecortin cells, which was not evident in untreated APP-/- mice, with this re-emergence in line with reports elsewhere (Ramaswamy et al., 2005; Rola et al., 2006) Interestingly doublecortin expressing late neural progenitors have been shown to be more susceptible to injury than early neural progenitors that do not express doublecortin (Yu et al., 2008). Given the significant amount of cell damage evident within the dentate gyrus of the APP-/- mice when compared to APP+/+ mice, the

results seen here may simply reflect a loss of early progenitors rather than an inhibition of maturation of these precursors. Thus APP+/+ mice may have had a remaining pool of early progenitors to repopulate the lost doublecortin expressing late progenitors by 7 days post-injury, which were not present in APP-/- mice. Regardless of the mechanism, given the time frame, it is highly unlikely that the decrease in neurogenesis observed in the APP-/- mice contributed to their greater functional deficits observed in this study, with further studies needed to assess the long term effects of knockout of APP on neurogenesis following TBI.

As sAPPα was able to rescue the exacerbation of deficits seen in APP-/- mice these findings do not support the premise that sAPPα requires the presence of endogenous APP to exert its protective effects. This is contrary to previous reports, which have shown that application of sAPPα to neuroblastoma cells only provided protection from metabolic stress when APP was present (Gralle et al., 2009) and that sAPPα did not stimulate neurite outgrowth in primary neuronal cells in the absence of APP (Young-Pearse et al., 2008). In these studies it was suggested that full length APP was responsible for promoting neuronal death and inhibiting neurite outgrowth, with sAPPα acting by disrupting the activity of cell surface APP. Although a similar toxic role for cell surface transmembrane APP has been postulated elsewhere (Bouron et al., 2004; Rohn et al., 2000; Sudo et al., 2000), it has also been reported to stimulate neurite outgrowth without the presence of sAPPα (Qiu et al., 1995), suggesting that the functional role of full length APP is not yet fully understood. Furthermore knock in of sAPPα *in vivo* was found to be sufficient to mediate the postnatal physiological actions of APP in APP-/- mice, with these animals exhibiting normal brain and somatic growth, normal grip strength development, normal spontaneous home cage activity and normal spatial learning and long term potentiation in aged mice (Ring et al., 2007), areas which are usually affected by knockout of APP (Dawson et al., 1999; Tremml et al., 1998; Zheng et al., 1995). Different mechanisms of action of sAPPα may be present in the *in vivo* compared to the *in vitro* environment, accounting for the discrepancy in results. Alternatively, given the similarity of APLP1 and APLP2 to APP, the actions of these proteins are thought to be enhanced in the absence of APP (Heber et al., 2000; Kaden et al., 2009), and this could provide an alternate route for sAPPα to mediate its effects.

This study further supports the role of endogenous APP as a neuroprotective agent following TBI. Despite the increase in injury severity, knockout of APP increased motor and cognitive deficits, enhanced cell death and inhibited the induction of a reparative response following a moderate focal injury. This can be attributed to lack of the APP metabolite, sAPPα, as treatment with this peptide

was sufficient to restore APP-/- mice to the level of injury seen in APP+/+ mice, providing further evidence of its important role as an endogenous neuroprotective agent.

Chapter 7: The region encompassing the heparin binding site of the D1 domain of sAPPα is sufficient to rescue deficits in amyloid precursor protein knockout mice

7.1 Introduction

In Chapter 3, we found that the D1 and D6a domains, but not the D2 domain of sAPPα were as effective as the full length protein at improving outcome following a diffuse TBI injury in rats. To recap, the predominant isoform of sAPPα within the brain, APP695, consists of 4 domains: a growth-factor like domain (D1), a copper binding region (D2), an acidic region (D3) and a carbohydrate domain (D6), which can be further divided into an E2 domain (D6a) and a juxtamembrane region (D6b) (Reinhard et al., 2005; Storey and Cappai, 1999). As the D1 and D6a, but not the D2 domains contain a heparin binding site, it was hypothesised that the neuroprotective properties of sAPPα may relate to its ability to bind HSPGs.

Intriguingly, binding to heparin has been shown to induce dimerisation in the D1 domain (Dahms et al., 2010; Soba et al., 2005), as well as in the D6 domain (Lee et al., 2011; Wang and Ha, 2004), with this postulated to initiate intracellular signalling cascades (Reinhard et al., 2005). This is proposed as a potential mechanism for the neuroprotective actions of sAPPα, whereby sAPPα prevents the toxic actions of full length membrane bound APP, by disrupting their dimer formation by providing an alternate binding partner (Gralle et al., 2009; Young-Pearse et al., 2008). However, in the previous chapter we demonstrated that sAPPα was able to mediate its neuroprotective and neurotrophic actions without the presence of endogenous APP. This suggests that there may be other pathways through which sAPPα can mediate its actions which do not require heparin binding. Alternatively there may be other mechanisms whereby the binding of sAPPα to HSPGs provides neuroprotection. To investigate, this study examined the effects of treatment with the D1 and D6a domains, as well as their heparin binding sites, APP96-110 and APP416-447 on outcome in APP-/- mice following a moderate focal injury.

7.2 Methods

In this study a total of 28 APP-/- mice that were 10-13 weeks of age were used, with incorporation of the APP-/- shams and vehicle treated mice from the previous chapter, as parts of the study were conducted concurrently.

7.2.1 Induction of Traumatic Brain Injury

As previously described, TBI was induced using the CCI model of injury. Animals were anaesthetised with Avertin, with a craniotomy then performed in the centre of the right parietal bone. Following placement within a stereotaxic frame, a 2mm flat impactor tip was used to cause 1.3mm of deformation at a velocity of 5m/sec with a dwell time of 100 ms. Following the impact a cranioplasty was performed to cover the craniotomy site.

Animals were then randomly assigned to receive treatment with either the D1 domain (APP28-123), or the D6a domain (APP316-498) of sAPPα (n=6 per group), or their heparin bindings sites, APP96-110 or APP416-447 (n=8 per group) (Fig 7.1). The D1 and D6a domains were expressed as a secreted protein in the methylotrophic yeast, *Pichia pastoris* as previously described (Henry et al., 1997). APP96-110 and APP416-447 were produced through custom peptide synthesis (Auspep) using the following sequences, NWCKRGRKQCKTHPH and FNMLKKYVRAEQKDRQHTLKHFEHVRMVDPKK, and were N-terminally acetylated and C- terminally amidated. 150 µl of each peptide (25µM) was then mixed with 75µL of artificial CSF vehicle (Roch et al., 1994; Thornton et al., 2006) prior to administration. 2µl of the appropriate treatment was then administered at a rate of 0.5µl/min into the lateral ventricle as previously described in Chapter 2.

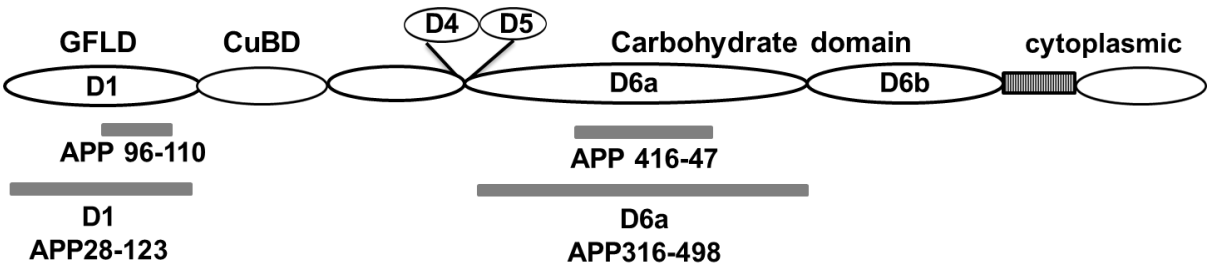

Fig 7.1: Schematic of the different peptides administered in relation to the full length protein

7.2.2 Motor Outcome

Motor deficits were assessed using the ledged beam test. Briefly mice were required to traverse a 1m long tapering beam with underhanging ledges (1cm), walking from the widest (3.5cm) to the

narrowest end (0.5cm). Animals were pre-trained for 3 days prior to injury and then tested daily for a week post-injury, which each mouse given 2 trials. The number of times the underhanging ledge was used (foot faults) by limbs on the side contralateral to the CCI injury were counted and averaged across the two trials.

7.2.3 Cognitive Outcome

Cognitive deficits were assessed using the Barnes Maze, where they were required to find the location of a previously learn escape box which was situated under 1 of 40 holes spaced around the perimeter of a white circular platform. Animals were pre-trained for 5 days prior to injury, with their best time taken as their pre-injury baseline level. Assessment was conducted on days 2, 4 and 6 post-injury, with escape latency (time in seconds) for the mice to find and enter the escape box with front paws and trunk recorded. On day 7 post-injury the escape box was moved to a different, randomly chosen hole to test the ability of mice to learn a new spatial contingency. Mice were allowed three trials, spaced 1 hr apart, to learn the location of the new hole with their escape latency recorded as above.

7.2.4 Tissue processing

For histological analysis animals were perfuse fixed at 7 days after CCI (n=3-5 per group) and were randomly chosen from those undergoing functional assessment. Mice were terminally anaesthetised with Pentobarbital and perfused transcardially with 10% formalin. Brains were then embedded in paraffin prior to sectioning. To ensure inclusion of the entire lesioned cortex, 5 µm sections were collected from Bregma +0.5 to -4mm.

7.2.5 Assessment of brain tissue damage

To determine the extent of cortical damage after CCI injury, 5 sections per brain (400µm apart) were stained with haematoxylin and eosin (H&E), representing the region Bregma -0.5 to -4, as described within Chapter 2. Briefly, the unaffected area of the cortex of each hemisphere was outlined, with the volumes of healthy tissue between successive pairs of sections then added to determine the total volume. This was then used to calculate the percentage of cortical tissue damage.

7.2.6 Assessment of hippocampal damage

Three sections located 200µm apart representing the region Bregma -1.2 to -2.1 were stained with H&E to assesses the degree of hippocampal damage to the CA region. Slides were scanned and viewed with the associated software to allow sequential imaging of the CA region at 40x magnification. These images were imported into Image J to allow manual counting of the number of neurons using the cell count software. To determine the effects of injury on the dentate gyrus, the area of the granular layer of the dentate gyrus was determined in 5 sections located 200µm apart (Bregma -1.5 to -3), with this then used to calculate the volume of the dentate gyrus.

7.2.7 Statistical Analysis

All data was analysed using either a one or two-way ANOVA as appropriate, (repeated measures for functional outcome analysis), followed by Bonferonni t tests using Graphpad Prism software. A p value of less than 0.05 was considered significant in all experiments.

7.3 Results

7.3.1 Motor outcome

Following injury, treatment with either the D1 (Fig 7.2A) or D6a domains (Fig 7.2B) of sAPPα led to a reduction in the number of foot faults in APP-/- mice, significant on days 2-4 ($p<0.05$) for the former and days 3 and 4 for the latter ($p<0.01$). Indeed by day 3 in the D1 treated mice and day 4 in the D6a treated mice, only a small and non-significant deficit in motor performance was noted in comparison to sham animals, whilst in vehicle treated APP-/- mice a much slower rate of improvement was evident. In contrast, treatment with APP96-110 (Fig 7.2A), but not APP416-447 (Fig 7.2B), had a positive effect on motor performance post-injury, with a significant reduction in foot faults on days 2 and 3 post-injury ($p<0.01$). Furthermore, there was a reduction in the number of foot faults for the rest of the testing period, with these mice performing in a similar manner to those treated with the entire D1 domain. In comparison the performance of mice treated with APP416-447 was indistinguishable from that of the vehicle treated APP-/- mice.

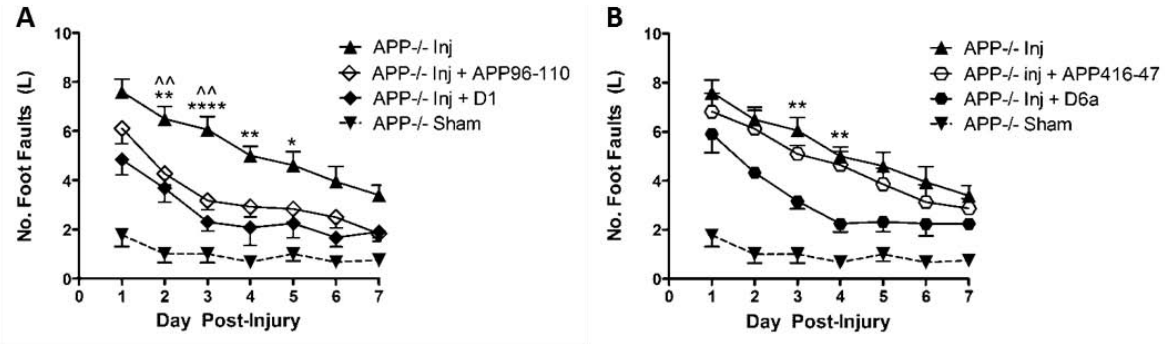

Fig 7.2: Motor outcome as assessed by the ledged beam in APP-/- treated with the D1 domain and its heparin binding site APP96-110 (A) and the D6a domain and its heparin binding site APP416-46 (B), demonstrating that the D1 and D6a domains and APP96-110, but not APP416-47 significantly reduced motor deficits in APP-/- mice. (D1 and D6a domain treated groups n =6; APP96-110 and APP416-47 n=8, vehicle treated APP-/- mice and APP-/- shams n=10) (*p<0.05, **p<0.01, ****p<0.0001 compared to D1 (A) and D6a (B) treated APP-/- mice; ^^p<0.01 compared to APP96-110 treated APP-/- mice)

7.3.2 Cognitive Outcome

Cognitive deficits were seen as an increase in escape latency on the Barnes Maze post-injury. Treatment with both the D1 domain and its heparin binding site, APP96-110, significantly decreased escape latency on days 2 and 4 post-injury ($p<0.05$) when compared to vehicle treated APP-/- mice (Fig 7.3A). In contrast the D6a domain, but not the region APP416-47, which encompasses its heparin binding site, was able to improve cognitive outcome following TBI, with a decrease in escape latency in all days tested post-injury injury in D6a treated mice (46.6, 35.2 and 28 secs vs 68.3, 65.3 and 45.1 secs) which reached significance on day 2. In contrast the time taken to find the location of the previously learnt escape hole in APP416-47 treated mice was similar to vehicle treated controls in 60.1, 62.5 and 42.8 secs (Fig 7.3B).

Similarly when tested on their ability to learn a new location for the escape hole on day 7 post-injury, treatment with the D1 or D6a domains of sAPPα or APP96-110 all significantly reduced escape latency on trial 2 ($p<0.05$) when compared to vehicle treated APP-/- mice. In contrast treatment with APP416-47 had minimal effect (Fig 7.3C&D). Indeed these animals took significantly longer than APP-/- shams on trial 2 ($p<0.05$), whilst the other treatment groups did not.

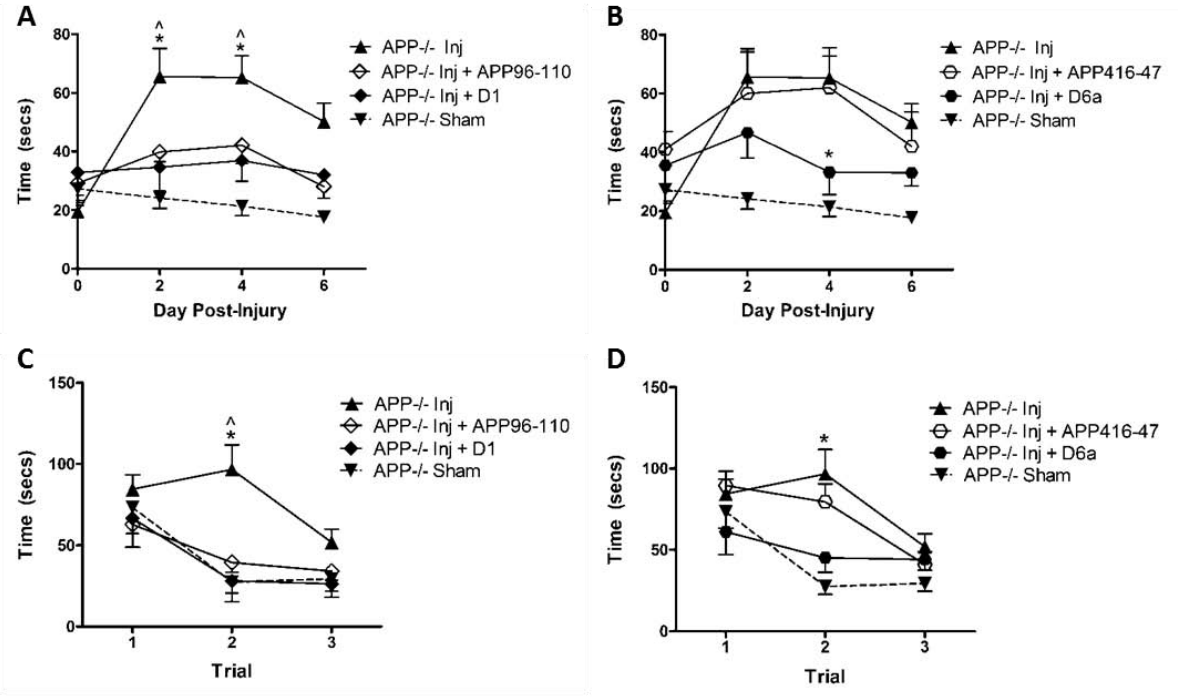

Fig 7.3: Cognitive outcome as assessed by the ability to find a previously learnt escape hole on the Barnes Maze (A&B) and the ability to learn a new location for the escape hole over 3 trials (C&D) in APP-/- treated with the D1 domain and its heparin binding site APP96-110 (A&C) and the D6a domain and its heparin binding site APP416-46 (B&D). This demonstrates that the D1 and D6a domains and APP96-110, but not APP416-47, significantly reduced cognitive deficits in APP-/- mice. (D1 and D6a domain treated groups n=6; APP96-110 and APP416-47 n=8, vehicle treated APP-/- mice and APP-/- shams n=10) (*p<0.05 compared to D1 (A) and to vehicle APP-/- mice (B, C & D); ^p<0.05 compared to APP96-110 treated APP-/- mice (A&C))

7.3.3 Lesion Volume

The extent of cortical tissue damage following TBI was assessed by comparing the volume of cortical tissue within the uninjured left hemisphere to that within the injured right hemisphere to determine a % cortical tissue damage of at 7 days post-injury (Fig 7.4). A significant decrease in cortical damage was evident within the mice treated with the D1 domain, APP96-110 or the D6a domain when compared to vehicle treated APP-/- mice

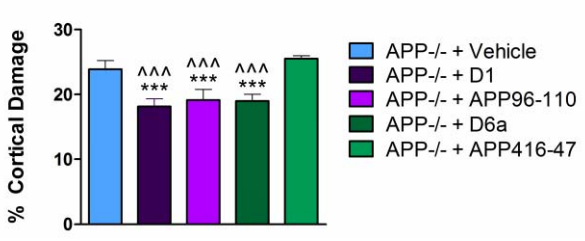

Fig 7.4: Cortical damage was assessed using H&E staining, showing a reduction in D1 or D6a domain and APP96-110 treated APP-/- mice, but not in APP416-47 treated APP-/- mice (Vehicle, APP96-110, APP426-47 treatment groups n=5; D1 and D6a domain treatment groups n=3) (*p<0.001 compared to APP-/- mice; ^^^p<0.001 compared to APP416-47 APP-/- treated mice)**

(p<0.001). Conversely treatment with APP416-47 had no effect on lesion volume, with these mice exhibiting significantly greater tissue damage than the other treatment groups (p<0.001).

7.3.4 Hippocampal Cell Damage

To evaluate the degree of hippocampal damage following TBI, H&E stained sections at 7 days post-injury were assessed, with representative images seen in Fig 7.5A-F. It is evident that there is greater preservation of the CA2/3 region of the hippocampus in APP-/- mice treated with the D1 or D6a domains of sAPPα, as well as those treated with APP96-110. In contrast there is minimal effect following treatment with APP416-47, although there appeared to be a small improvement when compared to vehicle treated mice. These observations were confirmed with a count of the remaining CA neurons showing a significant increase in the mice treated with the D1 domain, its heparin

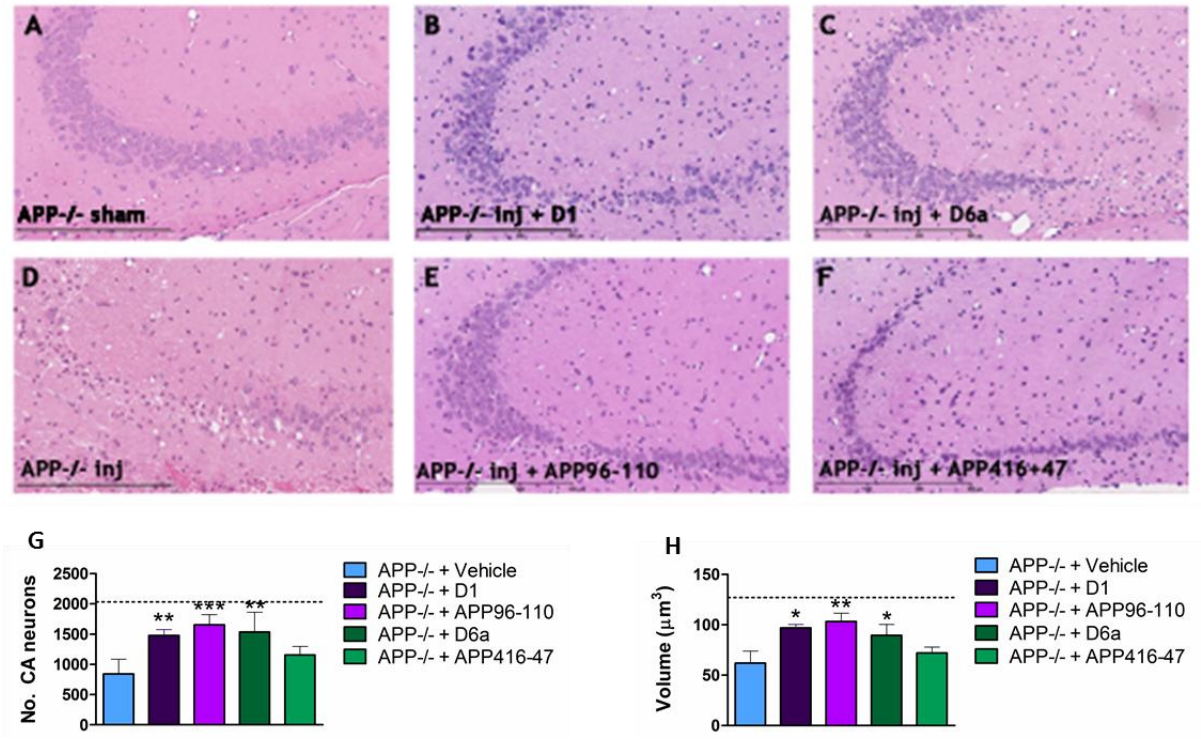

Fig 7.5: Representative images of the degree of hippocampal damage following CCI injury (A-F), showing greater preservation of the CA2/3 region in the D1 (B) and D6a (E) domain of sAPPα, as well as the APP96-110 (E) treated mice when compared to the vehicle treated mice (D) and those treated with APP416-47 (F). These observations were confirmed with counts of the number of remaining CA neurons (G) and determination of the volume of the dentate gyrus (H) (Vehicle, APP96-110, APP426-47 treatment groups n=5; D1 and D6a domain treatment groups n=3) (n=5 per group) (*p<0.05, **p<0.01, ***p<0.001 compared to vehicle treated APP-/- mice)

binding site APP96-110 or the D6a domain when compared to vehicle treated APP-/- mice (Fig 7.5G). A similar improvement in the volume of the dentate gyrus was noted in these treatment groups, whilst the APP416-47 peptide had no effect (Fig 7.5H).

7.4 Discussion

In this preliminary study, the D1 and D6a domains of sAPPα were shown to be as effective as each other in improving outcome in APP-/- mice following a CCI injury. However whilst the region encompassing the heparin binding site within the D1 domain, in APP96-110, was similarly capable of rescuing functional deficits and improving histological outcome in APP-/- mice, the peptide APP416-447, representing the heparin binding site of the D6a domain, had no effect.

Treatment with the peptide APP96-110 was able to reduce functional deficits, as detected by a reduction in the number of foot faults on the ledged beam and a decrease in escape latency on the Barnes Maze. This was accompanied by a significant reduction in the amount of cortical damage and significantly greater preservation of both the CA and dentate gyrus regions of the hippocampus. Indeed this peptide was as effective as the entire D1 domain of sAPPα, suggesting that it is this region that is responsible for its neuroprotective activity. The APP96-110 region contains a β hairpin loop formed by a disulphide bridge between cysteines 98 and 105 (Rossjohn et al., 1999; Small et al., 1994), with the presence of this bridge previously shown to be critical for promoting neurite outgrowth (Young-Pearse et al., 2008) and activation of MAP kinase (Greenberg and Kosik, 1995). This most likely relates to maintenance of the correct secondary structure to facilitate binding to heparin, with binding of this region to HSPGs known to promote neurite outgrowth from central and peripheral neurons (Small et al., 1994). Furthermore, an antibody that binds to this region inhibits functional synapse formation (Morimoto et al., 1998), completely abolishes depolarisation induced neurite outgrowth (Gakhar-Koppole et al., 2008) and prevents the effects of sAPPα in promoting the migration and differentiation of human neural stem cells (Kwak et al., 2006).

Although the lack of APP precludes the ability of APP96-110 to exert its effects through interaction with cell membrane bound APP, it may still be interacting with the APP paralogues, APLP1 or APLP2. Interaction with APLP2 is most likely as APLP1 lacks a heparin binding site within the D1 domain (Kaden et al., 2011). Physiologically, whilst individual knockout of APP, APLP1 or APLP2 has minimal effects, combined knockout of APP and APLP2 is perinatally lethal suggesting a degree of functional

overlap, at least developmentally (Heber et al., 2000; von Koch et al., 1997). sAPPα has previously been shown to promote neurite outgrowth *in vitro* in APP or APLP2 knockout neuronal cultures, but not with a combined knockout (Gakhar-Koppole et al., 2008). However, another study showed that sAPPα did not promote neurite outgrowth in primary neuronal cultures from APP-/- mice, suggesting that the presence of APLP2 did not compensate for the lack of APP (Young-Pearse et al., 2008). It is unclear what caused the discrepancy in these results, but could relate to factors such as the timing of analysis after plating or the substrate used. In terms of neuroprotection, whilst Gralle *et al* showed that full length APP was required for sAPPα to exert its protective effects against metabolic stress, it was not examined whether the presence of APLP2 would have a similar effect (Gralle et al., 2009). The B103 neuroblastoma cells used in the study do not have endogenous APP or APLPs (Schubert and Behl, 1993), with only the effects of transfection of these cells with APP studied.

Although it is unclear whether the presence of APLP2 can act as a mediator for the actions of sAPPα in the absence of APP, heterodimerisation between the APP family members has previously been shown to occur, with this reliant on the presence of the D1 domain (Bai et al., 2008; Soba et al., 2005). Indeed mutant APP and APLP constructs deficient in an extended version of the D1 domain, showed a reduction in the amount of coimmunoprecipiation indicative of a lack of dimer formation (Soba et al., 2005). Dimerisation of APP has been shown to require the presence of heparin (Dahms et al., 2010; Gralle et al., 2006). Furthermore, the APP96-110 region has been shown to be essential for dimerisation, as addition of a small peptide which interfered this loop region reduced the amount of dimerisation present (Kaden et al., 2008; Scheuermann et al., 2001). It is yet to be determined what functional effects relate to the phenomenon of homo- and heterodimerisation of APP family members, although it has been suggested to influence APP processing (Kaden et al., 2011). It is evident that further investigation is needed to determine the exact mechanisms whereby APP96-110 exerts its neuroprotective effects. It should be noted that although this region encompasses a heparin binding site, suggesting that binding to HSPGs in some manner is involved, the neuroprotective actions of this peptide could relate to another mechanism of action.

Although the region APP96-110, encompassing the heparin binding site of the D1 domain of sAPPα, was found to rescue deficits in APP-/- mice, the peptide APP417-446 representing the heparin binding site of the D6a domain of sAPPα had no effect. This is despite the fact that the D6a domain itself was found to be effective at reducing deficits in APP-/- mice. There are several reasons whereby the fragment APP417-446 of the D6a domain did not show efficacy in improving outcome in APP-/-

mice. Firstly the heparin binding site encompasses six basic residues from helices αC and αD of one monomer (Arg-375, His-382, Arg-424, Lys-428, His-432, His-439) and a conserved Arg-336 from helix αB′ of the second monomer (Wang and Ha, 2004). Although we included the key heparin binding residues in Arg-424, Lys-428, His-432, His-439, inclusion of the other residues was impractical, as the length of the peptide would have been too great to allow manufacture (R Cappai, personal communication). Hence, further studies will be needed to ensure whether this peptide has the appropriate secondary structure in order to have a functional effect. Alternatively, the heparin binding site within the D6a domain of sAPPα may not be responsible for its neuroprotective properties. As discussed extensively within Chapter 3, another putative site within this region, the pentapeptide motif `RERMS' (APP328-332), has been shown to be neurotrophic (Jin et al., 1994; Ninomiya et al., 1993; Roch et al., 1994) and neuroprotective (Yamamoto et al., 1994). However this remains controversial as other studies have failed to show a similar effect (Furukawa et al., 1996; Ohsawa et al., 1997). Finally, although this region could require the presence of endogenous APP to exert its protective effects, this seem unlikely since this study demonstrated that the D6a domain of sAPPα was able to reduce deficits in APP-/- mice.

This study has identified the region within the D1 domain, in APP96-110, which is capable of rescuing deficits in APP-/- mice, suggesting that binding to HSPGs are an important mechanism whereby sAPPα exerts its neuroprotective effects. However further research is needed to identify the site within the D6a domain which confers its protective activity. Whilst treatment with the D6a domain improved outcome in APP-/- mice, the region encompassing its heparin binding site in APP416-447 had no effect.

Chapter 8: Summary and Future Directions

The experiments within this thesis have demonstrated that knockout of APP worsens functional and histological outcome following both a mild diffuse and a moderate focal TBI. This is most likely due to lack of the APP metabolite sAPPα, as treatment with the peptide post-injury was able to rescue the exacerbation of deficits in APP-/- mice. The neuroprotective region within APP was initially narrowed down to the D1 and D6a domains of sAPPα, with preliminary investigations in APP-/- mice suggesting that the peptide APP96-110 is sufficient to provide neuroprotection.

8.1 Benefit of exogenous application of sAPPα following TBI

The studies within this thesis were based upon an initial investigation which demonstrated that exogenous application of sAPPα was able to improve motor outcome with an associated reduction in apoptotic cell death and axonal injury following a diffuse injury in rats (Thornton et al., 2006). These findings were replicated within this thesis, with sAPPα treatment found to improve motor and cognitive outcome following both a diffuse injury in rats and a moderate focal injury in mice, providing further evidence for its use as potential therapeutic agent following TBI.

Indeed, this was the first study to demonstrate that sAPPα treatment could also provide benefit following a focal TBI. However, as discussed extensively within Chapter 5, the improvement seen following the focal injury in mice was less impressive than that seen in rats. This was attributed to the greater spontaneous recovery seen in mice following TBI, as well as the more rapid rate of degeneration seen following a focal injury, making it more difficult to obtain a significant treament effect. Indeed de Olmos silver staining, which selectively stains degenerating neuronal axons and nerve terminals, demonstrated that minimal neurodegeneration is present at 24 hrs post-injury following a diffuse injury, with the peak of neurodegeneration in the cortex, hippocampus, and striatum observed at 3 days post-injury (Kupina et al., 2003). In contrast, following a moderate CCI injury a significant increase in silver staining is present by 6 hrs post-injury and peaks at 48 hrs, although there is minimal difference in the amount of staining from 28-72 hrs post-injury (Hall et al., 2008).

Interestingly a report published this year has indicated that use of a rounded tip, rather than the flat tip employed here, and indeed by many others (Dennis et al., 2009; Fox et al., 1998; Sandhir and Berman, 2010; Smith et al., 1995; Thompson et al., 2006; Whalen et al., 2008; Xiong et al., 2005), may slow the rate of neurodegeneration, potentially producing a focal injury that may be more

amenable to the testing of potential therapeutics (Pleasant et al., 2011). This is because use of a flat tip results in high tissue strains localised at the impactor rim, whereas a rounded tip leads to more radially distributed strains (Mao et al., 2010). Pleasant *et al* (2011) found that the peak of neuronal death within the cortex and hippocampus occurred at 4 hrs post-injury with the flat tip, whereas with the rounded tip the initial neocortical damage evident in the first 12 hrs post-injury was milder, although by 24 hrs the amount of damage was equivalent to flat tip impactor. Indeed there was no difference between the two types of impactors in terms of the size of the contusion or amount of axonal injury by 9 days post-injury or in the degree of neurobehavioural deficits. This suggested that it was only the rate of neurodegeneration that was altered, not the amount. Within our study there was also minimal expansion of the amount of cortical damage from 5 to 24 hrs (14.47%±0.76 vs 16.7%±0.98), but hippocampal damage, as measured by the number of FJC+ve neurons within the hippocampus, did increase within both the dentate gyrus (47±23.6 vs 133±17.4) and CA regions (68.6±33.4 vs 157±35.5). This suggests that there may be other factors apart from tip shape that influence the rate of neurodegeneration following injury. Indeed, histologically the depth of impact appeared greater within the Pleasant *et al* study (2011), with early damage to the CA1 region of the hippocampus that was not evident in this study. This reiterates the need to characterise an injury model, as the amount and rate of cell damage may differ between laboratories depending on the exact protocol employed. Regardless, comparison of treatment efficacy following CCI injury employing different tip shapes could be explored in the future. The predicted slower evolution of damage with use of a rounded tip may be more clinically relevant and allow a more accurate assessment of the usefulness of therapeutics in a focal injury.

8.2 The role of endogenous APP following TBI

Although exogenous sAPPα treatment was shown to improve outcome following both diffuse and focal TBI, it was unclear what role endogenous APP would play due to the disparate actions of its metabolites, neuroprotective sAPPα and toxic Aβ. However, mice deficient in APP were shown to have increased motor and cognitive deficits following both diffuse and focal TBI, with this associated with increased neuronal damage and an impaired reparative response. The differences noted within this thesis were not due to baseline phenotypic differences between APP+/+ and APP-/- mice, which include reductions in body weight, grip strength and brain weight in APP-/- mice (Zheng et al., 1995). Furthermore, with age, deficits are noted in spatial learning which are associated with decreased neocortical and hippocampal levels of synatophysin and reduced dendritic lengths of hippocampal

neurons (Dawson et al., 1999; Zheng et al., 1995). To counter these effects the APP-/- mice used were between 10-16 weeks of age, with sham APP+/+ and APP-/- mice identical in performance on the Barnes Maze, both during the acquistion phase and in post-surgery testing, indicating that no cognitive impairment was present. In addition, no differences in synaptophysin or MAP-2 staining intensity within the hippocampus were noted between the APP-/- and APP+/+ mice. Furthermore, no differences were seen in neuronal numbers within the CA and dentate gyrus regions of the hippocampus despite the reduction in brain weight, which is in line with previous reports which have not found major neuronal loss within the cortex or hippocampus of adult APP-/- mice (Herms et al., 2004; Phinney et al., 1999).

The injury parameters were also altered between APP+/+ and APP-/- mice for both the diffuse and focal injury models to ensure that the level of primary injury received was the same. Knockout strains can display different suceptibility to the impact (Flierl et al., 2009), with this of particular concern due to the phenotypic differences outlined above. Thus as described in the relevant chapters, for the diffuse injury the height from which the weight was released was reduced to ensure that righting time was the same between the groups, whilst for the focal injury depth of impact was reduced such that there was no histological difference in the amount of cortical or hippocampal damage at 5 hrs post-injury. As such the aggravation of deficits in APP-/- mice following TBI can be attributed to an increase in the level of secondary injury received, rather than a greater level of primary insult or due to baseline differences between the strains.

These results, showing that endogenous APP is protective following TBI *in vivo*, are contrary to earlier *in vitro* studies, which showed that there was no difference in survival rates between APP-/- and APP+/+ cortical neurons exposed to oxidative stress (Harper et al., 1998; White et al., 1998) or excitotoxicity (White et al., 1998). However our results are supported by another *in vitro* study which demonstrated that cultured cortical and hippocampal neurons from APP-/- mice were more susceptible to glutamate exposure, exhibiting less than 20% survival compared to 50% in wild-type neurons (Han et al., 2005). This deficit was primarily restored with the addition of sAPPα, which is in line with our finding that treatment with sAPPα post-injury was able to prevent exacerbation of neuronal damage and improve functional outcome in APP-/- mice, such that they were no longer different to APP+/+ mice. This further supports the theory that APP chiefly exerts its neuroprotective actions through its metabolite, sAPPα. As outlined throughout this thesis, sAPPα has previously been shown to be neuroprotective, with this attributed to its ability to activate high conductance

potassium channels which hyperpolarise the cell and thus reduce excitotoxic damage (Furukawa and Mattson, 1998), as well as activation of a number of anti-apoptotic pathways (Cheng et al., 2002; Stein et al., 2004).

The reparative response was also found to be inhibited in APP-/- mice following TBI, as detected by a decrease in levels of GAP-43. This is unsurprising given the extensive characterisation of the neurotrophic effects of sAPPα, with its application *in vitro* consistently found to increase neurite outgrowth (Araki et al., 1991; Bhasin et al., 1991; Ohsawa et al., 1997; Qiu et al., 1995; Saitoh et al., 1989). It should, however, be noted that within the studies in this thesis it cannot be determined whether the failure to demonstrate an increase in levels of GAP-43 is due to a direct inhibition of the reparative response due to lack of APP. The enhancement of the secondary injury cascade in APP-/- mice, seen as an increase in the amount of neuronal damage, may also have inhibited the reparative response (Thompson et al., 2006). It is evident that further studies will be necessary to identify the specific pathways that are activated following in TBI in order for sAPPα to exert its effects.

There is an upper limit to the protection provided by endogenous APP, with preliminary investigations showing no difference in functional outcome following a severe CCI injury induced by 2mm cortical deformation in APP+/+ mice and 1.8mm in APP-/- mice (data not shown). At this level of injury, as seen in Chapter 5, there is a considerable deformation of the hippocampus, suggesting that endogenous neuroprotective pathways may be overwhelmed when structural damage is extensive. The intensity of the secondary injury response may also play a role, as it may create an environment which acts to inhibit the reparative response. For example, although excessive calpain activation is known to occur following TBI due to injury induced calcium influx, calpain mediated spectrin breakdown was found to be a 100x greater than sham level following a severe CCI injury compared to 12x greater after a moderate CCI injury (Thompson et al., 2006). The preferred substrates for calpain include cytoskeletal proteins, membrane receptors and transporters and signalling transduction proteins (Carafoli and Molinari, 1998; Wang, 2000), with many of these substrates involved in neuroplasticity (Saatman et al., 1996). Indeed calpain substrates include cytoskeletal proteins like actin and specrin which are important for cytoskeletal remodeling (Chan and Mattson, 1999; Lynch and Baudry, 1987), as well as GAP-43, which promotes neuronal sprouting and neurite extension following TBI (Zakharov et al., 2005). This was seen in Chapter 5 where it was noted that whilst levels of cortical GAP 43 were increased from a mild to moderate level of CCI injury, in severely injured mice levels were decreased relative to the moderately injured mice.

Nonetheless, the results within this thesis support the theory that following a mild-moderate TBI, the neuroprotective properties of sAPPα outweigh any potential negative effects of other APP metabolites such as Aβ, AICD and C31, at least in the week following injury. These peptides are known to be pro-apoptotic (Bertrand et al., 2001; Kim et al., 2004; Lu et al., 2000; Mattson et al., 1998), with previous studies suggesting that they may be involved in enhancing the secondary injury cascade following TBI (Abrahamson et al., 2006; Loane et al., 2009; Stone et al., 2002). The long term implications of enhanced APP production, in relation to the risk of the later development of Alzheimer's disease remains controversial (reviewed in Van Den Heuvel et al., 2007), with the studies within this thesis not precluding the development of late negative effects of the presence of APP following TBI.

It should also be noted that although the studies within this thesis have shown that endogenous APP is neuroprotective following TBI, non-transgenic mice are unable to develop the Aβ plaque pathology that is seen in clinical TBI due to a three amino acid difference in Aβ sequence (Johnson et al., 2010). Furthermore, rodent Aβ is thought to be less toxic, as it does not reduce Cu (II) as effectively as human Aβ, which may affect its ability to promote oxidative stress. However, although rodent Aβ does not form plaques, it has been shown to form β-sheet fibrils *in vitro* (Fraser et al., 1992), but not as aggressively as human Aβ (Boyd-Kimball et al., 2004). Furthermore, induction of protein oxidation and lipid peroxidation in primary neurons has been demonstrated with rodent Aβ, with this triggering apoptosis and cell death, although at a slower rate than human Aβ (Boyd-Kimball et al., 2004).

Upregulation of soluble Aβ has been demonstrated following TBI in rodents (Blasko et al., 2004; Iwata et al., 2002; Loane et al., 2009; Mannix et al., 2010), as has aggregation of Aβ within damaged axons (Stone et al., 2002). This suggests that in rodent models increased Aβ production may still influence secondary injury mechanisms following TBI despite the lack of plaque formation. Indeed progressive cortical deterioration observed in injured adult APOε4 mice, who have reduced Aβ clearance, was associated with high levels of Aβ in both cerebral hemispheres at 1 month after injury (Mannix et al., 2010). Furthermore, increasing Aβ clearance without affecting APP processing through treatment with the cholesterol efflux transporter ABCA1 (ATP-binding cassette A1), improved functional recovery and significantly reduced lesion volume in non-transgenic mice (Loane et al., 2011). However, future studies in species with the human Aβ sequence may provide further evidence on the role that endogenous APP plays following TBI.

Interestingly, a recent report by Mannix *et al*, has challenged the idea that Aβ is neccessarily detrimental immediately following TBI, with knockout of BACE-1 in 8-12 week old mice found to worsen functional outcome, as assessed up to 10 days following injury (Mannix et al., 2011). It was suggested that this could be attributed to lack of the monomeric form of Aβ which is postulated to have a physiological function in depressing synaptic activity, thus providing feedback to prevent synaptic activity from becoming excessive (Kamenetz et al., 2003). Indeed these Aβ monomers have been shown to to enhance survival of developing neurons under conditions of trophic deprivation and protect mature neurons against excitotoxic death (Giuffrida et al., 2009). Recent studies employing intracerebral microdialysis to allow measurements of soluble Aβ within the extracellular space have found that levels of Aβ actually decrease following TBI in both mice (Schwetye et al., 2010) and humans (Brody et al., 2008). Furthermore, levels of Aβ increase as a patient recovers (Brody et al., 2008). This may, however, only be providing an indirect measure of neuronal activity, with suppression of activity following injury reducing the genesis of Aβ, whose production is correlated with the amount of synaptically coupled endocytic activity (Cirrito et al., 2008; Cirrito et al., 2005). Levels of Aβ then gradually increase as normal neuronal activity is restored. Furthermore, these microdialysis studies do not preclude a detrimental role for Aβ following TBI, as the decrease in extracellular soluble Aβ noted may simply reflect extracellular Aβ depostion into toxic insoluble aggregates or intracellular Aβ retention (Magnoni and Brody, 2010).

The worsening of functional outcome in young adult BACE-1-/- mice may also be due to loss of the effects of BACE-1 on other substrates, rather than due to a the lack of Aβ. For example neuroregulin-1 is known to be a substrate of BACE-1 (Evin et al., 2010), with treatment with neuroregulin-1 shown to improve cognitive outcome following TBI (Lok et al., 2007). Interestingly, the findings of the Mannix *et al* (2011) study are in direct contradiction of an earlier study by Loane *et al* (2009) who found that BACE-1 deletion decreased brain tissue damage and improved motor and cognitive deficits after CCI in aged mice (11-12 months). It was suggested that the disparity between these studies may be due to differences in Aβ dynamics following TBI with age. Indeed BACE-1 activity is known to increase with age (Miners et al., 2010), with the constitution of Aβ also changing, levels of insoluble Aβ increase whilst the amount of soluble Aβ decreases (van Helmond et al., 2010a) . Thus these differences in aged wildtype mice may mean that Aβ plays a greater role in the secondary injury process than seen in younger mice. In addition levels of sAPPα have been shown to decrease with age in rats. (Anderson et al., 1999). Inhibition of BACE-1 activity has been shown to increase levels of sAPPα (Sala Frigerio et al., 2010; Sankaranarayanan et al., 2008), and given the already

reduced levels in aged mice, there could be a greater difference in the levels of sAPPα in aged wildype versus BACE-1-/- mice than in the young adult mice. This could account to some degree for the dramatic improvement seen in aged BACE-1-/- mice that was not evident in the younger mice. Indeed in the younger mice any benefits of promotion of non-amyloidogenic processing may have been outweighed by other unrelated effects of BACE-1 knockout, for example by altering levels of neuroregulin-1, that are yet to be fully determined. The discrepancy between these studies highlight that age may influence the role of APP following TBI. It would be interesting to determine whether the difference in functional and histological outcome between APP-/- and APP+/+ mice decreases with age, although this would be a difficult study to perform due to the age related deficits noted in APP-/- mice.

8.3 Delineating the neuroprotective region within sAPPα

As well as examining the benefit of exogenous and endogenous sAPPα in improving outcome following TBI, we were also interested in determining the exact region within the protein that conferred this activity. Our Initial study, testing the efficacy of the D1, D2 and D6a domains of sAPPα in improving outcome in rats following a diffuse TBI indicated that either the D1 or D6a domains of sAPPα were as effective as the full length protein in improving outcome. This is in line with earlier reports that in the nematode *Caenorhabditis elegans* who have a single APP-related gene, APL-1, that knock-in of either the D1 or D6 domains was sufficient to rescue deficits in APL-1 deficient animals (Hornsten et al., 2007). As the D1 and D6a domains contain heparin binding sites, we suggested that the protective properties of sAPPα may relate to its ability to bind HSPGs. Heparin sulphate chains are normally attached to core proteins to form HSPGs which are located at the cell surface and in the ECM (Turnbull et al., 2001). These proteoglycans, which are glycoproteins with one or more GAG chains attached to the core protein, include the syndecan family of transmembrane proteins, the glypican family of proteins attached to the cell membrane and ECM proteins such as perlecan (Raman et al., 2005). Specific sequences in heparin sulphate chains are designed for interactions with certain proteins and regulate a number of functions such as cell signalling, cell adhesion and neurite outgrowth (Spillman and Lindahl, 1994). It is known that the the majority of binding sites for APP in the ECM are these HSPGs, with interference with the ability of APP to bind heparin preventing its neuroprotective (Furukawa et al., 1996) and neurotrophic actions (Williamson et al., 1996).

To investigate whether treatment with the regions encompassing the heparin binding sites within the D1 and D6a domains were sufficient to provide protection, we tested the ability of APP96-110 and APP416-447 respectively, to rescue deficits in APP-/- mice following a focal CCI injury. As these peptides were obtained 18 months after the completion of the study investigating the effects of treatment with different domains of sAPPα in rats, this precluded their inclusion within that study. Furthermore, given the modest benefit noted with sAPPα treatment in APP+/+ mice, it was determined that the greatest likelihood of seeing a significant improvement in outcome following TBI would be seen with treatment of APP-/- mice. Planned future studies will investigate the benefits of these peptides in non-transgenic animals, to determine whether they are sufficient to provide neuroprotection.

Nonetheless, this study found that APP96-110, but not APP416-447, was able to prevent exacerbation of deficits in APP-/- mice, improving motor and cognitive outcome with an accompanying reduction in cortical and hippocampal neuronal damage. It should be noted that this does not conclusively exclude the possibility that the heparin binding site is the active region within the D6a domain of sAPPα, as further studies will be needed to assess whether the APP416-447 peptide adopts the appropriate secondary structure to allow heparin binding. As discussed in Chapter 7, inclusion of all the amino acids thought to be involved in the heparin binding site was not practical, as the size of the peptide would have been too great to allow its manufacture. Indeed, there is evidence that the heparin binding site within the D6a region may play a role in regulating levels of intracellular calcium (Furukawa and Mattson, 1998), promoting neurite outgrowth (Qiu et al., 1995) and facilitating in dimerisation of APP (Lee et al., 2011; Wang and Ha, 2004). Alternatively another route of investigation would be to evaluate the abiilty of the putative neuroprotective region `RERMS', located within the D6a domain of sAPPα, to improve outcome following TBI.

The cyclic nature of the APP96-110 peptide, due to the presence of a disulphide bridge between cysteines 98 and 105 (Rossjohn et al., 1999; Small et al., 1994), ensures that it maintains the same secondary structure as would be seen in full length sAPPα, and thus maintains its ability to bind heparin. Although it is yet to be determined the exact mechanisms whereby the APP96-110 peptide exerts its effects, binding of this region to HSPGs has been shown to promote neurite outgrowth (Small et al., 1994). Furthermore an antibody that binds to this region inhibits its neurotrophic functions, preventing functional synapse formation (Morimoto et al., 1998) and depolarisation induced neurite outgrowth (Gakhar-Koppole et al., 2008). To definitely determine whether heparin

binding is required for the neuroprotective properties of this peptide, future studies could employ a mutated version which lacks the ability to bind heparin.

The ability of the APP96-110 peptide, and indeed of the D1 and D6a domains of sAPPα, as well as sAPPα itself, to rescue deficits in APP-/- mice suggests that sAPPα does not require the presence of endogenous APP to exert its neuroprotective effects. This disputes the claims that sAPPα acts by interrupting the toxic actions of APP dimers (Gralle et al., 2009; Young-Pearse et al., 2008), but corresponds with an earlier study that found that knock in of sAPPα was sufficient to rescue deficits in APP-/- mice (Ring et al., 2007)

It is possible that in the absence of APP, sAPPα, through its D1 and D6a domains, and more specifically the region APP96-110, may act through interactions with APLP2 and APLP1. As APP-/- mice age, levels of both APLP1 and APLP2 are known to increase in the brain relative to wildtype mice, suggesting they may compensate for some of the physiological activities of APP (Soba et al., 2005). Indeed, the functions of this family of proteins appear to be partially redundant, with only minor phenotypic effects of single knockout of any of these genes, or of APP/APLP1 knockout, whilst APP/APLP2 and APLP2/APLP1 knockout are perinatally lethal (Heber et al., 2000; von Koch et al., 1997). APP and both APLPs are highly conserved proteins, with many conserved regions over a large portions of the ectodomain and within the intracellular tail, although both APLP1 and APLP2 lack the Aβ region (Reinhard et al., 2005). A heparin binding site is found in all three proteins within the D6a domain, but only APP and APLP2 also have a heparin binding site within the D1 domain (Anliker and Muller, 2006). Given the importance of APLP2, as highlighted by the combined knockout studies, as well as its ability to interact with the heparin binding site of the D1 domain, it appears feasible that it could be an alternate receptor for sAPPα signalling in APP-/- mice.

Heparin binding has been shown to be important for promoting dimerisation of the ectodomain of APP through interactions within the region encompassing APP96-110 of the D1 domain (Kaden et al., 2008), as well as with the D6a domain (Lee et al., 2011). Heterodimersiation is also known to occur between the APP family members, with both *cis* and *trans* dimerisation demonstrated (Soba et al., 2005). Whereas *trans* dimerisation may play a role in cell-cell adhesion (Kaden et al., 2011; Soba et al., 2005), *cis*-dimerisation has been hypothesised to allow activation of intracellular signalling pathways (Gralle et al., 2009; Reinhard et al., 2005). Alternatively *cis* dimerisation may influence the processing of APP, possibly by changing its conformational state, thus decreasing its amyloidogenic

processing by preventing access of β-secretase to its cleavage site (Kaden et al., 2008). No consensus has yet been reached on the role of dimerisation of APP family members (Gralle et al., 2009; Kaden et al., 2008; Soba et al., 2005), the regions that are involved in promoting dimerisation (Soba et al., 2005; Wang and Ha, 2004), if heparin binding is required (Dahms et al., 2010; Gralle et al., 2006; Lee et al., 2011; Wang and Ha, 2004) or whether this dimerisation is dependent on cellular location (Dahms et al., 2010; Kaden et al., 2008; Soba et al., 2005). Indeed it is unclear whether cell surface full length APP or APLPs are primarily dimerised, or mainly present as monomers, with this having important implications for how these proteins may intereact with sAPPα (Dahms et al., 2010; Kaden et al., 2008; Soba et al., 2005). As such it is unclear whether the peptide APP96-110, or indeed sAPPα, requires the presence of APP family members to mediate its beneficial effects, or if other mechanisms of actions are involved, with further research needed into this issue.

8.4 Conclusion

The studies within this thesis identified a neuroprotective role for endogenous APP following TBI, as its knockout led to a worsening of motor and cognitive deficits, increased neuronal damage and an impaired reparative response following both a mild diffuse and moderate focal TBI. This was most likely due to lack of sAPPα, as treatment with sAPPα post-injury was able to rescue the exacerbation of deficits in APP-/- mice such that they were no longer different to APP+/+ mice. We were also able to confirm the benefits of exogenous sAPPα treatment following TBI, and specifically determined that both the D1 and D6a domains of sAPPα were sufficient to provide neuroprotection, potentially due to their ability to bind to HSPGs. This led to a preliminary investigation that determined that the region encompassing the heparin binding site of the D1 domain, in APP96-110, warrants further investigation as a putative neuroprotective agent following TBI, as it was significantly improved outcome in APP-/- mice.

References

Abou-Hamden A, Blumbergs PC, Scott G, Manavis J, Wainwright H, Jones N, McLean J. Axonal injury in falls. J Neurotrauma, 1997; 14: 699-713.

Abrahamson EE, Ikonomovic MD, Ciallella JR, Hope CE, Paljug WR, Isanski BA, Flood DG, Clark RS, DeKosky ST. Caspase inhibition therapy abolishes brain trauma-induced increases in Abeta peptide: implications for clinical outcome. Exp Neurol, 2006; 197: 437-50.

Adams JH, Doyle D, Ford I, Gennarelli TA, Graham DI, McLellan DR. Diffuse axonal injury in head injury: definition, diagnosis and grading. Histopathology, 1989; 15: 49-59.

Adle-Biassette H, Duyckaerts C, Wasowicz M, He Y, Fornes P, Foncin JF, Lecomte D, Hauw JJ. Beta AP deposition and head trauma. Neurobiol Aging, 1996; 17: 415-9.

Allinquant B, Hantraye P, Mailleux P, Moya K, Bouillot C, Prochiantz A. Downregulation of amyloid precursor protein inhibits neurite outgrowth in vitro. J Cell Biol, 1995; 128: 919-27.

Allinson TM, Parkin ET, Turner AJ, Hooper NM. ADAMs family members as amyloid precursor protein alpha-secretases. J Neurosci Res, 2003; 74: 342-52.

Andersen OM, Schmidt V, Spoelgen R, Gliemann J, Behlke J, Galatis D, McKinstry WJ, Parker MW, Masters CL, Hyman BT, Cappai R, Willnow TE. Molecular dissection of the interaction between amyloid precursor protein and its neuronal trafficking receptor SorLA/LR11. Biochemistry, 2006; 45: 2618-28.

Anderson JJ, Holtz G, Baskin PP, Wang R, Mazzarelli L, Wagner SL, Menzaghi F. Reduced cerebrospinal fluid levels of alpha-secretase-cleaved amyloid precursor protein in aged rats: correlation with spatial memory deficits. Neuroscience, 1999; 93: 1409-20.

Ando K, Iijima KI, Elliott JI, Kirino Y, Suzuki T. Phosphorylation-dependent regulation of the interaction of amyloid precursor protein with Fe65 affects the production of beta-amyloid. J Biol Chem, 2001; 276: 40353-61.

Anliker B, Muller U. The functions of mammalian amyloid precursor protein and related amyloid precursor-like proteins. Neurodegener Dis, 2006; 3: 239-46.

Annaert W, De Strooper B. Presenilins: molecular switches between proteolysis and signal transduction. Trends Neurosci, 1999; 22: 439-43.

Araki W, Kitaguchi N, Tokushima Y, Ishii K, Aratake H, Shimohama S, Nakamura S, Kimura J. Trophic effect of beta-amyloid precursor protein on cerebral cortical neurons in culture. Biochem Biophys Res Commun, 1991; 181: 265-71.

Ashkenazi A, Dixit VM. Death receptors: signaling and modulation. Science, 1998; 281: 1305-8.

Awasthi D, Church DF, Torbati D, Carey ME, Pryor WA. Oxidative stress following traumatic brain injury in rats. Surg Neurol, 1997; 47: 575-81; discussion 81-2.

Baek SH, Ohgi KA, Rose DW, Koo EH, Glass CK, Rosenfeld MG. Exchange of N-CoR corepressor and Tip60 coactivator complexes links gene expression by NF-kappaB and beta-amyloid precursor protein. Cell, 2002; 110: 55-67.

Bai Y, Markham K, Chen F, Weerasekera R, Watts J, Horne P, Wakutani Y, Bagshaw R, Mathews PM, Fraser PE, Westaway D, St George-Hyslop P, Schmitt-Ulms G. The in vivo brain interactome of the amyloid precursor protein. Mol Cell Proteomics, 2008; 7: 15-34.

Baldwin SA, Gibson T, Callihan CT, Sullivan PG, Palmer E, Scheff SW. Neuronal cell loss in the CA3 subfield of the hippocampus following cortical contusion utilizing the optical disector method for cell counting. J Neurotrauma, 1997; 14: 385-98.

Bandyopadhyay S, Goldstein LE, Lahiri DK, Rogers JT. Role of the APP non-amyloidogenic signaling pathway and targeting alpha-secretase as an alternative drug target for treatment of Alzheimer's disease. Curr Med Chem, 2007; 14: 2848-64.

Bandyopadhyay S, Hartley DM, Cahill CM, Lahiri DK, Chattopadhyay N, Rogers JT. Interleukin-1alpha stimulates non-amyloidogenic pathway by alpha-secretase (ADAM-10 and ADAM-17) cleavage of APP in human astrocytic cells involving p38 MAP kinase. J Neurosci Res, 2006; 84: 106-18.

Baranova AI, Whiting MD, Hamm RJ. Delayed, post-injury treatment with aniracetam improves cognitive performance after traumatic brain injury in rats. J Neurotrauma, 2006; 23: 1233-40.

Barnes CA. Memory deficits associated with senescence: a neurophysiological and behavioral study in the rat. J Comp Physiol Psychol, 1979; 93: 74-104.

Baskaya MK, Rao AM, Dogan A, Donaldson D, Dempsey RJ. The biphasic opening of the blood-brain barrier in the cortex and hippocampus after traumatic brain injury in rats. Neurosci Lett, 1997; 226: 33-6.

Beaumont A, Marmarou A, Hayasaki K, Barzo P, Fatouros P, Corwin F, Marmarou C, Dunbar J. The permissive nature of blood brain barrier (BBB) opening in edema formation following traumatic brain injury. Acta Neurochir Suppl, 2000; 76: 125-9.

Beer R, Franz G, Schopf M, Reindl M, Zelger B, Schmutzhard E, Poewe W, Kampfl A. Expression of Fas and Fas ligand after experimental traumatic brain injury in the rat. J Cereb Blood Flow Metab, 2000a; 20: 669-77.

Beer R, Franz G, Srinivasan A, Hayes RL, Pike BR, Newcomb JK, Zhao X, Schmutzhard E, Poewe W, Kampfl A. Temporal profile and cell subtype distribution of activated caspase-3 following experimental traumatic brain injury. J Neurochem, 2000b; 75: 1264-73.

Beher D, Hesse L, Masters CL, Multhaup G. Regulation of amyloid protein precursor (APP) binding to collagen and mapping of the binding sites on APP and collagen type I. J Biol Chem, 1996; 271: 1613-20.

Bell KF, Zheng L, Fahrenholz F, Cuello AC. ADAM-10 over-expression increases cortical synaptogenesis. Neurobiol Aging, 2006.

Belyaev ND, Kellett KA, Beckett C, Makova NZ, Revett TJ, Nalivaeva NN, Hooper NM, Turner AJ. The transcriptionally active amyloid precursor protein (APP) intracellular domain is preferentially produced from the 695 isoform of APP in a {beta}-secretase-dependent pathway. J Biol Chem, 2010; 285: 41443-54.

Bendotti C, Baldessari S, Pende M, Southgate T, Guglielmetti F, Samanin R. Relationship between GAP-43 expression in the dentate gyrus and synaptic reorganization of hippocampal mossy fibres in rats treated with kainic acid. Eur J Neurosci, 1997; 9: 93-101.

Bennett BD, Denis P, Haniu M, Teplow DB, Kahn S, Louis JC, Citron M, Vassar R. A furin-like convertase mediates propeptide cleavage of BACE, the Alzheimer's beta -secretase. J Biol Chem, 2000; 275: 37712-7.

Bertrand E, Brouillet E, Caille I, Bouillot C, Cole GM, Prochiantz A, Allinquant B. A short cytoplasmic domain of the amyloid precursor protein induces apoptosis in vitro and in vivo. Mol Cell Neurosci, 2001; 18: 503-11.

Besenski N. Traumatic injuries: imaging of head injuries. Eur Radiol, 2002; 12: 1237-52.

Beyreuther K, Pollwein P, Multhaup G, Monning U, Konig G, Dyrks T, Schubert W, Masters CL. Regulation and expression of the Alzheimer's beta/A4 amyloid protein precursor in health, disease, and Down's syndrome. Ann N Y Acad Sci, 1993; 695: 91-102.

Bhasin R, Van Nostrand WE, Saitoh T, Donets MA, Barnes EA, Quitschke WW, Goldgaber D. Expression of active secreted forms of human amyloid beta-protein precursor by recombinant baculovirus-infected insect cells. Proc Natl Acad Sci U S A, 1991; 88: 10307-11.

Blasko I, Beer R, Bigl M, Apelt J, Franz G, Rudzki D, Ransmayr G, Kampfl A, Schliebs R. Experimental traumatic brain injury in rats stimulates the expression, production and activity of Alzheimer's disease beta-secretase (BACE-1). J Neural Transm, 2004; 111: 523-36.

Blumbergs P. Pathology. In Reilly P, Bullock R, editors. Head Injury: Pathophysiology and Management of Severe Closed Injury. Chapman & Hall Medical: London, 1997: 39-70.

Blumbergs PC, Scott G, Manavis J, Wainwright H, Simpson DA, McLean AJ. Topography of axonal injury as defined by amyloid precursor protein and the sector scoring method in mild and severe closed head injury. J Neurotrauma, 1995; 12: 565-72.

Bouron A, Mbebi C, Loeffler JP, De Waard M. The beta-amyloid precursor protein controls a store-operated Ca2+ entry in cortical neurons. Eur J Neurosci, 2004; 20: 2071-8.

Boyd-Kimball D, Sultana R, Mohmmad-Abdul H, Butterfield DA. Rodent Abeta(1-42) exhibits oxidative stress properties similar to those of human Abeta(1-42): Implications for proposed mechanisms of toxicity. J Alzheimers Dis, 2004; 6: 515-25.

Braak H, Braak E. Frequency of stages of Alzheimer-related lesions in different age categories. Neurobiol Aging, 1997; 18: 351-7.

Bramlett HM, Dietrich WD. Pathophysiology of cerebral ischemia and brain trauma: similarities and differences. J Cereb Blood Flow Metab, 2004; 24: 133-50.

Bramlett HM, Kraydieh S, Green EJ, Dietrich WD. Temporal and regional patterns of axonal damage following traumatic brain injury: a beta-amyloid precursor protein immunocytochemical study in rats. J Neuropathol Exp Neurol, 1997; 56: 1132-41.

Braun H, Schafer K, Hollt V. BetaIII tubulin-expressing neurons reveal enhanced neurogenesis in hippocampal and cortical structures after a contusion trauma in rats. J Neurotrauma, 2002; 19: 975-83.

Bredesen DE. Programmed cell death mechanisms in neurological disease. Curr Mol Med, 2008; 8: 173-86.

Brody DL, Mac Donald C, Kessens CC, Yuede C, Parsadanian M, Spinner M, Kim E, Schwetye KE, Holtzman DM, Bayly PV. Electromagnetic controlled cortical impact device for precise, graded experimental traumatic brain injury. J Neurotrauma, 2007; 24: 657-73.

Brody DL, Magnoni S, Schwetye KE, Spinner ML, Esparza TJ, Stocchetti N, Zipfel GJ, Holtzman DM. Amyloid-beta dynamics correlate with neurological status in the injured human brain. Science, 2008; 321: 1221-4.

Bryant RA, O'Donnell ML, Creamer M, McFarlane AC, Clark CR, Silove D. The psychiatric sequelae of traumatic injury. Am J Psychiatry, 2010; 167: 312-20.

Buki A, Koizumi H, Povlishock JT. Moderate posttraumatic hypothermia decreases early calpain-mediated proteolysis and concomitant cytoskeletal compromise in traumatic axonal injury. Exp Neurol, 1999; 159: 319-28.

Buki A, Okonkwo DO, Wang KK, Povlishock JT. Cytochrome c release and caspase activation in traumatic axonal injury. J Neurosci, 2000; 20: 2825-34.

Buki A, Povlishock JT. All roads lead to disconnection?--Traumatic axonal injury revisited. Acta Neurochir (Wien), 2006; 148: 181-93; discussion 93-4.

Bullock R, Zauner A, Woodward JJ, Myseros J, Choi SC, Ward JD, Marmarou A, Young HF. Factors affecting excitatory amino acid release following severe human head injury. J Neurosurg, 1998; 89: 507-18.

Bush AI, Multhaup G, Moir RD, Williamson TG, Small DH, Rumble B, Pollwein P, Beyreuther K, Masters CL. A novel zinc(II) binding site modulates the function of the beta A4 amyloid protein precursor of Alzheimer's disease. J Biol Chem, 1993; 268: 16109-12.

Buxbaum JD, Koo EH, Greengard P. Protein phosphorylation inhibits production of Alzheimer amyloid beta/A4 peptide. Proc Natl Acad Sci U S A, 1993; 90: 9195-8.

Buxbaum JD, Liu KN, Luo Y, Slack JL, Stocking KL, Peschon JJ, Johnson RS, Castner BJ, Cerretti DP, Black RA. Evidence that tumor necrosis factor alpha converting enzyme is involved in regulated alpha-secretase cleavage of the Alzheimer amyloid protein precursor. J Biol Chem, 1998; 273: 27765-7.

Buxbaum JD, Oishi M, Chen HI, Pinkas-Kramarski R, Jaffe EA, Gandy SE, Greengard P. Cholinergic agonists and interleukin 1 regulate processing and secretion of the Alzheimer beta/A4 amyloid protein precursor. Proc Natl Acad Sci U S A, 1992; 89: 10075-8.

Bye N, Habgood MD, Callaway JK, Malakooti N, Potter A, Kossmann T, Morganti-Kossmann MC. Transient neuroprotection by minocycline following traumatic brain injury is associated with attenuated microglial activation but no changes in cell apoptosis or neutrophil infiltration. Exp Neurol, 2007; 204: 220-33.

Caille I, Allinquant B, Dupont E, Bouillot C, Langer A, Muller U, Prochiantz A. Soluble form of amyloid precursor protein regulates proliferation of progenitors in the adult subventricular zone. Development, 2004; 131: 2173-81.

Canevari L, Abramov AY, Duchen MR. Toxicity of amyloid beta peptide: tales of calcium, mitochondria, and oxidative stress. Neurochem Res, 2004; 29: 637-50.

Cao X, Sudhof TC. A transcriptionally [correction of transcriptively] active complex of APP with Fe65 and histone acetyltransferase Tip60. Science, 2001; 293: 115-20.

Capell A, Steiner H, Willem M, Kaiser H, Meyer C, Walter J, Lammich S, Multhaup G, Haass C. Maturation and pro-peptide cleavage of beta-secretase. J Biol Chem, 2000; 275: 30849-54.

Caporaso GL, Gandy SE, Buxbaum JD, Ramabhadran TV, Greengard P. Protein phosphorylation regulates secretion of Alzheimer beta/A4 amyloid precursor protein. Proc Natl Acad Sci U S A, 1992; 89: 3055-9.

Cappai R, White AR. Amyloid beta. Int J Biochem Cell Biol, 1999; 31: 885-9.

Carafoli E, Molinari M. Calpain: a protease in search of a function? Biochem Biophys Res Commun, 1998; 247: 193-203.

Carey RM, Balcz BA, Lopez-Coviella I, Slack BE. Inhibition of dynamin-dependent endocytosis increases shedding of the amyloid precursor protein ectodomain and reduces generation of amyloid beta protein. BMC Cell Biol, 2005; 6: 30.

Cernak I. Animal models of head trauma. NeuroRx, 2005; 2: 410-22.

Cernak I, Chapman SM, Hamlin GP, Vink R. Temporal characterisation of pro- and anti-apoptotic mechanisms following diffuse traumatic brain injury in rats. J Clin Neurosci, 2002; 9: 565-72.

Cernak I, Vink R, Zapple DN, Cruz MI, Ahmed F, Chang T, Fricke ST, Faden AI. The pathobiology of moderate diffuse traumatic brain injury as identified using a new experimental model of injury in rats. Neurobiol Dis, 2004; 17: 29-43.

Chan SL, Griffin WS, Mattson MP. Evidence for caspase-mediated cleavage of AMPA receptor subunits in neuronal apoptosis and Alzheimer's disease. J Neurosci Res, 1999; 57: 315-23.

Chan SL, Mattson MP. Caspase and calpain substrates: roles in synaptic plasticity and cell death. J Neurosci Res, 1999; 58: 167-90.

Checler F. Processing of the beta-amyloid precursor protein and its regulation in Alzheimer's disease. J Neurochem, 1995; 65: 1431-44.

Checler F, Sunyach C, Pardossi-Piquard R, Sevalle J, Vincent B, Kawarai T, Girardot N, St George-Hyslop P, da Costa CA. The gamma/epsilon-secretase-derived APP intracellular domain fragments regulate p53. Curr Alzheimer Res, 2007; 4: 423-6.

Chen AC, Selkoe DJ. Response to: Pardossi-Piquard et al., "Presenilin-Dependent Transcriptional Control of the Abeta-Degrading Enzyme Neprilysin by Intracellular Domains of betaAPP and APLP." Neuron 46, 541-554. Neuron, 2007; 53: 479-83.

Chen XH, Iwata A, Nonaka M, Browne KD, Smith DH. Neurogenesis and glial proliferation persist for at least one year in the subventricular zone following brain trauma in rats. J Neurotrauma, 2003; 20: 623-31.

Chen XH, Johnson VE, Uryu K, Trojanowski JQ, Smith DH. A lack of amyloid beta plaques despite persistent accumulation of amyloid beta in axons of long-term survivors of traumatic brain injury. Brain Pathol, 2009; 19: 214-23.

Chen XH, Siman R, Iwata A, Meaney DF, Trojanowski JQ, Smith DH. Long-term accumulation of amyloid-beta, beta-secretase, presenilin-1, and caspase-3 in damaged axons following brain trauma. Am J Pathol, 2004; 165: 357-71.

Cheng G, Yu Z, Zhou D, Mattson MP. Phosphatidylinositol-3-kinase-Akt kinase and p42/p44 mitogen-activated protein kinases mediate neurotrophic and excitoprotective actions of a secreted form of amyloid precursor protein. Exp Neurol, 2002; 175: 407-14.

Cherian L, Goodman JC, Robertson CS. Brain nitric oxide changes after controlled cortical impact injury in rats. J Neurophysiol, 2000; 83: 2171-8.

Chiaretti A, Antonelli A, Mastrangelo A, Pezzotti P, Tortorolo L, Tosi F, Genovese O. Interleukin-6 and nerve growth factor upregulation correlates with improved outcome in children with severe traumatic brain injury. J Neurotrauma, 2008; 25: 225-34.

Chirgadze DY, Hepple J, Byrd RA, Sowdhamini R, Blundell TL, Gherardi E. Insights into the structure of hepatocyte growth factor/scatter factor (HGF/SF) and implications for receptor activation. FEBS Lett, 1998; 430: 126-9.

Christman CW, Salvant JB, Jr., Walker SA, Povlishock JT. Characterization of a prolonged regenerative attempt by diffusely injured axons following traumatic brain injury in adult cat: a light and electron microscopic immunocytochemical study. Acta Neuropathol, 1997; 94: 329-37.

Cifu DX, Kreutzer JS, Marwitz JH, Miller M, Hsu GM, Seel RT, Englander J, High WM, Jr., Zafonte R. Etiology and incidence of rehospitalization after traumatic brain injury: a multicenter analysis. Arch Phys Med Rehabil, 1999; 80: 85-90.

Cirrito JR, Kang JE, Lee J, Stewart FR, Verges DK, Silverio LM, Bu G, Mennerick S, Holtzman DM. Endocytosis is required for synaptic activity-dependent release of amyloid-beta in vivo. Neuron, 2008; 58: 42-51.

Cirrito JR, Yamada KA, Finn MB, Sloviter RS, Bales KR, May PC, Schoepp DD, Paul SM, Mennerick S, Holtzman DM. Synaptic activity regulates interstitial fluid amyloid-beta levels in vivo. Neuron, 2005; 48: 913-22.

Clark RS, Carcillo JA, Kochanek PM, Obrist WD, Jackson EK, Mi Z, Wisneiwski SR, Bell MJ, Marion DW. Cerebrospinal fluid adenosine concentration and uncoupling of cerebral blood flow and oxidative metabolism after severe head injury in humans. Neurosurgery, 1997a; 41: 1284-92; discussion 92-3.

Clark RS, Chen J, Watkins SC, Kochanek PM, Chen M, Stetler RA, Loeffert JE, Graham SH. Apoptosis-suppressor gene bcl-2 expression after traumatic brain injury in rats. J Neurosci, 1997b; 17: 9172-82.

Clark RS, Kochanek PM, Adelson PD, Bell MJ, Carcillo JA, Chen M, Wisniewski SR, Janesko K, Whalen MJ, Graham SH. Increases in bcl-2 protein in cerebrospinal fluid and evidence for programmed cell death in infants and children after severe traumatic brain injury. J Pediatr, 2000; 137: 197-204.

Clarris HJ, Nurcombe V, Small DH, Beyreuther K, Masters CL. Secretion of nerve growth factor from septum stimulates neurite outgrowth and release of the amyloid protein precursor of Alzheimer's disease from hippocampal explants. J Neurosci Res, 1994; 38: 248-58.

Clausen F, Hanell A, Bjork M, Hillered L, Mir AK, Gram H, Marklund N. Neutralization of interleukin-1beta modifies the inflammatory response and improves histological and cognitive outcome following traumatic brain injury in mice. Eur J Neurosci, 2009; 30: 385-96.

Clement AB, Hanstein R, Schroder A, Nagel H, Endres K, Fahrenholz F, Behl C. Effects of neuron-specific ADAM-10 modulation in an in vivo model of acute excitotoxic stress. Neuroscience, 2008; 152: 459-68.

Clinton J, Ambler MW, Roberts GW. Post-traumatic Alzheimer's disease: preponderance of a single plaque type. Neuropathol Appl Neurobiol, 1991; 17: 69-74.

Conrad CD, Galea LA, Kuroda Y, McEwen BS. Chronic stress impairs rat spatial memory on the Y maze, and this effect is blocked by tianeptine pretreatment. Behav Neurosci, 1996; 110: 1321-34.

Conte V, Rojo N, Shimizu S, Saatman K, Watson D, Graham D, Stocchetti N, McIntosh TK. Neurotrophic Factors: Pathophysiology and Therapeutic Applications in Traumatic Brain Injury. Eur. J. Trauma, 2004; 35: 335-55.

Copanaki E, Chang S, Vlachos A, Tschape JA, Muller UC, Kogel D, Deller T. sAPPα lpha antagonizes dendritic degeneration and neuron death triggered by proteasomal stress. Mol Cell Neurosci, 2010; 44: 386-93.

Corrigan JD, Selassie AW, Orman JA. The epidemiology of traumatic brain injury. J Head Trauma Rehabil, 2010; 25: 72-80.

Couillard-Despres S, Winner B, Schaubeck S, Aigner R, Vroemen M, Weidner N, Bogdahn U, Winkler J, Kuhn HG, Aigner L. Doublecortin expression levels in adult brain reflect neurogenesis. Eur J Neurosci, 2005; 21: 1-14.

Dahlgren KN, Manelli AM, Stine WB, Jr., Baker LK, Krafft GA, LaDu MJ. Oligomeric and fibrillar species of amyloid-beta peptides differentially affect neuronal viability. J Biol Chem, 2002; 277: 32046-53.

Dahms SO, Hoefgen S, Roeser D, Schlott B, Guhrs KH, Than ME. Structure and biochemical analysis of the heparin-induced E1 dimer of the amyloid precursor protein. Proc Natl Acad Sci U S A, 2010; 107: 5381-6.

Dash PK, Mach SA, Moore AN. Enhanced neurogenesis in the rodent hippocampus following traumatic brain injury. J Neurosci Res, 2001; 63: 313-9.

Dash PK, Orsi SA, Zhang M, Grill RJ, Pati S, Zhao J, Moore AN. Valproate administered after traumatic brain injury provides neuroprotection and improves cognitive function in rats. PLoS One, 2010; 5: e11383.

Davis AA, Fritz JJ, Wess J, Lah JJ, Levey AI. Deletion of M1 muscarinic acetylcholine receptors increases amyloid pathology in vitro and in vivo. J Neurosci, 2010; 30: 4190-6.

Davis AE. Mechanisms of traumatic brain injury: biomechanical, structural and cellular considerations. Crit Care Nurs Q, 2000; 23: 1-13.

Dawson GR, Seabrook GR, Zheng H, Smith DW, Graham S, O'Dowd G, Bowery BJ, Boyce S, Trumbauer ME, Chen HY, Van der Ploeg LH, Sirinathsinghji DJ. Age-related cognitive deficits, impaired long-term potentiation and reduction in synaptic marker density in mice lacking the beta-amyloid precursor protein. Neuroscience, 1999; 90: 1-13.

De Strooper B, Annaert W. Proteolytic processing and cell biological functions of the amyloid precursor protein. J Cell Sci, 2000; 113 (Pt 11): 1857-70.

De Strooper B, Umans L, Van Leuven F, Van Den Berghe H. Study of the synthesis and secretion of normal and artificial mutants of murine amyloid precursor protein (APP): cleavage of APP occurs in a late compartment of the default secretion pathway. J Cell Biol, 1993; 121: 295-304.

DeKosky ST, Abrahamson EE, Taffe KM, Dixon CE, Kochanek PM, Ikonomovic MD. Effects of post-injury hypothermia and nerve growth factor infusion on antioxidant enzyme activity in the rat: implications for clinical therapies. J Neurochem, 2004; 90: 998-1004.

Dennis AM, Haselkorn ML, Vagni VA, Garman RH, Janesko-Feldman K, Bayir H, Clark RS, Jenkins LW, Dixon CE, Kochanek PM. Hemorrhagic shock after experimental traumatic brain injury in mice: effect on neuronal death. J Neurotrauma, 2009; 26: 889-99.

Dewji NN, Do C. Heat shock factor-1 mediates the transcriptional activation of Alzheimer's beta-amyloid precursor protein gene in response to stress. Brain Res Mol Brain Res, 1996; 35: 325-8.

Dewji NN, Singer SJ. Cell surface expression of the Alzheimer disease-related presenilin proteins. Proc Natl Acad Sci U S A, 1997; 94: 9926-31.

Dixon CE, Clifton GL, Lighthall JW, Yaghmai AA, Hayes RL. A controlled cortical impact model of traumatic brain injury in the rat. J Neurosci Methods, 1991; 39: 253-62.

Dixon CE, Lyeth BG, Povlishock JT, Findling RL, Hamm RJ, Marmarou A, Young HF, Hayes RL. A fluid percussion model of experimental brain injury in the rat. J Neurosurg, 1987; 67: 110-9.

Edbauer D, Willem M, Lammich S, Steiner H, Haass C. Insulin-degrading enzyme rapidly removes the beta-amyloid precursor protein intracellular domain (AICD). J Biol Chem, 2002; 277: 13389-93.

Ek CJ, Habgood MD, Callaway JK, Dennis R, Dziegielewska KM, Johansson PA, Potter A, Wheaton B, Saunders NR. Spatio-temporal progression of grey and white matter damage following contusion injury in rat spinal cord. PLoS One, 2010; 5: e12021.

Emery DL, Raghupathi R, Saatman KE, Fischer I, Grady MS, McIntosh TK. Bilateral growth-related protein expression suggests a transient increase in regenerative potential following brain trauma. J Comp Neurol, 2000; 424: 521-31.

Emery DL, Royo NC, Fischer I, Saatman KE, McIntosh TK. Plasticity following injury to the adult central nervous system: is recapitulation of a developmental state worth promoting? J Neurotrauma, 2003; 20: 1271-92.

Ennaceur A, Delacour J. A new one-trial test for neurobiological studies of memory in rats. 1: Behavioral data. Behav Brain Res, 1988; 31: 47-59.

Enriquez P, Bullock R. Molecular and cellular mechanisms in the pathophysiology of severe head injury. Curr Pharm Des, 2004; 10: 2131-43.

Eriksson PS, Perfilieva E, Bjork-Eriksson T, Alborn AM, Nordborg C, Peterson DA, Gage FH. Neurogenesis in the adult human hippocampus. Nat Med, 1998; 4: 1313-7.

Escorihuela RM, Fernandez-Teruel A, Gil L, Aguilar R, Tobena A, Driscoll P. Inbred Roman high- and low-avoidance rats: differences in anxiety, novelty-seeking, and shuttlebox behaviors. Physiol Behav, 1999; 67: 19-26.

Evin G, Barakat A, Masters CL. BACE: Therapeutic target and potential biomarker for Alzheimer's disease. Int J Biochem Cell Biol, 2010; 42: 1923-6.

Faden AI, Demediuk P, Panter SS, Vink R. The role of excitatory amino acids and NMDA receptors in traumatic brain injury. Science, 1989; 244: 798-800.

Faden AI, Stoica B. Neuroprotection: challenges and opportunities. Arch Neurol, 2007; 64: 794-800.

Farkas O, Povlishock JT. Cellular and subcellular change evoked by diffuse traumatic brain injury: a complex web of change extending far beyond focal damage. Prog Brain Res, 2007; 161: 43-59.

Ferreiro E, Oliveira CR, Pereira C. Involvement of endoplasmic reticulum Ca2+ release through ryanodine and inositol 1,4,5-triphosphate receptors in the neurotoxic effects induced by the amyloid-beta peptide. J Neurosci Res, 2004; 76: 872-80.

Finfer SR, Cohen J. Severe traumatic brain injury. Resuscitation, 2001; 48: 77-90.

Finnie JW, Blumbergs PC. Traumatic brain injury. Vet Pathol, 2002; 39: 679-89.

Fleminger S, Oliver DL, Lovestone S, Rabe-Hesketh S, Giora A. Head injury as a risk factor for Alzheimer's disease: the evidence 10 years on; a partial replication. J Neurol Neurosurg Psychiatry, 2003; 74: 857-62.

Flierl MA, Stahel PF, Beauchamp KM, Morgan SJ, Smith WR, Shohami E. Mouse closed head injury model induced by a weight-drop device. Nat Protoc, 2009; 4: 1328-37.

Foda MA, Marmarou A. A new model of diffuse brain injury in rats. Part II: Morphological characterization. J Neurosurg, 1994; 80: 301-13.

Folkerts MM, Berman RF, Muizelaar JP, Rafols JA. Disruption of MAP-2 immunostaining in rat hippocampus after traumatic brain injury. J Neurotrauma, 1998; 15: 349-63.

Forloni G. Neurotoxicity of beta-amyloid and prion peptides. Curr Opin Neurol, 1996; 9: 492-500.

Fortune N, Wen X. The definition, incidence and prevalence of acquired brain injury in Australia. Australian Institute of Health and Welfare: Canberra, 2007.

Fox GB, Fan L, LeVasseur RA, Faden AI. Effect of traumatic brain injury on mouse spatial and nonspatial learning in the Barnes circular maze. J Neurotrauma, 1998; 15: 1037-46.

Fragkouli A, Tzinia AK, Charalampopoulos I, Gravanis A, Tsilibary EC. Matrix Metalloproteinase-9 Participates in NGF-Induced alpha-Secretase Cleavage of Amyloid-beta Protein Precursor in PC12 Cells. J Alzheimers Dis, 2011.

Fraser PE, Nguyen JT, Chin DT, Kirschner DA. Effects of sulfate ions on Alzheimer beta/A4 peptide assemblies: implications for amyloid fibril-proteoglycan interactions. J Neurochem, 1992; 59: 1531-40.

Fratiglioni L, Ahlbom A, Viitanen M, Winblad B. Risk factors for late-onset Alzheimer's disease: a population-based, case-control study. Ann Neurol, 1993; 33: 258-66.

Fujimoto ST, Longhi L, Saatman KE, Conte V, Stocchetti N, McIntosh TK. Motor and cognitive function evaluation following experimental traumatic brain injury. Neurosci Biobehav Rev, 2004; 28: 365-78.

Furukawa K, Mattson MP. Secreted amyloid precursor protein alpha selectively suppresses N-methyl-D-aspartate currents in hippocampal neurons: involvement of cyclic GMP. Neuroscience, 1998; 83: 429-38.

Furukawa K, Sopher BL, Rydel RE, Begley JG, Pham DG, Martin GM, Fox M, Mattson MP. Increased activity-regulating and neuroprotective efficacy of alpha-secretase-derived secreted amyloid precursor protein conferred by a C-terminal heparin-binding domain. J Neurochem, 1996; 67: 1882-96.

Gabuzda D, Busciglio J, Yankner BA. Inhibition of beta-amyloid production by activation of protein kinase C. J Neurochem, 1993; 61: 2326-9.

Gaetz M. The neurophysiology of brain injury. Clin Neurophysiol, 2004; 115: 4-18.

Gage FH, Kempermann G, Palmer TD, Peterson DA, Ray J. Multipotent progenitor cells in the adult dentate gyrus. J Neurobiol, 1998; 36: 249-66.

Gakhar-Koppole N, Hundeshagen P, Mandl C, Weyer SW, Allinquant B, Muller U, Ciccolini F. Activity requires soluble amyloid precursor protein alpha to promote neurite outgrowth in neural stem cell-derived neurons via activation of the MAPK pathway. Eur J Neurosci, 2008; 28: 871-82.

Galli C, Piccini A, Ciotti MT, Castellani L, Calissano P, Zaccheo D, Tabaton M. Increased amyloidogenic secretion in cerebellar granule cells undergoing apoptosis. Proc Natl Acad Sci U S A, 1998; 95: 1247-52.

Garcia-Ladona FJC, Huss Y, Frey P, Ghandour MS. Oligodendrocytes express different isoforms of beta-amyloid precursor protein in chemically defined cell culture conditions: in situ hybridization and immunocytochemical detection. J Neurosci Res, 1997; 50: 50-61.

Garcia-Verdugo JM, Doetsch F, Wichterle H, Lim DA, Alvarez-Buylla A. Architecture and cell types of the adult subventricular zone: in search of the stem cells. J Neurobiol, 1998; 36: 234-48.

Gentleman SM, Graham DI, Roberts GW. Molecular pathology of head trauma: altered beta APP metabolism and the aetiology of Alzheimer's disease. Prog Brain Res, 1993a; 96: 237-46.

Gentleman SM, Greenberg BD, Savage MJ, Noori M, Newman SJ, Roberts GW, Griffin WS, Graham DI. A beta 42 is the predominant form of amyloid beta-protein in the brains of short-term survivors of head injury. Neuroreport, 1997; 8: 1519-22.

Gentleman SM, Nash MJ, Sweeting CJ, Graham DI, Roberts GW. Beta-amyloid precursor protein (beta APP) as a marker for axonal injury after head injury. Neurosci Lett, 1993b; 160: 139-44.

Gershtein L, Dmitrieva N, Sergutina A. Cytochemical characteristics of the brain in rats differing in active avoidance learning ability. Bull Exp Biol Med, 2000; 130: 838-9.

Gervais FG, Xu D, Robertson GS, Vaillancourt JP, Zhu Y, Huang J, LeBlanc A, Smith D, Rigby M, Shearman MS, Clarke EE, Zheng H, Van Der Ploeg LH, Ruffolo SC, Thornberry NA, Xanthoudakis S, Zamboni RJ, Roy S, Nicholson DW. Involvement of caspases in proteolytic cleavage of Alzheimer's amyloid-beta precursor protein and amyloidogenic A beta peptide formation. Cell, 1999; 97: 395-406.

Giliberto L, d'Abramo C, Acker CM, Davies P, D'Adamio L. Transgenic expression of the amyloid-beta precursor protein-intracellular domain does not induce Alzheimer's Disease-like traits in vivo. PLoS One, 2010; 5: e11609.

Giuffrida ML, Caraci F, Pignataro B, Cataldo S, De Bona P, Bruno V, Molinaro G, Pappalardo G, Messina A, Palmigiano A, Garozzo D, Nicoletti F, Rizzarelli E, Copani A. Beta-amyloid monomers are neuroprotective. J Neurosci, 2009; 29: 10582-7.

Glenn TC, Kelly DF, Boscardin WJ, McArthur DL, Vespa P, Oertel M, Hovda DA, Bergsneider M, Hillered L, Martin NA. Energy dysfunction as a predictor of outcome after moderate or severe head injury: indices of oxygen, glucose, and lactate metabolism. J Cereb Blood Flow Metab, 2003; 23: 1239-50.

Globus MY, Alonso O, Dietrich WD, Busto R, Ginsberg MD. Glutamate release and free radical production following brain injury: effects of posttraumatic hypothermia. J Neurochem, 1995; 65: 1704-11.

Goodger ZV, Rajendran L, Trutzel A, Kohli BM, Nitsch RM, Konietzko U. Nuclear signaling by the APP intracellular domain occurs predominantly through the amyloidogenic processing pathway. J Cell Sci, 2009; 122: 3703-14.

Goodman Y, Mattson MP. Secreted forms of beta-amyloid precursor protein protect hippocampal neurons against amyloid beta-peptide-induced oxidative injury. Exp Neurol, 1994; 128: 1-12.

Gordon-Krajcer W, Gajkowska B. Excitotoxicity-induced expression of amyloid precursor protein (beta-APP) in the hippocampus and cortex of rat brain. an electron-microscopy and biochemical study. Folia Neuropathol, 2001; 39: 163-73.

Goss JR, O'Malley ME, Zou L, Styren SD, Kochanek PM, DeKosky ST. Astrocytes are the major source of nerve growth factor upregulation following traumatic brain injury in the rat. Exp Neurol, 1998; 149: 301-9.

Graef IA, Mermelstein PG, Stankunas K, Neilson JR, Deisseroth K, Tsien RW, Crabtree GR. L-type calcium channels and GSK-3 regulate the activity of NF-ATc4 in hippocampal neurons. Nature, 1999; 401: 703-8.

Graham D, Gennarelli T, McIntosh TK. Greenfield's Neuropathology. Arnold: New York, 2002.

Graham DI, McIntosh TK, Maxwell WL, Nicoll JA. Recent advances in neurotrauma. J Neuropathol Exp Neurol, 2000a; 59: 641-51.

Graham DI, Raghupathi R, Saatman KE, Meaney D, McIntosh TK. Tissue tears in the white matter after lateral fluid percussion brain injury in the rat: relevance to human brain injury. Acta Neuropathol, 2000b; 99: 117-24.

Graham SH, Chen J, Clark RS. Bcl-2 family gene products in cerebral ischemia and traumatic brain injury. J Neurotrauma, 2000c; 17: 831-41.

Gralle M, Botelho MG, Wouters FS. Neuroprotective secreted amyloid precursor protein acts by disrupting amyloid precursor protein dimers. J Biol Chem, 2009; 284: 15016-25.

Gralle M, Oliveira CL, Guerreiro LH, McKinstry WJ, Galatis D, Masters CL, Cappai R, Parker MW, Ramos CH, Torriani I, Ferreira ST. Solution conformation and heparin-induced dimerisation of the full-length extracellular domain of the human amyloid precursor protein. J Mol Biol, 2006; 357: 493-508.

Greenberg SM, Kosik KS. Secreted beta-APP stimulates MAP kinase and phosphorylation of tau in neurons. Neurobiol Aging, 1995; 16: 403-7; discussion 7-8.

Griesbach GS, Hovda DA, Molteni R, Gomez-Pinilla F. Alterations in BDNF and synapsin I within the occipital cortex and hippocampus after mild traumatic brain injury in the developing rat: reflections of injury-induced neuroplasticity. J Neurotrauma, 2002; 19: 803-14.

Guenette SY, Chen J, Ferland A, Haass C, Capell A, Tanzi RE. hFE65L influences amyloid precursor protein maturation and secretion. J Neurochem, 1999; 73: 985-93.

Guo Z, Cupples LA, Kurz A, Auerbach SH, Volicer L, Chui H, Green RC, Sadovnick AD, Duara R, DeCarli C, Johnson K, Go RC, Growdon JH, Haines JL, Kukull WA, Farrer LA. Head injury and the risk of AD in the MIRAGE study. Neurology, 2000; 54: 1316-23.

Haass C. Take five--BACE and the gamma-secretase quartet conduct Alzheimer's amyloid beta-peptide generation. Embo J, 2004; 23: 483-8.

Haass C, Koo EH, Mellon A, Hung AY, Selkoe DJ. Targeting of cell-surface beta-amyloid precursor protein to lysosomes: alternative processing into amyloid-bearing fragments. Nature, 1992; 357: 500-3.

Halcomb E, Daly J, Davidson P, Elliott D, Griffiths R. Life beyond severe traumatic injury: an integrative review of the literature. Aust Crit Care, 2005; 18: 17-8, 20-4.

Hall ED, Bryant YD, Cho W, Sullivan PG. Evolution of post-traumatic neurodegeneration after controlled cortical impact traumatic brain injury in mice and rats as assessed by the de Olmos silver and fluorojade staining methods. J Neurotrauma, 2008; 25: 235-47.

Hall ED, Gibson TR, Pavel KM. Lack of a gender difference in post-traumatic neurodegeneration in the mouse controlled cortical impact injury model. J Neurotrauma, 2005; 22: 669-79.

Hall KD, Lifshitz J. Diffuse traumatic brain injury initially attenuates and later expands activation of the rat somatosensory whisker circuit concomitant with neuroplastic responses. Brain Res, 2010; 1323: 161-73.

Hallam TM, Floyd CL, Folkerts MM, Lee LL, Gong QZ, Lyeth BG, Muizelaar JP, Berman RF. Comparison of behavioral deficits and acute neuronal degeneration in rat lateral fluid percussion and weight-drop brain injury models. J Neurotrauma, 2004; 21: 521-39.

Hamm RJ, Pike BR, O'Dell DM, Lyeth BG, Jenkins LW. The rotarod test: an evaluation of its effectiveness in assessing motor deficits following traumatic brain injury. J Neurotrauma, 1994; 11: 187-96.

Han P, Dou F, Li F, Zhang X, Zhang YW, Zheng H, Lipton SA, Xu H, Liao FF. Suppression of cyclin-dependent kinase 5 activation by amyloid precursor protein: a novel excitoprotective mechanism involving modulation of tau phosphorylation. J Neurosci, 2005; 25: 11542-52.

Han X, Tong J, Zhang J, Farahvar A, Wang E, Yang J, Samadani U, Smith DH, Huang JH. Imipramine Treatment Improves Cognitive Outcome Associated with Enhanced Hippocampal Neurogenesis after Traumatic Brain Injury in Mice. J Neurotrauma, 2011.

Hanell A, Clausen F, Bjork M, Jansson K, Philipson O, Nilsson LN, Hillered L, Weinreb PH, Lee D, McIntosh TK, Gimbel DA, Strittmatter SM, Marklund N. Genetic deletion and pharmacological inhibition of Nogo-66 receptor impairs cognitive outcome after traumatic brain injury in mice. J Neurotrauma, 2010; 27: 1297-309.

Haniu M, Denis P, Young Y, Mendiaz EA, Fuller J, Hui JO, Bennett BD, Kahn S, Ross S, Burgess T, Katta V, Rogers G, Vassar R, Citron M. Characterization of Alzheimer's beta -secretase protein BACE. A pepsin family member with unusual properties. J Biol Chem, 2000; 275: 21099-106.

Harper SJ, Bilsland JG, Shearman MS, Zheng H, Van der Ploeg L, Sirinathsinghji DJ. Mouse cortical neurones lacking APP show normal neurite outgrowth and survival responses in vitro. Neuroreport, 1998; 9: 3053-8.

Harter L, Keel M, Hentze H, Leist M, Ertel W. Caspase-3 activity is present in cerebrospinal fluid from patients with traumatic brain injury. J Neuroimmunol, 2001; 121: 76-8.

Hartlage-Rubsamen M, Zeitschel U, Apelt J, Gartner U, Franke H, Stahl T, Gunther A, Schliebs R, Penkowa M, Bigl V, Rossner S. Astrocytic expression of the Alzheimer's disease beta-secretase (BACE1) is stimulus-dependent. Glia, 2003; 41: 169-79.

Hartley DM, Walsh DM, Ye CP, Diehl T, Vasquez S, Vassilev PM, Teplow DB, Selkoe DJ. Protofibrillar intermediates of amyloid beta-protein induce acute electrophysiological changes and progressive neurotoxicity in cortical neurons. J Neurosci, 1999; 19: 8876-84.

Hass MR, Yankner BA. A {gamma}-secretase-independent mechanism of signal transduction by the amyloid precursor protein. J Biol Chem, 2005; 280: 36895-904.

Heath DL, Vink R. Improved motor outcome in response to magnesium therapy received up to 24 hours after traumatic diffuse axonal brain injury in rats. J Neurosurg, 1999; 90: 504-9.

Heber S, Herms J, Gajic V, Hainfellner J, Aguzzi A, Rulicke T, von Kretzschmar H, von Koch C, Sisodia S, Tremml P, Lipp HP, Wolfer DP, Muller U. Mice with combined gene knock-outs reveal essential and partially redundant functions of amyloid precursor protein family members. J Neurosci, 2000; 20: 7951-63.

Hengartner MO, Bryant JA. Apoptotic cell death: from worms to wombats ... but what about the weeds? Symp Soc Exp Biol, 2000; 52: 1-12.

Henry A, Masters CL, Beyreuther K, Cappai R. Expression of human amyloid precursor protein ectodomains in Pichia pastoris: analysis of culture conditions, purification, and characterization. Protein Expr Purif, 1997; 10: 283-91.

Herard AS, Besret L, Dubois A, Dauguet J, Delzescaux T, Hantraye P, Bonvento G, Moya KL. siRNA targeted against amyloid precursor protein impairs synaptic activity in vivo. Neurobiol Aging, 2006; 27: 1740-50.

Herms J, Anliker B, Heber S, Ring S, Fuhrmann M, Kretzschmar H, Sisodia S, Muller U. Cortical dysplasia resembling human type 2 lissencephaly in mice lacking all three APP family members. EMBO J, 2004; 23: 4106-15.

Herreman A, Van Gassen G, Bentahir M, Nyabi O, Craessaerts K, Mueller U, Annaert W, De Strooper B. gamma-Secretase activity requires the presenilin-dependent trafficking of nicastrin through the Golgi apparatus but not its complex glycosylation. J Cell Sci, 2003; 116: 1127-36.

Hirsch-Reinshagen V, Wellington CL. Cholesterol metabolism, apolipoprotein E, adenosine triphosphate-binding cassette transporters, and Alzheimer's disease. Curr Opin Lipidol, 2007; 18: 325-32.

Hoey SE, Williams RJ, Perkinton MS. Synaptic NMDA receptor activation stimulates alpha-secretase amyloid precursor protein processing and inhibits amyloid-beta production. J Neurosci, 2009; 29: 4442-60.

Hornsten A, Lieberthal J, Fadia S, Malins R, Ha L, Xu X, Daigle I, Markowitz M, O'Connor G, Plasterk R, Li C. APL-1, a Caenorhabditis elegans protein related to the human beta-amyloid precursor protein, is essential for viability. Proc Natl Acad Sci U S A, 2007; 104: 1971-6.

Huber G, Bailly Y, Martin JR, Mariani J, Brugg B. Synaptic beta-amyloid precursor proteins increase with learning capacity in rats. Neuroscience, 1997; 80: 313-20.

Huh JW, Raghupathi R, Laurer HL, Helfaer MA, Saatman KE. Transient loss of microtubule-associated protein 2 immunoreactivity after moderate brain injury in mice. J Neurotrauma, 2003; 20: 975-84.

Hulsebosch CE, DeWitt DS, Jenkins LW, Prough DS. Traumatic brain injury in rats results in increased expression of Gap-43 that correlates with behavioral recovery. Neurosci Lett, 1998; 255: 83-6.

Huse JT, Pijak DS, Leslie GJ, Lee VM, Doms RW. Maturation and endosomal targeting of beta-site amyloid precursor protein-cleaving enzyme. The Alzheimer's disease beta-secretase. J Biol Chem, 2000; 275: 33729-37.

Hussain I, Powell D, Howlett DR, Tew DG, Meek TD, Chapman C, Gloger IS, Murphy KE, Southan CD, Ryan DM, Smith TS, Simmons DL, Walsh FS, Dingwall C, Christie G. Identification of a novel aspartic protease (Asp 2) as beta-secretase. Mol Cell Neurosci, 1999; 14: 419-27.

Hutchinson PJ, O'Connell MT, Rothwell NJ, Hopkins SJ, Nortje J, Carpenter KL, Timofeev I, Al-Rawi PG, Menon DK, Pickard JD. Inflammation in human brain injury: intracerebral concentrations of IL-1alpha, IL-1beta, and their endogenous inhibitor IL-1ra. J Neurotrauma, 2007; 24: 1545-57.

Hyder AA, Wunderlich CA, Puvanachandra P, Gururaj G, Kobusingye OC. The impact of traumatic brain injuries: a global perspective. NeuroRehabilitation, 2007; 22: 341-53.

Ikezu T, Trapp BD, Song KS, Schlegel A, Lisanti MP, Okamoto T. Caveolae, plasma membrane microdomains for alpha-secretase-mediated processing of the amyloid precursor protein. J Biol Chem, 1998; 273: 10485-95.

Ikonomovic MD, Uryu K, Abrahamson EE, Ciallella JR, Trojanowski JQ, Lee VM, Clark RS, Marion DW, Wisniewski SR, DeKosky ST. Alzheimer's pathology in human temporal cortex surgically excised after severe brain injury. Exp Neurol, 2004; 190: 192-203.

Ivins KJ, Bui ET, Cotman CW. Beta-amyloid induces local neurite degeneration in cultured hippocampal neurons: evidence for neuritic apoptosis. Neurobiol Dis, 1998; 5: 365-78.

Iwamoto Y, Yamaki T, Murakami N, Umeda M, Tanaka C, Higuchi T, Aoki I, Naruse S, Ueda S. Investigation of morphological change of lateral and midline fluid percussion injury in rats, using magnetic resonance imaging. Neurosurgery, 1997; 40: 163-7.

Iwata A, Chen XH, McIntosh TK, Browne KD, Smith DH. Long-term accumulation of amyloid-beta in axons following brain trauma without persistent upregulation of amyloid precursor protein genes. J Neuropathol Exp Neurol, 2002; 61: 1056-68.

Jacobs G, Aeron-Thomas A, Astrop A. Estimating Global Road Fatalities. Transport Research Laboratory: Crowthorne, 2000.

Jacobsen JS, Spruyt MA, Brown AM, Sahasrabudhe SR, Blume AJ, Vitek MP, Muenkel HA, Sonnenberg-Reines J. The release of Alzheimer's disease beta amyloid peptide is reduced by phorbol treatment. J Biol Chem, 1994; 269: 8376-82.

Jin LW, Ninomiya H, Roch JM, Schubert D, Masliah E, Otero DA, Saitoh T. Peptides containing the RERMS sequence of amyloid beta/A4 protein precursor bind cell surface and promote neurite extension. J Neurosci, 1994; 14: 5461-70.

Johnson VE, Stewart W, Smith DH. Traumatic brain injury and amyloid-beta pathology: a link to Alzheimer's disease? Nat Rev Neurosci.

Kaden D, Munter LM, Joshi M, Treiber C, Weise C, Bethge T, Voigt P, Schaefer M, Beyermann M, Reif B, Multhaup G. Homophilic interactions of the amyloid precursor protein (APP) ectodomain are regulated by the loop region and affect beta-secretase cleavage of APP. J Biol Chem, 2008; 283: 7271-9.

Kaden D, Munter LM, Reif B, Multhaup G. The amyloid precursor protein and its homologues: Structural and functional aspects of native and pathogenic oligomerization. Eur J Cell Biol, 2011.

Kaden D, Voigt P, Munter LM, Bobowski KD, Schaefer M, Multhaup G. Subcellular localization and dimerisation of APLP1 are strikingly different from APP and APLP2. J Cell Sci, 2009; 122: 368-77.

Kadomatsu K, Muramatsu T. [Role of basigin, a glycoprotein belonging to the immunoglobulin superfamily, in the nervous system]. Tanpakushitsu Kakusan Koso, 2004; 49: 2417-24.

Kaether C, Lammich S, Edbauer D, Ertl M, Rietdorf J, Capell A, Steiner H, Haass C. Presenilin-1 affects trafficking and processing of betaAPP and is targeted in a complex with nicastrin to the plasma membrane. J Cell Biol, 2002; 158: 551-61.

Kakuda N, Funamoto S, Yagishita S, Takami M, Osawa S, Dohmae N, Ihara Y. Equimolar production of amyloid beta-protein and amyloid precursor protein intracellular domain from beta-carboxyl-terminal fragment by gamma-secretase. J Biol Chem, 2006; 281: 14776-86.

Kalish H, Phillips TM. Analysis of neurotrophins in human serum by immunoaffinity capillary electrophoresis (ICE) following traumatic head injury. J Chromatogr B Analyt Technol Biomed Life Sci, 2010; 878: 194-200.

Kamal A, Almenar-Queralt A, LeBlanc JF, Roberts EA, Goldstein LS. Kinesin-mediated axonal transport of a membrane compartment containing beta-secretase and presenilin-1 requires APP. Nature, 2001; 414: 643-8.

Kamenetz F, Tomita T, Hsieh H, Seabrook G, Borchelt D, Iwatsubo T, Sisodia S, Malinow R. APP processing and synaptic function. Neuron, 2003; 37: 925-37.

Kampfl A, Pfausler B, Haring HP, Denchev D, Donnemiller E, Schmutzhard E. Impaired microcirculation and tissue oxygenation in human cerebral malaria: a single photon emission computed tomography and near-infrared spectroscopy study. Am J Trop Med Hyg, 1997; 56: 585-7.

Kao SC, Krichevsky AM, Kosik KS, Tsai LH. BACE1 suppression by RNA interference in primary cortical neurons. J Biol Chem, 2004; 279: 1942-9.

Kawahara M, Kuroda Y. Molecular mechanism of neurodegeneration induced by Alzheimer's beta-amyloid protein: channel formation and disruption of calcium homeostasis. Brain Res Bull, 2000; 53: 389-97.

Kawarabayashi T, Shoji M, Harigaya Y, Yamaguchi H, Hirai S. Expression of APP in the early stage of brain damage. Brain Res, 1991; 563: 334-8.

Kay AD, Petzold A, Kerr M, Keir G, Thompson E, Nicoll JA. Alterations in cerebrospinal fluid apolipoprotein E and amyloid beta-protein after traumatic brain injury. J Neurotrauma, 2003; 20: 943-52.

Keane RW, Kraydieh S, Lotocki G, Alonso OF, Aldana P, Dietrich WD. Apoptotic and antiapoptotic mechanisms after traumatic brain injury. J Cereb Blood Flow Metab, 2001; 21: 1189-98.

Keyvani K, Schallert T. Plasticity-associated molecular and structural events in the injured brain. J Neuropathol Exp Neurol, 2002; 61: 831-40.

Kim HS, Kim EM, Kim NJ, Chang KA, Choi Y, Ahn KW, Lee JH, Kim S, Park CH, Suh YH. Inhibition of histone deacetylation enhances the neurotoxicity induced by the C-terminal fragments of amyloid precursor protein. J Neurosci Res, 2004; 75: 117-24.

Kim HS, Kim EM, Lee JP, Park CH, Kim S, Seo JH, Chang KA, Yu E, Jeong SJ, Chong YH, Suh YH. C-terminal fragments of amyloid precursor protein exert neurotoxicity by inducing glycogen synthase kinase-3beta expression. Faseb J, 2003; 17: 1951-3.

Kim HS, Lee JH, Lee JP, Kim EM, Chang KA, Park CH, Jeong SJ, Wittendorp MC, Seo JH, Choi SH, Suh YH. Amyloid beta peptide induces cytochrome C release from isolated mitochondria. Neuroreport, 2002; 13: 1989-93.

Kim SH, Kim YK, Jeong SJ, Haass C, Kim YH, Suh YH. Enhanced release of secreted form of Alzheimer's amyloid precursor protein from PC12 cells by nicotine. Mol Pharmacol, 1997; 52: 430-6.

King GD, Scott Turner R. Adaptor protein interactions: modulators of amyloid precursor protein metabolism and Alzheimer's disease risk? Exp Neurol, 2004; 185: 208-19.

Kinoshita A, Whelan CM, Berezovska O, Hyman BT. The gamma secretase-generated carboxyl-terminal domain of the amyloid precursor protein induces apoptosis via Tip60 in H4 cells. J Biol Chem, 2002; 277: 28530-6.

Kleinig T. The role of substance P in experimental intracerebral haemorrhage. Anatomy and Pathology. The University of Adelaide: Adelaide, 2010.

Kneafsey R, Gawthorpe D. Head injury: long-term consequences for patients and families and implications for nurses. J Clin Nurs, 2004; 13: 601-8.

Knoblach SM, Nikolaeva M, Huang X, Fan L, Krajewski S, Reed JC, Faden AI. Multiple caspases are activated after traumatic brain injury: evidence for involvement in functional outcome. J Neurotrauma, 2002; 19: 1155-70.

Kojro E, Gimpl G, Lammich S, Marz W, Fahrenholz F. Low cholesterol stimulates the nonamyloidogenic pathway by its effect on the alpha -secretase ADAM 10. Proc Natl Acad Sci U S A, 2001; 98: 5815-20.

Koo EH, Squazzo SL, Selkoe DJ, Koo CH. Trafficking of cell-surface amyloid beta-protein precursor. I. Secretion, endocytosis and recycling as detected by labeled monoclonal antibody. J Cell Sci, 1996; 109 (Pt 5): 991-8.

Koopmans G, Blokland A, van Nieuwenhuijzen P, Prickaerts J. Assessment of spatial learning abilities of mice in a new circular maze. Physiol Behav, 2003; 79: 683-93.

Kossmann T, Stahel PF, Lenzlinger PM, Redl H, Dubs RW, Trentz O, Schlag G, Morganti-Kossmann MC. Interleukin-8 released into the cerebrospinal fluid after brain injury is associated with blood-brain barrier dysfunction and nerve growth factor production. J Cereb Blood Flow Metab, 1997; 17: 280-9.

Kowaltowski AJ, Castilho RF, Vercesi AE. Ca(2+)-induced mitochondrial membrane permeabilization: role of coenzyme Q redox state. Am J Physiol, 1995; 269: C141-7.

Kuan YH, Gruebl T, Soba P, Eggert S, Nesic I, Back S, Kirsch J, Beyreuther K, Kins S. PAT1a modulates intracellular transport and processing of amyloid precursor protein (APP), APLP1, and APLP2. J Biol Chem, 2006; 281: 40114-23.

Kuo YM, Emmerling MR, Vigo-Pelfrey C, Kasunic TC, Kirkpatrick JB, Murdoch GH, Ball MJ, Roher AE. Water-soluble Abeta (N-40, N-42) oligomers in normal and Alzheimer disease brains. J Biol Chem, 1996; 271: 4077-81.

Kupina NC, Detloff MR, Bobrowski WF, Snyder BJ, Hall ED. Cytoskeletal protein degradation and neurodegeneration evolves differently in males and females following experimental head injury. Exp Neurol, 2003; 180: 55-73.

Kwak YD, Choumkina E, Sugaya K. Amyloid precursor protein is involved in staurosporine induced glial differentiation of neural progenitor cells. Biochem Biophys Res Commun, 2006; 344: 431-7.

Lah JJ, Levey AI. Endogenous presenilin-1 targets to endocytic rather than biosynthetic compartments. Mol Cell Neurosci, 2000; 16: 111-26.

Lambert MP, Barlow AK, Chromy BA, Edwards C, Freed R, Liosatos M, Morgan TE, Rozovsky I, Trommer B, Viola KL, Wals P, Zhang C, Finch CE, Krafft GA, Klein WL. Diffusible, nonfibrillar ligands derived from Abeta1-42 are potent central nervous system neurotoxins. Proc Natl Acad Sci U S A, 1998; 95: 6448-53.

Lammich S, Kojro E, Postina R, Gilbert S, Pfeiffer R, Jasionowski M, Haass C, Fahrenholz F. Constitutive and regulated alpha-secretase cleavage of Alzheimer's amyloid precursor protein by a disintegrin metalloprotease. Proc Natl Acad Sci U S A, 1999; 96: 3922-7.

Lauderback CM, Hackett JM, Huang FF, Keller JN, Szweda LI, Markesbery WR, Butterfield DA. The glial glutamate transporter, GLT-1, is oxidatively modified by 4-hydroxy-2-nonenal in the Alzheimer's disease brain: the role of Abeta1-42. J Neurochem, 2001; 78: 413-6.

Laudon H, Winblad B, Naslund J. The Alzheimer's disease-associated gamma-secretase complex: functional domains in the presenilin 1 protein. Physiol Behav, 2007; 92: 115-20.

Launer LJ, Andersen K, Dewey ME, Letenneur L, Ott A, Amaducci LA, Brayne C, Copeland JR, Dartigues JF, Kragh-Sorensen P, Lobo A, Martinez-Lage JM, Stijnen T, Hofman A. Rates and risk factors for dementia and Alzheimer's disease: results from EURODEM pooled analyses. EURODEM Incidence Research Group and Work Groups. European Studies of Dementia. Neurology, 1999; 52: 78-84.

Laurer HL, McIntosh TK. Experimental models of brain trauma. Curr Opin Neurol, 1999; 12: 715-21.

Le Y, Gong W, Tiffany HL, Tumanov A, Nedospasov S, Shen W, Dunlop NM, Gao JL, Murphy PM, Oppenheim JJ, Wang JM. Amyloid (beta)42 activates a G-protein-coupled chemoattractant receptor, FPR-like-1. J Neurosci, 2001; 21: RC123.

LeBlanc A. Increased production of 4 kDa amyloid beta peptide in serum deprived human primary neuron cultures: possible involvement of apoptosis. J Neurosci, 1995; 15: 7837-46.

LeBlanc A, Liu H, Goodyer C, Bergeron C, Hammond J. Caspase-6 role in apoptosis of human neurons, amyloidogenesis, and Alzheimer's disease. J Biol Chem, 1999; 274: 23426-36.

Lee RK, Wurtman RJ, Cox AJ, Nitsch RM. Amyloid precursor protein processing is stimulated by metabotropic glutamate receptors. Proc Natl Acad Sci U S A, 1995; 92: 8083-7.

Lee S, Xue Y, Hu J, Wang Y, Liu X, Demeler B, Ha Y. The E2 Domains of APP and APLP1 Share a Conserved Mode of Dimerisation. Biochemistry, 2011; 50: 5453-64.

Leissring MA, Murphy MP, Mead TR, Akbari Y, Sugarman MC, Jannatipour M, Anliker B, Muller U, Saftig P, De Strooper B, Wolfe MS, Golde TE, LaFerla FM. A physiologic signaling role for the gamma - secretase-derived intracellular fragment of APP. Proc Natl Acad Sci U S A, 2002; 99: 4697-702.

Lenzlinger PM, Morganti-Kossmann MC, Laurer HL, McIntosh TK. The duality of the inflammatory response to traumatic brain injury. Mol Neurobiol, 2001; 24: 169-81.

Lesne S, Ali C, Gabriel C, Croci N, MacKenzie ET, Glabe CG, Plotkine M, Marchand-Verrecchia C, Vivien D, Buisson A. NMDA receptor activation inhibits alpha-secretase and promotes neuronal amyloid-beta production. J Neurosci, 2005; 25: 9367-77.

Lewen A, Fujimura M, Sugawara T, Matz P, Copin JC, Chan PH. Oxidative stress-dependent release of mitochondrial cytochrome c after traumatic brain injury. J Cereb Blood Flow Metab, 2001; 21: 914-20.

Lewen A, Matz P, Chan PH. Free radical pathways in CNS injury. J Neurotrauma, 2000; 17: 871-90.

Leyssen M, Ayaz D, Hebert SS, Reeve S, De Strooper B, Hassan BA. Amyloid precursor protein promotes post-developmental neurite arborization in the Drosophila brain. Embo J, 2005; 24: 2944-55.

Li J, Xu M, Zhou H, Ma J, Potter H. Alzheimer presenilins in the nuclear membrane, interphase kinetochores, and centrosomes suggest a role in chromosome segregation. Cell, 1997; 90: 917-27.

Lighthall JW. Controlled cortical impact: a new experimental brain injury model. J Neurotrauma, 1988; 5: 1-15.

Lin H, Bhatia R, Lal R. Amyloid beta protein forms ion channels: implications for Alzheimer's disease pathophysiology. Faseb J, 2001; 15: 2433-44.

Lin LH, Bock S, Carpenter K, Rose M, Norden JJ. Synthesis and transport of GAP-43 in entorhinal cortex neurons and perforant pathway during lesion-induced sprouting and reactive synaptogenesis. Brain Res Mol Brain Res, 1992; 14: 147-53.

Lindner MD, Plone MA, Cain CK, Frydel B, Francis JM, Emerich DF, Sutton RL. Dissociable long-term cognitive deficits after frontal versus sensorimotor cortical contusions. J Neurotrauma, 1998; 15: 199-216.

Loane DJ, Pocivavsek A, Moussa CE, Thompson R, Matsuoka Y, Faden AI, Rebeck GW, Burns MP. Amyloid precursor protein secretases as therapeutic targets for traumatic brain injury. Nat Med, 2009; 15: 377-9.

Loane DJ, Washington PM, Vardanian L, Pocivavsek A, Hoe HS, Duff KE, Cernak I, Rebeck GW, Faden AI, Burns MP. Modulation of ABCA1 by an LXR agonist reduces beta-amyloid levels and improves outcome after traumatic brain injury. J Neurotrauma, 2011; 28: 225-36.

Lok J, Wang H, Murata Y, Zhu HH, Qin T, Whalen MJ, Lo EH. Effect of neuregulin-1 on histopathological and functional outcome after controlled cortical impact in mice. J Neurotrauma, 2007; 24: 1817-22.

Loncarevic-Vasiljkovic N, Pesic V, Tanic N, Milanovic D, Popic J, Kanazir S, Ruzdijic S. Changes in markers of neuronal and glial plasticity after cortical injury induced by food restriction. Exp Neurol, 2009; 220: 198-206.

Longhi L, Perego C, Ortolano F, Zanier ER, Bianchi P, Stocchetti N, McIntosh TK, De Simoni MG. C1-inhibitor attenuates neurobehavioral deficits and reduces contusion volume after controlled cortical impact brain injury in mice. Crit Care Med, 2009; 37: 659-65.

Lorenzo A, Yankner BA. Beta-amyloid neurotoxicity requires fibril formation and is inhibited by congo red. Proc Natl Acad Sci U S A, 1994; 91: 12243-7.

Lu DC, Rabizadeh S, Chandra S, Shayya RF, Ellerby LM, Ye X, Salvesen GS, Koo EH, Bredesen DE. A second cytotoxic proteolytic peptide derived from amyloid beta-protein precursor. Nat Med, 2000; 6: 397-404.

Lu DC, Soriano S, Bredesen DE, Koo EH. Caspase cleavage of the amyloid precursor protein modulates amyloid beta-protein toxicity. J Neurochem, 2003; 87: 733-41.

Lue LF, Kuo YM, Roher AE, Brachova L, Shen Y, Sue L, Beach T, Kurth JH, Rydel RE, Rogers J. Soluble amyloid beta peptide concentration as a predictor of synaptic change in Alzheimer's disease. Am J Pathol, 1999; 155: 853-62.

Lyeth BG, Jenkins LW, Hamm RJ, Dixon CE, Phillips LL, Clifton GL, Young HF, Hayes RL. Prolonged memory impairment in the absence of hippocampal cell death following traumatic brain injury in the rat. Brain Res, 1990; 526: 249-58.

Lynch G, Baudry M. Brain spectrin, calpain and long-term changes in synaptic efficacy. Brain Res Bull, 1987; 18: 809-15.

Ma G, Chen S, Wang X, Ba M, Yang H, Lu G. Short-term interleukin-1(beta) increases the release of secreted APP(alpha) via MEK1/2-dependent and JNK-dependent alpha-secretase cleavage in neuroglioma U251 cells. J Neurosci Res, 2005; 80: 683-92.

Ma H, Lesne S, Kotilinek L, Steidl-Nichols JV, Sherman M, Younkin L, Younkin S, Forster C, Sergeant N, Delacourte A, Vassar R, Citron M, Kofuji P, Boland LM, Ashe KH. Involvement of beta-site APP cleaving enzyme 1 (BACE1) in amyloid precursor protein-mediated enhancement of memory and activity-dependent synaptic plasticity. Proc Natl Acad Sci U S A, 2007; 104: 8167-72.

Maas AI, Roozenbeek B, Manley GT. Clinical trials in traumatic brain injury: past experience and current developments. Neurotherapeutics, 2010; 7: 115-26.

Maas AI, Stocchetti N, Bullock R. Moderate and severe traumatic brain injury in adults. Lancet Neurol, 2008; 7: 728-41.

Magnoni S, Brody DL. New perspectives on amyloid-beta dynamics after acute brain injury: moving between experimental approaches and studies in the human brain. Arch Neurol, 2010; 67: 1068-73.

Mahley RW. Apolipoprotein E: cholesterol transport protein with expanding role in cell biology. Science, 1988; 240: 622-30.

Manley GT, Rosenthal G, Lam M, Morabito D, Yan D, Derugin N, Bollen A, Knudson MM, Panter SS. Controlled cortical impact in swine: pathophysiology and biomechanics. J Neurotrauma, 2006; 23: 128-39.

Mannix R, Zhang J, Park J, Lee C, Whalen M. Detrimental effect of genetic inhibition of beta-site app cleaving enzyme 1 on functional outcome after controlled cortical impact in young adult mice. J Neurotrauma, 2011.

Mannix RC, Zhang J, Park J, Zhang X, Bilal K, Walker K, Tanzi RE, Tesco G, Whalen MJ. Age-dependent effect of apolipoprotein E4 on functional outcome after controlled cortical impact in mice. J Cereb Blood Flow Metab, 2010; 31: 351-61.

Mao H, Yang KH, King AI, Yang K. Computational neurotrauma-design, simulation, and analysis of controlled cortical impact model. Biomech Model Mechanobiol, 2010.

Markakis EA, Gage FH. Adult-generated neurons in the dentate gyrus send axonal projections to field CA3 and are surrounded by synaptic vesicles. J Comp Neurol, 1999; 406: 449-60.

Markgraf CG, Clifton GL, Aguirre M, Chaney SF, Knox-Du Bois C, Kennon K, Verma N. Injury severity and sensitivity to treatment after controlled cortical impact in rats. J Neurotrauma, 2001; 18: 175-86.

Marklund N, Blennow K, Zetterberg H, Ronne-Engstrom E, Enblad P, Hillered L. Monitoring of brain interstitial total tau and beta amyloid proteins by microdialysis in patients with traumatic brain injury. J Neurosurg, 2009; 110: 1227-37.

Marmarou A. Pathophysiology of traumatic brain edema: current concepts. Acta Neurochir Suppl, 2003; 86: 7-10.

Marmarou A, Foda MA, van den Brink W, Campbell J, Kita H, Demetriadou K. A new model of diffuse brain injury in rats. Part I: Pathophysiology and biomechanics. J Neurosurg, 1994; 80: 291-300.

Marmarou CR, Prieto R, Taya K, Young HF, Marmarou A. Marmarou Weight Drop Injury Model. In Chen J, editor. Animal Models of Acute Neurological Injuries: New York, 2009.

Marmarou CR, Walker SA, Davis CL, Povlishock JT. Quantitative analysis of the relationship between intra- axonal neurofilament compaction and impaired axonal transport following diffuse traumatic brain injury. J Neurotrauma, 2005; 22: 1066-80.

Masliah E, Westland CE, Rockenstein EM, Abraham CR, Mallory M, Veinberg I, Sheldon E, Mucke L. Amyloid precursor proteins protect neurons of transgenic mice against acute and chronic excitotoxic injuries in vivo. Neuroscience, 1997; 78: 135-46.

Mattson MP. Cellular actions of beta-amyloid precursor protein and its soluble and fibrillogenic derivatives. Physiol Rev, 1997; 77: 1081-132.

Mattson MP. Impairment of membrane transport and signal transduction systems by amyloidogenic proteins. Methods Enzymol, 1999; 309: 733-46.

Mattson MP. Pathways towards and away from Alzheimer's disease. Nature, 2004; 430: 631-9.

Mattson MP. Secreted forms of beta-amyloid precursor protein modulate dendrite outgrowth and calcium responses to glutamate in cultured embryonic hippocampal neurons. J Neurobiol, 1994; 25: 439-50.

Mattson MP, Chan SL. Neuronal and glial calcium signaling in Alzheimer's disease. Cell Calcium, 2003; 34: 385-97.

Mattson MP, Cheng B, Culwell AR, Esch FS, Lieberburg I, Rydel RE. Evidence for excitoprotective and intraneuronal calcium-regulating roles for secreted forms of the beta-amyloid precursor protein. Neuron, 1993; 10: 243-54.

Mattson MP, Partin J, Begley JG. Amyloid beta-peptide induces apoptosis-related events in synapses and dendrites. Brain Res, 1998; 807: 167-76.

Maxwell WL, Povlishock JT, Graham DL. A mechanistic analysis of nondisruptive axonal injury: a review. J Neurotrauma, 1997; 14: 419-40.

Mayeux R, Ottman R, Maestre G, Ngai C, Tang MX, Ginsberg H, Chun M, Tycko B, Shelanski M. Synergistic effects of traumatic head injury and apolipoprotein-epsilon 4 in patients with Alzheimer's disease. Neurology, 1995; 45: 555-7.

Mbye LH, Singh IN, Sullivan PG, Springer JE, Hall ED. Attenuation of acute mitochondrial dysfunction after traumatic brain injury in mice by NIM811, a non-immunosuppressive cyclosporin A analog. Exp Neurol, 2008; 209: 243-53.

McIntosh TK, Noble L, Andrews B, Faden AI. Traumatic brain injury in the rat: characterization of a midline fluid-percussion model. Cent Nerv Syst Trauma, 1987; 4: 119-34.

McIntosh TK, Raghupathi R. Cell stress genes and acute CNS injury. Neuropathol Appl Neurobiol, 1995; 21: 477-9.

McIntosh TK, Vink R, Noble L, Yamakami I, Fernyak S, Soares H, Faden AL. Traumatic brain injury in the rat: characterization of a lateral fluid-percussion model. Neuroscience, 1989; 28: 233-44.

McKay R. Stem cells in the central nervous system. Science, 1997; 276: 66-71.

McKinney RA, Luthi A, Bandtlow CE, Gahwiler BH, Thompson SM. Selective glutamate receptor antagonists can induce or prevent axonal sprouting in rat hippocampal slice cultures. Proc Natl Acad Sci U S A, 1999; 96: 11631-6.

McLean CA, Cherny RA, Fraser FW, Fuller SJ, Smith MJ, Beyreuther K, Bush AI, Masters CL. Soluble pool of Abeta amyloid as a determinant of severity of neurodegeneration in Alzheimer's disease. Ann Neurol, 1999; 46: 860-6.

Meziane H, Dodart JC, Mathis C, Little S, Clemens J, Paul SM, Ungerer A. Memory-enhancing effects of secreted forms of the beta-amyloid precursor protein in normal and amnestic mice. Proc Natl Acad Sci U S A, 1998; 95: 12683-8.

Mills J, Laurent Charest D, Lam F, Beyreuther K, Ida N, Pelech SL, Reiner PB. Regulation of amyloid precursor protein catabolism involves the mitogen-activated protein kinase signal transduction pathway. J Neurosci, 1997; 17: 9415-22.

Mills J, Reiner PB. Regulation of amyloid precursor protein cleavage. J Neurochem, 1999; 72: 443-60.

Minambres E, Ballesteros MA, Mayorga M, Marin MJ, Munoz P, Figols J, Lopez-Hoyos M. Cerebral Apoptosis in Severe Traumatic Brain Injury Patients: An In Vitro, In Vivo, and Postmortem Study. J Neurotrauma, 2008.

Miners JS, van Helmond Z, Kehoe PG, Love S. Changes with age in the activities of beta-secretase and the Abeta-degrading enzymes neprilysin, insulin-degrading enzyme and angiotensin-converting enzyme. Brain Pathol, 2010; 20: 794-802.

Molina-Holgado E, Ortiz S, Molina-Holgado F, Guaza C. Induction of COX-2 and PGE(2) biosynthesis by IL-1beta is mediated by PKC and mitogen-activated protein kinases in murine astrocytes. Br J Pharmacol, 2000; 131: 152-9.

Morganti-Kossman MC, Lenzlinger PM, Hans V, Stahel P, Csuka E, Ammann E, Stocker R, Trentz O, Kossmann T. Production of cytokines following brain injury: beneficial and deleterious for the damaged tissue. Mol Psychiatry, 1997; 2: 133-6.

Morganti-Kossmann MC, Satgunaseelan L, Bye N, Kossmann T. Modulation of immune response by head injury. Injury, 2007; 38: 1392-400.

Morimoto T, Ohsawa I, Takamura C, Ishiguro M, Nakamura Y, Kohsaka S. Novel domain-specific actions of amyloid precursor protein on developing synapses. J Neurosci, 1998; 18: 9386-93.

Mortimer JA, van Duijn CM, Chandra V, Fratiglioni L, Graves AB, Heyman A, Jorm AF, Kokmen E, Kondo K, Rocca WA, et al. Head trauma as a risk factor for Alzheimer's disease: a collaborative re-analysis of case-control studies. EURODEM Risk Factors Research Group. Int J Epidemiol, 1991; 20 Suppl 2: S28-35.

Murai H, Pierce JE, Raghupathi R, Smith DH, Saatman KE, Trojanowski JQ, Lee VM, Loring JF, Eckman C, Younkin S, McIntosh TK. Twofold overexpression of human beta-amyloid precursor proteins in transgenic mice does not affect the neuromotor, cognitive, or neurodegenerative sequelae following experimental brain injury. J Comp Neurol, 1998; 392: 428-38.

Murakami N, Yamaki T, Iwamoto Y, Sakakibara T, Kobori N, Fushiki S, Ueda S. Experimental brain injury induces expression of amyloid precursor protein, which may be related to neuronal loss in the hippocampus. J Neurotrauma, 1998; 15: 993-1003.

Nakagawa Y, Reed L, Nakamura M, McIntosh TK, Smith DH, Saatman KE, Raghupathi R, Clemens J, Saido TC, Lee VM, Trojanowski JQ. Brain trauma in aged transgenic mice induces regression of established abeta deposits. Exp Neurol, 2000; 163: 244-52.

Nathoo N, Narotam PK, Agrawal DK, Connolly CA, van Dellen JR, Barnett GH, Chetty R. Influence of apoptosis on neurological outcome following traumatic cerebral contusion. J Neurosurg, 2004; 101: 233-40.

Navone F, Jahn R, Di Gioia G, Stukenbrok H, Greengard P, De Camilli P. Protein p38: an integral membrane protein specific for small vesicles of neurons and neuroendocrine cells. J Cell Biol, 1986; 103: 2511-27.

Nicotera P, Leist M, Ferrando-May E. Apoptosis and necrosis: different execution of the same death. Biochem Soc Symp, 1999; 66: 69-73.

Nie HZ, Shi S, Lukas RJ, Zhao WJ, Sun YN, Yin M. Activation of alpha7 nicotinic receptor affects APP processing by regulating secretase activity in SH-EP1-alpha7 nAChR-hAPP695 cells. Brain Res, 2010; 1356: 112-20.

Nielsen MS, Gustafsen C, Madsen P, Nyengaard JR, Hermey G, Bakke O, Mari M, Schu P, Pohlmann R, Dennes A, Petersen CM. Sorting by the cytoplasmic domain of the amyloid precursor protein binding receptor SorLA. Mol Cell Biol, 2007; 27: 6842-51.

Nihashi T, Inao S, Kajita Y, Kawai T, Sugimoto T, Niwa M, Kabeya R, Hata N, Hayashi S, Yoshida J. Expression and distribution of beta amyloid precursor protein and beta amyloid peptide in reactive astrocytes after transient middle cerebral artery occlusion. Acta Neurochir (Wien), 2001; 143: 287-95.

Ninomiya H, Roch JM, Jin LW, Saitoh T. Secreted form of amyloid beta/A4 protein precursor (APP) binds to two distinct APP binding sites on rat B103 neuron-like cells through two different domains, but only one site is involved in neuritotropic activity. J Neurochem, 1994; 63: 495-500.

Ninomiya H, Roch JM, Sundsmo MP, Otero DA, Saitoh T. Amino acid sequence RERMS represents the active domain of amyloid beta/A4 protein precursor that promotes fibroblast growth. J Cell Biol, 1993; 121: 879-86.

Nitsch RM, Deng M, Growdon JH, Wurtman RJ. Serotonin 5-HT2a and 5-HT2c receptors stimulate amyloid precursor protein ectodomain secretion. J Biol Chem, 1996; 271: 4188-94.

Nitsch RM, Slack BE, Wurtman RJ, Growdon JH. Release of Alzheimer amyloid precursor derivatives stimulated by activation of muscarinic acetylcholine receptors. Science, 1992; 258: 304-7.

Nitsch RM, Wurtman RJ, Growdon JH. Regulation of proteolytic processing of the amyloid beta-protein precursor by first messengers. A novel potential approach for the treatment of Alzheimer's disease. Arzneimittelforschung, 1995; 45: 435-8.

Nowotny P, Gorski SM, Han SW, Philips K, Ray WJ, Nowotny V, Jones CJ, Clark RF, Cagan RL, Goate AM. Posttranslational modification and plasma membrane localization of the Drosophila melanogaster presenilin. Mol Cell Neurosci, 2000; 15: 88-98.

Nudo RJ, Plautz EJ, Frost SB. Role of adaptive plasticity in recovery of function after damage to motor cortex. Muscle Nerve, 2001; 24: 1000-19.

O'Connor C, Heath DL, Cernak I, Nimmo AJ, Vink R. Effects of daily versus weekly testing and pre-training on the assessment of neurologic impairment following diffuse traumatic brain injury in rats. J Neurotrauma, 2003; 20: 985-93.

O'Connor CA, Cernak I, Johnson F, Vink R. Effects of progesterone on neurologic and morphologic outcome following diffuse traumatic brain injury in rats. Exp Neurol, 2007; 205: 145-53.

O'Connor CA, Cernak I, Vink R. The temporal profile of edema formation differs between male and female rats following diffuse traumatic brain injury. Acta Neurochir Suppl, 2006; 96: 121-4.

Ohkawara T, Nagase H, Koh CS, Nakayama K. The amyloid precursor protein intracellular domain alters gene expression and induces neuron-specific apoptosis. Gene, 2011; 475: 1-9.

Ohsawa I, Takamura C, Kohsaka S. The amino-terminal region of amyloid precursor protein is responsible for neurite outgrowth in rat neocortical explant culture. Biochem Biophys Res Commun, 1997; 236: 59-65.

Olsson A, Csajbok L, Ost M, Hoglund K, Nylen K, Rosengren L, Nellgard B, Blennow K. Marked increase of beta-amyloid(1-42) and amyloid precursor protein in ventricular cerebrospinal fluid after severe traumatic brain injury. J Neurol, 2004; 251: 870-6.

Ommaya AK, Goldsmith W, Thibault L. Biomechanics and neuropathology of adult and paediatric head injury. Br J Neurosurg, 2002; 16: 220-42.

Onyszchuk G, Al-Hafez B, He YY, Bilgen M, Berman NE, Brooks WM. A mouse model of sensorimotor controlled cortical impact: characterization using longitudinal magnetic resonance imaging, behavioral assessments and histology. J Neurosci Methods, 2007; 160: 187-96.

Oyesiku NM, Evans CO, Houston S, Darrell RS, Smith JS, Fulop ZL, Dixon CE, Stein DG. Regional changes in the expression of neurotrophic factors and their receptors following acute traumatic brain injury in the adult rat brain. Brain Res, 1999; 833: 161-72.

Ozaki T, Li Y, Kikuchi H, Tomita T, Iwatsubo T, Nakagawara A. The intracellular domain of the amyloid precursor protein (AICD) enhances the p53-mediated apoptosis. Biochem Biophys Res Commun, 2006; 351: 57-63.

Palmer AM, Marion DW, Botscheller ML, Swedlow PE, Styren SD, DeKosky ST. Traumatic brain injury-induced excitotoxicity assessed in a controlled cortical impact model. J Neurochem, 1993; 61: 2015-24.

Paola D, Domenicotti C, Nitti M, Vitali A, Borghi R, Cottalasso D, Zaccheo D, Odetti P, Strocchi P, Marinari UM, Tabaton M, Pronzato MA. Oxidative stress induces increase in intracellular amyloid beta-protein production and selective activation of betaI and betaII PKCs in NT2 cells. Biochem Biophys Res Commun, 2000; 268: 642-6.

Paradis E, Douillard H, Koutroumanis M, Goodyer C, LeBlanc A. Amyloid beta peptide of Alzheimer's disease downregulates Bcl-2 and upregulates bax expression in human neurons. J Neurosci, 1996; 16: 7533-9.

Pardon MC. Role of neurotrophic factors in behavioral processes: implications for the treatment of psychiatric and neurodegenerative disorders. Vitam Horm, 2010; 82: 185-200.

Pardossi-Piquard R, Petit A, Kawarai T, Sunyach C, Alves da Costa C, Vincent B, Ring S, D'Adamio L, Shen J, Muller U, St George Hyslop P, Checler F. Presenilin-dependent transcriptional control of the Abeta-degrading enzyme neprilysin by intracellular domains of betaAPP and APLP. Neuron, 2005; 46: 541-54.

Paxinos G, Franklin KBJ. The Mouse Brain in Stereotaxic Coordinates, 3rd ed. Academic Press: San Diego, 2007.

Paxinos GWC. The Rat Brain in Stereotaxic Coordinates. Academic Press: San Diego, 1998.

Pellegrini L, Passer BJ, Tabaton M, Ganjei JK, D'Adamio L. Alternative, non-secretase processing of Alzheimer's beta-amyloid precursor protein during apoptosis by caspase-6 and -8. J Biol Chem, 1999; 274: 21011-6.

Perez RG, Zheng H, Van der Ploeg LH, Koo EH. The beta-amyloid precursor protein of Alzheimer's disease enhances neuron viability and modulates neuronal polarity. J Neurosci, 1997; 17: 9407-14.

Petchprapai N, Winkelman C. Mild traumatic brain injury: determinants and subsequent quality of life. A review of the literature. J Neurosci Nurs, 2007; 39: 260-72.
Pettmann B, Henderson CE. Neuronal cell death. Neuron, 1998; 20: 633-47.

Pettus EH, Christman CW, Giebel ML, Povlishock JT. Traumatically induced altered membrane permeability: its relationship to traumatically induced reactive axonal change. J Neurotrauma, 1994; 11: 507-22.

Phinney AL, Calhoun ME, Wolfer DP, Lipp HP, Zheng H, Jucker M. No hippocampal neuron or synaptic bouton loss in learning-impaired aged beta-amyloid precursor protein-null mice. Neuroscience, 1999; 90: 1207-16.

Pierce JE, Trojanowski JQ, Graham DI, Smith DH, McIntosh TK. Immunohistochemical characterization of alterations in the distribution of amyloid precursor proteins and beta-amyloid peptide after experimental brain injury in the rat. J Neurosci, 1996; 16: 1083-90.

Pietrzik CU, Yoon IS, Jaeger S, Busse T, Weggen S, Koo EH. FE65 constitutes the functional link between the low-density lipoprotein receptor-related protein and the amyloid precursor protein. J Neurosci, 2004; 24: 4259-65.

Pike CJ, Cummings BJ, Cotman CW. beta-Amyloid induces neuritic dystrophy in vitro: similarities with Alzheimer pathology. Neuroreport, 1992; 3: 769-72.

Pike CJ, Walencewicz AJ, Glabe CG, Cotman CW. In vitro aging of beta-amyloid protein causes peptide aggregation and neurotoxicity. Brain Res, 1991; 563: 311-4.

Pleasant JM, Carlson SW, Mao H, Scheff SW, Yang KH, Saatman KE. Rate of Neurodegeneration in the Mouse Controlled Cortical Impact Model is Influenced by Impactor Tip Shape: Implications for Mechanistic and Therapeutic Studies. J Neurotrauma, 2011.

Popa-Wagner A, Schroder E, Walker LC, Kessler C. beta-Amyloid precursor protein and ss-amyloid peptide immunoreactivity in the rat brain after middle cerebral artery occlusion: effect of age. Stroke, 1998; 29: 2196-202.

Portera-Cailliau C, Price DL, Martin LJ. Excitotoxic neuronal death in the immature brain is an apoptosis-necrosis morphological continuum. J Comp Neurol, 1997; 378: 70-87.

Povlishock JT. Pathophysiology of neural injury: therapeutic opportunities and challenges. Clin Neurosurg, 2000; 46: 113-26.

Povlishock JT, Erb DE, Astruc J. Axonal response to traumatic brain injury: reactive axonal change, deafferentation, and neuroplasticity. J Neurotrauma, 1992; 9 Suppl 1: S189-200.

Povlishock JT, Hayes RL, Michel ME, McIntosh TK. Workshop on animal models of traumatic brain injury. J Neurotrauma, 1994; 11: 723-32.

Povlishock JT, Katz DI. Update of neuropathology and neurological recovery after traumatic brain injury. J Head Trauma Rehabil, 2005; 20: 76-94.

Povlishock JT, Pettus EH. Traumatically induced axonal damage: evidence for enduring changes in axolemmal permeability with associated cytoskeletal change. Acta Neurochir Suppl, 1996; 66: 81-6.

Price DL, Tanzi RE, Borchelt DR, Sisodia SS. Alzheimer's disease: genetic studies and transgenic models. Annu Rev Genet, 1998; 32: 461-93.

Qiu J, Whalen MJ, Lowenstein P, Fiskum G, Fahy B, Darwish R, Aarabi B, Yuan J, Moskowitz MA. Upregulation of the Fas receptor death-inducing signaling complex after traumatic brain injury in mice and humans. J Neurosci, 2002; 22: 3504-11.

Qiu WQ, Ferreira A, Miller C, Koo EH, Selkoe DJ. Cell-surface beta-amyloid precursor protein stimulates neurite outgrowth of hippocampal neurons in an isoform-dependent manner. J Neurosci, 1995; 15: 2157-67.

Quiroz-Baez R, Rojas E, Arias C. Oxidative stress promotes JNK-dependent amyloidogenic processing of normally expressed human APP by differential modification of alpha-, beta- and gamma-secretase expression. Neurochem Int, 2009; 55: 662-70.

Raber J, Rola R, LeFevour A, Morhardt D, Curley J, Mizumatsu S, VandenBerg SR, Fike JR. Radiation-induced cognitive impairments are associated with changes in indicators of hippocampal neurogenesis. Radiat Res, 2004; 162: 39-47.

Raby CA, Morganti-Kossmann MC, Kossmann T, Stahel PF, Watson MD, Evans LM, Mehta PD, Spiegel K, Kuo YM, Roher AE, Emmerling MR. Traumatic brain injury increases beta-amyloid peptide 1-42 in cerebrospinal fluid. J Neurochem, 1998; 71: 2505-9.

Racchi M, Mazzucchelli M, Pascale A, Sironi M, Govoni S. Role of protein kinase Calpha in the regulated secretion of the amyloid precursor protein. Mol Psychiatry, 2003; 8: 209-16.

Raghupathi R. Cell death mechanisms following traumatic brain injury. Brain Pathol, 2004; 14: 215-22.

Raghupathi R, Graham DI, McIntosh TK. Apoptosis after traumatic brain injury. J Neurotrauma, 2000; 17: 927-38.

Raghupathi R, McIntosh TK, Smith DH. Cellular responses to experimental brain injury. Brain Pathol, 1995; 5: 437-42.

Raman R, Sasisekharan V, Sasisekharan R. Structural insights into biological roles of protein-glycosaminoglycan interactions. Chem Biol, 2005; 12: 267-77.

Ramaswamy S, Goings GE, Soderstrom KE, Szele FG, Kozlowski DA. Cellular proliferation and migration following a controlled cortical impact in the mouse. Brain Res, 2005; 1053: 38-53.

Rasmusson DX, Brandt J, Martin DB, Folstein MF. Head injury as a risk factor in Alzheimer's disease. Brain Inj, 1995; 9: 213-9.

Reid TR, Torti FM, Ringold GM. Evidence for two mechanisms by which tumor necrosis factor kills cells. J Biol Chem, 1989; 264: 4583-9.

Reinhard C, Hebert SS, De Strooper B. The amyloid-beta precursor protein: integrating structure with biological function. Embo J, 2005; 24: 3996-4006.

Ren Z, Schenk D, Basi GS, Shapiro IP. Amyloid beta-protein precursor juxtamembrane domain regulates specificity of gamma-secretase-dependent cleavages. J Biol Chem, 2007; 282: 35350-60.

Ring S, Weyer SW, Kilian SB, Waldron E, Pietrzik CU, Filippov MA, Herms J, Buchholz C, Eckman CB, Korte M, Wolfer DP, Muller UC. The secreted beta-amyloid precursor protein ectodomain APPs alpha is sufficient to rescue the anatomical, behavioral, and electrophysiological abnormalities of APP-deficient mice. J Neurosci, 2007; 27: 7817-26.

Ringheim GE, Aschmies S, Petko W. Additive effects of basic fibroblast growth factor and phorbol ester on beta-amyloid precursor protein expression and secretion. Neurochem Int, 1997; 30: 475-81.

Rink A, Fung KM, Trojanowski JQ, Lee VM, Neugebauer E, McIntosh TK. Evidence of apoptotic cell death after experimental traumatic brain injury in the rat. Am J Pathol, 1995; 147: 1575-83.

Roberts GW, Gentleman SM, Lynch A, Graham DI. beta A4 amyloid protein deposition in brain after head trauma. Lancet, 1991; 338: 1422-3.

Robertson CL. Mitochondrial dysfunction contributes to cell death following traumatic brain injury in adult and immature animals. J Bioenerg Biomembr, 2004; 36: 363-8.

Roch JM, Masliah E, Roch-Levecq AC, Sundsmo MP, Otero DA, Veinbergs I, Saitoh T. Increase of synaptic density and memory retention by a peptide representing the trophic domain of the amyloid beta/A4 protein precursor. Proc Natl Acad Sci U S A, 1994; 91: 7450-4.

Rohn TT, Ivins KJ, Bahr BA, Cotman CW, Cribbs DH. A monoclonal antibody to amyloid precursor protein induces neuronal apoptosis. J Neurochem, 2000; 74: 2331-42.

Rola R, Mizumatsu S, Otsuka S, Morhardt DR, Noble-Haeusslein LJ, Fishman K, Potts MB, Fike JR. Alterations in hippocampal neurogenesis following traumatic brain injury in mice. Exp Neurol, 2006; 202: 189-99.

Roses AD. Apolipoprotein E alleles as risk factors in Alzheimer's disease. Annu Rev Med, 1996; 47: 387-400.

Rossjohn J, Cappai R, Feil SC, Henry A, McKinstry WJ, Galatis D, Hesse L, Multhaup G, Beyreuther K, Masters CL, Parker MW. Crystal structure of the N-terminal, growth factor-like domain of Alzheimer amyloid precursor protein. Nat Struct Biol, 1999; 6: 327-31.

Rothwell N. Interleukin-1 and neuronal injury: mechanisms, modification, and therapeutic potential. Brain Behav Immun, 2003; 17: 152-7.

Royo NC, Conte V, Saatman KE, Shimizu S, Belfield CM, Soltesz KM, Davis JE, Fujimoto ST, McIntosh TK. Hippocampal vulnerability following traumatic brain injury: a potential role for neurotrophin-4/5 in pyramidal cell neuroprotection. Eur J Neurosci, 2006; 23: 1089-102.

Rubin LL. Neuronal cell death: an updated view. Prog Brain Res, 1998; 117: 3-8.

Ruifrok AC, Johnston DA. Quantification of histochemical staining by colour deconvolution. Anal Quant Cytol Histol, 2001; 23: 291-9.

Ryan KA, Pimplikar SW. Activation of GSK-3 and phosphorylation of CRMP2 in transgenic mice expressing APP intracellular domain. J Cell Biol, 2005; 171: 327-35.

Saatman KE, Abai B, Grosvenor A, Vorwerk CK, Smith DH, Meaney DF. Traumatic axonal injury results in biphasic calpain activation and retrograde transport impairment in mice. J Cereb Blood Flow Metab, 2003; 23: 34-42.

Saatman KE, Bozyczko-Coyne D, Marcy V, Siman R, McIntosh TK. Prolonged calpain-mediated spectrin breakdown occurs regionally following experimental brain injury in the rat. J Neuropathol Exp Neurol, 1996; 55: 850-60.

Saatman KE, Feeko KJ, Pape RL, Raghupathi R. Differential behavioral and histopathological responses to graded cortical impact injury in mice. J Neurotrauma, 2006; 23: 1241-53.

Sabo SL, Lanier LM, Ikin AF, Khorkova O, Sahasrabudhe S, Greengard P, Buxbaum JD. Regulation of beta-amyloid secretion by FE65, an amyloid protein precursor-binding protein. J Biol Chem, 1999; 274: 7952-7.

Saitoh T, Sundsmo M, Roch JM, Kimura N, Cole G, Schubert D, Oltersdorf T, Schenk DB. Secreted form of amyloid beta protein precursor is involved in the growth regulation of fibroblasts. Cell, 1989; 58: 615-22.

Sala Frigerio C, Fadeeva JV, Minogue AM, Citron M, Van Leuven F, Staufenbiel M, Paganetti P, Selkoe DJ, Walsh DM. beta-Secretase cleavage is not required for generation of the intracellular C-terminal domain of the amyloid precursor family of proteins. FEBS J, 2010; 277: 1503-18.

Salib E, Hillier V. Head injury and the risk of Alzheimer's disease: a case control study. Int J Geriatr Psychiatry, 1997; 12: 363-8.

Sandbrink R, Masters CL, Beyreuther K. APP gene family. Alternative splicing generates functionally related isoforms. Ann N Y Acad Sci, 1996; 777: 281-7.

Sandhir R, Berman NE. Age-dependent response of CCAAT/enhancer binding proteins following traumatic brain injury in mice. Neurochem Int, 2010; 56: 188-93.

Sankaranarayanan S, Price EA, Wu G, Crouthamel MC, Shi XP, Tugusheva K, Tyler KX, Kahana J, Ellis J, Jin L, Steele T, Stachel S, Coburn C, Simon AJ. In vivo beta-secretase 1 inhibition leads to brain Abeta lowering and increased alpha-secretase processing of amyloid precursor protein without effect on neuregulin-1. J Pharmacol Exp Ther, 2008; 324: 957-69.

Sansone M, Battaglia M, Pavone F. Attenuation by nimodipine of amitriptyline-induced avoidance impairment in mice. Pharmacol Biochem Behav, 1999; 62: 613-8.

Santiard-Baron D, Langui D, Delehedde M, Delatour B, Schombert B, Touchet N, Tremp G, Paul MF, Blanchard V, Sergeant N, Delacourte A, Duyckaerts C, Pradier L, Mercken L. Expression of human FE65 in amyloid precursor protein transgenic mice is associated with a reduction in beta-amyloid load. J Neurochem, 2005; 93: 330-8.

Sastry PS, Rao KS. Apoptosis and the nervous system. J Neurochem, 2000; 74: 1-20.

Scheff SW, Baldwin SA, Brown RW, Kraemer PJ. Morris water maze deficits in rats following traumatic brain injury: lateral controlled cortical impact. J Neurotrauma, 1997; 14: 615-27.

Scheff SW, Price DA, Hicks RR, Baldwin SA, Robinson S, Brackney C. Synaptogenesis in the hippocampal CA1 field following traumatic brain injury. J Neurotrauma, 2005; 22: 719-32.

Scheuermann S, Hambsch B, Hesse L, Stumm J, Schmidt C, Beher D, Bayer TA, Beyreuther K, Multhaup G. Homodimerisation of amyloid precursor protein and its implication in the amyloidogenic pathway of Alzheimer's disease. J Biol Chem, 2001; 276: 33923-9.

Scheuner D, Eckman C, Jensen M, Song X, Citron M, Suzuki N, Bird TD, Hardy J, Hutton M, Kukull W, Larson E, Levy-Lahad E, Viitanen M, Peskind E, Poorkaj P, Schellenberg G, Tanzi R, Wasco W, Lannfelt L, Selkoe D, Younkin S. Secreted amyloid beta-protein similar to that in the senile plaques of Alzheimer's disease is increased in vivo by the presenilin 1 and 2 and APP mutations linked to familial Alzheimer's disease. Nat Med, 1996; 2: 864-70.

Schmidt RH, Grady MS. Regional patterns of blood-brain barrier breakdown following central and lateral fluid percussion injury in rodents. J Neurotrauma, 1993; 10: 415-30.

Schmued LC, Albertson C, Slikker W, Jr. Fluoro-Jade: a novel fluorochrome for the sensitive and reliable histochemical localization of neuronal degeneration. Brain Res, 1997; 751: 37-46.

Schubert D, Behl C. The expression of amyloid beta protein precursor protects nerve cells from beta-amyloid and glutamate toxicity and alters their interaction with the extracellular matrix. Brain Res, 1993; 629: 275-82.

Schwetye KE, Cirrito JR, Esparza TJ, Mac Donald CL, Holtzman DM, Brody DL. Traumatic brain injury reduces soluble extracellular amyloid-beta in mice: a methodologically novel combined microdialysis-controlled cortical impact study. Neurobiol Dis, 2010; 40: 555-64.

Selkoe DJ. Toward a comprehensive theory for Alzheimer's disease. Hypothesis: Alzheimer's disease is caused by the cerebral accumulation and cytotoxicity of amyloid beta-protein. Ann N Y Acad Sci, 2000; 924: 17-25.

Selkoe DJ, Wolfe MS. Presenilin: running with scissors in the membrane. Cell, 2007; 131: 215-21.

Semple BD, Bye N, Rancan M, Ziebell JM, Morganti-Kossmann MC. Role of CCL2 (MCP-1) in traumatic brain injury (TBI): evidence from severe TBI patients and CCL2-/- mice. J Cereb Blood Flow Metab, 2010a; 30: 769-82.

Semple BD, Bye N, Ziebell JM, Morganti-Kossmann MC. Deficiency of the chemokine receptor CXCR2 attenuates neutrophil infiltration and cortical damage following closed head injury. Neurobiol Dis, 2010b; 40: 394-403.

Senechal Y, Kelly PH, Dev KK. Amyloid precursor protein knockout mice show age-dependent deficits in passive avoidance learning. Behav Brain Res, 2008; 186: 126-32.

Serbest G, Burkhardt MF, Siman R, Raghupathi R, Saatman KE. Temporal profiles of cytoskeletal protein loss following traumatic axonal injury in mice. Neurochem Res, 2007; 32: 2006-14.

Shankar GM, Leissring MA, Adame A, Sun X, Spooner E, Masliah E, Selkoe DJ, Lemere CA, Walsh DM. Biochemical and immunohistochemical analysis of an Alzheimer's disease mouse model reveals the presence of multiple cerebral Abeta assembly forms throughout life. Neurobiol Dis, 2009; 36: 293-302.

Shear DA, Tate MC, Archer DR, Hoffman SW, Hulce VD, Laplaca MC, Stein DG. Neural progenitor cell transplants promote long-term functional recovery after traumatic brain injury. Brain Res, 2004; 1026: 11-22.

Sheibani N, Grabowski EF, Schoenfeld DA, Whalen MJ. Effect of granulocyte colony-stimulating factor on functional and histopathologic outcome after traumatic brain injury in mice. Crit Care Med, 2004; 32: 2274-8.

Shohami E, Ginis I, Hallenbeck JM. Dual role of tumor necrosis factor alpha in brain injury. Cytokine Growth Factor Rev, 1999; 10: 119-30.

Shojo H, Kibayashi K. Changes in localization of synaptophysin following fluid percussion injury in the rat brain. Brain Res, 2006; 1078: 198-211.

Shors TJ, Dryver E. Effect of stress and long-term potentiation (LTP) on subsequent LTP and the theta burst response in the dentate gyrus. Brain Res, 1994; 666: 232-8.

Simmons LK, May PC, Tomaselli KJ, Rydel RE, Fuson KS, Brigham EF, Wright S, Lieberburg I, Becker GW, Brems DN, et al. Secondary structure of amyloid beta peptide correlates with neurotoxic activity in vitro. Mol Pharmacol, 1994; 45: 373-9.

Simons M, de Strooper B, Multhaup G, Tienari PJ, Dotti CG, Beyreuther K. Amyloidogenic processing of the human amyloid precursor protein in primary cultures of rat hippocampal neurons. J Neurosci, 1996; 16: 899-908.

Sisodia SS, Koo EH, Hoffman PN, Perry G, Price DL. Identification and transport of full-length amyloid precursor proteins in rat peripheral nervous system. J Neurosci, 1993; 13: 3136-42.

Slack BE, Ma LK, Seah CC. Constitutive shedding of the amyloid precursor protein ectodomain is up-regulated by tumour necrosis factor-alpha converting enzyme. Biochem J, 2001; 357: 787-94.

Slomnicki LP, Lesniak W. A putative role of the Amyloid Precursor Protein Intracellular Domain (AICD) in transcription. Acta Neurobiol Exp (Wars), 2008; 68: 219-28.

Small DH, Nurcombe V, Reed G, Clarris H, Moir R, Beyreuther K, Masters CL. A heparin-binding domain in the amyloid protein precursor of Alzheimer's disease is involved in the regulation of neurite outgrowth. J Neurosci, 1994; 14: 2117-27.

Smith-Swintosky VL, Pettigrew LC, Craddock SD, Culwell AR, Rydel RE, Mattson MP. Secreted forms of beta-amyloid precursor protein protect against ischemic brain injury. J Neurochem, 1994; 63: 781-4.

Smith DH, Chen XH, Nonaka M, Trojanowski JQ, Lee VM, Saatman KE, Leoni MJ, Xu BN, Wolf JA, Meaney DF. Accumulation of amyloid beta and tau and the formation of neurofilament inclusions following diffuse brain injury in the pig. J Neuropathol Exp Neurol, 1999; 58: 982-92.

Smith DH, Meaney DF, Shull WH. Diffuse axonal injury in head trauma. J Head Trauma Rehabil, 2003; 18: 307-16.

Smith DH, Nakamura M, McIntosh TK, Wang J, Rodriguez A, Chen XH, Raghupathi R, Saatman KE, Clemens J, Schmidt ML, Lee VM, Trojanowski JQ. Brain trauma induces massive hippocampal neuron death linked to a surge in beta-amyloid levels in mice overexpressing mutant amyloid precursor protein. Am J Pathol, 1998; 153: 1005-10.

Smith DH, Soares HD, Pierce JS, Perlman KG, Saatman KE, Meaney DF, Dixon CE, McIntosh TK. A model of parasagittal controlled cortical impact in the mouse: cognitive and histopathologic effects. J Neurotrauma, 1995; 12: 169-78.

Soba P, Eggert S, Wagner K, Zentgraf H, Siehl K, Kreger S, Lower A, Langer A, Merdes G, Paro R, Masters CL, Muller U, Kins S, Beyreuther K. Homo- and heterodimerisation of APP family members promotes intercellular adhesion. Embo J, 2005; 24: 3624-34.

Sodhi CP, Perez RG, Gottardi-Littell NR. Phosphorylation of beta-amyloid precursor protein (APP) cytoplasmic tail facilitates amyloidogenic processing during apoptosis. Brain Res, 2008; 1198: 204-12.

Spillman D, Lindahl L. Glycosaminoglycan–protein interactions: a question of specificity. Curr. Opin. Struct Biol, 1994; 4: 667-82.

Spoelgen R, von Arnim CA, Thomas AV, Peltan ID, Koker M, Deng A, Irizarry MC, Andersen OM, Willnow TE, Hyman BT. Interaction of the cytosolic domains of sorLA/LR11 with the amyloid precursor protein (APP) and beta-secretase beta-site APP-cleaving enzyme. J Neurosci, 2006; 26: 418-28.

Stein TD, Anders NJ, DeCarli C, Chan SL, Mattson MP, Johnson JA. Neutralization of transthyretin reverses the neuroprotective effects of secreted amyloid precursor protein (APP) in APPSW mice resulting in tau phosphorylation and loss of hippocampal neurons: support for the amyloid hypothesis. J Neurosci, 2004; 24: 7707-17.

Stoica BA, Faden AI. Cell death mechanisms and modulation in traumatic brain injury. Neurotherapeutics, 2010; 7: 3-12.

Stone JR, Okonkwo DO, Singleton RH, Mutlu LK, Helm GA, Povlishock JT. Caspase-3-mediated cleavage of amyloid precursor protein and formation of amyloid Beta peptide in traumatic axonal injury. J Neurotrauma, 2002; 19: 601-14.

Stone JR, Singleton RH, Povlishock JT. Intra-axonal neurofilament compaction does not evoke local axonal swelling in all traumatically injured axons. Exp Neurol, 2001; 172: 320-31.

Storey E, Cappai R. The amyloid precursor protein of Alzheimer's disease and the Abeta peptide. Neuropathol Appl Neurobiol, 1999; 25: 81-97.

Strauss KI, Narayan RK, Raghupathi R. Common patterns of bcl-2 family gene expression in two traumatic brain injury models. Neurotox Res, 2004; 6: 333-42.

Stroemer RP, Kent TA, Hulsebosch CE. Neocortical neural sprouting, synaptogenesis, and behavioral recovery after neocortical infarction in rats. Stroke, 1995; 26: 2135-44.

Sudo H, Jiang H, Yasukawa T, Hashimoto Y, Niikura T, Kawasumi M, Matsuda S, Takeuchi Y, Aiso S, Matsuoka M, Murayama Y, Nishimoto I. Antibody-regulated neurotoxic function of cell-surface beta-amyloid precursor protein. Mol Cell Neurosci, 2000; 16: 708-23.

Suh YH, Checler F. Amyloid precursor protein, presenilins, and alpha-synuclein: molecular pathogenesis and pharmacological applications in Alzheimer's disease. Pharmacol Rev, 2002; 54: 469-525.

Sullivan PG, Keller JN, Bussen WL, Scheff SW. Cytochrome c release and caspase activation after traumatic brain injury. Brain Res, 2002; 949: 88-96.

Susin SA, Lorenzo HK, Zamzami N, Marzo I, Snow BE, Brothers GM, Mangion J, Jacotot E, Costantini P, Loeffler M, Larochette N, Goodlett DR, Aebersold R, Siderovski DP, Penninger JM, Kroemer G. Molecular characterization of mitochondrial apoptosis-inducing factor. Nature, 1999; 397: 441-6.

Svedberg MM, Hall H, Hellstrom-Lindahl E, Estrada S, Guan Z, Nordberg A, Langstrom B. [(11)C]PIB-amyloid binding and levels of Abeta40 and Abeta42 in postmortem brain tissue from Alzheimer patients. Neurochem Int, 2009; 54: 347-57.

Tachida Y, Nakagawa K, Saito T, Saido TC, Honda T, Saito Y, Murayama S, Endo T, Sakaguchi G, Kato A, Kitazume S, Hashimoto Y. Interleukin-1beta up-regulates TACE to enhance alpha-cleavage of APP in neurons: resulting decrease in Abeta production. J Neurochem, 2008; 104: 1387-93.

Tagliaferri F, Compagnone C, Korsic M, Servadei F, Kraus J. A systematic review of brain injury epidemiology in Europe. Acta Neurochir (Wien), 2006; 148: 255-68; discussion 68.

Tamagno E, Guglielmotto M, Aragno M, Borghi R, Autelli R, Giliberto L, Muraca G, Danni O, Zhu X, Smith MA, Perry G, Jo DG, Mattson MP, Tabaton M. Oxidative stress activates a positive feedback between the gamma- and beta-secretase cleavages of the beta-amyloid precursor protein. J Neurochem, 2008; 104: 683-95.

Tamagno E, Parola M, Bardini P, Piccini A, Borghi R, Guglielmotto M, Santoro G, Davit A, Danni O, Smith MA, Perry G, Tabaton M. Beta-site APP cleaving enzyme up-regulation induced by 4-hydroxynonenal is mediated by stress-activated protein kinases pathways. J Neurochem, 2005; 92: 628-36.

Tamagno E, Parola M, Guglielmotto M, Santoro G, Bardini P, Marra L, Tabaton M, Danni O. Multiple signaling events in amyloid beta-induced, oxidative stress-dependent neuronal apoptosis. Free Radic Biol Med, 2003; 35: 45-58.

Tanahashi H, Tabira T. Characterization of an amyloid precursor protein-binding protein Fe65L2 and its novel isoforms lacking phosphotyrosine-interaction domains. Biochem J, 2002; 367: 687-95.

Tanzi RE, Bertram L. Twenty years of the Alzheimer's disease amyloid hypothesis: a genetic perspective. Cell, 2005; 120: 545-55.

Taupin V, Toulmond S, Serrano A, Benavides J, Zavala F. Increase in IL-6, IL-1 and TNF levels in rat brain following traumatic lesion. Influence of pre- and post-traumatic treatment with Ro5 4864, a peripheral-type (p site) benzodiazepine ligand. J Neuroimmunol, 1993; 42: 177-85.

Tavazzi B, Signoretti S, Lazzarino G, Amorini AM, Delfini R, Cimatti M, Marmarou A, Vagnozzi R. Cerebral oxidative stress and depression of energy metabolism correlate with severity of diffuse brain injury in rats. Neurosurgery, 2005; 56: 582-9; discussion -9.

Thompson SN, Gibson TR, Thompson BM, Deng Y, Hall ED. Relationship of calpain-mediated proteolysis to the expression of axonal and synaptic plasticity markers following traumatic brain injury in mice. Exp Neurol, 2006; 201: 253-65.

Thornton E, Vink R, Blumbergs PC, Van Den Heuvel C. Soluble amyloid precursor protein alpha reduces neuronal injury and improves functional outcome following diffuse traumatic brain injury in rats. Brain Res, 2006; 1094: 38-46.

Tolias CM, Bullock MR. Critical appraisal of neuroprotection trials in head injury: what have we learned? NeuroRx, 2004; 1: 71-9.

Tomita S, Kirino Y, Suzuki T. Cleavage of Alzheimer's amyloid precursor protein (APP) by secretases occurs after O-glycosylation of APP in the protein secretory pathway. Identification of intracellular compartments in which APP cleavage occurs without using toxic agents that interfere with protein metabolism. J Biol Chem, 1998; 273: 6277-84.

Tong Y, Zhou W, Fung V, Christensen MA, Qing H, Sun X, Song W. Oxidative stress potentiates BACE1 gene expression and Abeta generation. J Neural Transm, 2005; 112: 455-69.

Townsend M, Shankar GM, Mehta T, Walsh DM, Selkoe DJ. Effects of secreted oligomers of amyloid beta-protein on hippocampal synaptic plasticity: a potent role for trimers. J Physiol, 2006; 572: 477-92.

Tremml P, Lipp HP, Muller U, Ricceri L, Wolfer DP. Neurobehavioral development, adult openfield exploration and swimming navigation learning in mice with a modified beta-amyloid precursor protein gene. Behav Brain Res, 1998; 95: 65-76.

Tremml P, Lipp HP, Muller U, Wolfer DP. Enriched early experiences of mice underexpressing the beta-amyloid precursor protein restore spatial learning capabilities but not normal openfield behavior of adult animals. Genes Brain Behav, 2002; 1: 230-41.

Truettner J, Schmidt-Kastner R, Busto R, Alonso OF, Loor JY, Dietrich WD, Ginsberg MD. Expression of brain-derived neurotrophic factor, nerve growth factor, and heat shock protein HSP70 following fluid percussion brain injury in rats. J Neurotrauma, 1999; 16: 471-86.

Turnbull J, Powell A, Guimond S. Heparan sulfate: decoding a dynamic multifunctional cell regulator. Trends Cell Biol, 2001; 11: 75-82.

Turner PR, O'Connor K, Tate WP, Abraham WC. Roles of amyloid precursor protein and its fragments in regulating neural activity, plasticity and memory. Prog Neurobiol, 2003; 70: 1-32.

Ulus IH, Wurtman RJ. Metabotropic glutamate receptor agonists increase release of soluble amyloid precursor protein derivatives from rat brain cortical and hippocampal slices. J Pharmacol Exp Ther, 1997; 281: 149-54.

Uryu K, Chen XH, Martinez D, Browne KD, Johnson VE, Graham DI, Lee VM, Trojanowski JQ, Smith DH. Multiple proteins implicated in neurodegenerative diseases accumulate in axons after brain trauma in humans. Exp Neurol, 2007; 208: 185-92.

Uryu K, Laurer H, McIntosh T, Pratico D, Martinez D, Leight S, Lee VM, Trojanowski JQ. Repetitive mild brain trauma accelerates Abeta deposition, lipid peroxidation, and cognitive impairment in a transgenic mouse model of Alzheimer amyloidosis. J Neurosci, 2002; 22: 446-54.

Van Den Heuvel C, Blumbergs P, Finnie J, Manavis J, Lewis S, Jones N, Reilly P, Pereira R. Upregulation of amyloid precursor protein and its mRNA in an experimental model of paediatric head injury. J Clin Neurosci, 2000; 7: 140-5.

Van den Heuvel C, Blumbergs PC, Finnie JW, Manavis J, Jones NR, Reilly PL, Pereira RA. Upregulation of amyloid precursor protein messenger RNA in response to traumatic brain injury: an ovine head impact model. Exp Neurol, 1999; 159: 441-50.

Van Den Heuvel C, Thornton E, Vink R. Traumatic brain injury and Alzheimer's disease: a review. Prog Brain Res, 2007; 161: 303-16.

van den Heuvel C, Vink R. The role of magnesium in traumatic brain injury. Clin Calcium, 2004; 14: 9-14.

van Helmond Z, Miners JS, Kehoe PG, Love S. Higher soluble amyloid beta concentration in frontal cortex of young adults than in normal elderly or Alzheimer's disease. Brain Pathol, 2010a; 20: 787-93.

van Helmond Z, Miners JS, Kehoe PG, Love S. Oligomeric Abeta in Alzheimer's disease: relationship to plaque and tangle pathology, APOE genotype and cerebral amyloid angiopathy. Brain Pathol, 2010b; 20: 468-80.

van Landeghem FK, Weiss T, Oehmichen M, von Deimling A. Decreased expression of glutamate transporters in astrocytes after human traumatic brain injury. J Neurotrauma, 2006; 23: 1518-28.

Vanderploeg RD, Curtiss G, Belanger HG. Long-term neuropsychological outcomes following mild traumatic brain injury. J Int Neuropsychol Soc, 2005; 11: 228-36.

Varma MR, Dixon CE, Jackson EK, Peters GW, Melick JA, Griffith RP, Vagni VA, Clark RS, Jenkins LW, Kochanek PM. Administration of adenosine receptor agonists or antagonists after controlled cortical impact in mice: effects on function and histopathology. Brain Res, 2002; 951: 191-201.

Vassar R, Bennett BD, Babu-Khan S, Kahn S, Mendiaz EA, Denis P, Teplow DB, Ross S, Amarante P, Loeloff R, Luo Y, Fisher S, Fuller J, Edenson S, Lile J, Jarosinski MA, Biere AL, Curran E, Burgess T, Louis JC, Collins F, Treanor J, Rogers G, Citron M. Beta-secretase cleavage of Alzheimer's amyloid precursor protein by the transmembrane aspartic protease BACE. Science, 1999; 286: 735-41.

Verweij BH, Muizelaar JP, Vinas FC, Peterson PL, Xiong Y, Lee CP. Impaired cerebral mitochondrial function after traumatic brain injury in humans. J Neurosurg, 2000; 93: 815-20.

Vink R, O'Connor CA, Nimmo AJ, Heath DL. Magnesium attenuates persistent functional deficits following diffuse traumatic brain injury in rats. Neurosci Lett, 2003a; 336: 41-4.

Vink R, Van Den Heuvel C. Recent advances in the development of multifactorial therapies for the treatment of traumatic brain injury. Expert Opin Investig Drugs, 2004; 13: 1263-74.

Vink R, Young A, Bennett CJ, Hu X, Connor CO, Cernak I, Nimmo AJ. Neuropeptide release influences brain edema formation after diffuse traumatic brain injury. Acta Neurochir Suppl, 2003b; 86: 257-60.

von Bohlen Und Halbach O. Immunohistological markers for staging neurogenesis in adult hippocampus. Cell Tissue Res, 2007; 329: 409-20.

von Koch CS, Zheng H, Chen H, Trumbauer M, Thinakaran G, van der Ploeg LH, Price DL, Sisodia SS. Generation of APLP2 KO mice and early postnatal lethality in APLP2/APP double KO mice. Neurobiol Aging, 1997; 18: 661-9.

von Rotz RC, Kohli BM, Bosset J, Meier M, Suzuki T, Nitsch RM, Konietzko U. The APP intracellular domain forms nuclear multiprotein complexes and regulates the transcription of its own precursor. J Cell Sci, 2004; 117: 4435-48.

Wallace WC, Akar CA, Lyons WE. Amyloid precursor protein potentiates the neurotrophic activity of NGF. Brain Res Mol Brain Res, 1997; 52: 201-12.

Walsh DM, Klyubin I, Fadeeva JV, Cullen WK, Anwyl R, Wolfe MS, Rowan MJ, Selkoe DJ. Naturally secreted oligomers of amyloid beta protein potently inhibit hippocampal long-term potentiation in vivo. Nature, 2002; 416: 535-9.

Walsh DM, Tseng BP, Rydel RE, Podlisny MB, Selkoe DJ. The oligomerization of amyloid beta-protein begins intracellularly in cells derived from human brain. Biochemistry, 2000; 39: 10831-9.

Wang HW, Pasternak JF, Kuo H, Ristic H, Lambert MP, Chromy B, Viola KL, Klein WL, Stine WB, Krafft GA, Trommer BL. Soluble oligomers of beta amyloid (1-42) inhibit long-term potentiation but not long-term depression in rat dentate gyrus. Brain Res, 2002; 924: 133-40.

Wang J, Dickson DW, Trojanowski JQ, Lee VM. The levels of soluble versus insoluble brain Abeta distinguish Alzheimer's disease from normal and pathologic aging. Exp Neurol, 1999; 158: 328-37.

Wang KK. Calpain and caspase: can you tell the difference? Trends Neurosci, 2000; 23: 20-6.

Wang Y, Ha Y. The X-ray structure of an antiparallel dimer of the human amyloid precursor protein E2 domain. Mol Cell, 2004; 15: 343-53.

Wang Y, Neumann M, Hansen K, Hong SM, Kim S, Noble-Haeusslein LJ, Liu J. Fluoxetine increases hippocampal neurogenesis and induces epigenetic factors but does not improve functional recovery after traumatic brain injury. J Neurotrauma, 2011; 28: 259-68.

Werner C, Engelhard K. Pathophysiology of traumatic brain injury. Br J Anaesth, 2007; 99: 4-9.

Whalen MJ, Dalkara T, You Z, Qiu J, Bermpohl D, Mehta N, Suter B, Bhide PG, Lo EH, Ericsson M, Moskowitz MA. Acute plasmalemma permeability and protracted clearance of injured cells after controlled cortical impact in mice. J Cereb Blood Flow Metab, 2008; 28: 490-505.

White AR, Zheng H, Galatis D, Maher F, Hesse L, Multhaup G, Beyreuther K, Masters CL, Cappai R. Survival of cultured neurons from amyloid precursor protein knock-out mice against Alzheimer's amyloid-beta toxicity and oxidative stress. J Neurosci, 1998; 18: 6207-17.

Williamson TG, Mok SS, Henry A, Cappai R, Lander AD, Nurcombe V, Beyreuther K, Masters CL, Small DH. Secreted glypican binds to the amyloid precursor protein of Alzheimer's disease (APP) and inhibits APP-induced neurite outgrowth. J Biol Chem, 1996; 271: 31215-21.

Wolfe MS. When loss is gain: reduced presenilin proteolytic function leads to increased Abeta42/Abeta40. Talking Point on the role of presenilin mutations in Alzheimer disease. EMBO Rep, 2007; 8: 136-40.

Wolfe MS, Guenette SY. APP at a glance. J Cell Sci, 2007; 120: 3157-61.
Xia W, Yang T, Shankar G, Smith IM, Shen Y, Walsh DM, Selkoe DJ. A specific enzyme-linked immunosorbent assay for measuring beta-amyloid protein oligomers in human plasma and brain tissue of patients with Alzheimer disease. Arch Neurol, 2009; 66: 190-9.

Xiao AY, Wang XQ, Yang A, Yu SP. Slight impairment of Na+,K+-ATPase synergistically aggravates ceramide- and beta-amyloid-induced apoptosis in cortical neurons. Brain Res, 2002; 955: 253-9.
Xiong Y, Shie FS, Zhang J, Lee CP, Ho YS. Prevention of mitochondrial dysfunction in post-traumatic mouse brain by superoxide dismutase. J Neurochem, 2005; 95: 732-44.

Yakovlev AG, Knoblach SM, Fan L, Fox GB, Goodnight R, Faden AI. Activation of CPP32-like caspases contributes to neuronal apoptosis and neurological dysfunction after traumatic brain injury. J Neurosci, 1997; 17: 7415-24.

Yamamoto K, Miyoshi T, Yae T, Kawashima K, Araki H, Hanada K, Otero DA, Roch JM, Saitoh T. The survival of rat cerebral cortical neurons in the presence of trophic APP peptides. J Neurobiol, 1994; 25: 585-94.

Yang L, Tao LY, Chen XP. Roles of NF-kappaB in central nervous system damage and repair. Neurosci Bull, 2007; 23: 307-13.

Yang X, Yang S, Zhang J, Xue L, Hu Z. Role of Caspase 3 in neuronal apoptosis after acute brain injury. Chin J Traumatol, 2002; 5: 250-3.

Yang Z, Cool BH, Martin GM, Hu Q. A dominant role for FE65 (APBB1) in nuclear signaling. J Biol Chem, 2006; 281: 4207-14.

Yao XL, Liu J, Lee E, Ling GS, McCabe JT. Progesterone differentially regulates pro- and anti-apoptotic gene expression in cerebral cortex following traumatic brain injury in rats. J Neurotrauma, 2005; 22: 656-68.

Yi JH, Hazell AS. Excitotoxic mechanisms and the role of astrocytic glutamate transporters in traumatic brain injury. Neurochem Int, 2006; 48: 394-403.

Yin KJ, Lee JM, Chen SD, Xu J, Hsu CY. Amyloid-beta induces Smac release via AP-1/Bim activation in cerebral endothelial cells. J Neurosci, 2002; 22: 9764-70.

You Z, Savitz SI, Yang J, Degterev A, Yuan J, Cuny GD, Moskowitz MA, Whalen MJ. Necrostatin-1 reduces histopathology and improves functional outcome after controlled cortical impact in mice. J Cereb Blood Flow Metab, 2008; 28: 1564-73.

Young-Pearse TL, Chen AC, Chang R, Marquez C, Selkoe DJ. Secreted APP regulates the function of full-length APP in neurite outgrowth through interaction with integrin beta1. Neural Dev, 2008; 3: 15.

Yu S, Kaneko Y, Bae E, Stahl CE, Wang Y, van Loveren H, Sanberg PR, Borlongan CV. Severity of controlled cortical impact traumatic brain injury in rats and mice dictates degree of behavioral deficits. Brain Res, 2009; 1287: 157-63.

Yu TS, Zhang G, Liebl DJ, Kernie SG. Traumatic brain injury-induced hippocampal neurogenesis requires activation of early nestin-expressing progenitors. J Neurosci, 2008; 28: 12901-12.

Zakharov VV, Bogdanova MN, Mosevitsky MI. Specific proteolysis of neuronal protein GAP-43 by calpain: characterization, regulation, and physiological role. Biochemistry (Mosc), 2005; 70: 897-907.

Zhang X, Chen J, Graham SH, Du L, Kochanek PM, Draviam R, Guo F, Nathaniel PD, Szabo C, Watkins SC, Clark RS. Intranuclear localization of apoptosis-inducing factor (AIF) and large scale DNA fragmentation after traumatic brain injury in rats and in neuronal cultures exposed to peroxynitrite. J Neurochem, 2002; 82: 181-91.

Zhang X, Chen Y, Jenkins LW, Kochanek PM, Clark RS. Bench-to-bedside review: Apoptosis/programmed cell death triggered by traumatic brain injury. Crit Care, 2005; 9: 66-75.

Zhao G, Cui MZ, Mao G, Dong Y, Tan J, Sun L, Xu X. gamma-Cleavage is dependent on zeta-cleavage during the proteolytic processing of amyloid precursor protein within its transmembrane domain. J Biol Chem, 2005; 280: 37689-97.

Zheng H, Jiang M, Trumbauer ME, Sirinathsinghji DJ, Hopkins R, Smith DW, Heavens RP, Dawson GR, Boyce S, Conner MW, Stevens KA, Slunt HH, Sisoda SS, Chen HY, Van der Ploeg LH. beta-Amyloid precursor protein-deficient mice show reactive gliosis and decreased locomotor activity. Cell, 1995; 81: 525-31.

Zhong Z, Higaki J, Murakami K, Wang Y, Catalano R, Quon D, Cordell B. Secretion of beta-amyloid precursor protein involves multiple cleavage sites. J Biol Chem, 1994; 269: 627-32.

Zhu G, Wang D, Lin YH, McMahon T, Koo EH, Messing RO. Protein kinase C epsilon suppresses Abeta production and promotes activation of alpha-secretase. Biochem Biophys Res Commun, 2001; 285: 997-1006.

Zhu T, Yao Z, Yuan HN, Lu BG, Yang SY. Changes of interleukin-1 beta, tumor necrosis factor alpha and interleukin-6 in brain and plasma after brain injury in rats. Chin J Traumatol, 2004; 7: 32-5.

Zohar O, Lavy R, Zi X, Nelson TJ, Hongpaisan J, Pick CG, Alkon DL. PKC activator therapeutic for mild traumatic brain injury in mice. Neurobiol Dis, 2010; 41: 329-37.

Zong WX, Thompson CB. Necrotic death as a cell fate. Genes Dev, 2006; 20: 1-15.